1 OF 2

PB80

219249

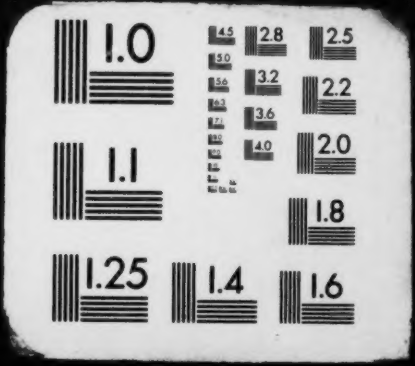
1.0
4.5
5.0
5.6
6.3
7.1
8.0
9.0
2.8
3.2
3.6
4.0
2.5
2.2
2.0
1.1
1.8
1.25
1.4
1.6

PB80-219249

Experimental/Engineering Support for EPA's FBC Program: Final Report. Volume II. Particulate Nitrogen Oxide, and Trace Element Control

Westinghouse Research and Development Center
Pittsburgh, PA

Prepared for

Industrial Environmental Research Lab.
Research Triangle Park, NC

Jan 80

U.S. Department of Commerce
National Technical Information Service
NTIS

PB80-219249

United States
Environmental Protection
Agency

Industrial Environmental Research
Laboratory
Research Triangle Park NC 27711

EPA-600/7-80-015b
January 1980

EPA

Experimental/ Engineering Support for EPA's FBC Program:
Final Report - Volume II. Particulate, Nitrogen Oxide, and Trace Element Control

Interagency
Energy/Environment
R&D Program Report

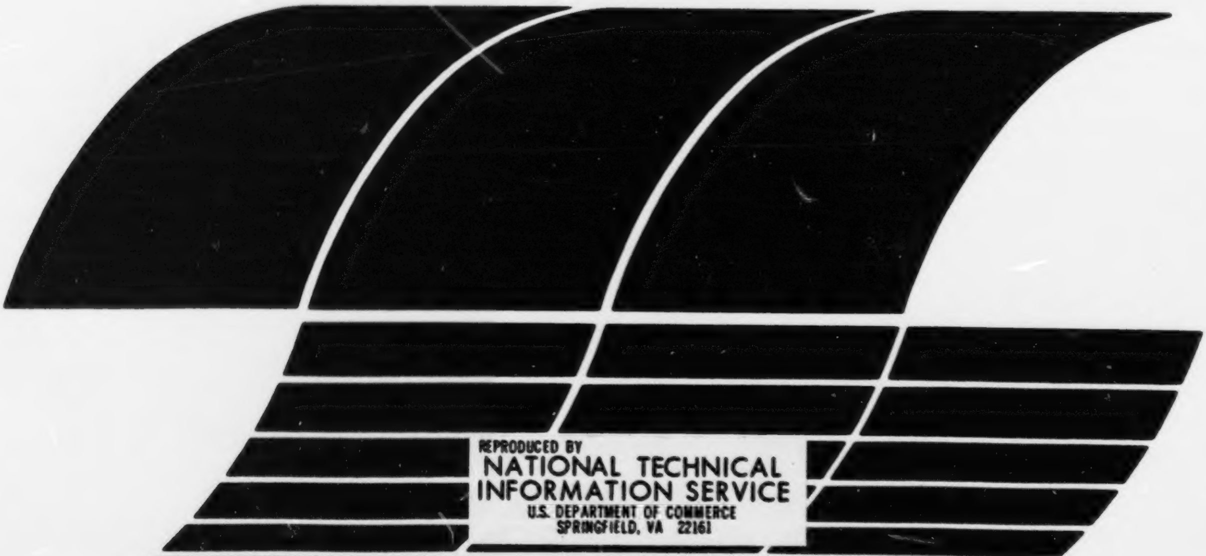

REPRODUCED BY
NATIONAL TECHNICAL
INFORMATION SERVICE
U.S. DEPARTMENT OF COMMERCE
SPRINGFIELD, VA 22161

RESEARCH REPORTING SERIES

Research reports of the Office of Research and Development, U.S. Environmental Protection Agency, have been grouped into nine series. These nine broad categories were established to facilitate further development and application of environmental technology. Elimination of traditional grouping was consciously planned to foster technology transfer and a maximum interface in related fields. The nine series are:

1. Environmental Health Effects Research
2. Environmental Protection Technology
3. Ecological Research
4. Environmental Monitoring
5. Socioeconomic Environmental Studies
6. Scientific and Technical Assessment Reports (STAR)
7. Interagency Energy-Environment Research and Development
8. "Special" Reports
9. Miscellaneous Reports

This report has been assigned to the INTERAGENCY ENERGY-ENVIRONMENT RESEARCH AND DEVELOPMENT series. Reports in this series result from the effort funded under the 17-agency Federal Energy/Environment Research and Development Program. These studies relate to EPA's mission to protect the public health and welfare from adverse effects of pollutants associated with energy systems. The goal of the Program is to assure the rapid development of domestic energy supplies in an environmentally-compatible manner by providing the necessary environmental data and control technology. Investigations include analyses of the transport of energy-related pollutants and their health and ecological effects; assessments of, and development of, control technologies for energy systems; and integrated assessments of a wide range of energy-related environmental issues.

EPA REVIEW NOTICE

This report has been reviewed by the participating Federal Agencies, and approved for publication. Mention of trade names or commercial products does not constitute endorsement or recommendation for use.

This document is available to the public through the National Technical Information Service, Springfield, Virginia 22161.

TECHNICAL REPORT DATA

(Please read Instructions on the reverse before completing)

1. REPORT NO. EPA-600/7-80-015b	2.	3. RECIPIENT'S ACCESSION NO. PB80 219249
4. TITLE AND SUBTITLE Experimental/Engineering Support for EPA's FBC Program: Final Report--Volume 2. Particulate, Nitrogen Oxide, and Trace Element Control		5. REPORT DATE January 1980 6. PERFORMING ORGANIZATION CODE
7. AUTHOR(S) D. F. Ciliberti, M. M. Ahmed, N. H. Ulerich, M. A. Alvin, and D. L. Keairns		8. PERFORMING ORGANIZATION REPORT NO.
9. PERFORMING ORGANIZATION NAME AND ADDRESS Westinghouse Research and Development Center 1310 Beulah Road Pittsburgh, Pennsylvania 15235		10. PROGRAM ELEMENT NO. INE825 11. CONTRACT/GRANT NO. 68-02-2132
12. SPONSORING AGENCY NAME AND ADDRESS EPA, Office of Research and Development Industrial Environmental Research Laboratory Research Triangle Park, NC 27711		13. TYPE OF REPORT AND PERIOD COVERED Final; 12/75 - 12/78 14. SPONSORING AGENCY CODE EPA/600/13

15. SUPPLEMENTARY NOTES IERL-RTP project officer is D. Bruce Henschel, Mail Drop 61, 919/541-2825. EPA-600/7-78-050 also relates to this work.

16. ABSTRACT The report gives results of an investigation of particulate, NOx, and trace element control for atmospheric and pressurized fluidized-bed combustion (FBC) systems used with coal. A model, developed previously to project the loading and size distribution of particulate emissions from FBC systems, was used to permit an integrated analysis of particle control options for FBC. An experimental 150 scf/sec high-temperature/-pressure particulate control test facility, treating simulated flue gas, was constructed and shaken down to permit investigation of alternative particulate control devices. Available data on NOx emissions from FBC, and on NOx formation and decomposition, are reviewed to identify significant FBC operating parameters affecting NOx emissions, and to assess formation/decomposition mechanisms that may be controlling in FBC. The previous thermodynamic projections of trace element emissions from FBC were expanded to include aluminum, iron, titanium, cobalt, chromium, manganese, molybdenum, and nickel. These projections provide a first-level approximation of the distribution of volatile and condensed phases of compounds of these metals in FBC effluent streams.

17. KEY WORDS AND DOCUMENT ANALYSIS

a. DESCRIPTORS		b. IDENTIFIERS/OPEN ENDED TERMS	c. COSATI Field/Group
Pollution	Metals	Pollution Control	13B
Combustion		Stationary Sources	21B
Fluidized Bed Processing		Particulate	13H, 07A
Coal		Trace Metals	21D
Dust			11G
Nitrogen Oxides			07B

18. DISTRIBUTION STATEMENT Release to Public	19. SECURITY CLASS *(This Report)* Unclassified	21. NO. OF PAGES
	20. SECURITY CLASS *(This page)* Unclassified	22. PRICE

EPA Form 2220-1 (9-73)

EPA-600/7-80-015b
January 1980

Experimental/Engineering Support for EPA's FBC Program:
Final Report - Volume II. Particulate, Nitrogen Oxide, and Trace Element Control

by

D.F. Ciliberti, M.M. Ahmed, N.H. Ulerich,
M.A. Alvin, and D.L. Keairns

Westinghouse Research and Development Center
1310 Beulah Road
Pittsburgh, Pennsylvania 15235

Contract No. 68-02-2132
Program Element No. INE825

EPA Project Officer: D. Bruce Henschel

Industrial Environmental Research Laboratory
Office of Environmental Engineering and Technology
Research Triangle Park, NC 27711

Prepared for

U.S. ENVIRONMENTAL PROTECTION AGENCY
Office of Research and Development
Washington, DC 20460

PREFACE

The Westinghouse R&D Center is carrying out a program to provide experimental and engineering support for the development of fluidized-bed combustion systems under contract to the Industrial Environmental Research Laboratory (IERL), U. S. Environmental Protection Agency (EPA), at Research Triangle Park, NC. The contract scope includes atmospheric (AFBC) and pressurized (PFBC) fluidized-bed combustion processes as they may be applied for steam generation, electric power generation, or process heat. Specific tasks include work on calcium-based sulfur removal systems (e.g., sorption kinetics, regeneration, attrition, modeling), alternative sulfur sorbents, nitrogen oxide (NO_x) emissions, particulate emissions and control, trace element emissions and control, spent sorbent and ash disposal, and systems evaluation (e.g., impact of new source performance standards (NSPS) on FBC system design and cost).

This report contains the results of work defined and completed under the particulate, NO_x, and trace element control tasks of the contract. Work on these tasks was performed from January 1976 to January 1979 and is documented in the following EPA contract reports:

- The present report, which presents perspective on particulate profiles and control requirements for FBC systems, construction of a high-pressure and -temperature particulate control test facility, perspective on available NO_x emission data and mechanisms of NO_x generation and reduction, projections of trace element fate in FBC systems, and evaluation of available trace element emission data
- Report on the "Effect of SO_2 Emission Requirements on Fluidized-Bed Combustion Systems: Preliminary Technical/Economic Assessment," issued in August 1978 (EPA-600/7-78-163, NTIS PB 286 871/7ST).[1]

- Report on "Evaluation of Trace Element Release from Fluidized-Bed Combustion Systems," issued in March 1978 (EPA-600/7-78-050, NTIS PB 281 321).[2]

The final report also includes:

Volume 1: "Sulfur Oxide Control," EPA-600/7-80-15a
Volume 3: "Solid Residue Study," EPA-600/7-80-15c
Volume 4: "Engineering Studies," EPA-600/7-80-15d.

ABSTRACT

Particulate, nitrogen oxide, and trace element control are investigated for atmospheric and pressurized fluidized-bed combustor AFBC and PFBC systems. A detailed particle profile model was developed to permit integrated analysis of particle size distributions, particle carry-over rates, and control efficiency in these systems. An experimental high-temperature/high-pressure particulate control test facility was constructed to permit investigation of alternative particulate control equipment performance. Shakedown has been completed and the facility is operational. Available data on NO_x formation-decomposition are reviewed to assess formation-decomposition mechanisms and to identify significant operating parameters. These considerations provide the basis for performing engineering assessments of NO_x control. Thermodynamic projections of trace and minor element profiles for AFBC and PFBC operating conditions are presented. These provide a first-level approximation for the distribution of volatile and condensed phases present and a basis for further work on potential toxicity and process constraints.

TABLE OF CONTENTS

		Page
1	INTRODUCTION	1
2	SUMMARY AND CONCLUSIONS	3
	Particulate Control	3
	Nitrogen Oxide Emissions	5
	Trace Elements	7
3	RECOMMENDATIONS	9
	Particulate Control	9
	Nitrogen Oxide Emissions	9
	Trace Elements	10
4	PARTICULATE CONTROL	12
	Effect of Particulate Emission Requirements on FBC Systems	12
	Design and Operating Considerations for PFBC Particulate Control Systems	14
	High-Temperature, High-Pressure Gas-Cleaning Particle Removal Equipment	39
	Test Facility	41
	Particulate Sampling	54
5	NITROGEN OXIDE EMISSIONS	60
	Literature Review	60
	Data Analysis	67
	Assessment	75
6	TRACE ELEMENT RELEASE	78
	Introduction	78
	Thermodynamic Projections	89
	Assessment	109
7	REFERENCES	114

Preceding page blank

TABLE OF CONTENTS (Continued)

Page

APPENDICES

A NITROGEN OXIDE EMISSIONS IN FLUID-BED COMBUSTION EXPERIMENTS 121

B LITERATURE SUMMARY OF NITROGEN OXIDE EMISSIONS IN FLUIDIZED-BED COMBUSTION 141

C EFFECTS OF PRESSURE, EXCESS AIR, AND GASEOUS SULFUR CONTENT ON VOLATILE TRACE AND MINOR SPECIES AT EQUILIBRIUM IN FBC PROCESSES 149

D EQUILIBRIUM CALCULATIONS FOR FBC OPERATION AT 100 PERCENT EXCESS AIR, 90 PERCENT SULFUR REMOVAL, AND 1013 kPa TOTAL PRESSURE 159

LIST OF FIGURES

Page

1. Schematic of Solids Flow Diagram 1

2. Fractional Efficiency of Cyclones 24

3. Grade Efficiency for Ambient Temperature and Pressure, Laboratory-Scale Granular-Bed Filter 25

4. Baghouse Performance at Sunbury Steam Electric Station 26

5. Particle Size Distributions 28

6. Elutriation Correlation of Yagi and Aochi 28

7. Loading from Recycle Cyclone (Ash + Sorbent) 31

8. Combined Sorbent and Ash Size Distributions from Final Filter 31

9. Loading to Turbine as Function of Ca/S and Attrition for Fabric-Filter Performance 33

10. Loading to Turbine as Function of Ca/S and Attrition for Granular-Bed Performance 33

11. Incremental Cost of Electricity and Life of Turbine Blades and Vanes as a Function of Particulate Loading and Particle Erosivity 37

12. Schematic Diagram of Westinghouse Hot-Gas Cleanup Facility 42

13. Particulate Control Test System and Support Facility 42

14. Centrifugal Compressor 43

15. Three-Stage Cooper Bessemer Compressor 44

16. Test Passage Air Preheaters 45

17. Fuel Blend Tanks and Facilities 46

LIST OF FIGURES (CONT'D)

Page

18. High-Temperature and -Pressure Particulate Removal Test Facility (Side Inlet) 47

19. High-Temperature and -Pressure Particulate Removal Test Facility (Split Inlet) 47

20. High-Temperature and -Pressure Particulate Removal Test Facility (Top Inlet) 48

21. High-Temperature and -Pressure Test Facility Pressure Vessel 49

22. High-Temperature and -Pressure Test Facility Pressure Vessel with Aerodyne Installed 50

23. High-Temperature and -Pressure Test Facility Pressure Vessel Aerodyne Installation 51

24. High-Temperature and -Pressure Test Facility Control Room 52

25. High-Temperature and -Pressure Test Facility 53

26. Schematic of Sampling Train 56

27. Photograph of Particulate Sampling Train 57

28. Particulate Injection System 58

29. Effect of Fluidized-Bed Combustor Size 70

30. Effect of Coal Nitrogen Content - AFBC 70

31. Effect of Coal Nitrogen Content - PFBC 70

32. Effect of Temperature and Excess Air - PFBC 71

33. Effect of Temperature and Excess Air - AFBC 71

34. Plot of Residuals - Statistical Analysis 73

35. Regression Fit NO_x Projections 74

36. NO Decomposition Model - Pseudo-First-Order Rate Constants 76

LIST OF TABLES

Page

1. Illustrative Factors Determining Particles Leaving Fluidized-Bed Combustor 17

2. High -Temperature and -Pressure Test Facility 55

3. AFBC NO_x Emission Data 68

4. Fusion of Mineral Particles in a Coal Gas Flame - Typifying Commercial Ash Products 80

5. Average Trace Element Content of Regional Coals throughout the U. S. 81

6. Average Trace Element Content of Ash from U. S. Coals of Various Ranks 82

7. Trace Elements in Coal and Sorbent Materials 83

8. Trace Element Concentration as a Function of Particle Size as Reported by Lyon 86

9. Trace Element Concentration as a Function of Particle Size as Reported by Cowherd 87

10. Trace Element Concentration as a Function of Particle Size as Reported by Cato 88

11. Coal Composition 89

12. C-H-N-O-S-Cl Species Considered in Fluid-Bed Combustion Reaction 92

13. Trace and Minor Species Considered in Fluid-Bed Combustion Reactions 93

14. Partial Pressure of Gaseous Compounds and Moles of Condensed Compounds in PFBC Processes at Combustion Temperatures 105

15. Summary of Trace and Minor Element Reactions in Fluidized-Bed Combustion Systems 107

NOMENCLATURE

AFBC	Atmospheric Fluidized-Bed Combustion
ANL	Argonne National Laboratory
B&W	Babcock and Wilcox
EPA	U. S. Environmental Protection Agency
CTIU	Component Test and Integration Unit
Conoco	Consolidated Coal Company
FBC	Fluidized-Bed Combustion
ICP	Inductively Coupled Plasma Emission Spectroscopy
MIT	Massachusetts Institute of Technology
NAA	Neutron Activation Analysis
NCB	National Coal Board, London, UK
PER	Pope, Evans and Robbins
PFBC	Pressurized Fluidized-Bed Combustion
SSMS	Spark Source Mass Spectroscopy

PARTICULATE CONTROL

A	rate constant in expression for shrinkage of solid particles, sec^{-1}
A_2	mass flow rate of attrited solids,g/s
D	diameter of solids, microns
D_m	smallest solids diameter, microns
D_M	largest solids diameter, microns
F_o	mass flow of solids in feed, g/s
F_1	mass flow of solids in outflow, g/s
F_2	mass flow of solids in carry-over, g/s
H	height of unfluidized bed, cm
k	rate constant in expression for shrinkage of solid particles, sec^{-1}
K	elutriation constant, sec^{-1}
m	mass of an individual solid particle, g
P	pressure, atm
p_a	size distribution of attrited solids, cm^{-1}

P_b	size distribution of solids in bed, cm^{-1}
P_1	size distribution of solids in outflow, cm^{-1}
P_2	size distribution of solids in carry-over, cm^{-1}
$R=\frac{dD}{dt}$	rate of shrinkage of solid particles, cm/s
t	time, s
T	temperature, °C
U_o	superficial velocity of fluidizing medium, cm/s
W	total mass of solids in bed, g
z	cumulative size distribution function, cm^{-1}
z_c	cumulative size distribution of the combined (A_2+F_2) stream, cm^{-1}
Δ	difference
η	efficiency of solids removal device
ρ_s	density of solids, g/cm^3
ε	bed porosity
$\sum$	summation

NITROGEN OXIDE CONTROL

h	bed depth, m
k	specific reaction rate constant, $(hr)^{-1}$
p	pressure, kpa
T	temperature, °C
U	superficial gas velocity, m/s
X	percent excess air

TRACE ELEMENTS

G	Gibbs free energy
H°	standard state molar enthalpy
S°	standard state molar entropy
Cp°	standard state specific heat
M	molar chemical potential
M°	molar chemical potential at unit fugacity
n	moles
R	universal gas constant

ACKNOWLEDGMENT

We want to express our high regard for and acknowledge the contribution of D. B. Henschel who served as the EPA project officer. P. P. Turner and R. P. Hangebrauck, Industrial Environmental Research Laboratory, EPA, are acknowledged for their continuing contributions through discussions and support of the program.

We gratefully acknowledge the contributions of A. Y. Ranadive for his assistance in developing the particle profile model and computer program and in performing FBC evaluations; of personnel at the Westinghouse Advanced Coal Conversion Department, who, under the supervision of W. J. Havener, installed and operate the particulate control test facility; of E. A. DeZubay for his work on NO_x emissions; of C. A. Hill in developing an NO_x emission data base; and of R. W. Liebermann who developed the free-energy minimization programs that form the basis of the trace element analysis. The particle profile-turbine performance analysis is based on an extension of the evaluation presented in Volume IV of the report. J. R. Hamm and R. W. Wolfe are acknowledged for their coordination of the turbine analysis work. R. A. Wenglarz contributed to the review of and subsequent extensions to the turbine tolerance modeling.

1. INTRODUCTION

The design of fluidized-bed combustion (FBC) systems for electric power generation, industrial steam or process heat, or cogeneration applications depends on an understanding of particle history, particulate control, and nitrogen oxide (NO_x) emission and a perspective on the fate of trace elements in order to achieve energy cost and environmental objectives and requirements. Fluidized-bed combustion systems can offer energy, cost, and environmental advantages over alternative processes if the system design incorporates an understanding of the component/subsystem performance, limitations, and available trade-offs as a function of operating and design parameters. Particulate carry-over and control equipment performance, and NO_x generation and reduction mechanisms represent two subjects that must be understood when design and operating parameters that will achieve the process objectives and environmental requirements at the lowest energy cost are selected. An understanding of trace element history in FBC systems is important for process considerations in pressurized fluidized-bed combustion (PFBC) systems and for identifying any potential environmental concerns. The results reported in this document extend our previous understanding of these phenomena to provide a basis for FBC design and performance evaluation.

An understanding of the particle loadings and size distributions of particulate emissions and of the control of particulate emitted from FBC processes is important for successfully meeting both environmental and process constraints. The goal of the particulate work has been to develop methods that give consistent and reliable estimates of particulate emissions for FBC processes. These, in turn, can be used to project both the environmental and the economic consequences of FBC technology. Three areas of work are presented: the impact of emission requirements and fluidized-bed combustor design and operating conditions on FBC particulate control requirements and plant economics; the utilization of a particle profile model to develop an understanding of the critical fluidized-bed combustor and particulate control system design parameters in order to meet turbine performance and emission requirements for FBC systems; and the construction of a high-temperature high-pressure (HTHP) test facility to investigate particulate control equipment performance and provide experimental data on new and conventional devices.

An understanding of the mechanisms of NO_x generation and destruction in FBC is required in order to define the design and operating parameters necessary for minimizing NO_x emissions and achieving environmental standards. We have carried out work in two areas to develop such an understanding: the statistical treatment of data presently available that may present clues to the reaction mechanisms and the evolution of a model to permit selection of design and operating criteria and to project plant performance.

In assessing the environmental impact of FBC processes one must determine the chemical fate of trace and minor elements to assess their potential toxicity and their potential for corrosion or deposition in process equipment. In previous work reported under this contract, Westinghouse applied a thermodynamic model to project the chemical fate (and emissions) of four trace elements in coal-fired FBC systems: lead (Pb), beryllium (Be), mercury (Hg), and fluorine (F). This work has been extended to project the chemical fate in the FBC system of eight additional metals by using the same thermodynamic model: aluminum (Al), iron (Fe), titanium (Ti), cobalt (Co), chromium (Cr), manganese (Mn), molybdenum (Mo), and nickel (Ni). An evaluation of available trace element emission data from conventional boilers and FBC systems is presented.

2. SUMMARY AND CONCLUSIONS

Westinghouse has completed work that provides perspective on particulate control, NO_x emissions, and the fate of trace elements in fluidized-bed combustion systems.

PARTICULATE CONTROL

- A particle profile model for fluidized-bed combustion systems has been developed.
- The effect of the degree of gas cleaning on the cost of electricity and turbine blade life for a FBC system was developed by combining the particle profile model with an existing turbine erosion model.
- The description and status of a high-temperature and -pressure (HTHP) particulate control test facility is discussed.

Particle Profile Model

Westinghouse has developed a particle profile model that is a powerful tool for the parametric assessment of the effects on particle emissions of such operating and design parameters as:

- Superficial velocity
- Attrition characteristics
- Bed depth
- Recycle cyclone design
- Calcium-to-sulfur (Ca/S) ratios
- Sorbent feed size distributions
- Elutriation characteristics.

The model in its current state yields qualitative results. Its greatest potential lies in its ability to give quick, consistent results that indicate major effects and trends.

PFBC Particle Profile-Turbine Performance Analysis

The application of the model to a specific set of design and operating conditions (described herein) using alternative particle cleanup performance is used to illustrate the determination of turbine blade life and electricity costs and to provide perspective on the important design and operating parameters.

Some conclusions from the analysis are:

- Analytical tools are available to permit analyses that can give perspective on trade-offs between FBC, gas cleaning, and turbine design and operating parameters.
- Particle size distribution and materials erosion characteristics are two important factors that determine turbine life. Projections using particle size distributions from filters with 5 to 20 percent >5 μm particles and nickel-based turbine alloy erosion characteristics indicate loadings as low as 0.0046 g/m^3 (0.002 gr/scf or 3.7 ppm) could be required to achieve acceptable performance. Reducing the >5 μm particle loading and erosion-resistant coatings would increase this tolerance.
- Turbine tolerance requirements to achieve acceptable life will control the selection of particle control equipment for the specific case analyzed. Particulate control performance to reduce the >5 μm particles and improved material erosion characteristics could result in tolerance requirements approaching 0.039 g/m^3 (0.017 gr/scf or 30 ppm) which is the equivalent environmental limit for a 20 percent excess air PFBC design. Standards for fine

particulates could also result in environmental requirements controlling the selection of particulate control equipment.

- The filter design is of primary importance since the filter performance determines the particle size distribution and loading presented to the turbine and emitted to the environment.
- The selection of feed materials and the fluidized-bed combustor design will affect particle loading to the turbine and the environment for a given filter performance. A tenfold increase in attrition rate may increase mass loading to the turbine and environment by a factor of 2.
- Ash particle size distribution, sorbent attrition rates, and attrited sorbent size distributions are critical parameters since they determine the bulk of material presented to the final filter.
- The design of the fluidized-bed combustor so as to minimize the sorbent requirements and particle attrition is important for minimizing particles in the turbine and the environment.

Particulate Control Test Facility

A new HTHP particulate control test facility, along with such subsystems as the dust injection and hot, pressurized sampling systems, has been constructed. The system described is one in which pilot-scale experimentation can be undertaken at actual PFBC conditions without the cost and complications of pilot plant runs. This flexible test facility will play an important and unique role in the development of hot gas-cleaning technology.

NITRIC OXIDE EMISSIONS

The objectives of this task have been to develop an understanding of the nitrogen oxide (NO_x) generation and destruction mechanisms in fluidized-bed combustion (FBC) systems. Information available in the literature has been briefly reviewed to gain an insight into the relationship between NO_x formation and destruction reactions and the fluidized-bed combustor design and operating parameters. We have gathered the NO_x emission data from PFBC and/or AFBC systems of Argonne National Laboratory (ANL), Babcock and Wilcox (B&W), Combustion Power Company, Consolidated Coal Company (Conoco), Exxon, National Coal Board (NCB) and Pope, Evans and Robbins (PER); and from these, we have attempted to develop a model for the selection of FBC design and operating criteria and to project plant performance. Among the various sources there exist significant differences in FBC design and operating conditions, coal and sorbents used, and NO_x detection methods. Hence, the conclusions drawn in this study should be used with caution.

The important observations reported in the literature are:

- In fluidized-bed combustion fuel-bound nitrogen is the primary source of NO_x emissions. The conversion of fuel-bound nitrogen is less than 100 percent, suggesting the decomposition of once-formed NO.
- Thermal fixation of molecular nitrogen is less favored under fluidized-bed combustion conditions.
- The conversion of fuel-bound nitrogen to NO seems to depend strongly on excess air level. Rapid production of NO immediately above the distributor plate with substantial reduction in NO concentration in the splash region and in the freeboard have been observed.
- NO_x emissions seem to exhibit a temperature maximum between 750 to 800°C, suggesting that NO formation-decomposition mechanisms and/or rate-determining steps change with temperature.
- NO_x emissions from PFBC operations seem to be less than those from AFBC systems.
- Nitrogen-containing coal volatiles (NH_3, amines, etc.), CO, H_2, and char have been observed to reduce NO to N_2.

- Staged combustion has the potential to further limit NO_x emissions.
- Precise kinetic information for NO formation and reduction reactions in fluidized-bed combustion are lacking.

Some of the characteristic features of the data gathered from AFBC and AFBC development units follow:

- NO_x emissions from the relatively smaller units of ANL and Exxon seem to be considerably greater than those from the bigger units of PER, B&W, and NCB. This difference could be due to the differences in the mixing pattern, local stoichiometry, and mass transfer effects in the various units.
- Data gathered from fluidized-bed combustion development units indicate a similarity in temperature maximum, reduced emissions at higher pressures, and increased emissions with increased excess air with those previously observed in the controlled laboratory-scale experiments.
- Data from relatively larger FBC development units suggest that excess air levels of 15 to 20 percent in the proposed commercial designs could result in NO_x emissions of 129 to 301 ng NO_2/J (0.3-0.7 lb $NO_2/10^6$ Btu).
- Regression analysis of the data from various FBC development units resulted in a poor fit, possibly because scatter and variations in the raw data from different sources and/or the functional dependencies (first-order and second-order terms) on pressure, temperature, excess air level, and gas residence time chosen may not be representative of the NO_x formation-decomposition reactions.
- Currently, there is no generalized model available for _a priori_ prediction of NO_x emissions level in FBC.

TRACE ELEMENTS

Theoretical projections at equilibrium were carried out to project the quantity and the chemical form of the trace and minor elements from coal and sorbent feed materials formed in both AFBC and PFBC systems.

Westinghouse has applied a thermodynamic model to project the chemical fate of lead (Pb), beryllium (Be), mercury (Hg), and fluorine (F) in coal-fired FBC systems. The previous thermodynamic analysis indicated that essentially all the lead, beryllium, mercury, and fluorine can be volatilized in the high-temperature zone in the fluidized-bed combustor but did not attempt to demonstrate the reaction of the trace species with either the clay or the carbonate constituents in the feedstock material. The areas selected for this study include:

- Further evaluation of available trace element emission data from conventional boilers and FBC systems.
- Application of the thermodynamic model to project the chemical fate in the FBC system of eight additional elements: aluminum (Al), iron (Fe), titanium (Ti), cobalt (Co), chromium (Cr), manganese (Mn), molybdenum (Mo), and nickel (Ni).

We conclude from the thermodynamic equilibrium model that the trace and minor elements for AFBC and PFBC systems may be categorized as those that yield:

- Potentially complete volatilization at 927°C: Mo (100%), Pb (100%), Be (100%), Hg (100%), and F (100%)
- Partial volatilization at 927°C: Co (14%), Cr (79%), Mn (∿2%), and Ni (∿5%)
- Almost no volatilization at 927°C: Al (0.02%), Ti (0%), and Fe (0%).

3. RECOMMENDATIONS

PARTICULATE CONTROL

Particulate profile modeling should be extended to:

- Improve the modeling of sorbent attrition, including breakage functions
- Obtain more experimental data to support attrition models
- Develop a better understanding of such ash characteristics as size distribution
- Develop reliable particulate control equipment operating at the PFBC system temperature and pressure to achieve the required particulate loading and size distributions for economic turbine life. We recommend that alternative concepts be tested in the dedicated HTHP test facility to efficiently and economically screen candidate systems prior to plant operation.
- Gain understanding of turbine performance through turbine tolerance modeling which would include experimental determination of actual blade erosion damage as a function of operating conditions in order to define particulate control requirements.

NITROGEN OXIDE EMISSIONS

The following recommendations are made for further work on NO_x emissions:

- Mechanistic and kinetic information for NO_x reduction reactions should be developed.

- Comprehensive reporting of FBC development-unit data, such as on reducing agents (NH_3, H_2, CO, char) concentrations in the bed, is required for assessing the NO_x formation-reduction mechanisms proposed on the basis of controlled laboratory experiments.
- NO_x emission control options proposed should be assembled on the basis of mechanisms that are identified and are at least partially confirmed through the observation of data trends.
- Continue the modeling work to provide a basis for projecting NO_x emissions in FBC systems, and for the technical/economic assessment of NO_x control options necessary for meeting EPA requirements.

TRACE ELEMENTS

Although the equilibrium model predicted the volatilization of lead as lead tetrachloride ($PbCl_4$), measurements to determine the fate of lead in a cyclone-fed power plant indicated that 10 percent of the lead was lost as an atmospheric discharge. The kinetics of conversion of feedstock lead compounds to $PbCl_4$ may be so intrinsically slow that equilibrium within the combustor was not attained. Alternatively, there may be more stable lead complexes, as silicates or borates, which may be formed in the combustor. Similarly, we projected molybdenum at equilibrium to volatilize completely at high combustion temperatures, but its readsorption onto entrained fly ash particles may account for the reduced emission percentages cited in the literature. The remaining elements are partitioned in the solid fractions removed in the waste and spent sorbent process, thus reducing the elemental concentration in the stack gases. Relative agreement exists between the thermodynamic projections and the data obtained at the various coal-fired steam plants.

We recommend continued investigation of additional trace and minor element reactions, with emphasis on the potential chemical interactions in the fluidized-bed combustor. Such an investigation would include:

- An expansion of the thermodynamic equilibrium model to include an additional set of 25 trace and minor elements, with parametric studies conducted to demonstrate the interactions of the elements with the clay and carbonate feedstock constituents for anticipated operating ranges of various fluidized-bed combustor designs.
- A correlation of the equilibrium projections with in-field data that would identify the elemental partitioning between stack gas emissions and ash formations
- Modeling throughout the various AFBC and PFBC systems once the chemical reactions and interactions of the trace and minor elements are defined. Assessment of the potential toxicity of the projected gaseous emissions should be made, and control criteria for minimizing any potentially toxic trace or minor element concentration in the stack emissions should be advanced.

4. PARTICULATE CONTROL

The understanding and control of particulates emitted from FBC processes is important for successfully meeting both environmental and process constraints. To better understand the loadings and size distributions of emitted particulate, we must develop the basis for projecting carry-over from the fluidized bed and the performance of various particulate control systems. The goal of this work has been to achieve methods that give consistent and reliable estimates of particulate emissions for FBC processes. These, in turn, can be used to make projections of both the environmental and the economic consequences of this technology.

Work performed under this contract includes:

- Determining the impact of emission requirements and fluidized-bed combustor design and operating conditions on FBC particulate control requirements and plant economics
- Developing an understanding of the critical fluidized-bed combustor and particulate control system design parameters to meet turbine performance and emission requirements for pressurized FBC systems
- Constructing a high-temperature high-pressure (HTHP) test facility to investigate particulate control equipment performance and to provide experimental data on new and conventional devices.

EFFECT OF PARTICULATE EMISSION REQUIREMENTS ON FBC SYSTEMS

We evaluated the implications of more stringent degrees of particulate control on FBC plant design and cost. The previous particulate new source performance standard (NSPS) of 43.0 ng/J (0.1 lb/MBtu) for large coal-fired boilers and the newly-promulgated standard of 12.9 ng/J (0.03 lb/MBtu) for utility boilers were considered.

Particulate control in AFBC and in PFBC are quite different in nature. Conventional technology exists for AFBC - hot electrostatic precipitators (ESP) (~400°C) or fabric filter techniques (baghouses) - that should, by suitable design, be capable of controlling particulate emissions to the 12.9 ng/J (0.03 lb/MBtu) level. Testing these control options on operating fluidized-bed combustors, however, is necessary before actual control performance and any operating problems can be firmly defined. AFBC plants now under construction and initial operation will provide a basis for such an evaluation.

The protection of the gas turbine from erosion and deposition damage for PFBC may require that particulate emissions be controlled to levels lower than 12.9 ng/J (0.03 lb/MBtu), depending on size distribution and composition. Granular bed filters, ceramic filters, and high-temperature precipitators have been proposed for hot-gas cleaning but have not yet been demonstrated.

Evaluation of the effects of the more stringent NSPS particulate standards (12.9 to 107.5 ng/J) for both AFBC and PFBC systems is presented in a separate topical report.[1] The total loading and particle size distribution of particulates attrited and elutriated from a fluidized-bed combustor are projected there using a Westinghouse model; these projections are compared with the expected performance of particle control equipment that might reasonably be employed. The projections suggest that over the range of Ca/S ratios considered (up to 10), within the variability of sorbent attrition performance expected and based on the current data available, particulate emission levels of 12.9 ng/J (0.03 lb/MBtu) should be economically achievable for AFBC and PFBC.

The major uncertainties with AFBC involve details of the equipment specifications (filter materials, face velocities, etc.) and operating and maintenance procedures (e.g., prevention of bag fires). Factors such as resistivity of FBC ash and sorbent fines, and adhesion and flow resistance properties of filter cake, are not yet well understood and can significantly influence equipment design.

The level of particulate emissions standards may have little effect on the development of PFBC since turbine life requirements may impose more stringent requirements on expansion gas quality. Even encouraging results with conventional cyclones that have resulted in particle size distributions with only about 10 percent >5 to 6 μm particles do not meet the standard.[3] Fine material can arrive on the blades by turbulent and molecular diffusion and can result in deposition and result in passage choking problems. This may also require further cleaning, which may be achieved on line.

Should it prove necessary we can develop more rugged turbines that could accept higher particle loadings. This tactic, of course, will trade off efficiency against capital costs and cleanup system costs.

As with sulfur removal, the combustor design and operating conditions greatly effect the control of particulate emissions. With little cost penalty we can design and operate the combustor (e.g., at low velocities) to limit particle attrition and elutriation, though very efficient final-stage particulate control devices will still probably be required for AFBC and PFBC systems. The coal sulfur content and the Ca/S ratio have a far greater effect on the particulate control requirements for FBC than do either coal ash control or coal heating value (i.e., sorbent feed rate has the primary effect on particulate emissions).

DESIGN AND OPERATING CONSIDERATIONS FOR PFBC PARTICULATE CONTROL SYSTEMS

The commercial operation of coal-fired PFBC processes utilizing gas turbine expanders depends on reliable operation of the gas turbine. Reliable operation of the turbine, in turn, is related to the particulate and chemical composition of the gases that it expands. Erosion due to micron-sized particles, deposition of submicron particles, and the formation of corrosive deposits from alkali metal sulfates are of concern. The scope of this assessment, however, is limited to the control of particulates and their effect on the erosion of turbine components. The effects of alkali-induced corrosion and fine particle deposits were not within the scope of this effort.

An understanding of the character of the particulates and the development of appropriate methods for removing the particulates that result from FBC processes is important in meeting environmental and process constraints. Several aspects of the problem must be understood in order to develop and specify both particulate control requirements and equipment. These include an understanding of: particulate properties, loadings, and size distributions from the fluidized-bed combustor; their impact on gas turbine performance and life; and the environmental emission standards for concentration and size.

Perspective on the particulate control system requirements and control options have been previously presented.[4] The present study extends this earlier work to develop an understanding of the critical FBC and particulate control system design parameters that effect the particulates reaching the gas turbine and an understanding of the impact of these parameters on turbine life and plant cost.

This study is based on the removal of particulates at the combustor outlet temperature. Since the cost of particulate removal equipment is a strong function of the operating temperature, the removal of particulates at a reduced temperature was investigated and presented in a previous report.[5] Two alternatives were investigated in the earlier study: cooling the combustion gases by a convection-type boiler and removing particulates at intermediate temperature, and cooling the combustion gases with a recuperator, followed by a scrubber-cooler with subsequent reheating of the gas. Results from the study show the low-temperature cleanup option may be competitive with a conventional plant with flue gas desulfurization (FGD) but does not provide an economic or efficiency margin for development. The present work is focused on high-temperature particulate control.

Particle Profile Projections

Projections of the nature of the particles entering the turbine expander must be developed in order to estimate the effect of particulate erosion on turbine life. To make these projections we have developed a particle profile model that incorporates the fluidized-bed combustor and the particulate control subsystems. The computer model permits rational, consistent estimates of particle loadings and size distributions throughout FBC systems. The model is used to perform parametric studies on the effect of different FBC design and operating conditions on particulate emissions. The effect of the selection of FBC design and operating conditions on particulate carry-over is discussed along with a discussion of the model. Then the particulate control system selected for this study is considered. The particulate that would enter the turbine is then characterized for the parameters selected. The objective is to provide perspective on important operating and design choices.

Model for Fluidized-Bed Combustor Particulate Carry-over and Control

The FBC design and operating parameters, along with the coal and sulfur sorbent characteristics, will determine the concentration, size, physical character, and chemical composition of the particulate leaving the combustor. A representative list of important factors is presented in Table 1.

A particle profile model has been developed to project particle loadings and size distributions in the carry-over from fluidized-bed combustors and throughout any subsequent series of specified cleanup devices. Westinghouse developed the early form of this model for ANL in

Table 1

ILLUSTRATIVE FACTORS DETERMINING PARTICLES LEAVING FLUIDIZED-BED COMBUSTOR

Feed Materials
- Coal and sorbent (limestone or dolomite)
- Chemical and physical properties, size reduction equipment

Design Parameters
- Temperature control system design,
  - heat transfer surface, excess air
- Carbon control system design,
  - recycle, carbon burnup cell, in-bed temperature/bed depth/excess air
- Feed system design,
  - coal and sorbent feed introduction and location
- Air distributor design
- Combustor configuration,
  - bed configuration, freeboard design

Operating Parameters
- Temperature
- Pressure
- Gas velocity
- Bed depth

Environmental Regulations
- Sulfur removal,
  - sorbent requirements
- Nitrogen oxides

support of their Component Integration and Test Unit (CTIU) program. The model is capable of analyzing FBC configurations that employ a recycle cyclone for carbon utilizations as well as those that use a carbon burnup cell (CBC).

In the following, we present a brief review of the derivation of the carry-over model. Details of the derivation and extensions of the model are presented in Reference 6. A procedure for saving the resulting performance equation is presented and a particulate control performance model is incorporated.

The model employed to describe particle carry-over from the bed (Figure 1) is based on a mass balance of particles in a certain size range. The method used to estimate the rate at which particles are carried out of the bed requires that a correlation for the elutriation rate constant be available. This elutriation rate constant is defined by

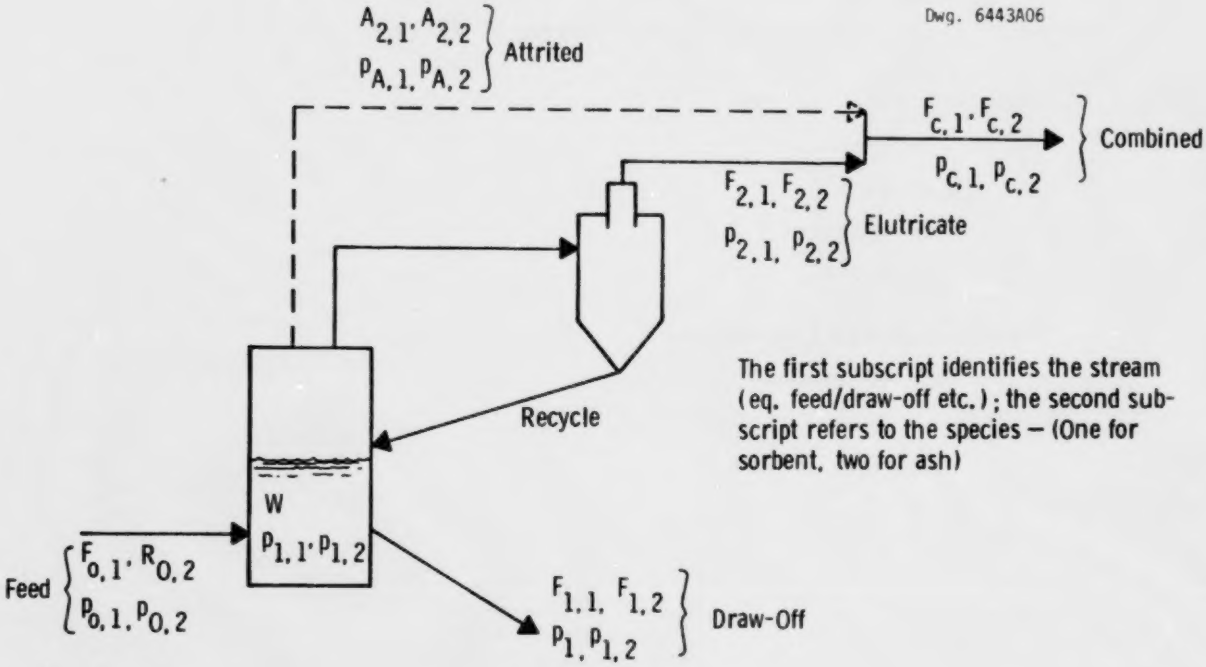
Dwg. 6443A06
$A_{2,1}, A_{2,2}$
$p_{A,1}, p_{A,2}$
Attrited
$F_{c,1}, F_{c,2}$
$p_{c,1}, p_{c,2}$
Combined
$F_{2,1}, F_{2,2}$
$p_{2,1}, p_{2,2}$
Elutricate
Recycle
The first subscript identifies the stream (eq. feed/draw-off etc.); the second subscript refers to the species – (One for sorbent, two for ash)
W
$p_{1,1}, p_{1,2}$
Feed
$F_{0,1}, R_{0,2}$
$p_{0,1}, p_{0,2}$
$F_{1,1}, F_{1,2}$
$p_{1}, p_{1,2}$
Draw-Off

Figure 1 - Schematic of Solids Flow System

asserting that the mass of particles of size D in the overhead is proportional to the mass of particles of size D in the bed, or that

$$K(D) = \frac{F_2 p_2(D)}{W p_b(D)} \quad . \qquad (1)$$

Many such correlations are available in the literature,[5,6] but none appears to be applicable to all systems.

The model treats attrition as if the surface of the large particles is gradually abraded away so that the large particle slowly shrinks in size according to some rate expression of the general form:

$$\frac{dD}{dt} = R(D) \qquad (2)$$

The fines ground from the large particle are considered to pass out of the system as if in the gas phase. The mass of these particles can be calculated, but their size distribution must be assumed, and they are not included in the recycle stream.

The general performance equation arises from a mass balance on particles of size between D and D + ΔD. In unit time,

$$\begin{pmatrix}\text{Solids entering}\\ \text{in feed}\end{pmatrix} - \begin{pmatrix}\text{Solids leaving}\\ \text{in overflow}\end{pmatrix} - \begin{pmatrix}\text{Solids leaving}\\ \text{in carry-over}\end{pmatrix} +$$

$$\begin{pmatrix}\text{Solids growing}\\ \text{into interval}\\ \text{from larger size}\end{pmatrix} - \begin{pmatrix}\text{Solids growing}\\ \text{out of interval}\\ \text{to smaller size}\end{pmatrix} + \begin{pmatrix}\text{Loss of mass}\\ \text{due to shrinking}\\ \text{within interval}\end{pmatrix} = 0 \qquad (3)$$

or

$$\int_D^{D + \Delta D} F_o p_o dD - \int_D^{D + \Delta D} F_1 p_1 dD - \int_D^{D + \Delta D} F_2 p_2 dD + \left(W p_b R\right)_{D + \Delta D}$$

$$- W p_b R_D + \int_D^{D + \Delta D} \frac{3 W p_b R dD}{D} = 0 \qquad (4)$$

Dividing by ΔD and taking limits as $\Delta D \rightarrow 0$, using equation (1) and with the assumption of backmix flow, i.e., $p_1 = p_b$, we obtain the following differential equation:

$$F_o p_o - F_1 p_1 - WK p_1 + W \frac{d(p_1 R)}{dD} + \frac{3\, W p_1 R}{D} = 0 \quad . \tag{5}$$

Further manipulation of this basic balance leads in the general performance equation of the model which is given as

$$\frac{W}{F_o} = \int_{D_m}^{D_M} \frac{\hat{D}^3 I(\hat{D}, D_M)}{R(\hat{D})} \int_{\hat{D}=\hat{D}}^{\hat{D}=D_M} \frac{p_o(D)\, d\hat{D}}{D^3 I(D, D_M)} \, d\hat{D} \tag{6}$$

where the $I(D,D_M)$ term is defined as

$$I(D,D_M) = \exp\left[-\int_{D_M}^{D} \frac{\frac{F_1}{W} + K}{R} \, dD \right] \quad . \tag{7}$$

The final form of the performance equation is that of the triple integral expressed in equation (6). To include the effect of a cyclone recycling coarse material to the bed, one need only modify the elutriation rate constant K by multiplying it by the cyclone penetration (1-efficiency) so that the K term of equation (7) is replaced by $(K(1-\eta)$.

Use of this equation generally requires an iterative procedure, since usually F_o and W are specified but F_1 is not. The solution algorithm proceeds as follows:

1. For given F_o and W, pick F_1.
2. Calculate the triple integral of equation (6).
3. Compare the result with W/F_o; if not sufficiently close, update F_1 value and iterate.

4. Once convergence to F_1 is achieved p_1 can be calculated from the expression:

$$p_1(D) = \frac{F_o D^3 I(D,D_M)}{W|R|} \int_{D}^{D_M} \frac{p_o(\hat{D})d\hat{D}}{\hat{D}^3 I(\hat{D},D_M)} \quad . \tag{8}$$

5. Knowing p_1 one can calculate F_2 as follows:

$$\int_{D_m}^{D_M} F_2 p_2 dD = F_2 = \int_{D_m}^{D_M} W\, K(1-\eta)p_1 dD \quad . \tag{9}$$

6. The size distribution of F_2 can be obtained directly from the elutriation rate expression

$$p_2 = (W/F_2)K(1-\eta)p_1 \quad . \tag{10}$$

7. The mass of the attrited material A_2 can be calculated by integration of the rate equation over the bed size distribution or, more simply, by overall mass balance

$$A_2 = F_o - F_1 - F_2 \quad . \tag{11}$$

The loading presented to the particulate removal train is obtained as the sum of A_2 and F_2. The size distribution of F_2 is known, but the size distribution of A_2 must be assumed (p_A). The cumulative size distribution of the combined stream is then obtained as

$$Z_c(D) = \int_{D_m}^{D} \frac{F_2 p_2 + A_2 p_A}{F_2 + A_2}\, dD \quad . \tag{12}$$

Loadings and cumulative size distributions from any subsequent particle removal device can be calculated if the efficiency of the device is known as a function of particle size. If $\eta_i(D)$ is the grade efficiency of the ith device and the size distribution of A_2 and F_2 combined is given by $p_c(D)$ (i.e., $p_c(D) = dz_c/dD\ (D)$, then the cumulative size distribution of the particles emerging from the the ith device is given by

$$Z_i(D) = \int_{D_m}^{D} p_c(D)(1-\eta_1)\ (1-\eta_2)\cdots\cdot(1-\eta_i)d\hat{D} \quad . \qquad (13)$$

To include the effects of a second component, ash, in the fluidized-bed segment of the model, we have assumed that the single component particle balances on each species hold and the only coupling in the two species extension occurs in the elutriation from the bed surface. We presume this effect manifests itself by reducing the elutriation rate of a species in proportion to the mass fraction of this species in the bed. For example, if the bed were 0.80 sorbent and 0.20 ash, the single species elutriation rate calculated for the sorbent would be reduced by multiplication by the factor of 0.8 sorbent and 0.20, since roughly these portions of the bed surface would be occupied by the other species. In order to implement the approximation one must use a trial-and-error procedure to determine the proper fractions of each species in the bed. The basic algorithm used is as follows:

- Assume a fraction of sorbent.
- Calculate the withdrawal rates (F_1) for both ash and sorbent independently with the exception that the elutriation rate of each species is reduced as indicated above.
- Use F_1 (ash) and F_1 (sorbent) to calculate the fraction of each species in the bed and compare them with the assumed values.
- Up-date the initial guess of the sorbent fraction and iterate until convergence is achieved.

Having completed these calculations, one can carry out the remaining computations independently, giving loadings and size distributions throughout the system as well as the steady-state fractions of sorbent and ash in the bed.

Particulate Removal System

On the basis of a previous assessment[7] Westinghouse has estimated that a particle loading of 0.0046 g/m^3 (0.002 gr/scf) with essentially all particles smaller than 6 μm would be necessary to protect the gas turbines from rapid choking and erosion. As discussed in Reference 2, a ceramic filter or a granular-bed filter would probably be necessary in order to meet this goal at elevated temperatures and pressures. We believe these loadings and size constraints are conservative, however, and the less stringent goals set by others in the field may prove to be acceptable. Further discussion of the erosion analysis is presented in Volume 4.

In accordance with the more stringent goals used in this study, the particulate control train selected for this work consists of the following: a relatively low-efficiency recycle cyclone, followed by a secondary high-efficiency cyclone, followed by a granular-bed filter.

The recycle cyclone collection characteristics are shown in Figure 2. This grade efficiency was based on preliminary specifications set by Stearns-Roger for the "roughing" recycle cyclone in their plant design for the ANL CTIU effort.[7] This cyclone was purposely specified as a low efficiency unit, to avoid the possibility of inordinately high recycle rates of ash, and to operate at a total pressure of 1013 to 1216 kPa (10 to 12 atm) and at temperatures between 900 and 1000°C. The total pressure drop across the cyclone was specified to be less than 13.8 kPa (2 psi).

The secondary cyclone grade efficiency curve also shown in Figure 2 is based on an estimate supplied by a commercial vendor for particles with a density of 2.5 g/cm^3. The expected operating parameters for this cyclone at 1013 kPa (10 atm) and 900°C are as follows:

- Inlet velocity 19.8 m/s
- 160 cm wg. pressure drop.

Curve 713715-A

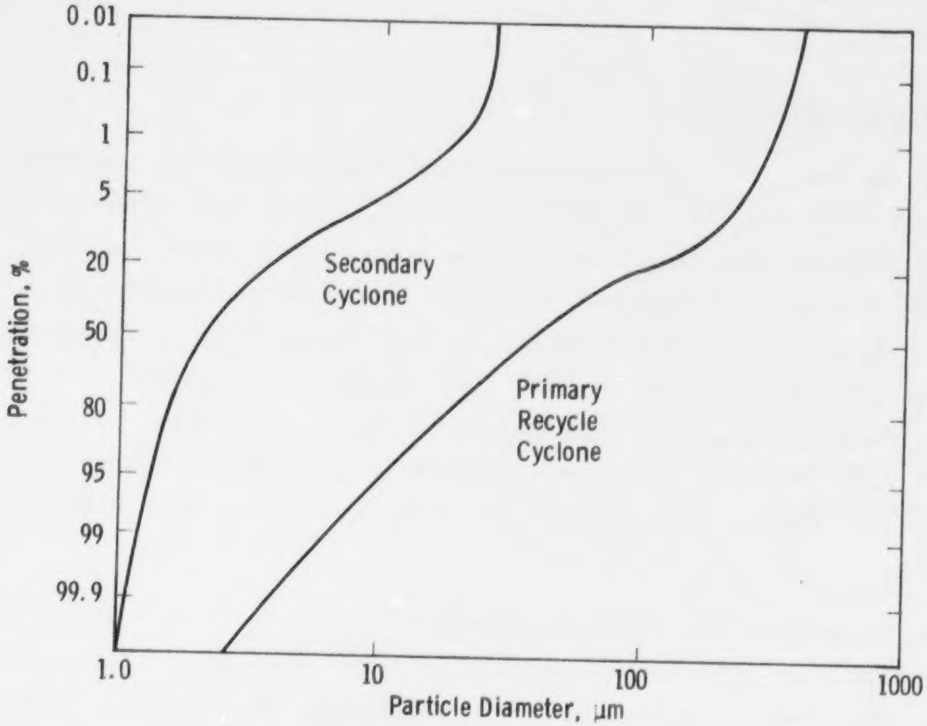

Figure 2 - Fractional Efficiency of Cyclones

As is indicated by the grade efficiency curve, the proposed secondary cyclone is a high-efficiency device and is intended to remove the bulk of solids from the hot gas stream.

To achieve the desired final degree of removal, we have assumed that a final stage of filtration will be required. Since actual commercial filtering devices capable of operation at elevated temperatures and pressures are not yet available, we made some assumptions about the desired particle collection abilities of the filter. Two cases were considered. For the first case the grade efficiency of the filter was based on Westinghouse experimental data obtained from operation of a small laboratory-scale granular-bed filter at ambient pressure and temperature. During these runs a superficial velocity of 18 cm/s was used through a 7.6 cm deep bed of Ottawa sand screened to be between 600 to 840 µm (20 to 30 mesh). The penetration vs. particle size curve determined by using cascade impactors is presented in Figure 3.

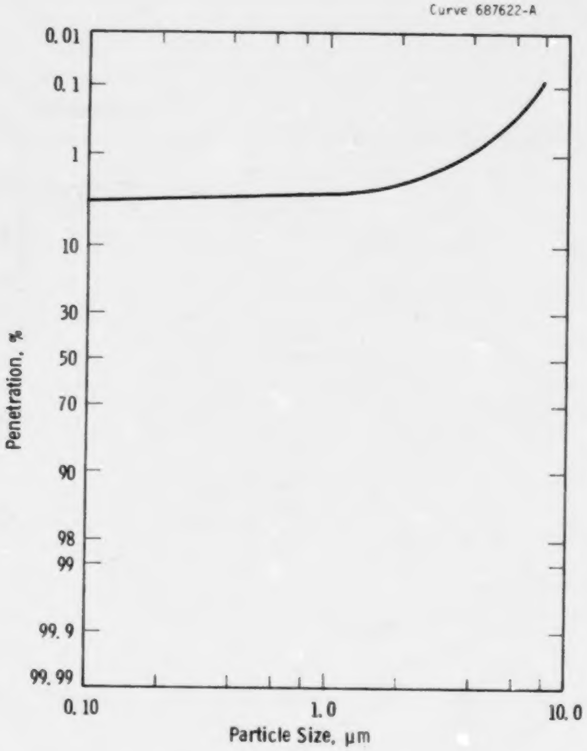

Figure 3 - Grade Efficiency for Ambient Temperature and Pressure, Laboratory-Scale Granular-Bed Filter

We obtained a second estimate of filter performance by assuming that the likely upper limit on HTHP cleaning devices might be estimated by using the grade efficiency of a conventional, low-temperature, fabric-filter system. Since actual data of large-scale baghouse operations were available they were used. The assumed performance is presented in Figure 4 along with the pertinent operating parameters.

Particle Profile Calculations

The model described above was employed to estimate particulate loadings and size distributions arriving at a gas turbine for chosen sets of PFBC conditions. Calcium-to-sulfur ratios were varied from 0 to 5 and two sorbent attrition rates (0.2 and 2 %/hr) were examined. The resultant loadings and size distributions escaping from the final filter were then used in an erosion model to estimate the blade life and

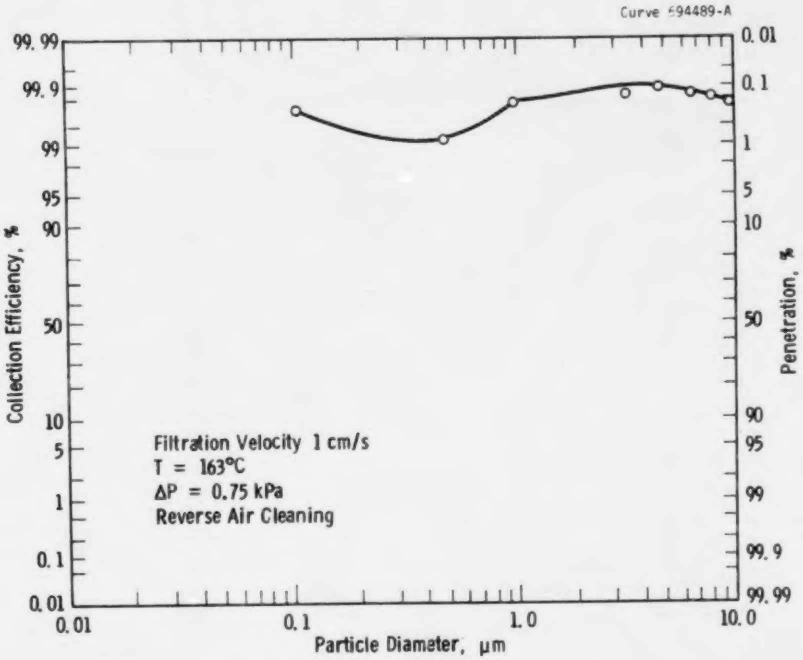

Figure 4 - Baghouse Performance at Sunbury Steam Electric Station

operating costs associated with different choices of operating parameters. This procedure allowed a consistent study of both the economic and environmental consequences of PFBC.

Base operating parameters chosen for this study were as follows:

Temperature	900°C
Pressure	1013 kPa (10 atm)
Superficial velocity	215 cm/s
Bed height	260 cm
Fines recycle	cyclone (Figure 2)
Coal	Illinois No. 6 (3% moist)
Excess air	20%

Ca/S	2:1; 5:1
Sorbent	• dolomite • minus 6350 μm • single screened • size distribution (Figure 5) • attrition 0.2 - 2%/hr • attrited size distribution (Figure 5)

The sorbent feed size distribution was based on actual measurements of a single-screened limestone. A standard sieve analysis was used for the larger sizes. Both Coulter Counter and cascade impactor techniques were used to establish the fines (44 to 0.5 μm) distributions.

The sorbent attrition used in this analysis is attributed to a continuous abrasion of the surface of particles. The fines abraded from the surface are assumed to leave the bed immediately and penetrate the recycle cylone. The mass of these fines can be calculated but, using the model as is, not their size distributions. An assumed size distribution must therefore be entered for these fines. Figure 5 presents the distribution assumed for this work. This distribution was based on preliminary experimental data obtained at Westinghouse with extrapolation to the smaller than 10 μm sizes. The larger particles that abrade from attrition and are elutriated from the bed are included in the model calculations, and both loadings and size distributions escaping from the recycle cyclone are calculated. Over the range of attrition rates studied, the size distribution of the particles elutriated (not attrited) did not change perceptably; it is presented in Figure 5.

Several models for elutriation have been offered in the literature[8,9]. For this work the correlation by Yagi and Aochi has been used and is presented in Figure 6. While this correlation cannot be used as a general prediction for particle carry-over, we have used it here for illustrative purposes.

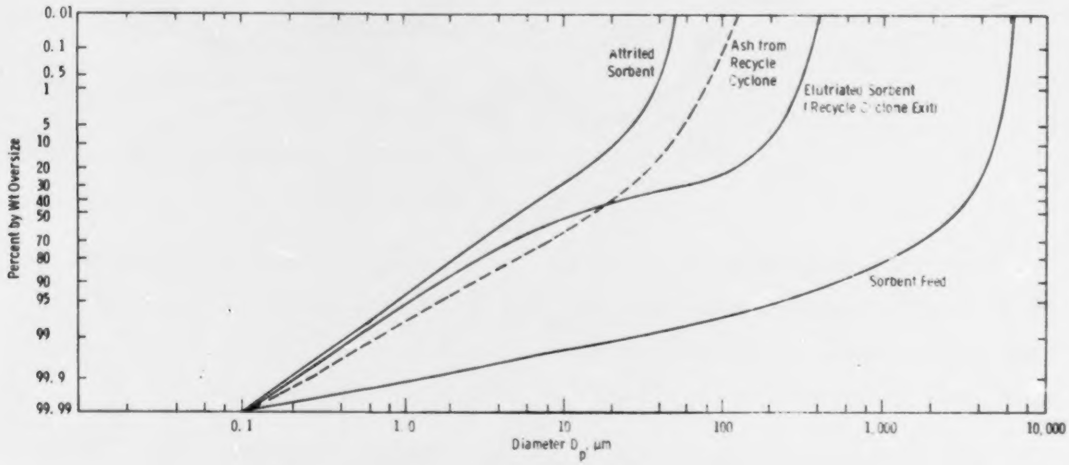

Figure 5 - Particle Size Distributions

Curve 69674[illegible]-A

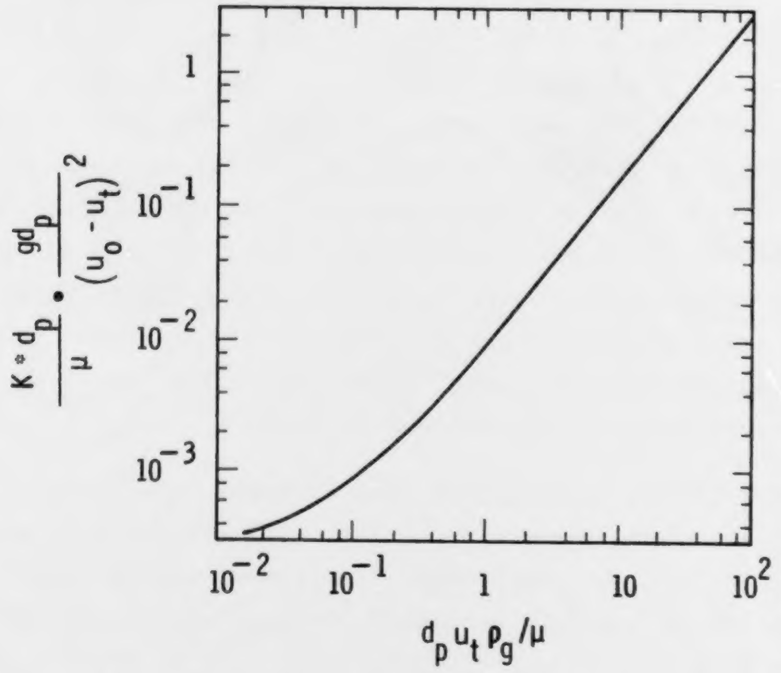

Figure 6 - Elutriation Correlation of Yagi and Aochi

Since estimation of attrition parameters for ash is obviously difficult, we employed the following strategy. We matched the mass of ash carry-over from the bed with NCB data[10] by adjusting the attrition rate constants and using the NCB emitted size distributions as the feed. This same size distribution was used to typify the attrited ash fractions. The result was thereby forced to give ash carry-over that was similar in mass flow and size distributions to experimental data. Subsequent calculations showed that the equilibrium bed fraction of ash was relatively constant at about 2.5 to 5 percent, which seems generally consistent with what we expected. The size distribuion of the ash calculated to be escaping from the recyle cyclone is presented in Figure 5.

The cleanup train consisted of the roughing recycle cyclone and the conventional high-efficiency cyclone, whose grade efficiency curves were presented in Figure 2. The final stage of cleaning was accomplished by using a granular-bed filter whose performance was assumed to be similar either to the laboratory data presented in Figure 3 or to the commercial-scale fabric filter data presented in Figure 4. Figure 5 can be used to present a summary of calculated size distributions of the materials leaving the recycle cyclone. Since the ash size distribution was essentially forced to agree with experimental data at this point, it did not change with variations in either Ca/S or sorbent attrition. Secondly, the sorbent size distribution tended to the "attrited" size distribution for the high (2%/hr) attrition rates and approached the "elutriated" size distribution for the low (0.2%/hr) attrition rates. The recycle cyclone exit loadings as a function of Ca/S ratio and attrition rates are presented in Figure 7. These loadings are generally in the range of 11-20 g/m^3 (5-10 gr/scf), which is in reasonable agreement with typical findings available from the Exxon miniplant and the Curtiss Wright test facilities.

These calculated loadings and the size distributions from the recycle cyclone are then sent through the remainder of the cleanup train model consisting of the secondary cyclone and final filter. This process has the effect of damping out differences in inlet distributions to a large degree and results in combined ash and sorbent size distributions emitted to the turbine that are very similar. This point is illustrated by Figure 8 where the combined size distributions for the following range of conditions are presented:

Δ - fabric filter, 2.0%/hr, 5/1 Ca/S
□ - fabric filter, 0.2%/hr, 2/1 Ca/S
o - Granular bed, 2.0%/hr, 5/1 Ca/S
x - Granular bed, 0.2%/hr, 2/1 Ca/S.

The calculations indicate that outlet size distributions from a given final filter are virtually independent of the Ca/S ratio and attrition rates. Additionally, the differences between outlet size distributions of the two different filters are relatively small, given the approximations and assumptions incorporated in the model. The calculated differences can be explained by comparison of the two grade efficiencies assumed (Figures 3 and 4). The baghouse performance curve is based on a full-scale utility installation and indicates a slight decline in efficiency around 8 to 10 μm, which explains why approximately 2% of the particles are larger than 10 μm for the fabric filter. The granular-bed filter performance data were taken on a small bench-scale rig where very high efficiencies for the >10 μm material were measured, thus explaining the absence of any material larger than 10 μm in the filter effluent.

Although there are very small differences in size distributions of the fabric filter and the granular-bed filter results, there is a large difference in overall efficiency or penetration. Figures 9 and 10 demonstrate this point by presenting a plot of total loading escaping the final filter as a function of Ca/S ratio for 2 and 0.2%/hr attrition rates. These figures indicate that there is almost an order of magnitude difference between the filters. For example, at Ca/S = 5 and a

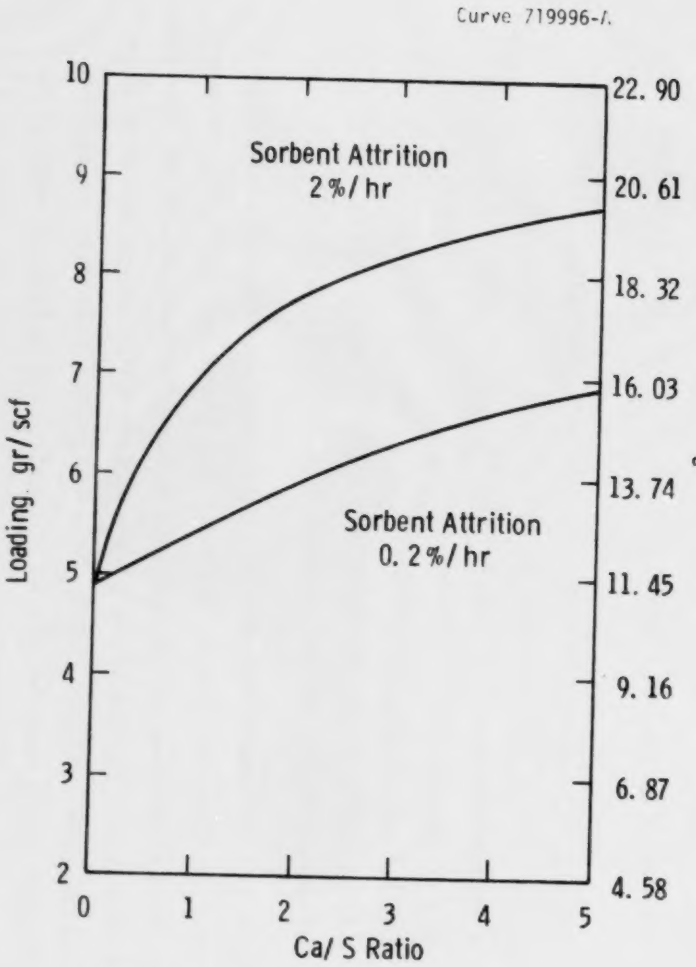

Figure 7 - Loading from Recycle Cyclone (Ash + Sorbent)

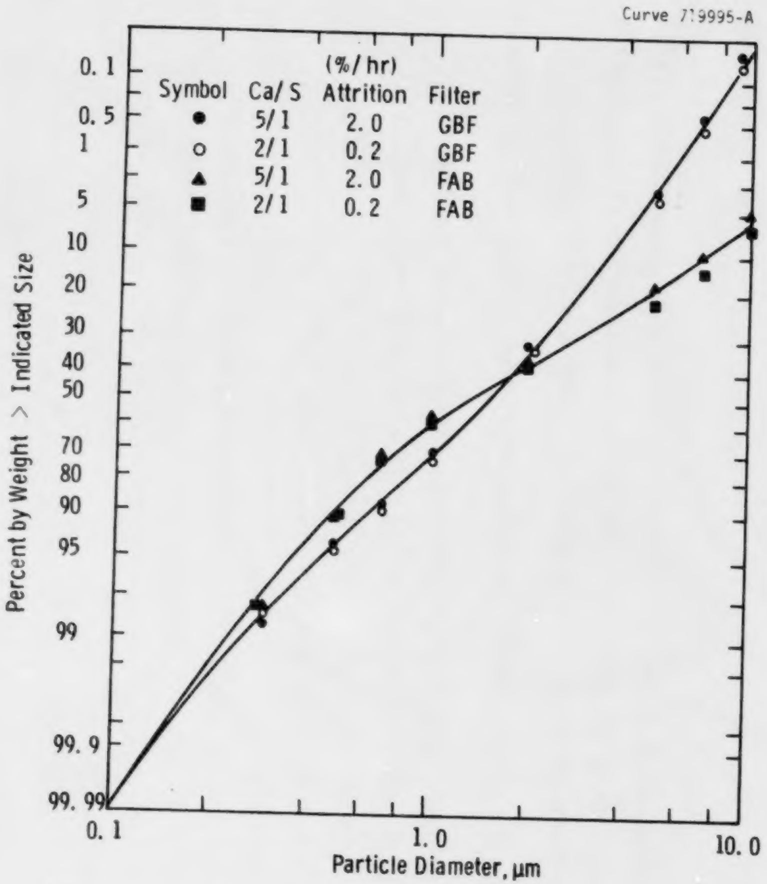

Figure 8 - Combined Sorbent and Ash Size Distributions from Final Filter

2%/hr attrition rate the fabric filter allows only about 0.006 g/m^3 (4.6 ppm) of dust to penetrate, while the granular-bed filter penetration is projected to be on the order of 0.048 g/m^3 (37 ppm).

General conclusions to be drawn from this example are as follows:

- A high-temperature/ -pressure filter device capable of performance similar to that of a conventional fabric filter will probably be necessary if turbine inlet grain loadings of 0.0046 g/m^3 or 3.7 ppm (0.002 gr/scf) are required.
- The filter design is of primary importance since the filter performance determines the particle size distribution and loading presented to the turbine and emitted to the environment.
- The selection of feed materials and the FBC design will effect particle loading to the turbine and the environment for a given filter performance. Figures 9 and 10 show that a tenfold increase in attrition rate may increase mass loading to the turbine and environment by a factor of 2.
- Ash particle size distribution, sorbent attrition rates, and attrited sorbent size distributions are critical parameters since they determine the bulk of material presented to the final filter.
- The design of the FBC to minimize sorbent requirements and particle attrition is important since it also, thus, minimizes particles in the turbine and the environment.

There are two factors that are of critical importance to be discussed when we consider these results. The first issue is that of projecting the performance of particulate collection devices in the smaller than 10 μm range. Particulates in the 0.1 to 10 μm range are very difficult to measure reliably, with the consequence that data on performance in this range must be viewed carefully and judgments made as to

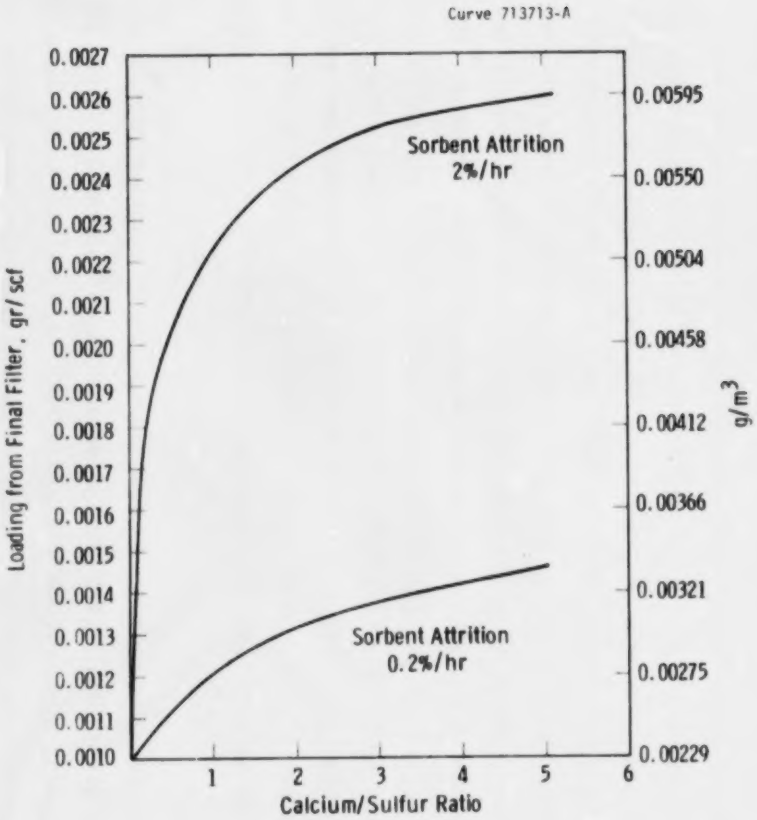

Figure 9 - Loading to Turbine as Function of Ca/S and Attrition for Fabric/Filter Performance

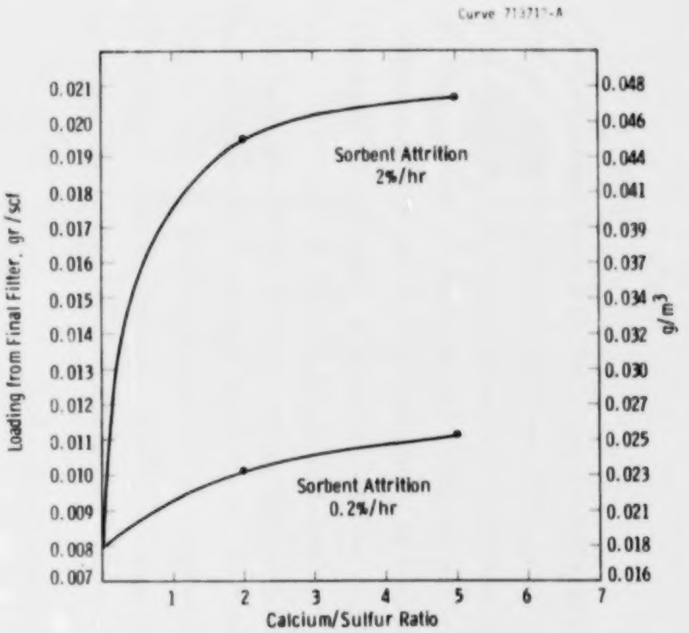

Figure 10 - Loading to Turbine as Function of Ca/S and Attrition for Granular-Bed Performance

real operating situations. This is especially true for the final-filter performance, since the upstream cyclones will probably have removed most of the large material and essentially all of the particulate fed to the final filter are in this <10 μm class. The second issue is similar in nature: the actual distribution of the fines emitted from the bed to the cleanup system are not well established. Typically, good data exist down to ~44 μm, and the distribution of the remainder of the material is reached by log-normal extrapolation with some analytical support. Although this <44 μm material may only represent a small fraction of the feed to the system, it is virtually 100 percent of the feed to the final-filter system. Small changes in this distribution, therefore, can greatly affect the calculated emissions to the turbine and atmosphere.

Turbine Tolerance Projections

Projections of the turbine tolerance of particulates are made to provide perspective on the requirements for environmental control. A turbine tolerance model previously developed by Westinghouse is used to provide guidance for the current study.[11] Calculations of particle trajectories through turbine blading have been carried out, including impact damage, bounce angle, and subsequent impacts. Using related data on the impact damage as a function of angle, velocity, and materials properties, we have calculated actual metal recession rates due to erosion that permit projection of turbine blade life for any given set of conditions. We have also studied the effect of fine particles, since these particles can arrive at blade surfaces by diffusion and can deposit on the blades and eventually unbalance or choke the flow through the blade passage. They can also serve as sites for corrosion to begin.

A considerable amount of work remains to be done in this area with respect to gathering impact damage data with actual PFBC ash and turbine blade alloys at temperature and pressure. As with the particle profile model, however, the turbine tolerance model provides perspective on development requirements and needs.

One must also recognize that the turbine tolerance will depend on the turbine design. The results presented are based on a machine designed to maximize the performance of a PFBC plant. Turbines operating at lower temperatures (e.g., <850°C) and with lower performance (i.e., reduced particle-blade relative velocities) can have increased particulate and chemical tolerances. Thus, an additional trade-off in plant performance, cost, and reliability must be considered.

Using the Westinghouse turbine tolerance model, we can estimate the erosion rate of the turbine blading as a function of particle size distribution, loading, and erosivity. The life of turbine blades is then estimated on the basis of the allowable metal recession. Figure 11 shows the blade life plotted as a function of particulate loading and erosivity. A constant particle size distribution is assumed for all values of particulate loading. The particle size distribution assumed is represented by the granular-bed-filter curve in Figure 8, which is generally a log-normal distribution of sizes between 0.1 and 10 μm. We do not feel that the accuracy of the carry-over and control model warrants differentiation between the curves presented in Figure 8. It is important to note, however, that actual values will have an important effect on turbine erosion, e.g., >10 μm particle loading.

The time between overhauls and the incremental cost of energy due to the turbine blade and vane replacement have been calculated on the basis of the following assumptions:

- The power plant is operated at full load whenever it is operated.
- The operating time per year is 5000 hr (capacity factor - 0.571).
- A spare rotor is normal practice with clean fuels.
- The power plant can be shut down for up to two weeks in spring and fall (off-peak periods) without incurring a penalty for not providing power to the grid.

- The operating time is divided equally between winter and summer periods.
- The penalty for replacing turbine parts in peak demand periods is 20 mills/kWh.
- The capacity factor in the middle of winter or summer is 80 percent.
- The time required to replace bladed rotor and turbine vanes is two weeks.
- The minimum practical overhaul period is three months.
- The effect of a boundary layer on erosion of turbine parts is zero.
- Overhaul periods will be multiples of six months.

Figure 11 shows the relationship between particulate loading and the incremental cost of electricity. For overhaul periods longer than six months the increment cost varies in a series of steps of increasing magnitude but on a constant slope base. For overhaul periods of less than six months, there is only one option (three months), and this is assumed to be the minimum practical overhaul period. With the three-month overhaul period, every other overhaul occurs in a peakload period so the 20 mills/kWh penalty is applied. This changes the slope of the step base at six months.

To use Figure 11 one enters through the particulate loading (for example 10^{-2} g/m^3). If one assumes the granular-bed filter size distribution of Figure 8 and an erosivity of 1/25 silicon carbide (SiC), one finds an incremental cost of electricity of about 1.2 mills/kWh over the use of perfectly clean fuel. This loading corresponds to a life of about 5000 hours and an overhaul schedule of about 12 months.

The maximum practical particulate loadings for the chosen size distribution is a function of erosivity. For an erosivity of 1/25 of SiC, the maximum practical loading is 5.5×10^2 g/m^3 (2.4×10^{-2} gr/scf), and for an erosivity of 1/50 of SiC it is 11×10^{-2} g/m^3 (4.8×10^{-2} gr/scf). Thus, the maximum practical particulate loading is inversely

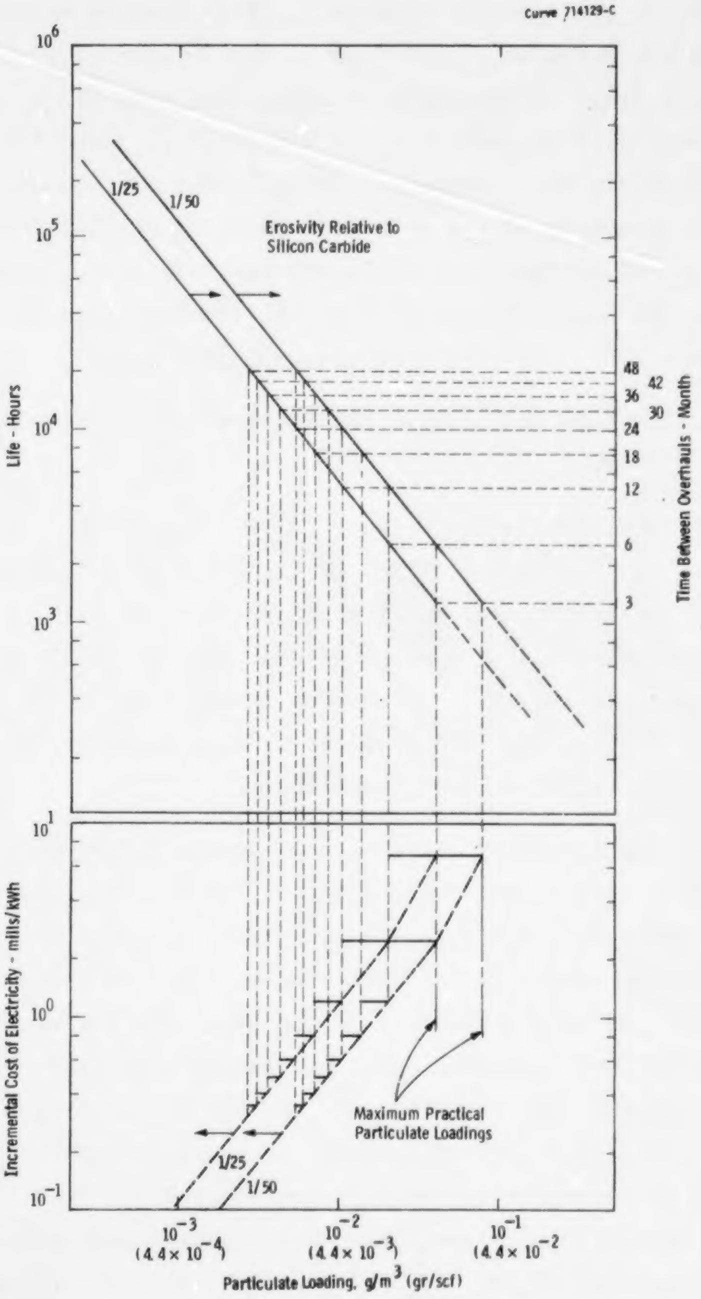

Figure 11 - Incremental Cost of Electricity and Life of Turbine Blades and Vanes as a Function of Particulate Loading and Particle Erosivity

proportional to the particle erosivity. This finding indicates that loadings in the range of 5 x 10^{-2} to 11 x 10^{-2} g/m^3 (0.02 - 0.05 gr/scf) with the size distribution could be acceptable only if an incremental cost of electricity of about 8 mills/kWh could be justified along with a three-month maintenance schedule. The specific performance and cost results are dependent on the selected operating characteristics. The purpose is to illustrate that tools are available to provide perspective on the important trade-offs that can result in choices leading to a reliable FBC plant achieving environmental goals.

Assumptions incorporated in the turbine tolerance model that are of importance are that:

- The estimates do not account for the appreciable slowing of 1 to 3 μm particles in the blade boundary layers; on this basis the erosion rate projections are high.
- The erosivity of the ash and spent sorbent is not well known; two erosivities are used in the projections which are 1/25 and 1/50 the erosivity of SiC particles striking a nickel alloy at room temperature.

Further discussion of the erosion analysis is presented in Volume IV of this report, EPA-600/7-80-015d. Estimates of gas turbine blade life and system costs assuming different degrees of final-stage filtrations were generated for PFBC systems using the carbon burn-up cell concept. In this earlier study the basis for the erosion analysis was similar to that presented here, but the methods used to project particle loadings and size distributions throughout the system were different and based on an earlier method for particle profile projection. The ability to incorporate a recycle cyclone had not been built into the carry-over model for that analysis. Westinghouse has carried out a subsequent application of the combined particle profile/turbine erosion model during 1979 under contract to EPRI (contract No. 1336-1). Results from this study are generally consistent with the present study, indicating that particulate loadings <~0.023 g/m^3 (0.01 gr/scf) (or

18 ppm) will be required for similar size distributions for 25,000-hr life. This was based on the Exxon miniplant particle size distribution ~10% > 5μm) and loading (58 ppm) measured during turbine cascade tests and on use of erosion-resistant turbine materials.

Environmental Requirements and Turbine Tolerance

The particulate control requirements for PFBC processes are determined by either environmental emission standards or turbine tolerance requirements to achieve reliable and economic plant operation. Which of these factors limits the design will depend on the PFBC concept, component designs, component life criteria, and the emission standards.

The preliminary work on turbine tolerance indicates that the erosion and deposition on the blading will control the selection of particulate control equipment for PFBC processes; however, the inclusion of a standard for fine particulates (e.g., <1 μm) could result in the environmental requirements controlling the selection of particulate removal equipment.

HIGH-TEMPERATURE, HIGH-PRESSURE GAS-CLEANING PARTICLE REMOVAL EQUIPMENT TEST FACILITY

Background

Hot gas cleaning is required in a PFBC power plant. Cooling the hot combustion gases, removing particles at low temperature by scrubbing or filtration, and reheating the clean gases prior to their expansion results in capital costs that are higher and operating efficiencies that are lower than those for a conventional coal-fired plant.[5] Westinghouse studies indicate that hot gas cleaning is also desirable in a coal gasification combined-cycle plant for reducing costs and improving efficiency.

A number of particle removal devices have been tested in previous work at Westinghouse.

- Cyclones. Both conventional and advanced rotary flow units. Flow patterns have been measured, and grade efficienty curves, presenting percent removal as a function of particle size, have been determined. Bench- and pilot-scale cyclones have been evaluated at 21 and 815°C (70 and 1500°F).
- Moving wire impactors. A device based on a revolving squirrel cage was devised, constructed, and evaluated as a means of removing particles from gases passing from the interior to the exterior of the cage. Fine particle adherence and agglomeration on the moving wires was apparently insufficient for effective operation of the device.
- Granular-bed filters. Filters involving the downward flow of dirty gases through a stationary bed of particles supported on a perforated plate have been evaluated on both a bench and pilot scale at both 21 and 760°C (70 and 1400°F). Grade efficiency curves have been determined. Collected particles have been effectively removed from the filter by briefly fuidizing the bed particles with a reverse upward flow of gases.
- Porous ceramic filters. Filters involving the flow of dirty gases through one of a stack of thin porous ceramic membranes separated by ceramic corrugations have been evaluated at both 21 and 760°C (70 and 1400°F). Collected particles have been effectively removed from the filter by a brief reverse flow of clean gases.

Other organizations have tested similar devices, such as fibrous ceramic filters, hot, pressurized, electrostatic precipitators, granular-bed filters, and cyclones of advanced and conventional design. It seems likely that a successful hot-gas cleaning, particle removal system for a PFBC or coal gasification combined-cycle power plant can be provided by scaling up one or more of these devices.

There is a need to test, at high temperature and high pressure, particle removal equipment large enough to permit extrapolation to the design of utility-scale units. Westinghouse, with the support of both EPA and DOE designed, constructed, and operated a test facility for evaluating particle removal equipment using simulated flue gases at temperatures up to 871°C (1600°F) and pressures up to 1520 kPa (15 atm). Hot gas flows up to 5.44 kg/s (12 lb/s), 42.5 m^3/s (150 scf/s), can be provided. Equipment up to 1.37 m (4.5 ft) diameter and 2.44 m (8 ft) length can be mounted within an insulated pressure shell for testing.

The DOE has supplied funding for the pressure vessel, flow and back-pressure valves, and bursting discs at a total cost on the order of $40,000. The EPA funded the purchase of the piping and the installation of that piping at the passage at a cost of about $85,000. Westinghouse has supplied the remainder of the equipment in the system at a cost of about $3,000,000.

TEST FACILITY

A functional schematic of the test passage is presented in Figure 12 and a floor plan of the entire test and development center in Figure 13. The high-pressure air for the system is supplied by either or both compressors available. A 1500 kW (2000 hp) centrifugal compressor (Figure 14) can supply 3.4 kg/s (7.6 lbm/sec) of air at 2026 kPa (300 psig). A second three-stage 900 kW (1200 hp) reciprocating compressor (Figure 15) can be run in parallel, providing flows up to 5.86 kg/s (12.9 lbm/sec). This high-pressure air flows from the compressor building to the laboratory where it can be heated to temperatures up to 650°C by either of two propane or oil-fired air preheaters (Figure 16).

The pressurized preheated air then flows through a combustor where enough No. 2 fuel is burned to raise the gases to the desired set point. The combustor fuel is pumped from the fuel-blending building (Figure 17) where several tanks are available for blending either corrosion inhibitors or promoters (combustible alkali organometallic

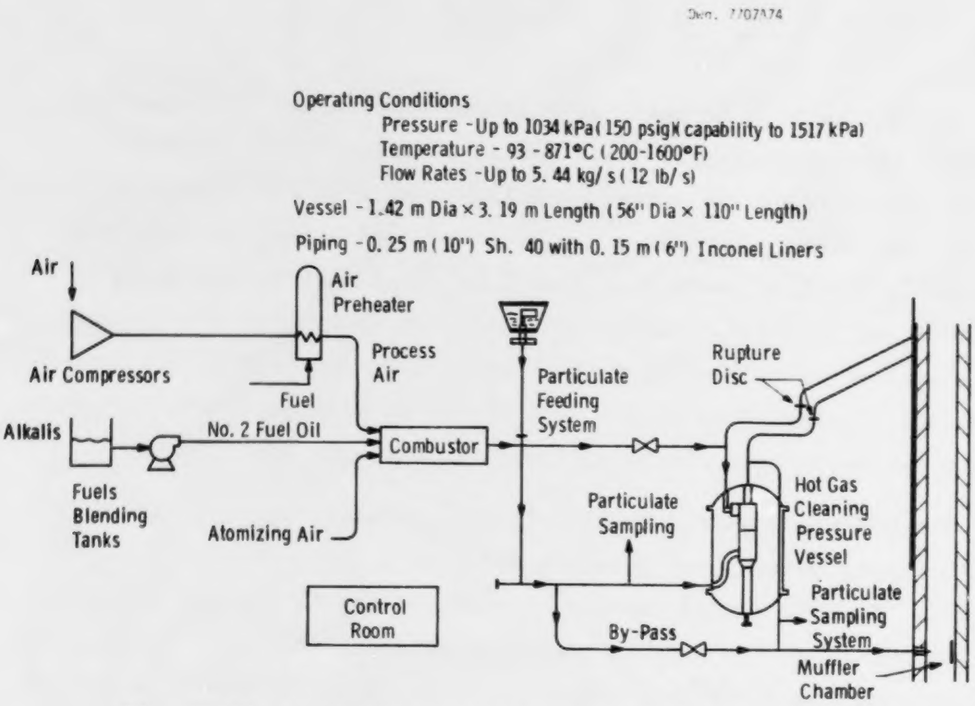
Dwg. 7707A74
Operating Conditions
Pressure - Up to 1034 kPa (150 psig) (capability to 1517 kPa)
Temperature - 93 - 871°C (200-1600°F)
Flow Rates - Up to 5.44 kg/s (12 lb/s)
Vessel - 1.42 m Dia × 3.19 m Length (56" Dia × 110" Length)
Piping - 0.25 m (10") Sh. 40 with 0.15 m (6") Inconel Liners
Air
Air Compressors
Air Preheater
Fuel
Process Air
Alkalis
Fuels Blending Tanks
No. 2 Fuel Oil
Combustor
Atomizing Air
Control Room
Particulate Feeding System
Particulate Sampling
By-Pass
Rupture Disc
Hot Gas Cleaning Pressure Vessel
Particulate Sampling System
Muffler Chamber

Figure 12 - Schematic Diagram of Westinghouse Hot-Gas Cleanup Facility

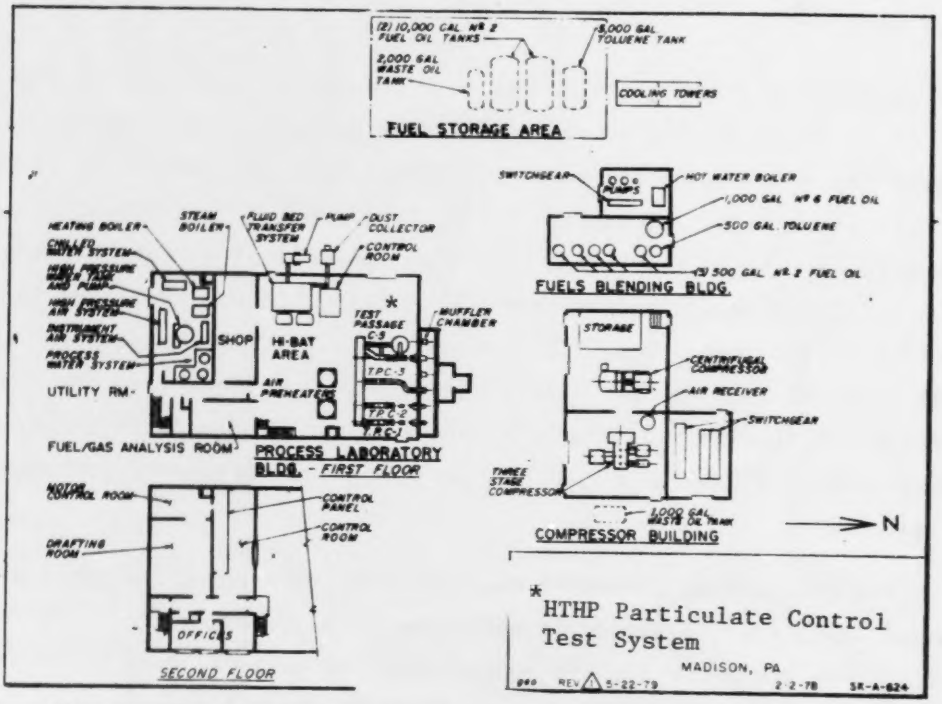
(2) 10,000 GAL Nº 2 FUEL OIL TANKS
2,000 GAL WASTE OIL TANK
5,000 GAL TOLUENE TANK
COOLING TOWERS
FUEL STORAGE AREA
SWITCHGEAR
PUMPS
HOT WATER BOILER
1,000 GAL Nº 6 FUEL OIL
500 GAL TOLUENE
(3) 500 GAL Nº 2 FUEL OIL
FUELS BLENDING BLDG.
HEATING BOILER
STEAM BOILER
FLUID BED TRANSFER SYSTEM
PUMP
DUST COLLECTOR
CONTROL ROOM
CHILLED WATER SYSTEM
HIGH PRESSURE WATER TANK AND PUMP
HIGH PRESSURE AIR SYSTEM
INSTRUMENT AIR SYSTEM
PROCESS WATER SYSTEM
UTILITY RM
SHOP
HI-BAY AREA
*
TEST PASSAGE C-5
TPC-3
TPC-2
TPC-1
MUFFLER CHAMBER
AIR PREHEATERS
FUEL/GAS ANALYSIS ROOM
PROCESS LABORATORY BLDG. - FIRST FLOOR
STORAGE
CENTRIFUGAL COMPRESSOR
AIR RECEIVER
SWITCHGEAR
THREE STAGE COMPRESSOR
1,000 GAL WASTE OIL TANK
COMPRESSOR BUILDING
N
MOTOR CONTROL ROOM
CONTROL PANEL
CONTROL ROOM
DRAFTING ROOM
OFFICES
SECOND FLOOR
*HTHP Particulate Control Test System
MADISON, PA
REV 1 5-22-79
2-2-78
SR-A-624

Figure 13 - Particulate Control Test System and Support Facility

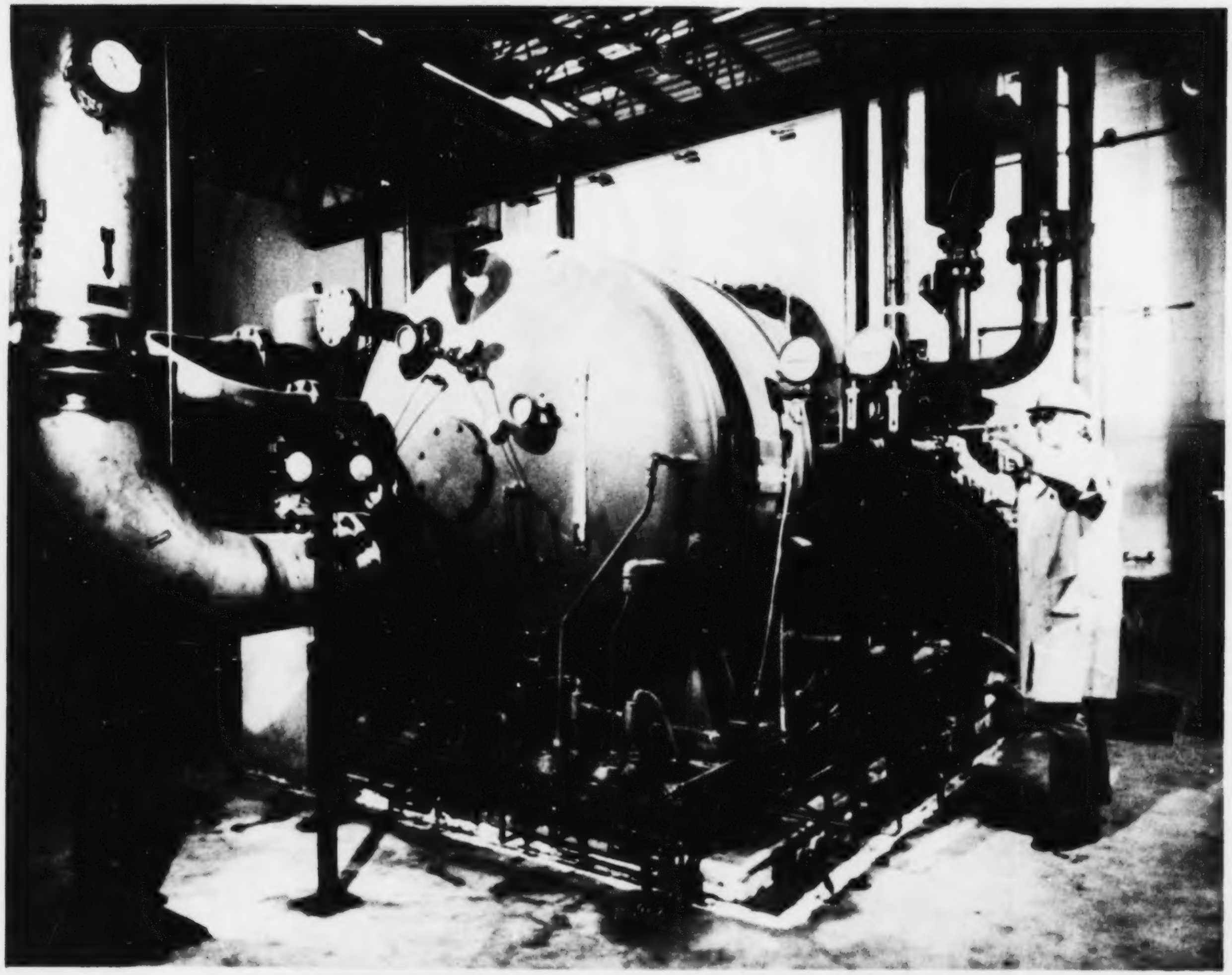

Figure 14 - Centrifugal Compressor

Figure 15 - Three-Stage Cooper Bessemer Compressor

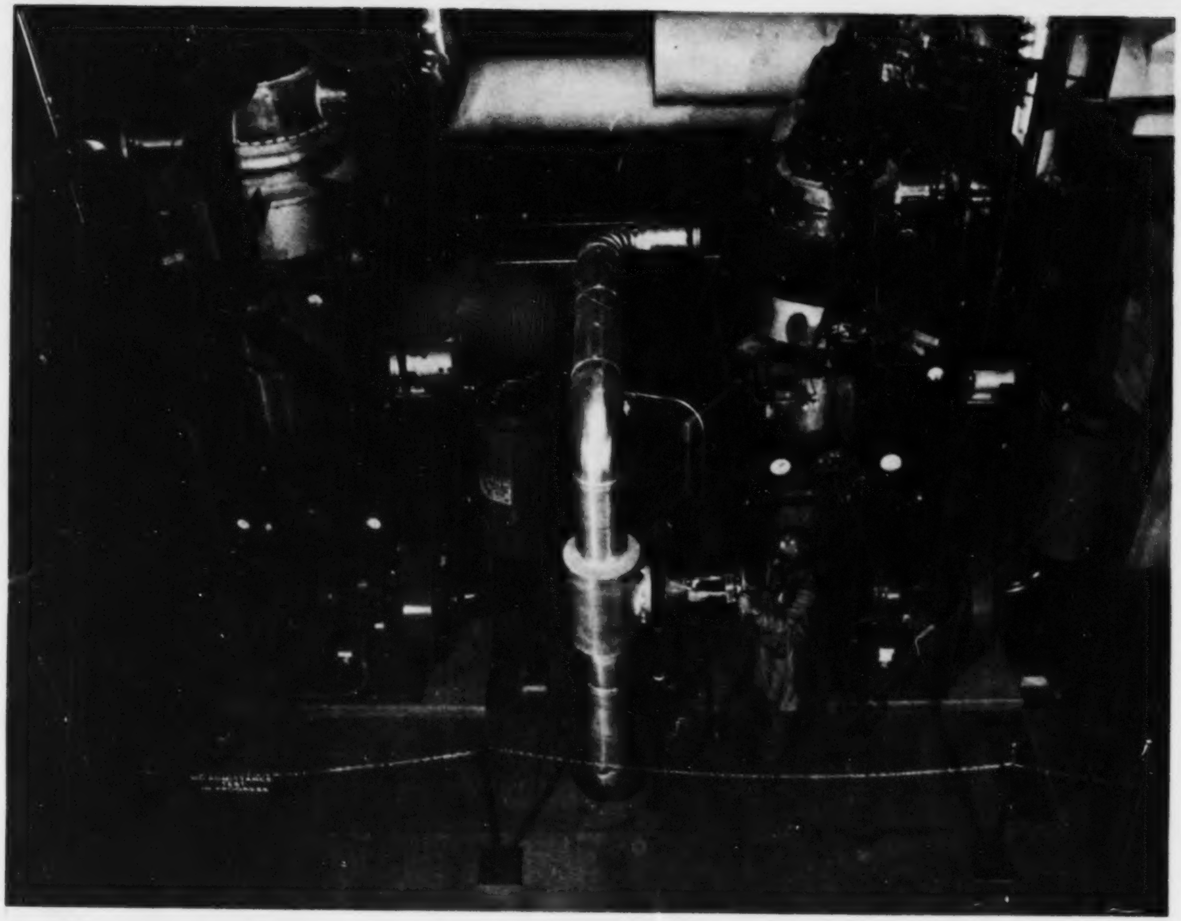

Figure 16 - Test Passage Air Preheaters

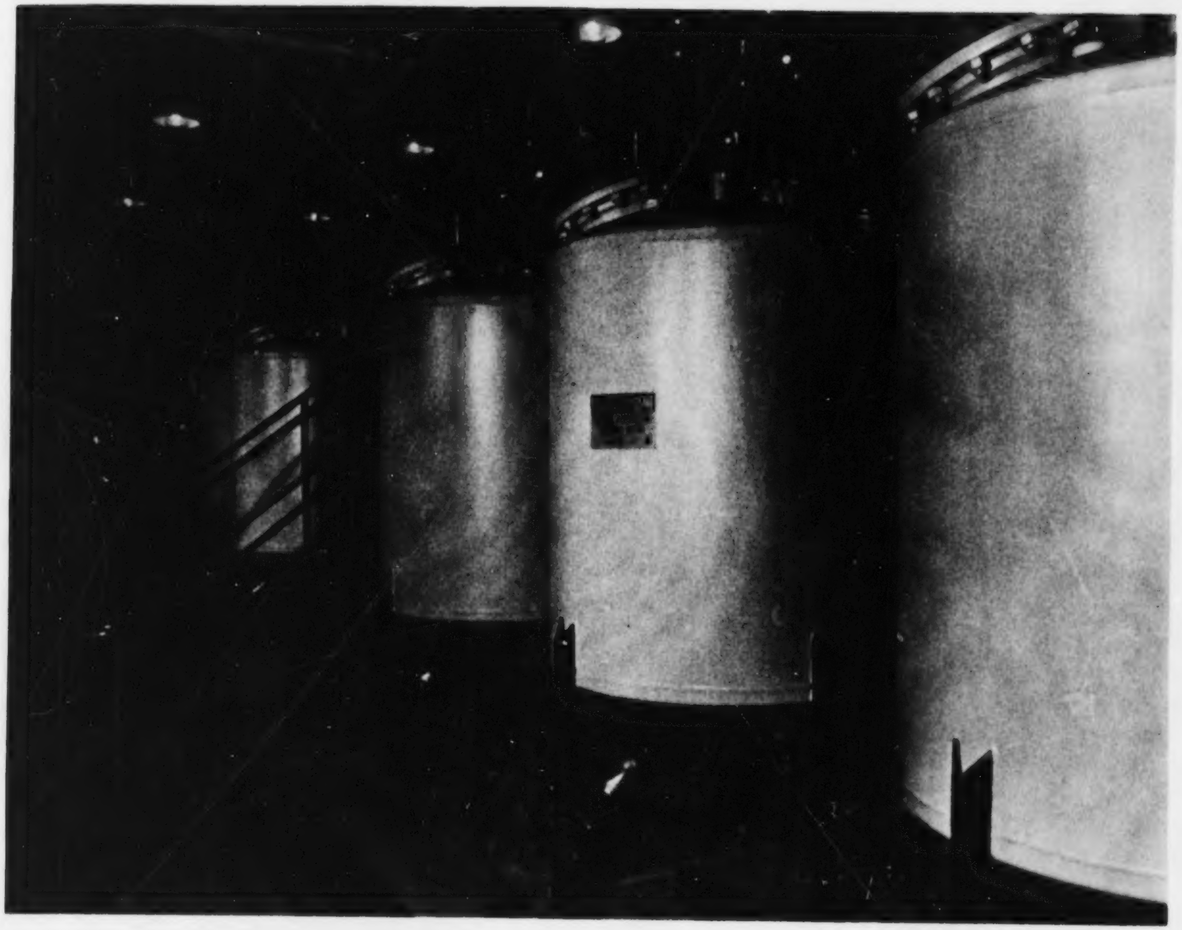

Figure 17 - Fuel Blend Tanks and Facilities

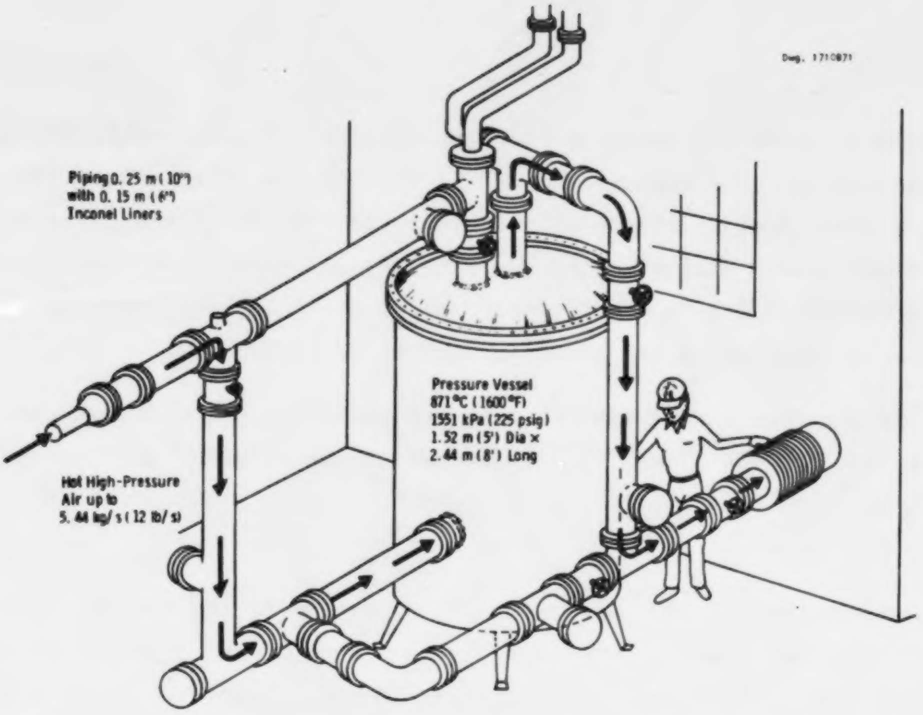
Dwg. 1710B71
Piping 0.25 m (10") with 0.15 m (6") Inconel Liners
Pressure Vessel 871°C (1600°F) 1551 kPa (225 psig) 1.52 m (5') Dia × 2.44 m (8') Long
Hot High-Pressure Air up to 5.44 kg/s (12 lb/s)

Figure 18 - High-Temperature and -Pressure Particulate Removal Test Facility (Side Inlet)

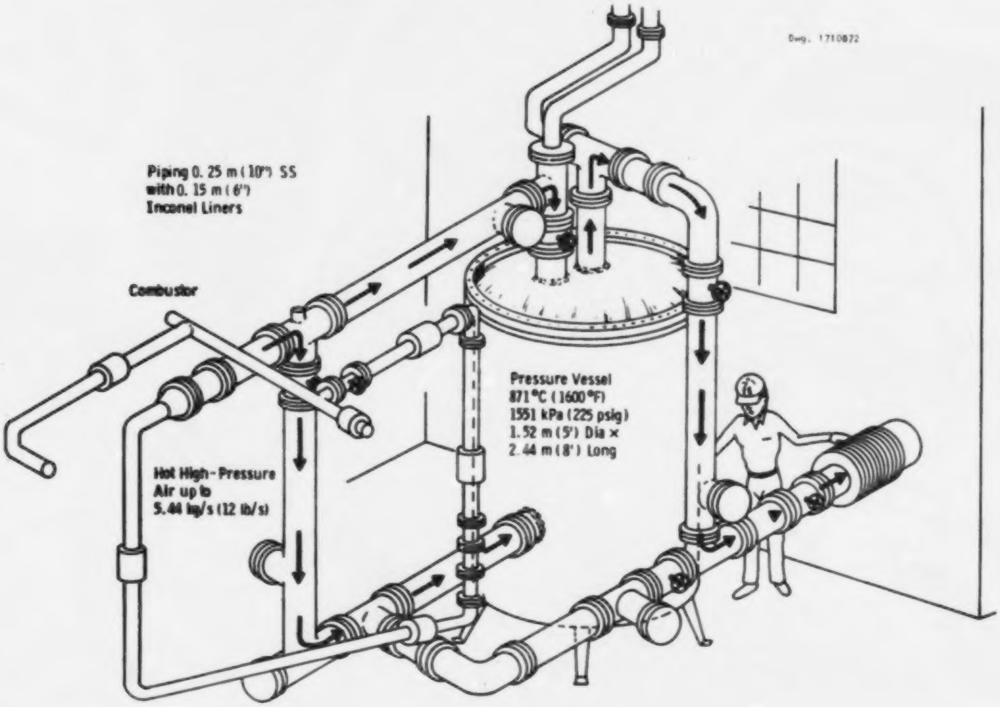
Dwg. 1710B72
Piping 0.25 m (10") SS with 0.15 m (6") Inconel Liners
Combustor
Pressure Vessel 871°C (1600°F) 1551 kPa (225 psig) 1.52 m (5') Dia × 2.44 m (8') Long
Hot High-Pressure Air up to 5.44 kg/s (12 lb/s)

Figure 19 - High-Temperature and -Pressure Particulate Removal Test Facility (Split Inlet)

compounds). From the combustor the hot pressurized gases enter the test passage piping. The passage piping and valving are fairly extensive, to allow a great deal of flexibility in the manner in which the gases are introduced to and exit from the pressure vessel, allowing virtually, any device that will fit in the pressure vessel to be tested. Several alternative flow paths are shown in Figures 18 through 20.

The pressure vessel used in this system is shown with dimensions in Figure 21. Figures 22 and 23 are photographs showing how the internal connections to a typical test device (an Aerodyne cyclone here) are made within the vessel.

Overall control and operation of the passage is carried out from the control room shown in Figure 24, although sampling and other operations must be carried out at the passage itself. Figure 25 shows a photograph of the passage pressure vessel and some of the piping.

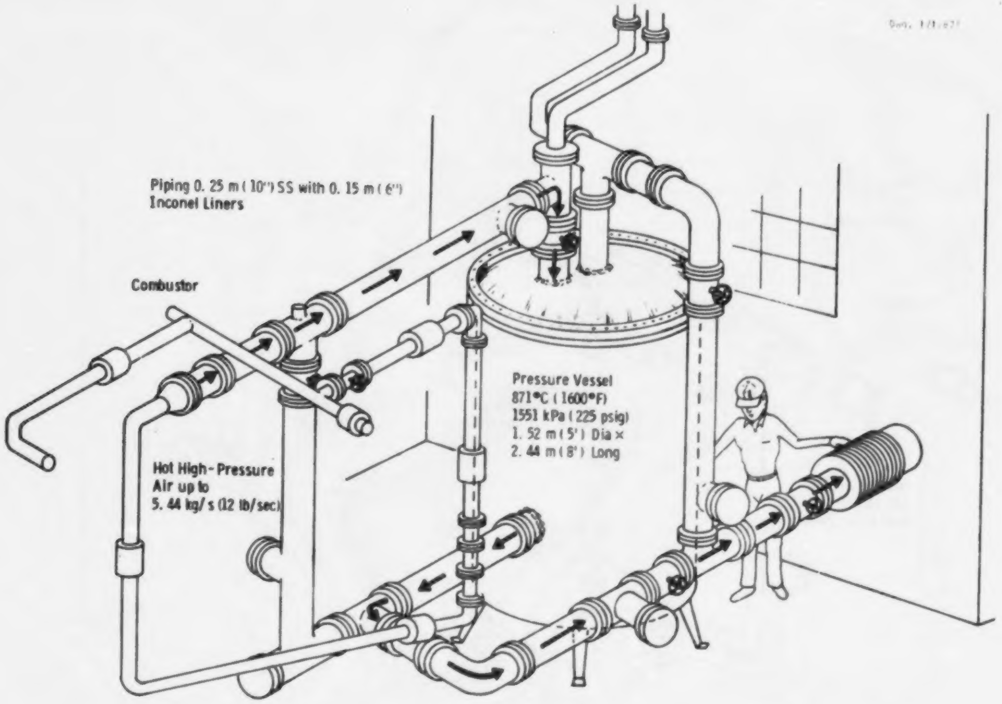
Piping 0.25 m (10") SS with 0.15 m (6")
Inconel Liners
Combustor
Pressure Vessel
871°C (1600°F)
1551 kPa (225 psig)
1.52 m (5') Dia ×
2.44 m (8') Long
Hot High-Pressure
Air up to
5.44 kg/s (12 lb/sec)

Figure 20 - High-Temperature -Pressure Particulate Removal Test Facility (Top Inlet)

Dwg. 7681A02

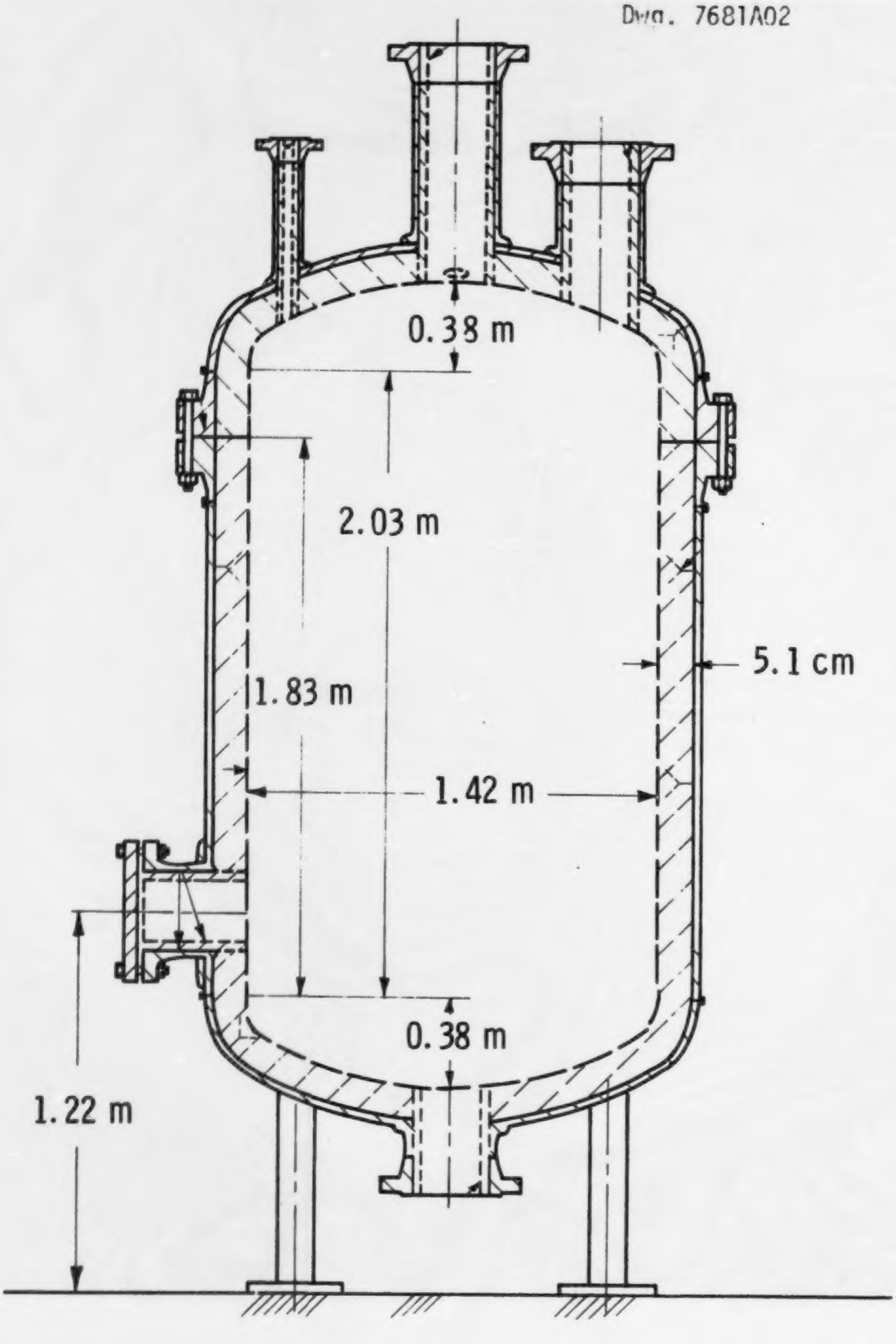
0.38 m
2.03 m
5.1 cm
1.83 m
1.42 m
0.38 m
1.22 m

Figure 21 - High-Temperature and -Pressure Test Facility Pressure Vessel

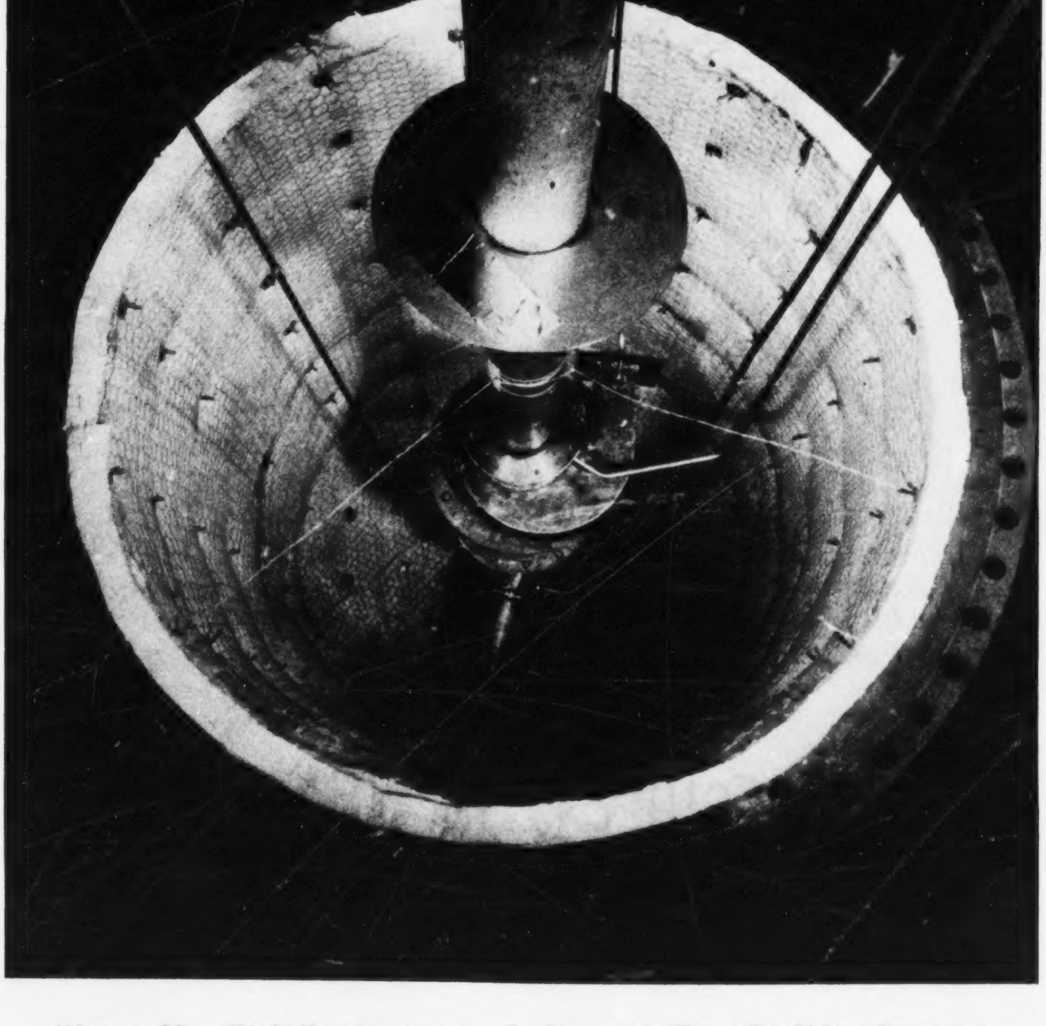

Figure 22 - High-Temperature and -Pressure Test Facility Pressure Vessel with Aerodyne Installed

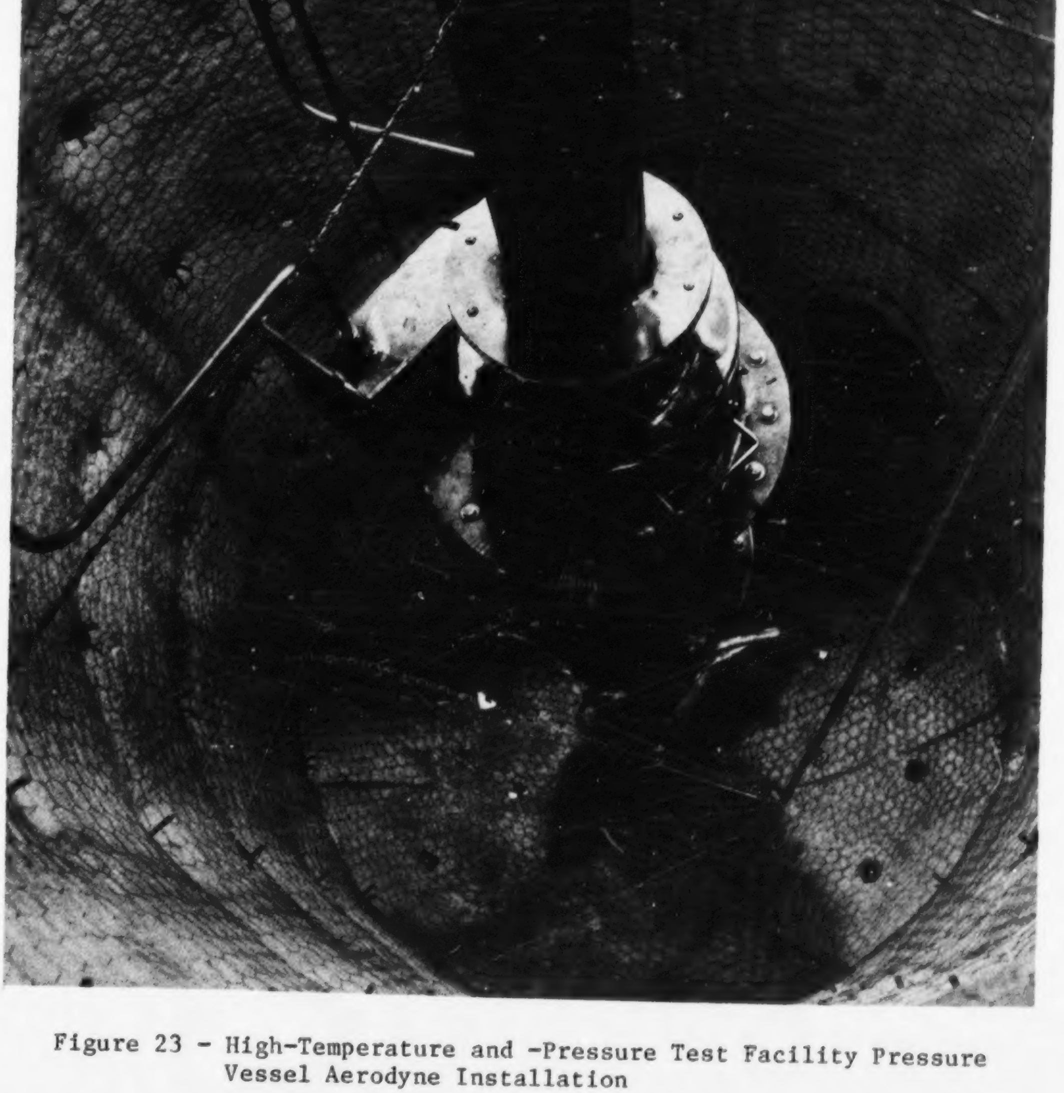

Figure 23 - High-Temperature and -Pressure Test Facility Pressure Vessel Aerodyne Installation

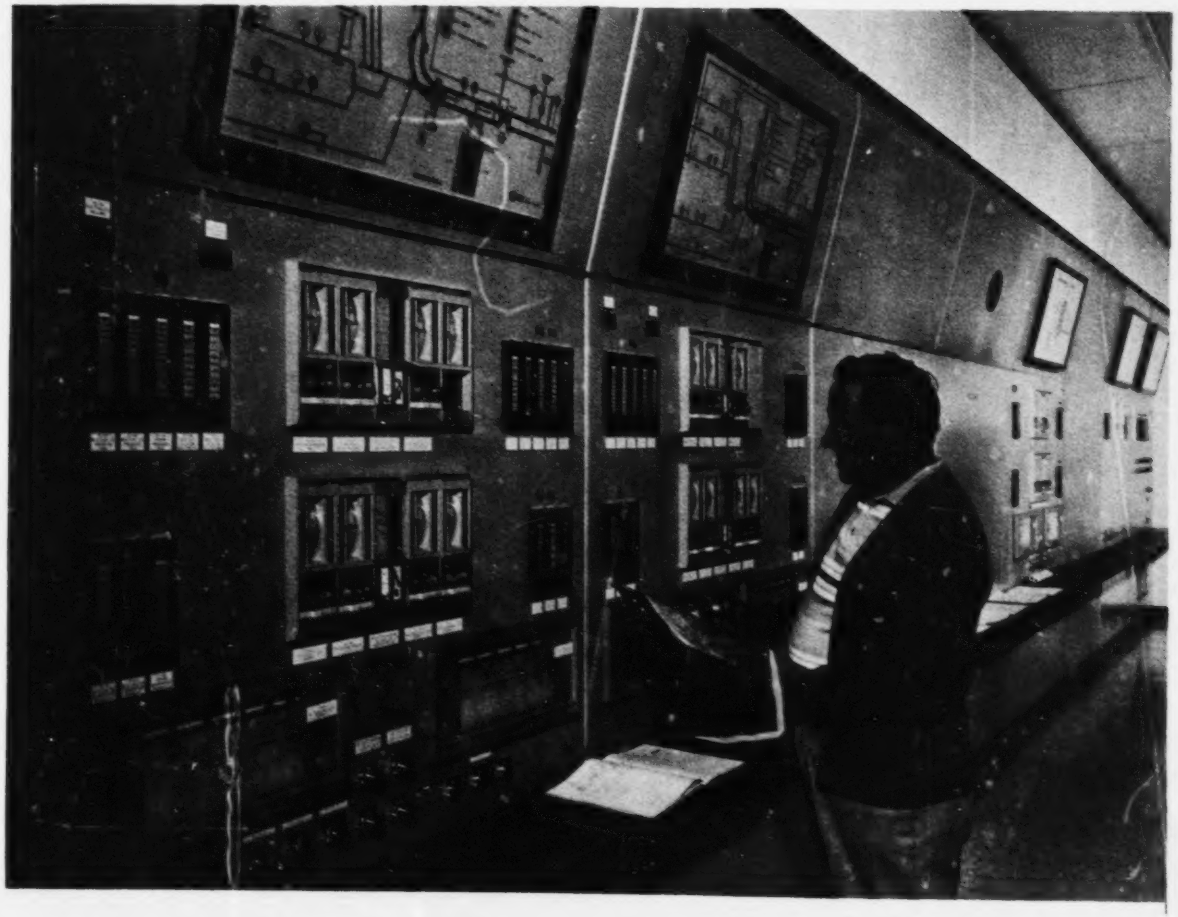

Figure 24 - High-Temperature and -Pressure Test Facility Control Room

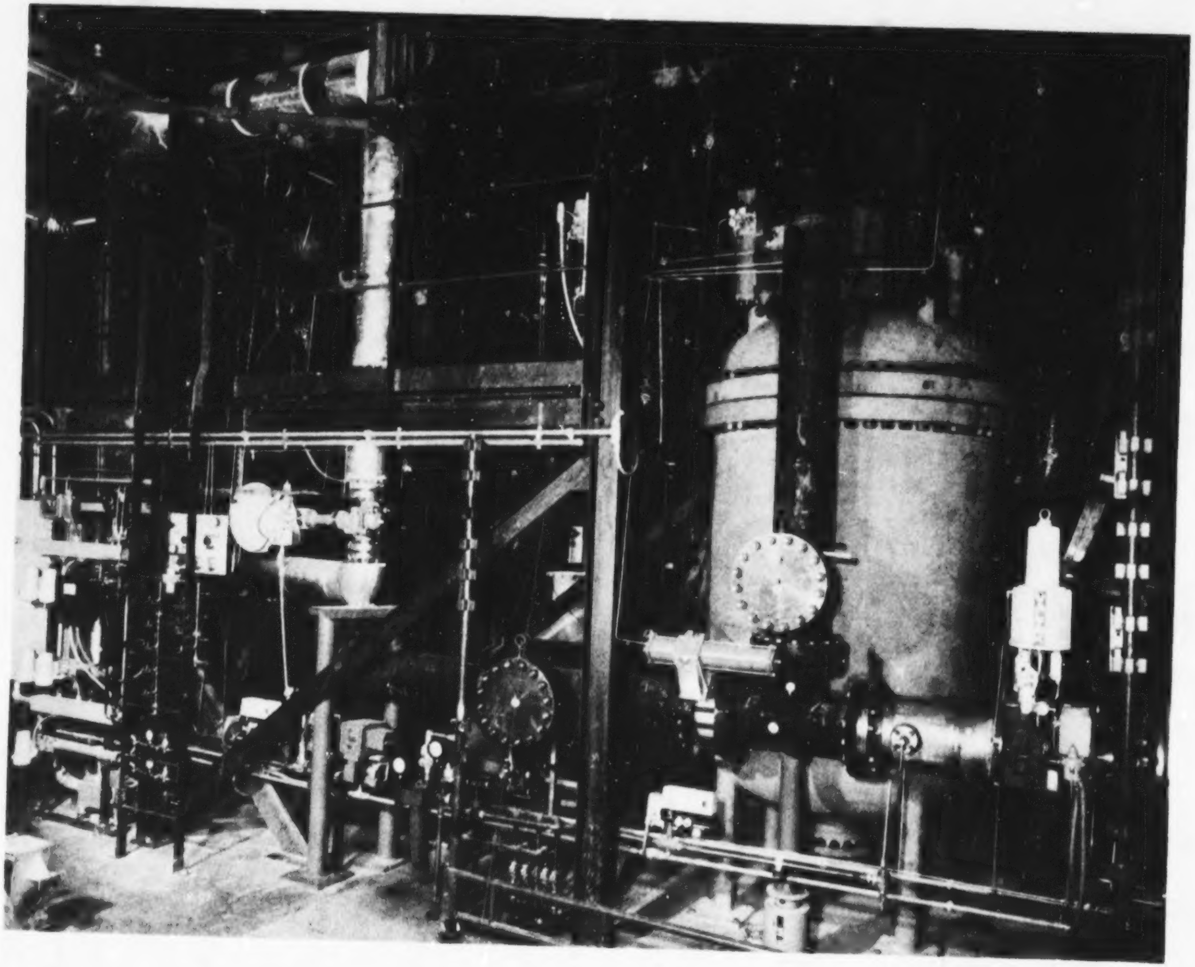

Figure 25 - High-Temperature and -Pressure Test Facility

Pertinent facts about the Westinghouse HTHP Particulate Removal Equipment Test Facility, its capabilities, and its operation are presented in Table 2. This facility provides the means for testing pilot-scale apparatus under carefully controlled conditions at minimum cost. The pressure vessel permits light construction of the particle removal apparatus, since the device itself needs to withstand only its own pressure drop.

PARTICULATE SAMPLING

Dust sampling parts have been included at several points in the system. Figure 26 shows a schematic of the usual sampling train when cascade impactors are used for mass loading and size distribution measurements. As indicated in the schematic, this system allows the impactor to be inserted directly into the passage piping for sampling. This system minimizes the risk of altering the sample when extracting it from the passage, conditioning it, and subsequently measuring its properties. Figure 27 presents a photograph of the sampling train used in the system.

Containment Injection

In order to be able to suitably simulate PFBC flue gas conditions provisions have been made for injection of solid particulate and gaseous species.

Particulate Injection

The injection and subsequent dispersal of fine powders at elevated pressures is a difficult task. Over a relatively long period a system has evolved that appears to be adequate for metering and dispersing fine test dusts. This system is shown schematically in Figure 28. The test dust is placed in a pressurized pipe section containing a variable-speed torque motor. The motor rotates a plate at the bottom of the dust hopper. This plate has a set number of through holes at a given radius,

Table 2

HIGH-TEMPERATURE AND -PRESSURE TEST FACILITY

Vessel	2.79 m (110") Length 2.03 m (80") Straight Sides 1.42 m (56") Diameter 4 - 25.4 cm (10") Nozzles (2 Head, 1 Side, 1 Bottom) 2 - 7.6 cm (3") Nozzles (Head)
Piping	25.4 cm (10") Carbon Steel 15.0 cm (6") Inconel Liners 5.1 cm (2") Fiber Frax Insulation
Flow Conditions	Up to 5.44 kg/s (12 lb/s) Temperature, 93-871°C (200-1600°F) Pressure, 0-1034 kPa (0-150 psig) Oxidizing Atmosphere
Subsystems	Provisions for Injection of Virtually any Dust Type, Size, and Rate Provisions for Sampling at All Vessel Inlet and Outlet Points Provisions for Adding Sulfur and/or Alkali Metal Compounds in Fuel
Typical Test Devices	Cyclones - Conventional and Rotary Flow Units Granular Bed Filters Ceramic Filters - Barrier or Bag Type Electrostatic Precipitators
Manpower Requirements	1 - Control Room Operator 1 - Auxiliary Equipment Monitor 1 - System Monitor 2 - Sampling Team Electricity Fuel and Water Costs $75/hr (est.)

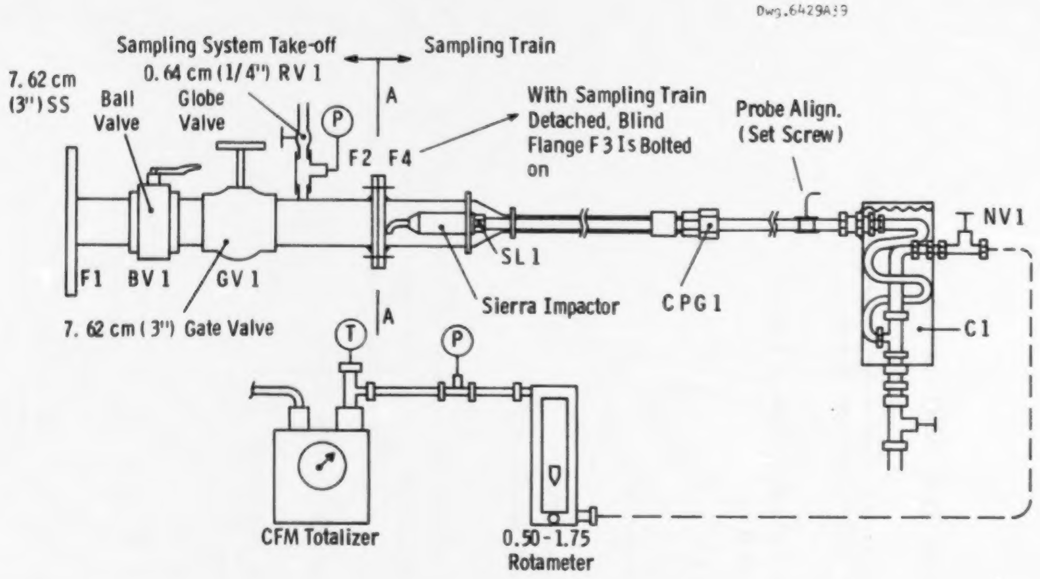
Dwg.6429A39
Sampling System Take-off
Sampling Train
7. 62 cm
(3") SS
0. 64 cm (1/4") RV 1
Ball
Valve
Globe
Valve
A
P
F2
F4
With Sampling Train
Detached, Blind
Flange F 3 Is Bolted
on
Probe Align.
(Set Screw)
NV 1
SL 1
F1
BV 1
GV 1
Sierra Impactor
CPG 1
C 1
7. 62 cm (3") Gate Valve
T
A
P
CFM Totalizer
0.50 - 1.75
Rotameter

Figure 26 - Schematic of Sampling Train

which fill with the test dust upon rotation. A stationary plate is supported below the rotating disk. This plate has a single through hole that is located so that the moving holes pass over the stationary hole. As they do, the dust in the moving hole is "puffed" down through the stationary hole by a high-pressure pulse from above. This action is enhanced by the action of a straight "through" ejector which is fastened to the bottom plate hole. This injector disperses and dilutes the delivered "pellet" of dust and feeds it to a second, conventional, orifice-type ejector where the dispersion is completed by a sonic flow of motive air. The dispersed dust is then blown directly into the test passage through connecting tubing.

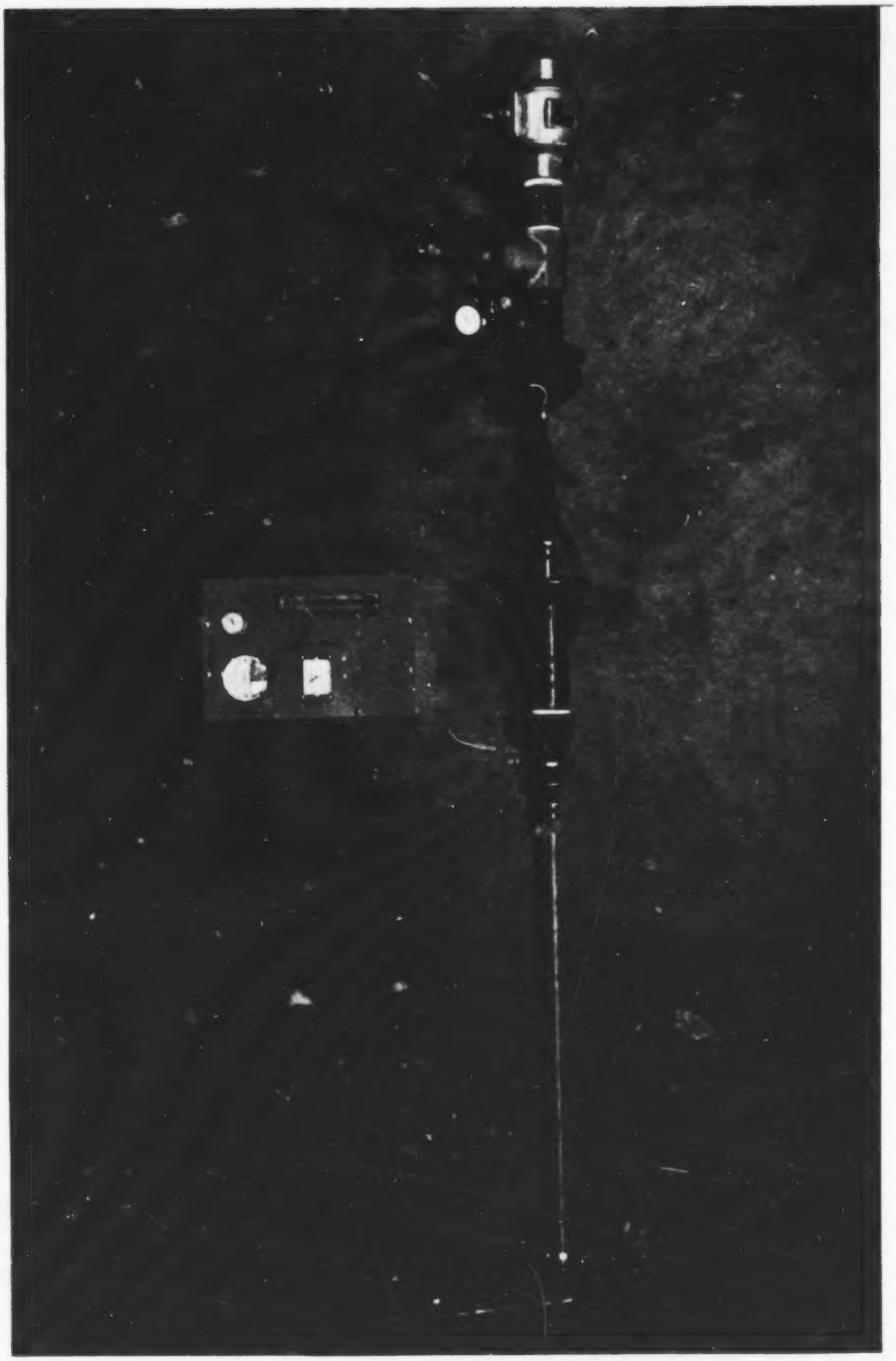

Figure 27 - Photograph of Particulate Sampling Train

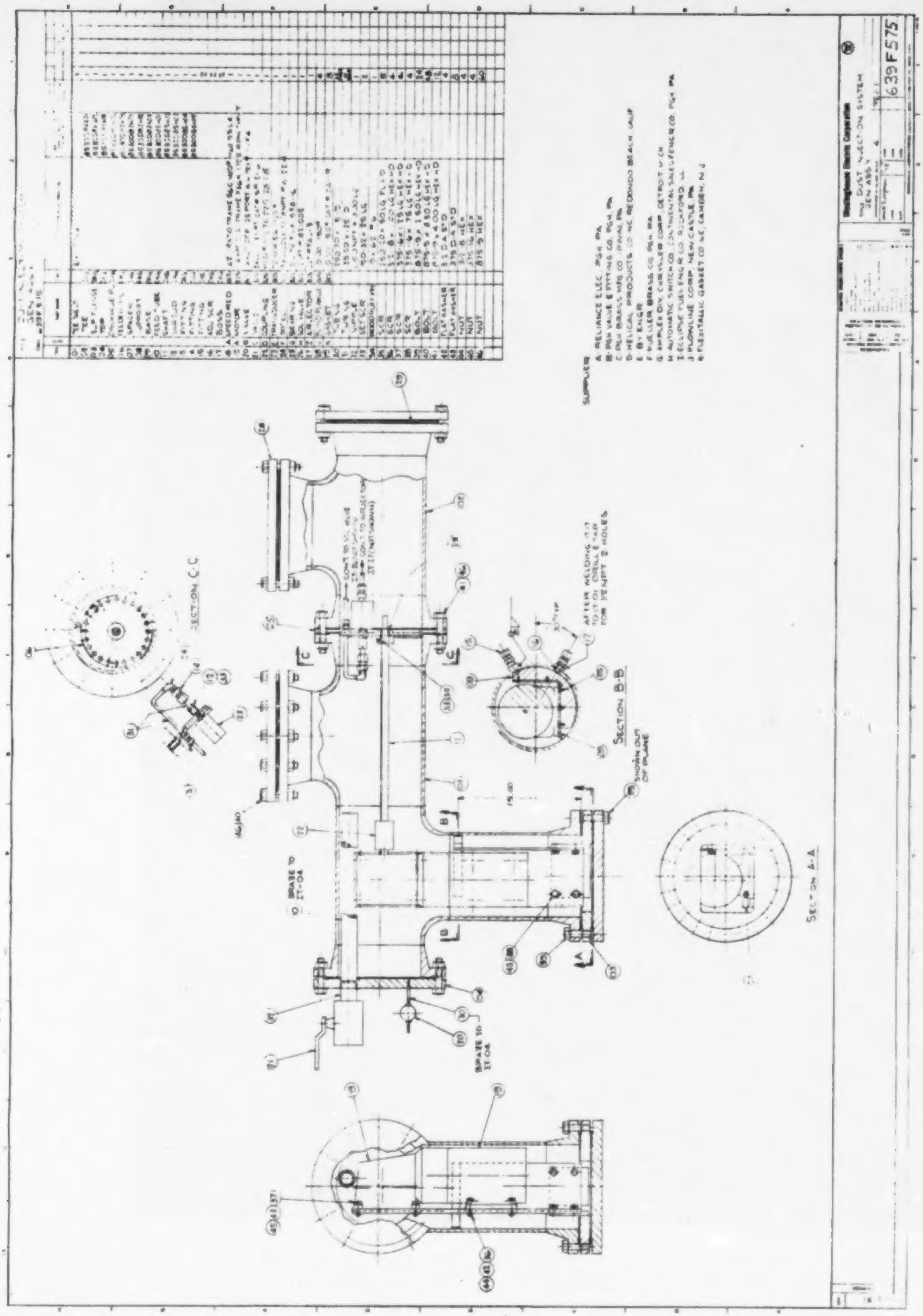
SECTION C-C
SECTION B-B
SECTION A-A
BRAZE TO IT-04
SUPPLIER
Westinghouse Electric Corporation
639F575

Figure 28 - Particulate Injection System

Gas Phase Contaminants

The introduction of gaseous species such as SO_2 is accomplished in a straightforward manner by connecting a high-pressure tank of the gas to an injection port and metering in the desired quantity.

Alkali metal contaminants can be injected into the system most easily by blending combustible organometallic compounds of the desired type into the combustor fuel. This technique has a long, successful history in combustion engineering research.

Test Facility Status

At this time the test facility construction is complete and operations for actually running the passage are shaken down and ready. To date, the major problems have been associated with adequate control of the dust injection rate and dispersion. The sampling system has been tried at temperature and pressure and operates well.

Test Program Status

At this time, two test programs are scheduled for the test facility. The first is a DOE-sponsored program (Contract EF-77-C-01-2787) to examine an advanced rotary flow cyclone's performance and compare it with a conventional cyclone design.

The second program is an ERPI-sponsored program to test two ceramic bag-filter concepts (Contract RP1336-1). The actual test program for this contract is expected to begin late in 1979.

5. NITROGEN OXIDE EMISSIONS

The objectives of this task are to develop an understanding of the mechanisms of NO_x generation and destruction in FBC so as to define the design and operating parameters required to permit the minimization of NO_x emissions. We have chosen a dual approach to obtain such understanding:

- The statistical treatment of data presently available that may present clues to the reaction mechanisms
- The evolution of a model to permit selection of design and operating criteria and to project plant performance.

LITERATURE REVIEW

Fluidized-bed combustion technology is being developed as an alternative to the conventional combustion techniques. The major emphasis is on limiting sulfur oxide (SO_x) emissions by using a suitable sorbent in the bed. In this section information available in the literature is reviewed briefly to offer insight into the NO_x formation mechanisms and into the effects of fluidized-bed design and operating parameters on NO_x emissions.

Mechanisms

In combustion processes nitric oxide (NO) can form by the thermal fixation of molecular nitrogen in the combustion air and/or by the oxidation of the chemically bound nitrogen in the fuel. The NO once formed can be reduced to molecular nitrogen by homogeneous gas phase reactions with carbon monoxide (CO), hydrogen, methane (CH_4), and SO_2, and/or by the heterogeneous reaction with char.

Source of NO

Thermal NO is believed to be formed largely through a relatively slow and a very temperature-dependent reaction path commonly referred to as the Zeldovich mechanism.[13] These reactions describe the NO formation in the postcombustion product gas stream, since there is no generally accepted reaction mechanism for NO formation during the combustion process. The relatively lower temperatures, less than 1000°C, encountered in FBC seem to be unfavorable for thermal fixation of atmospheric nitrogen. Experiments conducted by several investigators[14-16] using air and argon-oxygen mixtures as oxidizers have shown a general uniformity in the NO_x emissions from FBC that suggests fuel-bound nitrogen to be the major source. Relatively little is known about the nature of nitrogen-containing polynuclear structures present in coal and their conversion to NO. During the initial phases of combustion, such as devolatilization, some of the nitrogen in the coal can be released in the form of hydrogen cyanide (HCN), ammonia (NH_3), nitrogen-containing organic bases like pyridines, quinolines, and so on, while significant quantities of nitrogen may remain in the char particle.[17] As compared with molecular nitrogen, these nitrogen-containing structures can be oxidized at lower temperatures.

Relative Contribution of Volatile Matter and Char

Nitrogen in the coal has been observed to be distributed among the volatiles and the fixed carbon (char).[17] Pereira et al.[15] have shown that at temperatures below 750°C most of the NO_x is formed from the oxidation of nitrogen left in the char. At higher temperatures, however, 800°C and above, the volatiles seem to be the major source of NO_x emission. These observations suggest that nitrogen in the chars formed at higher temperatures is less easily oxidized.

Coal Nitrogen Content

In the case of liquid and gaseous fuels, combustion experiments conducted by doping the fuels with nitrogen compounds have shown decreased conversion of the total nitrogen present in the fuel mixture to NO.[18] Pereira et al.[19] and Chronowski and Molayem[20] have shown that NO_x emissions under similar operating conditions increase with an increase in the coal nitrogen content. Thus, there seems to be some indirect evidence showing a similar decrease in the percent of conversion of nitrogen in the coal to NO with an increase in the coal nitrogen content.[14,18,19] This observation, however, is based on results from burning different coals that may have significantly different combustion characteristics.

NO Reduction Reactions

Less than 100 percent conversion of fuel-bound nitrogen to NO is observed in FBC and can be explained by assuming the once-formed NO to be reduced by, for example, CO, hydrogen, NH_3, unburned hydrocarbons, and char, which may be present in the combustion mixture. Pereira[21] has proposed that the homogeneous gas phase reducing reactions limits NO_x emissions at temperatures below 750 to 800°C, while the heterogeneous reaction between NO and char is accelerated above 800°C, resulting in significantly decreased NO_x emissions. Jonke et al.[16] have shown that the NO_x emissions decrease in FBC in the presence of limestone. Vogel et al.[22] reported that NO_x emissions increase with an increase in the Ca/S molar ratio. A close examination of their data, however, indicated the possibility of increased emissions due to increased superficial gas velocity rather than to the increased Ca/S ratio. Hammons and Skopp[23] have shown that calcium sulfate ($CaSO_4$) can act as a catalyst during the catalytic reduction of NO by CO or by SO_2.

Effect of Fluidized-Bed Operating and Design Parameters

The NO_x formation and reduction reactions in FBC can be significantly influenced by the operating and design parameters. These influences are briefly described below.

Pressure

Nitrogen oxide emissions were found to decrease substantially between 101 and 304 to 405 kPa (1 and 3 to 4 atm) and then decrease less rapidly with a further increase in pressure.[23] Pressurized beds are usually deeper, providing increased gas residence times, and the fluid dynamics in them favor relatively smaller bubbles. These factors can have favorable influences on the interphase mass transfer steps involved in the homogeneous NO reduction reactions and also on the adsorption-desorption steps involved in the heterogeneous reduction of NO by char.

Temperature

A temperature maximum for NO_x emissions was found by Pereira, Beér, and Gibbs[19] at 750 to 800°C. They observed NO_x emissions to be substantially less than those corresponding to 100 percent conversion of fuel-bound nitrogen. They proposed that the relatively lower NO_x emissions at temperatures below 750°C can be due to the reducing action of CO, hydrogen, and unburned hydrocarbons, while at higher temperatures the decrease is caused by an accelerated reduction by char.

Excess Air

Studies[14-16] using air and argon-oxygen mixtures as oxidizers have shown few differences in NO_x emissions in FBC, suggesting the fuel-bound nitrogen to be the major source of NO_x emissions. The conversion of fuel-bound nitrogen to NO has been observed to depend strongly on the availability of oxygen and, hence, on the local stoichiometry. Furasawa et al.[14] have shown the NO_x emissions to increase substantially between 0 and 40 to 50 percent excess air and then to increase less rapidly with further increase in excess air. These observations suggest that the interphase mass transfer and diffusional resistances govern the NO_x formation and destruction kinetics. Gibbs and Beér,[24] using a 30 cm x 30 cm fluidized-bed combustor have shown rapid production of NO immediately above the distributor plate, with substantial reduction in NO concentration in the splash region and in the freeboard. They showed radial as well as axial concentration gradients for NO, indicating the importance of fluid dynamics, which determines the local stoichiometry of the combustion mixture. The NO concentration was observed to be higher at the walls than at the center of the combustor, suggesting that the NO formation takes place mainly in the particulate phase, where coal particles are being burned.

Gas Residence Time

Pereira et al.[15] have shown NO_x emissions first to increase and then to decrease with an increase in gas velocity at constant bed depth. This observation suggests a reaction mechanism in which NO could be treated as an intermediate product. For example:

$$O_2 \xrightarrow[\text{nitrogen}]{\text{+ fuel-bound}} NO \xrightarrow[\text{agent}]{\text{+ reducing}} N_2 \quad .$$

Particle Size

Gibbs et al.[24] have shown increased NO reduction in NO-char systems (in the absence of oxygen) with decreasing char particle size. This reduction can be due to the minimization of diffusional resistances involved in the heterogeneous NO-char reduction reactions. In fluidized-bed combustors decreasing the coal feed particle size can have an adverse affect on the combustion efficiency because of the possible increase in the elutriation of unburned char from the bed.

Staged Combustion

Experiments carried out by Gibbs et al.[24] have shown that air staging can substantially reduce NO_x emissions. In their study the primary stage of the bed was operated at substoichiometric conditions, and secondary combustion air was injected into the freeboard for improved combustion efficiency. Furusawa et al.[14] have also observed considerably lower NO_x emissions in staged combustion. The relatively lower NO_x

emissions observed in staged firing can be due to the enhancement of NO reduction reactions by CO, unburned hydrocarbons, and char in the primary stage.

Models to Project NO_x Emissions

Pereira and Beér[15] have developed a model describing the formation and destruction of NO in homogeneous reactions involving the coal volatiles. The model consists of two parts - the homogeneous reaction process of NO formation and destruction and the heterogeneous process of NO formation and the NO-char reduction. Simulated results from the theoretical model were observed to agree reasonably well with experimental data for temperatures between 600 and 800°C. Above 800°C, however, the discrepancies between model predictions and the experimental results were attributed to the lack of information on the fast reduction of NO by char. Recently, under the joint sponsorship of the DOE Fluidized Combustion Modeling and the EPA NO_x Emissions Control contracts, work has commenced at MIT to develop a model describing NO_x emissions due to the oxidation of nitrogenous compounds evolved from the devolatilized char.

The FBC NO_x emission models proposed need additional refinements so as to account for the release rate of nitrogen-containing volatiles, diffusion flames that may form during the rapid devolatilization stage, more detailed models of the oxidation and reduction reactions of coal nitrogen volatiles, and the catalytic and noncatalytic gas-solid NO_x formation and decomposition reactions involving the residual char. The heterogeneous nature and the differences among the various coal types can become a limiting factor for precise projections of NO_x emissions in FBC.

Summary

The important observations made by the research workers looking specifically at the NO_x formation-decomposition mechanisms in FBC are:

- Nitric oxide formation from fuel-bound nitrogen is the primary source of NO_x emission in FBC.
- Thermal NO formation from atmospheric nitrogen and oxygen is less favored under FBC conditions.
- Conversion of fuel-bound nitrogen is substantially less than 100 percent in FBC, suggesting that the once-formed NO is being decomposed, possibly by reducing agents such as nitrogen-containing coal volatiles (NH_3, amines, etc.), CO, hydrogen, and char, which may be present in the combustion mixture.
- Nitrogen oxide emissions from PFBC operation seem to be less than those from AFBC.
- Conversion of fuel-bound nitrogen to NO seems to depend strongly on the excess air level. Rapid production of NO immediately above the distributor plate, with substantial reduction in NO concentration in the splash region and in the freeboard, has been observed.
- Nitrogen oxide emissions seem to exhibit a temperature maximum around 750 to 800°C, suggesting that NO formation-decomposition mechanisms and/or rate-determining steps change with temperature.
- Nitrogen oxide emissions have been observed to show a gas residence time maximum, indicating the occurrence of consecutive series-type (NO formation-decomposition) reactions.
- The rate of NO-char reduction reaction seems to be influenced by pore diffusional effects.

- Staged combustion seems to reduce NO_x emissions substantially.
- Precise kinetic information for NO formation and decomposition reactions are lacking. The currently proposed NO_x emissions models also need additional refinements so as to account for reactor dynamics (mixing pattern, interphase and intraphase mass transfer effects), devolatilization rate, catalytic effects of char (carbon loading in the bed), etc.

DATA ANALYSIS

Pressurized and/or atmospheric pressure FBC NO_x emission data from ANL, B&W, Combustion Power Company, Conoco, Exxon, NCB, and PER have been gathered and are listed in Appendix A. These data consist of average NO_x emission values reported for batch combustor runs and the NO_x emissions observed at steady state from continuously operated fluidized-bed combustors.

To gain insight into the NO_x formation and destruction mechanisms, the characteristic features of the NO_x emission data collected are summarized in Appendix B. Plots showing the NO_x emissions from PFBC and AFBC as a function of temperature with percent excess air as a parameter are also included in Appendix A. Some of the observations that have been made for AFBC, for example, are briefly summarized in Table 3, which indicates an increase in NO_x emissions with an increase in percent excess air and/or temperature. In comparison with PFBC data, the NO_x emissions from AFBC units under similar operating temperatures and excess air levels seem to be higher.

Effect of Fluidized-Bed Combustor Size

The NO_x emission data reported by the various investigators for AFBC operations with excess air in the range of 15 to 20 percent are

Dwg. 2623C83

Table 3

AFBC NO_x EMISSION DATA

Source		Exxon		ANL		NCB		NCB		PER		B & W	
Unit Size		0. 07 m dia.		0. 15 m dia.		0. 68 m dia.		0. 91 m × 0. 45 m		0. 45 m × 1. 82 m		0. 91 m × 0. 91 m	
Superficial Velocity, m/s		0. 6 - 1. 2		0. 84 - 2. 7		1. 80 - 3. 3		0. 60 - 2. 45		3. 90		1. 31 - 3. 57	
Bed Depth, m		0. 15-0. 30		0. 60		0. 60		0. 63 - 2. 10		0. 32 - 0. 60		0. 28 - 0. 86	
Coal Nitrogen Content, wt%		1. 30		1. 11 - 1. 31		1. 40		1. 40		0. 99; 2. 55		0. 76; 0. 86	
Excess Air, %	Temperature, °C	No. of Data	ng NO_2/J	No. of Data	ng NO_2/J	No. of Data	ng NO_2/J	No. of Data	ng NO_2/J	No. of Data	ng NO_2/J	No. of Data	ng NO_2/J
0-5. 00	871	–	–	1	258	–	–	–	–	–	–	–	–
5. 01-10. 00	843	–	–	1	373	–	–	–	–	–	–	–	–
	871	–	–	2	246-306	–	–	–	–	–	–	–	–
	926	1	420	–	–	–	–	–	–	–	–	–	–
10. 01-15. 00	843	–	–	5	346-450	–	–	–	–	–	–	–	–
	845	–	–	–	–	–	–	–	–	–	–	1	146
	848	–	–	–	–	–	–	1	203	–	–	1	169
	871	1	347	9	141-353	–	–	–	–	–	–	–	–
	898	–	–	–	–	–	–	–	–	1	162	–	–
15. 01-20. 00	700	–	–	2	170; 182	–	–	–	–	–	–	–	–
	770-774	–	–	–	–	–	–	–	–	–	–	2	33; 181
	787	–	–	1	187	–	–	–	–	–	–	–	–
	798	–	–	–	–	–	–	3	121-204	–	–	–	–
	804	–	–	–	–	–	–	–	–	3	97-159	–	–
	810	–	–	–	–	–	–	–	–	1	123	–	–
	815	–	–	1	247	–	–	–	–	–	–	–	–
	818, 819	–	–	–	–	–	–	–	–	–	–	2	144; 180
	826	–	–	–	–	–	–	–	–	1	147	–	–
	829	–	–	–	–	–	–	–	–	–	–	2	128; 184
	838	–	–	–	–	–	–	–	–	–	–	2	127; 129
	843	–	–	2	162; 411	–	–	–	–	2	146; 175	1	176
	845	–	–	–	–	–	–	–	–	–	–	3	143-167
	848	–	–	–	–	–	–	9	125-286	–	–	–	–
	850	–	–	–	–	–	–	–	–	–	–	3	114-185
	854	–	–	–	–	1	202	–	–	4	170-193	–	–
	857	–	–	–	–	–	–	–	–	–	–	1	194
	860	–	–	–	–	–	–	–	–	3	121-146	–	–
	865	–	–	–	–	–	–	–	–	–	–	1	120
	871	3	395-483	14	219-357	–	–	–	–	3	153	–	–
	894	–	–	–	–	–	–	–	–	–	–	1	201
	898	–	–	3	387-411	–	–	–	–	–	–	–	–
	904	–	–	–	–	–	–	–	–	1	134	–	–
	915	–	–	–	–	–	–	–	–	1	166	–	–
	926	1	458	–	–	–	–	–	–	–	–	–	–
	932	–	–	–	–	–	–	–	–	1	136	–	–
	937	–	–	–	–	–	–	–	–	2	184, 212	–	–
	948	–	–	–	–	–	–	–	–	1	210	–	–
	965, 987	–	–	–	–	–	–	–	–	2	135; 152	–	–
20. 01-25. 00	766	–	–	–	–	–	–	1	224	–	–	–	–
	804	–	–	1	268	–	–	–	–	–	–	–	–
	815	–	–	–	–	1	231	–	–	–	–	–	–
	837	–	–	–	–	–	–	–	–	1	229	–	–
	843	–	–	2	414-454	2	265-272	–	–	–	–	–	–
	848	–	–	–	–	1	251	–	–	–	–	–	–
	854	–	–	–	–	1	211	–	–	–	–	–	–
	871	1	409	3	248-311	–	–	–	–	1	188	–	–
	898	–	–	1	444	1	258	–	–	–	–	–	–
25. 01-30. 00	837	–	–	–	–	1	267	–	–	–	–	–	–
	843	–	–	–	–	1	297	–	–	–	–	–	–
	871	3	398-456	–	–	–	–	–	–	–	–	–	–
	904	–	–	–	–	1	280	–	–	–	–	–	–
30. 01-35. 00	843	–	–	–	–	1	298	–	–	–	–	–	–
	854	–	–	–	–	1	194	–	–	–	–	–	–
35. 01-41. 00	843	–	–	–	–	2	256; 290	–	–	–	–	–	–
	871	1	502	–	–	–	–	–	–	–	–	–	–

plotted as a function of temperature in Figure 29. The NO_x emissions from the relatively smaller units of ANL and Exxon seem to be considerably higher than those from the bigger units of PER, B&W, and NCB, possibly because of differences in the fluid dynamics (mixing pattern), local stoichiometry, and mass transfer effects in the various units.

Effect of Coal Type and Nitrogen Content

The NO_x emission data from AFBC and PFBC units for excess air levels in the range of 15 to 20 percent and for different coals are plotted as a function of temperature in Figures 30 and 31, respectively. Apparently, under the operating conditions investigated, the NO_x emissions are independent or a weak function of the coal type and nitrogen content.

Effect of Fluidized-Bed Operating Conditions

Comparison of the NO_x emission data plotted in Figures 30 and 31 show relatively lower NO_x emissions from PFBC than from AFBC units. Apparently, for both PFBC and AFBC, there is a temperature maximum between 800 and 900°C. Additional data plotted in Figures 32 and 33 show increased NO_x emission with increasing excess air levels. The interpretation of the data to single out the effects of fluidizing velocity, bed depth, coal particle size, SO_2 emissions, and so on is difficult because of the accompanied variations in temperature and/or excess air levels.

The above analysis suggests that the temperature, excess air, and pressure are the most significant parameters. The trends observed should be assessed with caution, however, because the more precise effects may be concealed by variations in other operating parameters, fluidized-bed design variables, and analytical techniques.

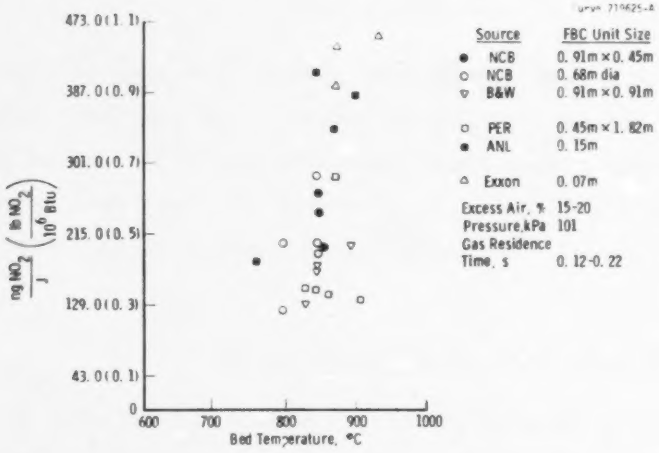

Figure 29 - Effect of Fluidized-Bed Combustor Size

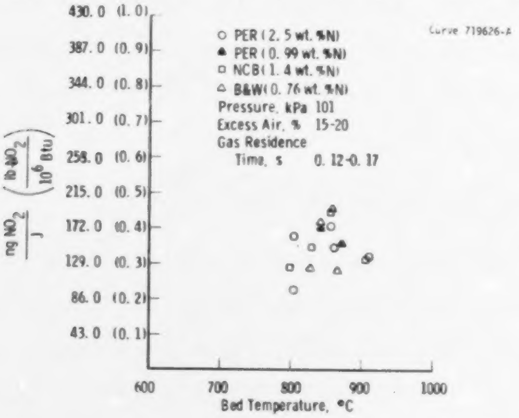

Figure 30 - Effect of Coal Nitrogen Content - AFBC

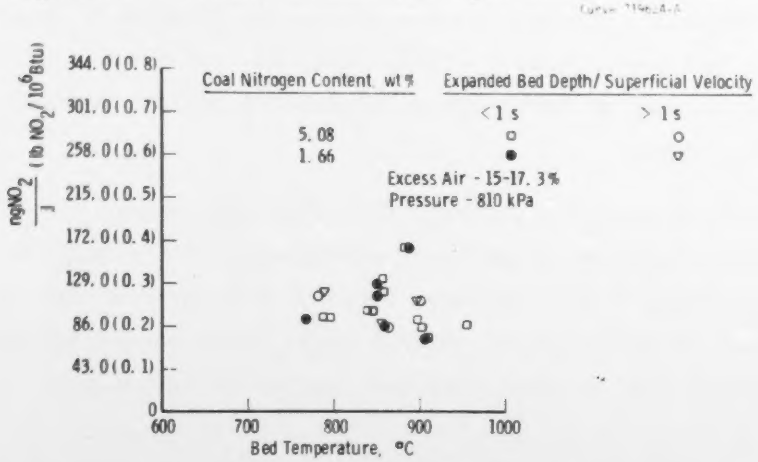

Figure 31 - Effect of Coal Nitrogen Content - PFBC

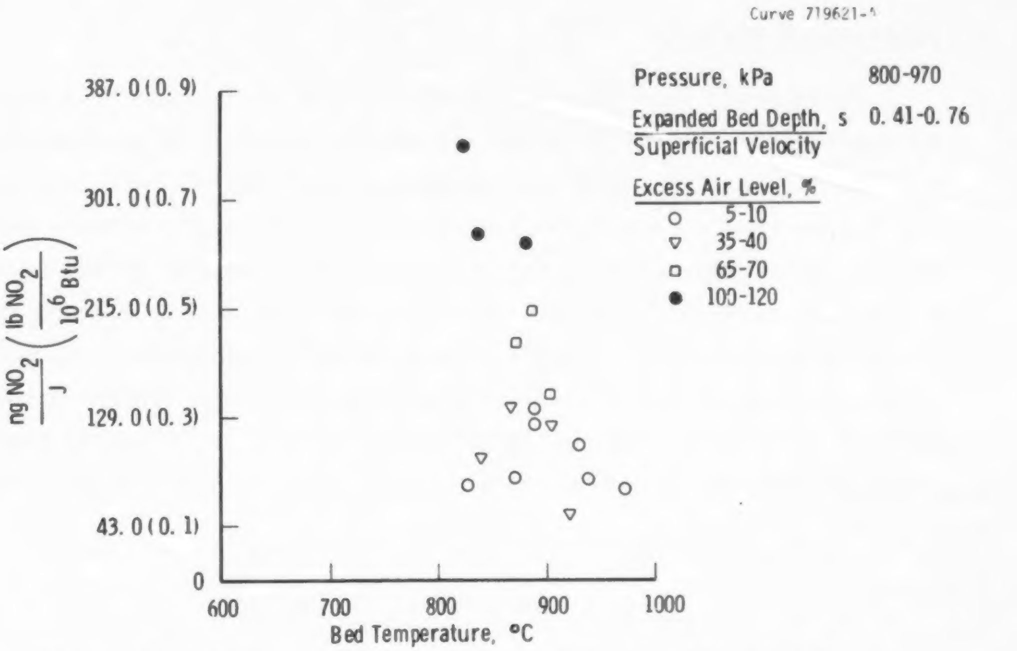

Figure 32 - Effect of Temperature and Excess Air - PFBC

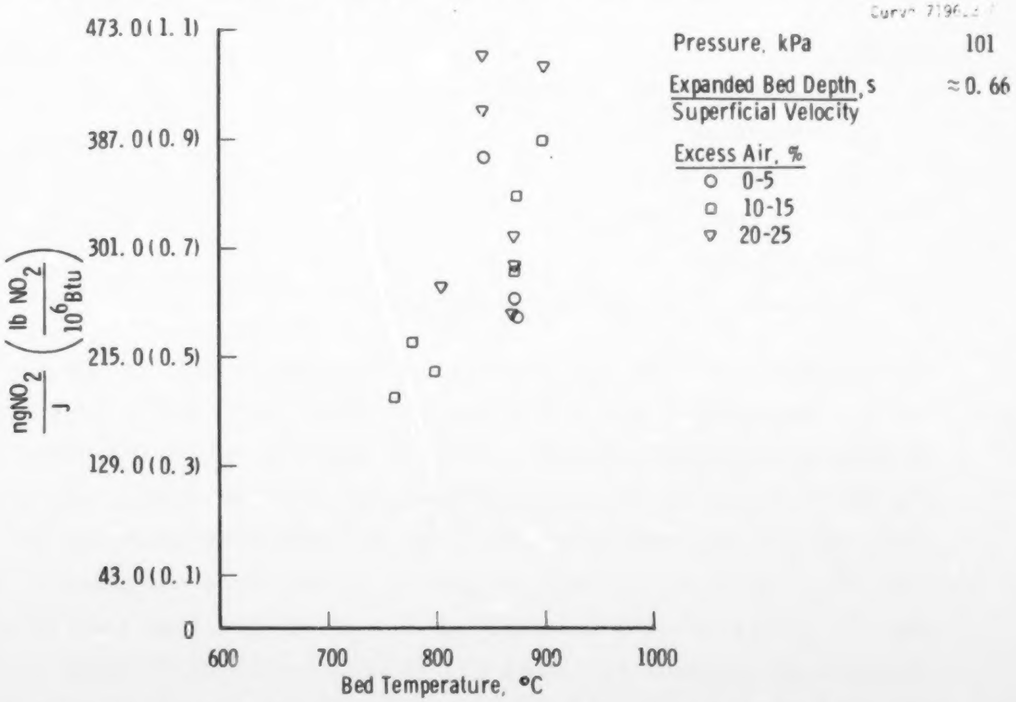

Figure 33 - Effect of Temperature and Excess Air - AFBC

Statistical Analysis

Assimilated data from both AFBC and PFBC tests have been subjected to regression analysis to develop a simple equation for projecting NO_x emissions as a function of FBC operating conditions. Data from continuously operated units have been used for regression fit because batch runs reported average emission values for NO_x that may not be representative of steady-state conditions. In the light of the discussions in the preceding sections, fluidized-bed operating pressure, temperature, percent excess air, and gas residence time have been chosen as the independent variables. Regression analysis yielded the following empirical equation describing the dependence of NO_x emissions on these variables:

$$\begin{aligned} NO_x = &- (0.5775)(P) + (4.135 \times 10^{-4})(P)^2 + (0.6598)(T) \\ &- (4.238 \times 10^{-4})(T)^2 + (1.1668)(X) \\ &- (2.759 \times 10^{-3})(X)^2 - (5.5066)(h/v) \end{aligned}$$

where

NO_x is expressed as ng NO_2/J, and
P = pressure, kPa
T = temperature, °C
X = percent excess air
h = bed depth, m
v = superficial gas velocity, m/s.

The residual variance and the correlation coefficient for the regression fit are 60 ng NO_2/J and 0.869, respectively. Such a low correlation coefficient predicts poor fit, and, as shown in Figure 34, there is considerable deviation in the experimentally observed values and in those predicted by the regression fit. The NO_x emissions predicted by the empirical equation for various operating conditions are plotted in Figure 35. These results show the experimentally observed trends, such as temperature maximum, increased NO_x emissions with an increase in excess air, and lower NO_x emissions at higher pressures. Due to the poor regression fit, however, an experimentally observed value of 43 ng NO_2/J

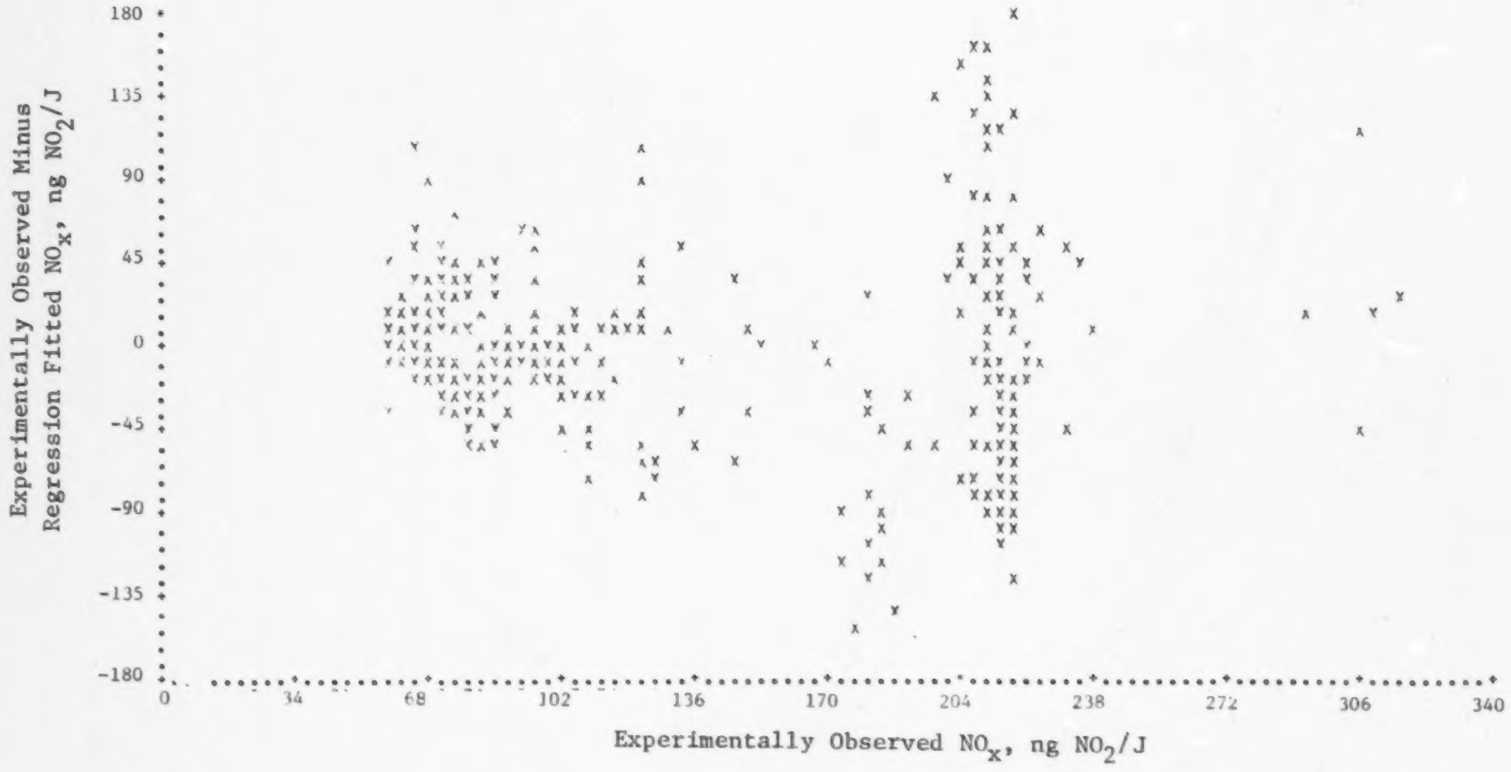

Figure 34 - Plot of Residuals - Statistical Analysis

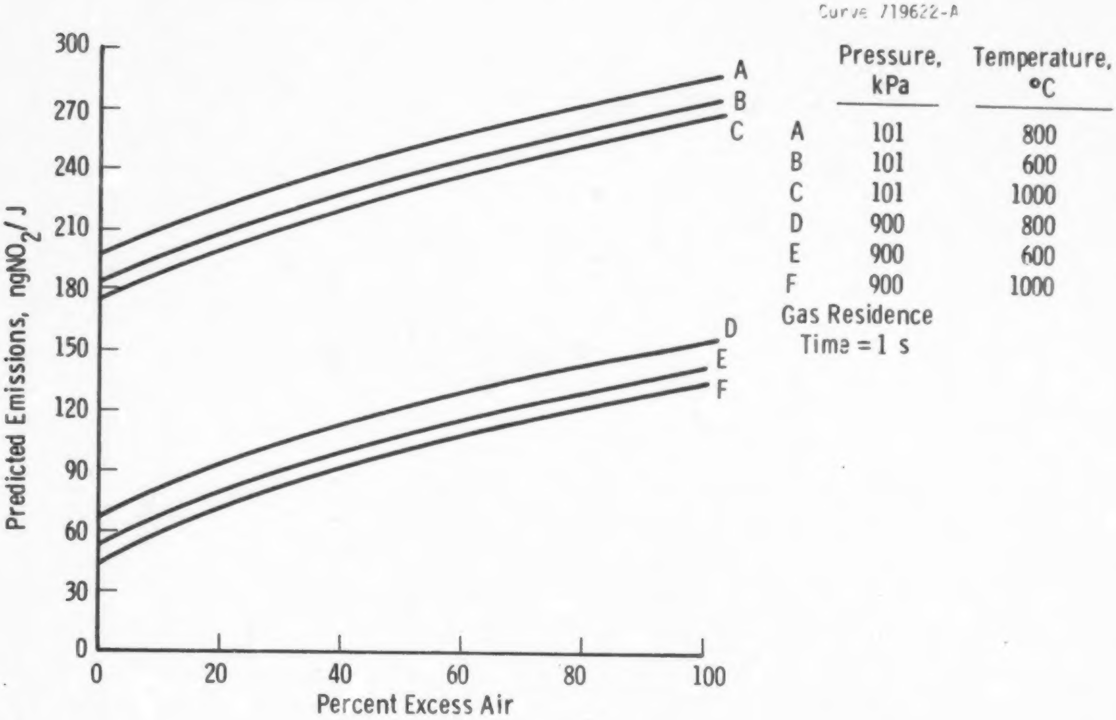

Figure 35 - Regression Fit NO_x Projections

could be predicted between 0 to 86 ng NO_2/J when the corresponding pressure, temperature, excess air, and gas residence time values were inserted in the above empirical equation. Similarly, an experimentally observed value of 215 ng NO_2/J could be predicted between 0 and 430 ng NO_2/J.

Data sets from different sources have been used in correlating the data with regression analysis. Among the various sources there exist significant variations in the fluidized-bed operating and design factors, the coal and sorbents used, and the NO_x detection methods. These differences result in an inherent scatter in the raw data used for regression analysis and could possibly explain the resulting poor regression fit. Also, it is possible that the functional dependence of NO_x emissions on the operating variables (first-order and second-order terms) chosen for regression fit are not representative of the NO_x formation-decomposition reaction mechanisms, reactor dynamics-like mixing pattern, interphase and intraphase mass transfer effects, and so on. Better regression correlations may be developed for each individual data set, but these will have limited application, and the overall objectives of the FBC technology assessment may not be fully served.

NO_x Decomposition Model

Most of the researchers investigating NO_x emissions in FBC have reported significantly higher concentrations of NO near the distributor plate (air inlet to the bed) and a decrease in NO concentration as the gas rises through the bed. NO-char reduction reactions at temperatures of 750°C and higher have been suggested to be mainly responsible for the decomposition of the once formed NO. In order to provide a preliminary test of this mechanism, we calculated kinetic rate constants for NO_x decomposition from available FBC data by assuming that all the nitrogen in the coal is released at the base of the bed and that the NO_x then decomposes according to first-order kinetics as it passes up through the depth of the bed (to reach the concentrations measured in the flue gas). The scatter in the first-order specific reaction rate constants plotted in Figure 36 show the inadequacy of the first-order decomposition model. These specific reaction rate constants, however, are within the range reported by NO-char reduction studies at MIT.

ASSESSMENT

Data sets from different sources have been gathered. Among the various sources there exist significant variations in the fluidized-bed operating and design factors, the coal and sorbents used, and the NO_x detection methods. The NO_x emission data from relatively larger fluidized-bed combustors are similar in temperature maximum, reduced emissions at higher pressures, and increased emissions with increased

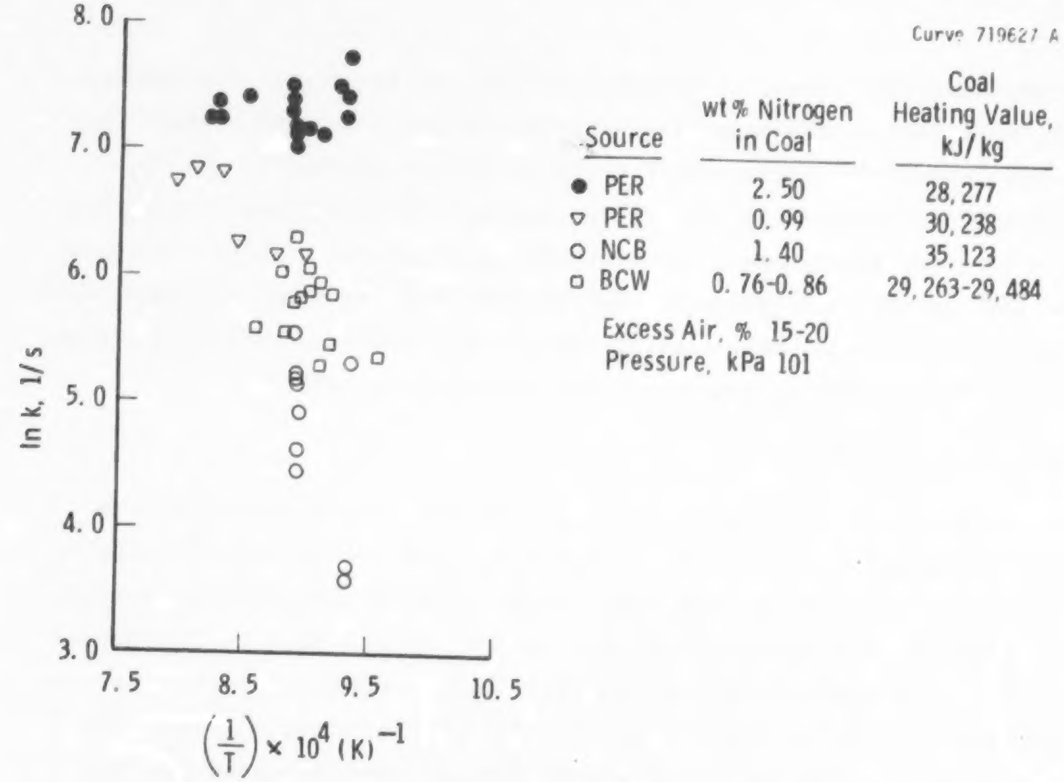

Figure 36 - NO Decomposition Model - Pseudo-First-Order Rate Constants

excess air to those previously observed in the controlled experiments in laboratory-scale fluidized-bed combustors. Data from relatively larger fluidized-bed combustors suggest that NO_x emissions under certain operating conditions could be less than 301 ng NO_2/J (0.7 lb NO_2/ 10^6 Btu). The range of excess air levels anticipated for commercial fluidized-bed combustor units is 15 to 20 percent. In this range the data from larger fluidized-bed combustors suggest that the NO_x emission levels could be on the order of 129 to 301 ng NO_2/J (0.3-0.7 lb NO_2/ 10^6 Btu). With fluidized bed combustor design modifications such as staged combustion the NO_x emissions could possibly be limited even further.

Currently, there is no generalized model available for a priori prediction of NO_x emissions in fluidized-bed combustion. Statistical analysis of the data gathered in this study resulted in poor regression fit, possibly due to the scatter in the raw data. Also, the functional dependence of NO_x emissions on the operating variables chosen for regression fit may not be representative of the NO_x formation-decomposition reaction mechanisms. Better regression correlations could be developed for each individual data set, but these would have limited application.

6. TRACE ELEMENT RELEASE

INTRODUCTION

Pilot-scale tests of the fluidized-bed combustion of coal have shown that air pollution from SO_2 and NO_x emissions can be reduced in order to meet EPA requirements. Coal contains many minor and trace elements in addition to carbon, hydrogen, nitrogen, oxygen, and sulfur, that are chemically changed or are released during combustion. In assessing the environmental impact of the FBC process, we must determine the chemical fate of these trace and minor elements and assess their potential toxicity.

In previously reported work under this contract,[2] Westinghouse applied a thermodynamic model to project the chemical fate (and emissions) of four trace elements in coal-fired FBC systems. These four elements were: lead (Pb), beryllium (Be), mercury (Hg) and fluorine (F). Since that earlier report was issued the trace element work has been extended to include further evaluation of available trace element emission data from conventional boilers and FBC systems and application of the thermodynamic model to project the chemical fate in the FBC system of eight additional elements: aluminum (Al), iron (Fe), titanium (Ti), cobalt (Co), chromium (Cr), manganese (Mn), molybdenum (Mo), and nickel (Ni).

This study emphasizes the chemical equilibrium reactions for the eight metals in the PFBC and AFBC systems operating at 100 percent excess air with 0, 90, and 99 sulfur removal efficiencies as a function of temperature. Correlation of these reaction projections with 10 and 300 percent excess air combustion covers the range expected in the alternative variations of the FBC process.

Trace Elements in Coals

Numerous reports in the literature[25-36] have indicated that the major mineral constituents of coal are silicon (Si), aluminum, titanium, calcium (Ca), magnesium (Mg), iron, phosphorous (P), sulfur (S), sodium (Na), and potassium (K). These mineral constituents exist either as aluminosilicates (illites, kaolinites, mixed layers of illite, and montmorillonite), sulfides and sulfates (pyrites, marcasites), carbonates (calcite, dolomite, siderite, ankerite), or as silica. At combustion temperatures of 750°C the clay auminosilicates release lattice-bound water and the sulfide fractions oxidize, releasing SO_2. The carbonate fractions calcine, releasing CO_2; quartz (silica) remains as a stable solid phase at high temperatures of combustion. Watt and Thorne[37] demonstrated that the ultimate fate of these constituents was principally associated with the final ash particle shape, color, and texture and could be directly related to specific initial mineral phases in coal that were present at the onset of combustion. By injecting powdered specimens of shale, kaolin, sulfides, carbonates, and accessory minerals into an air-coal gas or oxygen coal-gas flame (Table 4), they found that fused particles that had formed appeared similar to the commercial ash formed when pulverized coal is injected into boiler furnaces with sufficient air to maintain combustion.

The trace elements lead, beryllium, mercury, fluorine, cobalt, chromium, manganese, molybdenum, and nickel have the potential to exist in more than one form in coal. The exact nature of the trace element's occurrence in the coal particle may be an important factor in determining its behavior on combustion. Generally, the trace elements have been reported to be associated with either the aluminosilicate minerals (lithophilic) or the sulfide minerals (chalcophilic).[26] Miller et al.[38] correlated the trace element association of fluorine with the clay aluminosilicate fraction, beryllium with the sulfide and sulfate fraction, and mercury with both the clay and sulfur fractions. In addition to the lithophilic and chalcophilic categories, Miller classified manganese

Table 4

FUSION OF MINERAL PARTICLES IN A COAL GAS FLAME - TYPIFYING COMMERCIAL ASH PRODUCTS[37]

MINERAL GROUP	MINERAL SPECIES	FLAME COMPOSITION	APPEARANCE
SHALE	MUSCOVITE	AIR/COAL GAS	SPONGY PARTICLES GLASS SPHERES AND CENOSPHERES
	ILLITE	AIR/COAL GAS	SPONGY PARTICLES GLASS SPHERES
	MONTMORILLONITE	AIR/COAL GAS OXYGEN/COAL GAS	SPONGY PARTICLES GLASS SPHERES
KAOLIN	KAOLINITE	AIR/COAL GAS OXYGEN/COAL GAS	SPONGY PARTICLES GLASS SPHERES
CARBONATE	ANKERITE	OXYGEN/COAL GAS	OPAQUE NON-MAGNETIC SPHERES
SULPHIDE	PYRITE	OXYGEN/COAL GAS	OPAQUE MAGNETIC SPHERES AND ROUNDED PARTICLES. SOME RED HAEMATITE FRAGMENTS.
ACCESSORY SILICATE MINERALS	QUARTZ	OXYGEN/COAL GAS	UNFUSED PARTICES
	POTASSIUM FELDSPAR		GLASS SPHERES
	KYANITE		GLASS SPHERES
	HORNBLENDE		LIGHT BROWN GLASS SPHERES
	TOURMALINE		BROWN GLASS SPHERES
	BIOTITE		BROWN OPAQUE GLASS SPHERES

and molybdenum as elements associated with the carbonate or the quartz fraction in coal and chromium with quartz. The association of lead, cobalt, and nickel with either the aluminosilicate, sulfate, carbonate, or quartz fraction was not identified.

The heterogeneous nature of coal when analyzed produces a range of both trace and minor element concentrations that are the result of such factors as geographical location (Table 5), coal rank (Table 6), and location within the field or quarry. Illustrating the variation in trace and minor elements contained in both coal and sorbent materials, Table 7 presents a comprehensive listing of the elements and reported concentrations considered in this study. Consistently throughout this study only those values reported by Ruch and Gluskoter[25] will be used.

Trace Element Behavior during Combustion

The fate of these elements during coal combustion depends not only on the affinity, concentration, and distribution of each element with the inorganic coal matrix, but also on process conditions such as temperature, heating rate, exposure time at elevated temperatures,

Table 5

AVERAGE TRACE ELEMENT CONTENT OF REGIONAL COALS THROUGHOUT THE U.S, ppm[29]

Region / Element	West and Southwest	Eastern Interior	Northern Great Plains	Appalachian Region
Be	1.1	2.5	1.5	2.5
F				
Hg				
Pb				
Al				
Co	4.6	3.8	2.7	5.1
Cr	13	20	7	13
Fe				
Mn				
Mo	3.1	4.3	1.7	3.5
Ni	14	15	7.2	14
Ti	250	450	591	350

surrounding environment in either oxidizing or reducing conditions, type of coal firing, and waste process removal systems. In a fluidized-bed combustor, of course, some of these process conditions can be much different from those that exist in a conventional boiler. For example, the combustion temperature in a fluidized bed, 1100 to 1200 K, is much lower than in a 1650 K conventional boiler. The mechanism and chemical fate of the trace elements in fluidized-bed systems, however, has not been delineated because of the limited data reported in the literature and presently can only reflect an extension to low-temperature operation data from the conventionally fired boiler systems. Lyon et al.,[26] proposed the following mechanism for the behavior of the trace and minor elements during combustion in conventional coal-fired boilers:

- Complex aluminosilicates do not decompose but melt and coalesce to form slag or boiler bottom ash and fly ash.

Table 6

AVERAGE TRACE ELEMENT CONTENT OF ASH FROM U.S. COALS OF VARIOUS RANKS, ppm[29]

Rank / Element	Anthracite Coal	Bituminous Coals			Lignite
		Low Volatility	Medium Volatility	High Volatility	
Be	9	16	13	17	6
F					
Hg					
Pb	81	189	196	183	60
Al					
Co	81	172	105	64	45
Cr	304	221	169	193	54
Fe					
Mn	270	280	1432	120	688
Mo					
Ni	220	141	263	154	129
Ti					

- During initial stages of combustion, a reducing environment probably exists within the coal particle and its immediate vicinity. Under these conditions the chemical bonding of metallic elements and sulfur in sulfide mineral inclusions or between the elements and the organic matrix may be broken, with the elements forming volatile species. If the elements are dispersed in the coal organic matrix, they initially become dispersed in the gas stream when the coal is burned.
- Elements that initially are volatilized or dispersed in the flue gas stream may then be oxidized to form less volatile species that may then condense or be absorbed on the fly ash as the temperature of the flue gas drops.

Table 7

TRACE ELEMENTS IN COAL AND SORBENT MATERIALS (ppm)

COAL

ELEMENT	GLUSKOTER[25]	LYON[26]	MAGEE[27]	ORNL[28]	WEWERKA[29]	WEIR[30]
BE	1.61		0.64-3.1		2.2	0.16-2.1
F	60.94		50-160		190	54-372
HG	0.20	0.122-99	0.18			0.131-0.322
PB	34.78	4.9-7.4	4-14		17	0.15-41
AL	1.29%	1.0%-1.1%			3.1%	
CO	9.57	2.9%-3.95%			12	
CR	13.75	18-22		20	38	0.45-3.4
FE	1.92%	1.1%-1.6%			3.4%	
MN	49.40	33.8-53		34	69	16.0-142.0
MO	7.54	9-34			14.8	<0.13-1.3
NI	21.07	16			21	2.3-51.7
TI	0.07%	506-550		510	0.18%	

ELEMENT	MURTHY*[31]	KAAKINEN[32]	GOLDBERG[33]	MERRYMAN[34]	COWHERD[35]	CATO[36] (A)	(B)
BE	1.6		3	2	1.5,2.44	1.1	0.7
F	60.94			<3	121,82	117	61
HG	0.20		0.012	<2	1.91,0.15	<0.3	<0.3
PB	34.78		25	<1	3.72,9.5	8.5	8.1
AL	1.80%*	0.49+0.03%	1.0%	5%			
CO	0.57		5	10	1.45,4.8	2.3	1.5
CR	13.75			100	15.4,24	15	14
FE	2.32%*	0.37+0.02%	1.0%	NS%	2.3%	1.5%	0.74%
MN	49.4		50	100	35,50	25	57
MO	7.54	1+0.3	5	30			
NI	21.07		15	<10	14.8,15.0	4.6	<58
TI	0.09%*		500	5000	385,895	790	720

SORBENT

ELEMENT	WEIR[30]	MERRYMAN[34]	MURTHY[31] (A)	(B)
BE	0.14-3.0	<0.005		
F	103-307	~10		
HG	<.01-.02	<0.3	0.2	0.2
PB	1.3-26	3	0.2	5
AL		0.1%	0.24%	0.07%**
CO		0.3		
CR	0.57-3.5	5	~20	4.23
FE		0.02%	0.19%	1.16%**
MN	20.3-290	100	~200	42
MO	0.04-150	<3	~10	5
NI	4.3-<12	<2	~10	1
TI		2	0.02%	0.008%**

(*) Pittsburgh No. 8 Coal
(A) #1359 Limestone
(B) Tymochtee Dolomite
(**) Reported as oxides

- Since the slag is in contact with the flue gas for a short time and at a high temperature, condensation of volatiles on the slag is minimal.

Partitioning of the trace and minor elements in a conventional boiler results, according to this mechanism, between the volatile stack-gas emissions and the solid ash formation of either the slag or the fly ash. Analysis of the ash and outlet gases by Lyon[26] at the Allen Steam Plant in Memphis, Tennessee indicates that the trace and minor elements can be classified as:

- Elements that readily incorporate into slag formations: Al, Co, Cr, Fe, Mn, Ti, and possibly Ni. These elements do not volatilize in the combustion zone but form a melt of rather uniform composition, divided almost equally between the fly ash entering the electrostatic precipitator and the slag fraction. There is no apparent tendency to concentrate these elements on ash particles exiting from the electrostatic precipitator.
- Elements that concentrate in the inlet electrostatic precipitator fly ash instead of the slag, and in the outlet electrostatic precipitator fly ash instead of the inlet electrostatic precipitator fly ash: Pb and possibly Mo. These elements volatilize on combustion. With the removal of the slag in the combustion zone, lead has no opportunity to condense on the slag but condenses or becomes adsorbed on the fly ash as the flue gas cools.
- Elements that remain completely in the gas phase: Hg.

Natusch et al.,[39] proposed a volatilization-condensation or adsorption mechanism that accounted for the relation between the trace element concentration and the ash particle size. As the temperature of the flue gas decreases, volatiles condense and chemically react with or are absorbed onto the ash particle surface. Lyon[26], Cowherd[35], and Cato[36] have shown the concentration of the condensed element in a conventional boiler to be inversely proportional to the ash particle size as shown in Tables 8 through 10. This finding would be expected since the surface area increases as particle size decreases, thus increasing the concentration of condensed volatile material per unit area.

The volatile trace and minor elements emitted in the stack gases may be toxic. Cowherd et al.,[35] however, indicated that the concentration of emissions from conventional utility boilers at ground-level is less than the corresponding threshold limit value (TLV) for the various inorganic trace and minor elements, with only the concentration of beryllium approaching the level of potential concern. Limited information is reported on potentially hazardous organic emissions. Polycyclic organic material (POM) and polychlorinated biphenyls (PCB) could possibly be formed within the combustor prior to complete oxidation.

Although the exact chemical nature of the inorganic and organic trace and minor elements in the fluidized bed and stack gases is uncertain, thermodynamic calculations at equilibrium allow a first-level approximation for projecting the resulting product distribution in both the condensed and the gas phases. The chemical reactions of the trace and minor elements aluminum, cobalt, chromium, iron, molybdenum, manganese, nickel, and titanium, in addition to chlorine, have been studied for anticipated operating ranges of different fluidized-bed combustor designs. The data will be discussed in light of available experimental evidence or in-field data for the individual element reactions. An investigation of the chemical interactions of these elements is not to be presented in this report.

Table 8

TRACE ELEMENT CONCENTRATION AS A FUNCTION OF PARTICLE SIZE AS REPORTED BY LYON[26]

LOCATION: The Allen Plant, Memphis, Tennessee

DESCRIPTION: The boilers are fed with crushed coal via a cyclone arrangement.

FUEL ANALYSIS: 9.5% moisture, 34% volatile matter, 43% fixed carbon, approximately 13% ash, and 3.4% sulfur (as fired)

ASH COLLECTION: Approximately 60% goes through the slag tank, while 40% is collected by electrostatic precipitation.

Electrostatic Precipitator Inlet Fly Ash, ppm

	Microns						
Element	>15	14	9	6	4	3.5	1.4-0.5
Be							
F							
Hg							
Pb							
Al	99600	97100	100000	80000	105000	95000	92100
Co	56	49	45	50.6	67	65	83
Cr	433	240	250	320	420	490	634
Fe	181000	158000	140000	140000	160000	156000	174000
Mn	317	294	290	320	358	430	458
Mo	30	51	67	110	153	153	212
Ni							
Ti	5860	6350	6670	6810	8280	9510	9630

Electrostatic Precipitator Outlet Fly Ash, ppm

	Microns		
Element	11-2.9	2.0-1.3	0.9-0.6
Be			
F			
Hg			
Pb			
Al	57000	99200	86000
Co	60	90	80
Cr	1100	1300	1000
Fe	143000	170000	77000
Mn	404	405	430
Mo	100	165	223
Ni			
Ti	6670	12000	12600

Table 9

TRACE ELEMENT CONCENTRATION AS A FUNCTION OF PARTICLE SIZE AS REPORTED BY COWHERD[35]

LOCATION: Tennessee Valley Authority Widows Creek Steam Electric Generating Station-Unit 5

DESCRIPTION: The 125 MW utility boiler horizontally fired with pulverized coal was equipped with a mechanical fly ash collector. Sampled streams included: pulverized coal, furnace bottom ash, superheater ash, collection ash, and flue gases at the inlet and outlet of the fly ash collection.

FUEL ANALYSIS: 1.42% moisture, 34.28% volatile matter, 48.46% fixed carbon, 15.84% ash, and 3.47% sulfur (average weight percent reported values for the Appalachian coal)

ASH COLLECTION: Two four-bank multiclone units used for fly ash collection; V-type furnace bottom hoppers with water sluice for bottom ash sampling

Dust Collector Inlet Sample, ppm

	Microns				
Element	>3.96	2.35-3.96	1.61-2.35	0.87-1.61	0.56-0.87
Be	5.2	8.7	4.7	5.4	36.1
F					
Hg					
Pb	14.5	15.5	29.5	12.1	18.4
Al					
Co	26	30	28	58	75
Cr	251	458	1080	3080	4510
Fe	145000	155000	295000	121000	184000
Mn	149	274	189	569	654
Mo					
Ni	460	840	690	2460	689
Ti					

Dust Collector Outlet Sample, ppm

	Microns			
Element	>2.87	1.16-1.69	0.61-1.16	0.39-0.61
Be	12.6	8.3	3.5	86
F				
Hg				
Pb	10.5	9.3	6.8	18.5
Al				
Co	55	48	67	218
Cr	347	577	709	1790
Fe	105000	93000	68000	185000
Mn	199	288	376	1560
Mo				
Ni	414	319	478	512
Ti				

Table 10

TRACE ELEMENT CONCENTRATIONS AS A FUNCTION OF PARTICLE SIZE AS REPORTED BY CATO[36]

LOCATION: Fremont, Nebraska

DESCRIPTION: Boiler Number 6 at the Fremont Plant was an Erie City Iron Works water tube boiler with four Combustion Engineering gas- and coal-type RO burners.

FUEL ANALYSIS: 6.85-7.65% moisture, 38.26-38.75% volatile matter, 43.07-43.58% fixed carbon, 10.18-10.79% ash, 1.03-1.28% sulfur.

ASH COLLECTION: Dust collector was a mechanical cyclone type. Collected materials include: bottom ash, dust collector ash, flue gas collector inlet and outlet.

Inlet to Dust Collector, ppm

	Microns					
Element	15	3.4	2.1	1.4	0.69	0.34
Be	2.9	4.2	2.6	3.6	9.1	<10
F						
Hg						
Pb	10	270	260	570	300	560
Al						
Co	49	65	65	78	69	77
Cr	110	110	62	170	83	240
Fe						
Mn	1100	900	800	1000	1200	1300
Mo						
Ni	330	47	40	165	62	260
Ti	7700	8400	7000	6100	5400	<11000

Outlet from Dust Collector, ppm

	Microns					
Element	15	3.44	2.06	1.38	0.69	0.34
Be	4.3	3.3	3.5	6.3	<6.3	<15
F						
Hg						
Pb	200	360	360	400	320	410
Co	63	66	62	57	97	1100
Cr	92	58	62	55	<140	<360
Fe						
Mn	1300	780	1000	1200	1400	1300
Mo						
Ni	76	78	71	77	310	<340
Ti	6900	6600.	5700	4800	<14000	<36000

THERMODYNAMIC PROJECTIONS

In the previous Westinghouse study[2] the effect that sulfur, chlorine, and various fuel-to-air ratios have on the resulting partial pressures of fluorine, beryllium, mercury, and lead complexes was investigated in depth. The current study has extended this approach to projecting the reactions of aluminum, iron, titanium, cobalt, chromium, manganese, molybdenum, and nickel in the fluidized bed, where chlorine has the potential to act as an anionic carrier for each element.

The feedstock chosen in the fluidized-bed combustion study is a model 3 to 4 percent sulfur coal with a mean composition for the U.S. coals, as reported by Ruch and Gluskoter.[25] The calculated number of moles for each key element fed into the fluidized bed per 100 grams of coal burned is indicated in Table 11. Unlike the first Westinghouse

Table 11

COAL COMPOSITION[25]

Element	Wt%	Moles Fed to the Fluid-Bed per 100 grams of Coal Burned
C	70.28	5.8566
H	4.95	4.9107
N	1.30	0.0928
O	8.68	0.5425
S	3.27	0.1020
Cl	0.14	0.0039
Al	1.29	4.7811×10^{-2}
Co	9.57 ppm	1.6239×10^{-5}
Cr	13.75 ppm	2.6444×10^{-5}
Fe	1.92	3.4380×10^{-2}
Mn	49.40 ppm	8.9920×10^{-5}
Mo	7.54 ppm	7.859×10^{-6}
Ni	21.07 ppm	3.5889×10^{-5}
Ti	0.07	1.4614×10^{-3}

study, in which the concentrations for beryllium, fluorine, mercury, and lead were known for both coal and sorbent, in the present investigation only the elemental coal concentrations are used. If sufficient data were documented, reporting comprehensive elemental analyses for sorbent materials, one would expect a negligible contribution of the sorbent's trace or minor element concentration in the total (coal plus sorbent) concentration and subsequent negligible impact on the calculated trace element emission levels. Our approach has been to utilize one concentration level for the trace and minor elements for the first-order emissions estimate, emphasizing the potential chemical reactions and product distribution at equilibrium for FBC systems operating at 100 percent excess air with 0, 90, and 99 percent sulfur removal efficiencies as a function of bed temperature. We have treated the effects of the variable excess air ratios and system pressures as secondary in developing the in-bed and above-bed chemical reactions. The expectation that only minor variance in the partial pressure for the various volatile phases would result in the PFBC as against the AFBC, or in the 10 percent excess air as opposed to the 300 percent excess air system with 0 or 99 percent sulfur removal rather than the formation of additional phases, is confirmed (See Appendix C). The detailed results of the thermodynamic calculations at 100 percent excess air, 1013 kPa (10 atm) total pressure for 90 percent sulfur removal efficiencies are given in Appendix D.

Thermodynamic Equilibrium Calculation Basis

The equilibrium composition for trace element FBC conditions is calculated by minimizing the Gibbs free energy of the polyphase system, using the techniques of Geometric Programming,[40] in addition to satisfying the mass conservation equations.

The Gibbs free energy (G) of a multicomponent system is represented by a summation over the mixture chemical species; in other words,

$$G = \sum_{i} n_i G_i \quad , \tag{1}$$

where $G_i = \mu_i$ is the molar chemical potential and n_i is the number of moles of the i^{th} species. The molar chemical potential is expressed as

$$\mu_i = \mu_i^o + \delta\,(RT \ln P_i) \quad , \tag{2}$$

where for a gaseous species $\delta = 1.0$, and for a condensed species $\delta = 0$. In the above equation P_i is the partial pressure of the gaseous species, T is the gas temperature, R is the universal gas constant, and μ_i^o is the species's chemical potential at unit fugacity

$$\mu_i^o = H_i^o - TS_i^o \quad . \tag{3}$$

The molar enthalpy (H_i^o) and molar entropy (S_i^o) are the species's standard thermochemical properties which are functions of the species's standard specific heat ($C_{p,i}^o$) as shown in the following equations:

$$H_i^o\,(T) = \int_{T_r}^{T_o} C_{P,i}^o\,dT + \Delta H_f^o\,(T_r) \tag{4}$$

and

$$S_i(T) = \int_o^T \frac{C_{P,i}^o\,dT}{T} \quad , \tag{5}$$

The variable ΔH_f^o is the standard heat of formation for the compound at the reference temperature (T_r) of 298.15 K.

The chemical equilibrium program determines the value of n_i for each species in all possible solid, liquid, or gaseous phases, given the species's standard thermochemical data (as reported in the literature),[41-49] the total gas pressure, and the mass constraints on the system. Tables 12 and 13 illustrate the major combustion gas, minor, and trace species for which thermochemical data are available. The data for each species have been reduced and used as input for the chemical equilibrium calculations. It should be noted that this study considers only the reactions of compounds for which thermodynamic data are available. It is reasonable to assume that other compounds may form in the fluid-bed system, but data for such compounds have not been cited in the literature, nor have estimates of their free energy, heats of formation, or molecular constants been made in this study. We believe that compounds not reported in the literature are less likely to form than are those for which data are cited.

For each of the eight trace elements considered in the current study, the system used in the thermodynamic program was C-H-N-O-S-Cl-X,

Table 12

C-H-N-O-S-Cl SPECIES CONSIDERED IN FLUID-BED COMBUSTION REACTIONS

GASES

C
CCl
CCl_2
CCl_2O
CCl_3
CCl_4
CH
CHN
$CHNO$
CHO
CH_2
CH_2O
CH_3
CH_4
CN
CHN
CN_2
CO
CO_2
C_2
C_2Cl_4
C_2Cl_6
C_2H
C_2H_2
C_2H_4
C_2H_4O
C_2N
C_2N_2
C_2O
C_3
C_3O_2
C_4
C_4N_2
CS
COS
Cl
$ClHO$
ClO
ClO_2
Cl_2
Cl_2O
H
HCl
HNO
HNO_3
HO
HO_2
HS
H_2
H_2O
H_2S
H_2SO_4
N
NH
NH_2
NH_3
NO
NO_2
NO_3
NS
N_2
N_2H_2
N_2H_4
N_2O
N_2O_3
N_2O_4
N_2O_5
O
O_2
O_3
S
S_2
S_3
S_8
SO
SO_2
SO_3
S_2O

SOLIDS/LIQUIDS

C

Table 13

TRACE AND MINOR SPECIES CONSIDERED IN FLUID-BED COMBUSTION REACTIONS

GASES

Al
AlCl
AlClO
$AlCl_2$
$AlCl_3$
AlH
AlHO
$AlHO_2$
AlN
AlO
AlO_2
AlS
Al_2Cl_2
Al_2Cl_6
Al_2O
Al_2O_2
Co
CoCl
$CoCl_2$
$CoCl_3$
$CoCl_4$
Cr
CrCl
$CrCl_2$
$CrCl_3$
$CrCl_4$
CrN
CrO
CrO_2
CrO_2Cl_2
CrO_3
$CrO_2(OH)_2$
CrO_2OH
CrS
Cr_2
Fe
FeCl
$FeCl_2$
$FeCl_3$
Fe_2Cl_4
Fe_2Cl_6
FeH_2O_2
FeO
FeOCl
Mn
MnO
MnCl
$MnCl_2$
Mo
MoO
MoO_2
MoO_3
MoO_2Cl_2
$MoCl_4$
$MoCl_5$
$MoCl_6$
MoO_4H_2
Ni
NiO
NiCl
$NiCl_2$
NiH
$NiFe_2Cl_8$
$Ni(CO_4)_2$
$Ni(OH)_2$
Ti
TiS
TiO
TiO_2
TiCl
TiClO
$TiOCl_2$
$TiCl_3$
$TiCl_4$

SOLIDS/LIQUIDS

Al
AlClO
$AlCl_3$
$Al(OH)_3$
AlN
Al_2O_3
$Al(SO_4)_3$
Co
$CoCl_2$
CoO
$CoSO_4$
Co_3O_4
$CoS_{0.89}$
Cr
$Cr(CO)_6$
$CrCl_2$
CrN
CrO_2
CrO_3
CrS_3
$Cr_2(CO_3)_3$
Cr_2N
Cr_2O_3
Cr_2S_3
$Cr_2(SO_3)_3$
$Cr_2(SO_4)_3$
Cr_3C_2
Cr_4C
Cr_7C_3
$Cr_{23}C_6$
$FeCl_2$
$FeCl_3$
Fe
FeH_2O_2
FeH_3O_3
$FeO_{0.947}$
FeO
Fe_2O_3
$FeSO_4$
$Fe_2O_{12}S_3$
FeS
Fe_3O_4
Mn
$MnCO_3$
MnC_2
MnO
MnO_2
MnS
$MnSO_4$
$MnCl_2$
Mn_2O_3
Mn_3C
Mn_7C_3
Mn_3O_4
Mo
MoS_2
MoS_3
MoO
MoO_2
MoO_3
$MoCl_4$
$MoCl_5$
$MoCl_6$
$Mo(CO)_6$
Mo_2C
Mo_2N
Mo_2S_3
Mo_3C_2
Ni
NiS
NiO
$NiSO_4$
$NiCl_2$
Ni_3S_2
Ti
TiS_2
TiO
TiO_2
TiC_2
$TiCl_3$
$TiCl_4$
Ti_2O_3
Ti_3O_5
Ti_4O_7
TiH_2
TiC

where X is the specific trace or minor element involved. That is, interactions between the trace and minor constituents were not considered in the current discussion.

Thermodynamic Equilibrium Reactions for Noninteractive Trace and Minor Element Systems

Multiple reactions that occur in fluidized-bed combustors produce numerous solids, liquids, or gaseous compounds that are dependent on the pressure and temperature of the system. The final concentration of each phase is a function of the relative concentration of specific elements or compounds introduced into the reaction as constituents from feedstock materials. This study assumes 100 percent release of the feedstock elemental concentrations and does not account for partial conversion of the individual elements from one phase to another phase, the interaction between the various trace and minor elements with either the clay or carbonation fractions, or the kinetics of these reactions. The following sections simply describe the chemical reactions of each trace or minor element in fluidized-bed combustion systems.

Aluminum

The major chemical reaction of aluminum in FBC systems at equilibrium is the formation of aluminum oxide, $Al_2O_3(s)$. Temperatures within the various fluidized-bed coal combustion processes do not exceed the oxide melt temperature of 2054°C. Aluminum oxide, therefore, is expected to be stable as a solid principally within the temperature range of 27 to 972°C for sulfur-free processes. With 90 percent sulfur removal in systems utilizing a 3.27 percent sulfur coal, the resultant SO_x concentration in the effluent gas is sufficient at equilibrium to convert 80 percent of the $Al_2O_3(s)$ to aluminum sulfate ($Al_2(SO_4)_3(s)$) if operational temperatures are below 527°C as shown in the reaction

$$Al_2O_3(s) + 3SO_3(g) \longrightarrow Al_2(SO_4)_3(s) \quad . \qquad (6)$$

At temperatures typical of the fluidized bed (815-900°C), therefore, the major chemical form of aluminum is that of the oxide rather than the sulfate phase, as illustrated in the tables presented in Appendix D. For 0 percent sulfur removal systems where the maximum sulfur content has been released into the combustion stream, Al_2O_3 is no longer projected to be present as a solid below 527°C because of the total conversion of aluminum into the solid sulfate phase. The temperature of the oxide $\longrightarrow$ sulfate transition is a function of the total pressure of the system and sulfur concentration.

No major volatile compounds are projected to form over the Al_2O_3 (major phase)/$Al_2(SO_4)_3$ (potential minor phase) solids at fluidized-bed operating temperatures. Insignificant traces of gaseous aluminum trichloride ($AlCl_3$), aluminum oxycloride ($AlOCl$), aluminum dichloride ($AlCl_2$), aluminum dioxide (AlO_2), aluminum monoxyhydride ($AlOH$), aluminum monochloride ($AlCl$), aluminum monoxide (AlO), and aluminum trichloride dimer (Al_2Cl_6) are thermodynamically projected to exist in equilibrium with the solids at partial pressures of 10^{-12} kPa (10^{-14} atm) and below. The reaction of hydrogen chloride (HCl) with Al_2O_3 influences the formation of the volatile aluminum phases, as shown in reactions 7 and 8.

$$Al_2O_3(s) + 6HCl(g) \longrightarrow 2AlCl_3(g) + 3H_2O(g) \qquad (7)$$

$$Al_2O_3(s) + 2HCl(g) \longrightarrow 2AlOCl(g) + H_2O(g) \quad . \qquad (8)$$

In summary, the parametric calculations demonstrate that at fluidization temperatures, aluminum released from the combustion of coal will primarily exist as the solid oxide. The formation of an alternate phase, the most probable of which is the sulfate, has the potential to form from the reaction of aluminum with gaseous SO_x if equilibrium is attained locally within the bed where fluidization temperatures have decreased to below 527°C. The major chemical composition of the fines that are carried over from the bed into the cyclone are therefore projected as an oxide phase. Conversion of the fines, and subsequent stack gas emissions of the oxide to the sulfate, is not expected, nor has it been demonstrated in the presented first-level equilibrium calculations.

Iron

The principal reaction of iron in fluidized-bed combustion systems is the formation of hematite, Fe_3O_3, and diiron trisulfate, $Fe_2(SO_4)_3$. The relative concentration and stability of each compound is dependent on the concentration of sulfur and the operating temperature of the system. Hematite is the stable solid iron complex in fluidized-bed systems operating at temperatures of 815 to 900°C; transition into magnetite, Fe_3O_4, an alternate oxide structure as shown in reaction 9, would result when combustion temperatures exceeded 1462°C.

$$6Fe_2O_3(s) \longrightarrow 4Fe_3O_4(s) + O_2(g) \quad . \qquad (9)$$

The reaction of iron with sulfur released from the combustion of coal produces $Fe_2(SO_4)_3$ at low temperatures in the fluidized bed:

$$Fe_2O_3(s) + 3SO_3(g) \longrightarrow Fe_2(SO_4)_3(s) \quad , \qquad (10)$$

or

$$Fe_2O_3(s) + 3H_2SO_4(g) \longrightarrow Fe_2(SO_4)_3(s) + 3H_2O(g) \quad . \qquad (11)$$

For example, at equilibrium in fluidized-bed systems operating at 0 percent sulfur removal, solid Fe_2O_3 would be present until combustion temperatures were reduced to below 627°C, whereupon 100 percent of the iron released during combustion would react with sulfur, forming solid $Fe_2(SO_4)_3$. In the 90 percent sulfur removal systems considered in this study, Fe_2O_3 is the stable major phase formed at fluidizing temperatures and within cooler regimes, with $Fe_2(SO_4)_3(s)$ present as a seondary phase which is stable within the temperature range from 27°C to between 527 and 627°C.* Although FBC temperatures are well above 627°C, this lower temperature could be experienced by particulates carried out of the bed into the cooler flue gas zones.

For a typical U.S. mean coal the major volatile compounds, iron dihydroxide ($Fe(OH_2)$), iron dichloride ($FeCl_2$), iron trichloride ($FeCl_3$), formed pressures of 10^{-7} kPa (10^{-9} atm), as shown in Appendix D. These volatile phases have the potential to escape as stack gas emissions, to condense and deposit as iron oxide (Fe_2O_3) ($Fe_2(SO_4)_3$ if sufficient SO_x is present at equilibrium) on cooler metal surfaces, or to nucleate along the surface of entrained flue gas ash particulates. The possible series of reactions that could occur are illustrated below.

$$2Fe(OH)_2(g) + 1/2\ O_2(g) \rightarrow Fe_2O_3(s) + 2H_2O(g) \qquad (12)$$

$$(2Fe(OH)_2(g) + 2\ O_2(g) + 3SO_2(g) \rightarrow Fe_2(SO_4)_3(s) + 2H_2O(g))$$

$$2FeCl_2(g) + 2H_2O(g) + 1/2\ O_2(g) \rightarrow Fe_2O_3(s) + 4HCl(g) \qquad (13)$$

$$(2FeCl_2(g) + 2H_2O(g) + 2\ O_2(g) + 3SO_2(g) \rightarrow Fe_2(SO_4)_3(s) + 4HCl(g))$$

and

$$2FeCl_3(g) + 3H_2O(g) \rightarrow Fe_2O_3(s) + 6HCl(g) \qquad (14)$$

$$\begin{aligned}(2FeCl_3(g) &+ 3H_2O(g) + 3SO_2(g)\\ &+ 3/2\ O_2(g) \rightarrow Fe_2(SO_4)_3(s) + 6HCl(g)) \quad .\end{aligned}$$

Trace FeO, Fe_2Cl_4, FeCl, and $(Fe_2Cl_3)_2$ could be thermodynamically formed in addition to the major volatile compounds. These trace phases do not exert partial pressures greater than 10^{-14} kPa (10^{-16} atm) at combustion temperatures of 927°C.

---

*Parametric calculations were performed in 100 degree increments. Attempts at defining the specific transition or conversion temperature as a function of pressure and combustion gas compositions were not made.

Titanium

The projected equilibrium reaction of titanium in fluidized-bed combustion systems is the formation of rutile, TiO_2, as a stable solid under the various temperature, pressure, excess oxygen, and sulfur removal conditions. The major gaseous titanium compounds that could be formed in equilibrium with rutile are titanium oxydichloride ($TiOCl_2$), titanium tetrachloride ($TiCl_4$), and titanium dioxide (TiO_2), as shown in the following reactions:

$$TiO_2(s) + 2HCl(g) \xleftrightarrow{t > 727°C} TiOCl_2(g) + H_2O(g) \qquad (15)$$

$$TiCl_4(g) + 1/2\ O_2(g) \xleftrightarrow{t > 727°C} TiOCl_2(g) + 2Cl(g) \qquad (16)$$

$$TiO_2(s) + 4HCl(g) \xleftrightarrow{t < 727°C} TiCl_4(g) + 2H_2O(g) \qquad (17)$$

$$TiO_2(s) \longleftrightarrow TiO_2(g)\ . \qquad (18)$$

As shown in Appendix D, the partial pressures of none of these projected gaseous species exceed 10^{-15} kPa (10^{-17} atm) and, hence, are not considered significant.

With variation in pressure at temperatures in excess of 727°C and 10 percent excess air, the partial pressure of $TiOCl_2$ is projected to be greater than $TiCl_4$ and TiO_2, as shown in Appendix C. In systems operating at 100 percent excess air and 1013.6 to 1520.4 kPa (10-15 atm), the partial pressures of the resulting gases should be similar to those of the 10 percent excess air system ($ppTiOCl_2 > ppTiCl_4 > ppTiO_2$). If the total system pressure were decreased to 101.3 - 1520.4 kPa (1-15 atm), $TiOCl_2$ would be the major gaseous phase, with the partial pressure of TiO_2 exceeding the partial pressure of $TiCl_4$. Increasing the excess air content to 300 percent favors the formation of $TiOCl_2 > TiO_2 > TiCl_4$ at all system pressures.

When the temperature of the fluidized-bed system is less than 727°C the predominant gaseous phase is thermodynamically projected to be

$TiCl_4$. These reactions apply for both 0 and 90 percent sulfur removal systems. Variation in the sulfur content should not appreciably affect the resulting partial pressure of each gas phase. The slight decrease in the partial pressure of each compound at 90 percent sulfur removal, if monitored, would not be detectably different from that of the 0 percent sulfur removal system. Solid sulfur-titanium compounds are not expected to form in the FBC system.

Data for titanium hydroxide ($Ti(OH)_x$) compounds are not contained in the present data file. Consideration may be given later to the possible formation of these compounds.

Similarity in the degree of volatilization of the minor elements and solid formation has been projected for aluminum, iron, and titanium. The principal volatile phases that are likely to form include the chloride complexes, exerting generally insignificant partial pressures over the stable solid oxides.

Cobalt

Solid cobalt sulfate, $CoSO_4$, and cobalt oxides, CoO and Co_3O_4, are formed in FBC systems operating at 10, 100, and 300 percent excess air. The major chemical reactions include

$$3CoSO_4(s) + 1/2\ O_2(g) \longrightarrow Co_3O_4(s) + 3SO_3(g) \tag{19}$$

$$CoSO_4(s) \longrightarrow CoO(s) + SO_3(g) \tag{20}$$

$$Co_3O_4(s) \longrightarrow 3CoO(s) + 1/2\ O_2(g) \quad . \tag{21}$$

The transition of $CoSO_4$ to CoO occurs in three successive decomposition reactions as the temperature of the system is increased. Cobalt sulfate releases SO_3, forming Co_3O_4 at temperatures of 727 to 827°C for 10 percent excess air, 627 to 827°C for 100 percent excess air, and 627 to 727°C for 300 percent excess air for 0 percent sulfur removal conditions. In 90 percent sulfur removal systems the temperature at which $CoSO_4$ is stable is further reduced to between 627 and 727°C for 10 percent and 100 percent excess air, and to between 527 to 627°C for

300 percent excess air. Initially, the decomposition product is Co_3O_4, followed by the formation of a mixture of Co_3O_4 and CoO, and finally complete conversion to CoO as the temperature of the system is increased.

The major gaseous phase formed in equilibrium with the $CoSO_4/Co_3O_4/$ CoO solids is cobalt dichloride ($CoCl_2$), exerting a partial pressure of 10^{-4} kPa (10^{-6} atm) at fluidized-bed combustion bed temperatures. Depending on the operating system temperature the following reactions occur:

$$CoSO_4(s) + 2HCl(g) \longrightarrow CoCl_2(g) + H_2SO_4(g) \tag{22}$$

$$Co_3O_4(s) + 6HCl(g) \longrightarrow 3CoCl_2(g) + 3H_2O(g) + 1/2\ O_2(g) \tag{23}$$

$$CoO(s) + Cl_2(g) \longrightarrow CoCl_2(g) + 1/2\ O_2(g)\quad . \tag{24}$$

Further reaction of $CoCl_2$ with cloride yields cobalt trichloride ($CoCl_3$):

$$2CoCl_2(g) + Cl_2(g)^{*} \longrightarrow 2CoCl_3(g)\quad . \tag{25}$$

Trace quantities of the cobalt dichloride dimer, Co_2Cl_4, are formed at high combustion temperatures, in addition to cobalt monochloride, CoCl.

Data for cobalt hydroxides, oxychlorides, and oxide compounds are not contained in the present data file. Consideration may later be given to the possible formation of these compounds.

The concentration of cobalt released as a gas into the effluent stream after combustion of U.S. mean coal for a typical pressurized fluidized bed at 815 to 900°C, operating with 100 percent excess air levels and 90 percent sulfur removal efficiencies is approximately 7.0 ppm. Although cobalt is projected to be more volatile than either aluminum, iron or titanium, the projected trace emitted level is far below the minimum acute toxicity effluent level[50] of 100 ppm for cobalt fume and 1600 ppm for $CoCl_2$. Similar mechanisms of nucleation or condensation discussed for the preceding elements are applicable to the gaseous cobalt phase. Solid emissions from the bed may contain entrapped particles of either $CoSO_4$, Co_3O_4 or CoO, depending on the system's operating temperature.

---

*$Cl_2(g)$ at low temperatures; $2Cl(g)$ at high temperatures.

Chromium

In an oxidizing environment, chromium oxide, Cr_2O_3, forms as a stable solid over the temperature range of 27 to 927°C. In the presence of sulfur, conversion to the sulfate by the reaction

$$Cr_2O_3(s) + 3SO_3(g) \longrightarrow Cr_2(SO_4)_3(s) \qquad (26)$$

is not projected at conditions existing in the fluidized bed. Ash formed from combustion within the bed, therefore, and fines released into the effluent gas stream are projected to contain chromium as Cr_2O_3.

At temperatures greater than 727°C the major volatile phase projected to be formed in equilibrium with the oxide is dihydroxy-dioxychromium VI ($CrO_4H_2(g)$) as shown in reaction 27:

$$Cr_2O_3(s) + 2H_2O(g) + \frac{3}{2}\,O_2(g) \longrightarrow 2CrO_4H_2(g) \quad . \qquad (27)$$

As the local temperature within the bed decreases below 727°C, however, reaction with hydrogen chloride (HCl) and oxygen enhances the formation of the oxychloride rather than the hydroxide complex (reaction 28):

$$Cr_2O_3(s) + 4HCl(g) + \frac{3}{2}\,O_2(g) \longrightarrow 2CrO_2Cl_2(g) + 2H_2O(g) \quad . \qquad (28)$$

In addition to these major chromium volatiles, which exert maximum partial pressures of approximately 10^{-4} kPa (10^{-6} atm), trace levels of volatile chromium oxides and chlorides as CrO_3, CrO_2, $CrCl_3$, $CrCl_2$, $CrCl_4$, and CrO are projected to form at partial pressures less than 10^{-6} kPa (10^{-8} atm) for a 927°C fluidized bed.

Manganese

The thermochemical equilibrium reaction of manganese with FBC gases containing sulfur and HCl is the formation of solid manganese sulfate ($MnSO_4$) and/or the manganese oxides Mn_2O_3, and Mn_3O_4. At temperatures below 627°C $MnSO_4$ is the stable solid form in both 0 and 90 percent sulfur removal conditions. As the temperature is increased to 827°C at 10 percent excess air, and 927°C at 100 percent and 300 percent excess air, $MnSO_4(s)$ is converted to $Mn_2O_3(s)$ by the reaction

$$2MnSO_4(s) + 1/2\ O_2(g) \longrightarrow Mn_2O_3(s) + 2SO_3(g) \quad . \qquad (29)$$

At temperatures greater than 927°C $Mn_2O_3(s)$ releases oxygen, forming solid Mn_3O_4:

$$3Mn_2O_3(s) \longrightarrow 2Mn_3O_4(s) + 1/2\ O_2(g) \quad . \qquad (30)$$

The likeliest manganese complex in the fluidized bed, therefore, is Mn_2O_3, with the potential formation of $MnSO_4$ when the temperature of equilibrated bed material is reduced to below 727°C.

The principal manganese gaseous compounds projected to be formed in equilibrium with the manganese sulfate or oxide solid is manganese dichloride ($MnCl_2$). At 927°C operational temperatures the partial pressure exerted by the innocuous volatile $MnCl_2$ complex is approximately 10^{-4} kPa (10^{-6} atm). Additional gaseous phases of manganese chloride (MnCl), manganese oxide (MnO), and manganese are present at trace levels (10^{-12} kPa [$<10^{-14}$ atm]). Data for manganese hydroxides, oxides, and oxychlorides are not considered in the present data file and, hence, not included in the current study. Consideration may be given later to the possible formation of these compounds.

Molybdenum

When considering the fate of molybdenum in the combustion of coal, it is reasonable to propose that stable oxides will be formed. From the thermodynamic calculations molybdenum trioxide, MoO_3, is projected to form as the stable solid equilibrium product between 27 and 327°C. Volatilization of the compound should begin when the system temperature exceeds 327°C and is enhanced in the presence of water vapor at high temperatures, according to the reaction

$$MoO_3(s) + H_2O(g) \longrightarrow MoO_2(OH)_2(g) \quad . \qquad (31)$$

In fluidized-bed combustion gases containing chlorine, volatilization of solid MoO_3 is complete, with a subsequent reaction of molybdenum with chlorine, forming the dioxydichloride complex, MoO_2Cl_2, as shown in reactions 32 and 33.

$$MoO_3(s) + 2HCl(g) \longrightarrow MoO_2Cl_2(g) + H_2O(g) \qquad (32)$$

$$MoO_3(s) + Cl_2(g) \longrightarrow MoO_2Cl_2(g) + 1/2\ O_2(g) \quad . \qquad (33)$$

With the feedstock molybdenum concentration assumed for this study (Table 11), the partial pressures of molybdenum dioxydihydroxide ($MoO_2(OH)_2$) and MoO_2Cl_2 are thermodynamically projected to be as high as 10^{-13} and 10^{-16} kPa (10^{-15} and 10^{-18} atm) respectively, at the fluidized-bed temperature.

Gas phases that are projected to be formed in addition to $MoO_2(OH)_2$ and MoO_2Cl_2 include MoO_3, molybdenum dioxide (MoO_2), molybdenum tetrachloride ($MoCl_4$), molybdenum pentachloride ($MoCl_5$), molybdenum monoxide (MoO), and molybdenum hexachloride ($MoCl_6$) as shown in Appendix D.

In conclusion, the parametric calculations projected complete volatilization of molybdenum contained in the feed stock material. The ultimate fate of gaseous molybdenum complexes would appear to be released as stack emissions. The possiblity of condensation of molybdenum along cooled metal surfaces or nucleation by entrained ash particles should be considered as potential mechanisms that minimize the concentration of molybdenum in the stack gases. The current thermodynamic model has not taken into account potential removal sites in the process design. No data are available documenting the toxicity of molybdenum from industrial exposure.[51]

Nickel

The formation of stable nickel oxides and sulfate solids in the fluidized bed is dependent on the system parameters of temperature, pressure, excess air, and sulfur content. The major chemical reactions of nickel in fluidized-bed gas that occur at equilibrium include

$$NiO(s) \xrightarrow{t\ >\ 827°C} NiO(g) \tag{34}$$

$$NiSO_4(s) \xrightarrow{t\ =\ 527\ to\ 727°C} NiO(s) + SO_3(g) \tag{35}$$

$$NiSO_4(s) + 2HCl(g) \longrightarrow NiCl_2(g) + H_2SO_4(g) \tag{36}$$

$$NiO(s) + 2HCl(g) \longrightarrow NiCl_2(g) + H_2O(g) \tag{37}$$

$$NiSO_4(s) + H_2O(g) \longrightarrow Ni(OH)_2(g) + SO_3(g) \tag{38}$$

$$NiO(s) + H_2O(g) \longrightarrow Ni(OH)_2(g) \quad . \tag{39}$$

With 0 percent sulfur removal, nickel sulfate ($NiSO_4(s)$) is projected to be present at temperatures between 727 and 827°C for pressures of 506.5, 1013.6, and 1520.4 kPa (5, 10, and 15 atm) prior to the conversion of the solid complex into nickel oxide, NiO (reaction 35) when the operational temperature of the system is increased. The temperature of the sulfate/oxide conversion, however, is between 627 and 727°C for atmospheric, 0 percent sulfur removal systems. Similarly, Appendix D illustrates a typical 90 percent sulfur removal PFBC system operating at 100 percent excess air levels where the sulfate/oxide transition occurs between 627 and 727°C. Within the bed, therefore, the major chemical phase of nickel at equilibrium should be that of the oxide.

The major volatile nickel species projected to form over $NiSO_4(s)$ or $NiO(s)$ is nickel dichloride ($NiCl_2$). The partial pressures exerted by the chloride are approximately 10^{-4} kPa (10^{-6} atm) at the fluidized-bed temperature. Secondary gaseous phases that are projected to form include nickel hydroxide ($Ni(OH)_2$), nickel chloride (NiCl), NiO, nickel, and nickel hydride (NiH). These gaseous phases are not considered potentially toxic, even if the concentration in the stack gases were to approach the level of 100 percent release of the content in the feedstock materials during combustion. Nickel carbonyl, $Ni(CO)_4$, is considered most toxic of all the nickel compounds[51] but is not projected to form in the effluent combustion streams.

Summary of Reactions

Table 14 illustrates the resulting partial pressures of the gaseous aluminum, cobalt, chromium, iron, manganese, molybdenum, nickel, and titanium compounds and the number of moles of condensed phases if we assume 100 percent combustion release of the individual elements in the feedstock materials for a FBC system operating at 100 percent excess air and 1013 kPa (10 atm) total pressure, with 90 percent sulfur removal efficiencies. As indicated previously, these levels reflect combustion of a U.S. mean coal within the fluidized bed and do not present the reactions of interactions of carbonate (calcium and magnesium) and clay (aluminum and silicon) with the trace and minor elements.

The levels of sulfur present in the various parametric calculations were chosen to illustrate sulfur removal efficiencies (0, 90, and 99 percent removal) for systems in which the coal-to-sorbent feed ratios is approximately 3.6.

A summary of the trace and minor element equilibrium calculations indicating the principal condensed and volatile phases projected to be formed and the volatilization percentage of each element from the feedstock material is presented in Table 15. Thermodynamically, the elements may be classified as those that have the potential to volatilize completely at combustion temperatures within the fluidized bed (i.e., Mo), those that have the potential to volatilize partially (i.e., Co,

Table 14

PARTIAL PRESSURE OF GASEOUS COMPOUNDS AND MOLES OF CONDENSED COMPOUNDS IN PFBC PROCESSES AT COMBUSTION TEMPERATURES

Fluid Bed Combustion - Partial Pressure of Gaseous Compounds
100% Excess Air
90% Sulfur Removal
10 Atmospheres Total Pressure

Compound	927°C (1700°F)	827°C (1521°F)	727°C (1341°F)	627°C (1161°F)
CrO_4H_2	.3085-05	.1395-05	.5435-06	.1746-06
MoO_4H_2	.1158-05	.1143-05	.1122-05	.1073-05
CrO_2OH	.4485-06	.7081-07	.7670-08	.5036-09
$CoCl_2$	.3246-06	.9051-07	.1783-07	.1835-09
$MnCl_2$	.2928-06	.7825-07	.1563-07	.2956-09
$NiCl_2$	.2278-06	.8949-07	.2874-07	.6712-09
$Ni(OH)_2$	.3859-07	.5283-08	.4869-09	.2511-11
MoO_2Cl_2	.3466-08	.8095-08	.2183-07	.7003-07
CrO_3	.1995-08	.1805-09	.9972-11	.2854-12
$FeCl_2$	.1064-08	.1820-09	.2151-10	.1489-11
$Fe(OH)_2$	.3018-09	.1704-10	.5349-12	.7691-14
$CoCl_3$	.3573-10	.2421-10	.1383-10	.5198-12
$FeCl_3$	.2492-10	.1523-10	.8337-11	.3715-11
MoO_3	.1144-10	.1352-11	.1015-12	.4091-14
NiCl	.4614-11	.1513-12	.2454-14	.1485-17
CrO_2	.1721-12	.2221-14	.1178-16	.1908-19
CoCl	.1001-12	.1650-14	.1086-16	.1749-20
Co_2Cl_4	.5560-13	.1803-13	.3911-14	.3424-17
MnCl	.1255-13	.1644-15	.8772-18	.1981-21
NiO	.1113-13	.8044-16	.2135-18	.1430-22
$AlCl_3$	.1148-14	.2712-15	.4802-16	.5485-17
$CrCl_3$	.8902-15	.1881-15	.2839-16	.2706-17
$CrCl_2$	.3277-15	.1174-16	.2112-18	.1505-20
$TiOCl_2$	.7915-16	.3890-17	.1039-18	.1188-20
AlOCl	.7319-16	.1183-17	.8296-20	.1878-22
$CrCl_4$	.5618-16	.5141-16	.4514-16	.3700-16
FeO	.2248-16	.6581-19	.5811-22	.1031-25
MnO	.1609-16	.5125-19	.5032-22	.1448-26
Ni	.1907-16	.4735-19	.3494-22	.4908-27
$TiCl_4$	.5341-17	.3147-17	.1679-17	.7312-18
TiO_2	.3896-17	.1318-19	.1399-22	.3160-26
Fe_2Cl_4	.7713-18	.8209-19	.5444-20	.1769-21
Mn	.5051-19	.5707-22	.1619-25	.1023-30
FeCl	.4511-19	.1696-21	.2036-24	.5202-28
AlO_2	.1636-19	.4495-22	.3747-25	.6367-29

Table 14 (Cont'd)

$TiCl_3$	.6723-20	.4032-21	.1378-22	.2105-24
$AlCl_2$	.4300-20	.5440-22	.2843-24	.4405-27
CrO	.3581-20	.4201-23	.1253-26	.6004-31
MoO_2	.9955-21	.5174-23	.9090-26	.3688-29
NiH	.3757-21	.4356-24	.1287-27	.5905-33
Fe	.3134-21	.1960-24	.2727-28	.5076-33
CrCl	.1366-21	.2835-24	.1669-27	.1819-31
$(FeCl_3)_2$	.8435-22	.1064-21	.1399-21	.1732-21
TiOCl	.4497-23	.1105-25	.8068-29	.1143-22
AlOH	.5882-24	.5490-27	.1246-30	.4298-35
$MoCl_4$	.2616-24	.1082-24	.3638-25	.9093-26
AlCl	.1178-24	.1324-27	.3772-31	.1687-35
$TiCl_2$	.3466-26	.1041-28	.9714-32	.1832-35
Cr	.3024-27	.5195-31	.1548-35	<-35
AlO	.1933-27	.4842-31	.2268-35	<-35
TiO	.8097-29	.1031-32	<-35	<-35
$MoCl_5$	.5311-29	.4887-29	.4302-29	.3504-29
Al_2Cl_6	.1430-31	.2232-32	.2447-33	.1507-34
$MoCl_6$	.6073-37	.6452-37	.6775-37	.6880-37

Fluid Bed Combustion - Moles of Condensed Compounds
100% Excess Air
90% Sulfur Removal
10 Atmospheres Total Pressure

Compound	927°C (1700°F)	827°C (1521°F)	727°C (1341°F)	627°C (1161°F)
Al_2O_3	.2390-01	.2390-01	.2390-01	.2390-01
Co_3O_4	.4668-05	.5201-05	.0000	.0000
Co_5O_4	.0000	.0000	.1610-04	.1619-04
Cr_2O_3	.2790-05	.8579-05	.1306-04	.1306-04
Fe_2O_3	.1719-01	.1719-01	.1719-01	.1719-01
Mn_2O_3	.4397-04	.4470-04	.4491-04	.0000
$MnSO_4$	.0000	.0000	.0000	.8989-04
NiO	.3399-04	.3521-04	.3562-04	.0000
$NiSO_4$	.0000	.0000	.0000	.3576-04
TiO_2	.1460-02	.1460-02	.1460-02	.1460-02

Dwg. 2624C84

Table 15

SUMMARY OF TRACE AND MINOR ELEMENT REACTIONS IN FLUIDIZED-BED COMBUSTION SYSTEMS

Element	Coal Wt %/ppm	Condensed Phases	Sulfate/Oxide Conversion Reactions	Temperature Range for the Formation of Stable Oxide Solids	Temperature Range for 1% Volatilization	Volatile Phases*	Percent Volatilization at 927°C (1200 K)**
Al	1.29%	Al_2O_3, $Al_2(SO_4)_3$	$Al_2(SO_4)_3(s) \xrightarrow{700\text{-}800\ K} Al_2O_3(s) + 3SO_3(g)$	Al_2O_3 (800-1200 K)	> 1200 K	$AlCl_3$, AlOCl, $AlCl_2$, AlOH, AlCl, AlO, Al_2Cl_6	0.02
Co	9.57 ppm	$CoSO_4$, Co_3O_4, CoO	$3CoSO_4(s) + 1/2\ O_2(g) \xrightarrow{1000\text{-}1100\ K}$ $Co_3O_4(s) + 3SO_3(g)$	Co_3O_4 (1100-1200 K)	1000-1100 K	$CoCl_2$, $CoCl_3$, Co_2Cl_4, CoCl	13.76
Cr	13.75 ppm	Cr_2O_3	$Cr_2O_3(s)$	Cr_2O_3 (300-1200 K)	1000-1100 K	CrO_4H_2, CrO_2Cl_2, CrO_2OH, CrO_3, CrO_2, $CrCl_3$, $CrCl_2$, $CrCl_4$, CrO, CrCl, Cr	78.6
Fe	1.92%	Fe_2O_3, $Fe_2(SO_4)_3$	$Fe_2(SO_4)_3(s) \xrightarrow{800\text{-}900\ K}$ $Fe_2O_3(s) + 3SO_3(g)$	Fe_2O_3 (900-1200 K)	> 1200 K	$FeCl_2$, $Fe(OH)_2$, $FeCl_3$, FeO Fe_2Cl_4, FeCl, $(FeCl_3)_2$, Fe	0
Mn	49.40 ppm	$MnSO_4$, Mn_2O_3, Mn_3O_4	$2\ MnSO_4(s) + 1/2\ O_2(g) \xrightarrow{800\text{-}900\ K}$ $Mn_2O_3(s) + 2SO_3(g)$	Mn_2O_3 (1000-1200 K)	1000-1100 K	$MnCl_2$, MnCl, MnO, Mn	2.2
Mo	7.54 ppm	MoO_3	$MoO_3(s)$	MoO_3 (300-700 K)	400-500 K	MoO_4H_2, MoO_2Cl_2, MoO_3, MoO_2, $MoCl_4$, MoO, $MoCl_5$, $MoCl_6$	100
Ni	21.07 ppm	$NiSO_4$, NiO	$NiSO_4(s) \xrightarrow{900\text{-}1000\ K} NiO(s) + So_3(g)$	NiO (1000-1200 K)	1000-1100 K	$NiCl_2$, $Ni(OH)_2$, NiCl, NiO, Ni, NiH	5.05
Ti	0.07%	TiO_2	$TiO_2(s)$	TiO_2 (300-1200 K)	> 1200 K	$TiOCl_2$, $TiCl_3$, $TiCl_2$, TiCl, $TiCl_4$, TiOCl, TiO_2, TiO	0

*Major volatile phases are reported initially

**Percent volatilization at 927°C for a FBC system operating at 1013 kPa, with 90% sulfur removal and 100% excess air

Cr, Mn, Ni), and those that will remain in condensed ash phases with almost no volatilization (i.e., Al, Ti, Fe). The elements that partially or completely volatilize may condense along cooler metal surfaces within the system or nucleate through either a physical adsorption mechanism or chemical reaction with entrained flue gas ash particles. In the final particle control device (a fabric filter or electrostatic precipitator), for example, in an AFBC system operating between 150 and 375°C, condensation or nucleation reactions of the molybdenum, cobalt, chromium, manganese, nickel gaseous complexes with the entrained ash may occur, thus reducing the concentration of trace and minor elements in the stack gases. In a PFBC system with hot gas and particulate cleaning, however, a higher concentration of volatile complexes is likely to pass through the control device and escape as a stack gas emission product.* Utilizing the thermodynamic calculations for the trace and minor elemental product distribution in the fluidized bed as a first-level approximation for projecting the ultimate fate and stack gas emission concentration is therefore useful. With this basic understanding further modeling which requires additional information concerning the process design, the partitioning of gaseous phases with entrained ash materials, and reaction kinetics will aid in ultimately determining the fate of both innocuous and potentially toxic elements or complexes within the FBC system.

ASSESSMENT

Gas phase measurements of the volatilized trace and minor elements in the combustion zone of coal combustors and stack gas emission levels have not been made as such. The extent to which the trace and minor elements partially or fully volatilize on combustion, however, can be estimated from reported data by determining the depletion of the specific element in the various slag or ash formations in the particular systems. The appearance of the specific element in, for example, the fly ash fines, is not absolute evidence that volatilization is occurring. The element may be present in that portion of the coal mineral matter that is released as fly ash, without prior volatilization and recondensation. Consistently higher concentrations in increasingly finer ash particle fractions, however, certainly suggests that volatilization is a candidate, initial mechanism. Our equilibrium projections on the volatility percentages for specific trace and minor elements during coal combustion agree relatively well with the experimental data reported by Oak Ridge National Laboratory (ORNL)[28] for a conventional coal-fired steam plant. The following comparison results (Westinghouse PFBC projections of volatility in parentheses): aluminum ~0% (0.02%), cobalt 33% (14%), nickel 43% (5%), and molybdenum 73% (100%). We project cobalt and nickel to be thermodynamically less volatile than ORNL observed. This difference may be attributed to either an external contribution of the elements from process materials or alloys or, in part, to the inaccuracies in experimental data for the molecular constants of the various complexes used in this study. More practically, the higher volatility of cobalt and nickel in the conventional boiler system may be attributed to higher combustion temperatures.

---

*The thermodynamic emission levels for the projected volatile Al, Co, Cr, Fe, Mn, Mo, Ni, and Ti phases (without consideration given to the potential reduction in concentration when particulate removal systems are employed) are expected to be innocuous at equilibrium.

Although at equilibrum 100 percent of the total molybdenum content is projected to volatilize at PFBC temperatures, ORNL detects only 73 percent volatilization, even though the conventional furnace operates at higher combustion temperature concentrate on the surface of entrained ash particles. This result through either physical adsorption or chemical reaction of the gaseous oxyhydroxide or oxychloride molybdenum in the effluent streams when efficient particulate removal systems are employed. Similary, if particulate removal is not an integral part of the plant, or if particulate removal occurs prior to the condensation/adsorption reaction, emissions of molybdenum, possibly as MoO_3 fume, may be increased.

The sole exception to the relative agreement between the ORNL data and our projections is chromium. The ORNL study found the fly ash to be significantly enriched in chromium, even though the concentration in the slag fraction was not depleted. The ORNL sampling indicated an enrichment corresponding to between 24 and 40 percent of the original chromium content of the feedstock coal, as opposed to the thermodynamic calculations which predict 79 percent volatilization for FBC operations using a feedstock coal that contained a lower chromium content. The ORNL team suggested that chromium removed from the boiler tubes may be responsible for the enrichment. If the thermodynamic calculations were repeated using the ORNL's higher-chromium coal, the adjusted equilibrium value would predict 47 percent volatilization.

Based on experimental work by Swift[52] at ANL, where trace element mass balances around a 6 in. bench-scale combustor were conducted, emission levels of 25 percent for chromium (77%),* 0 to 20 percent for cobalt (14%), and 0 percent for iron (0%) and manganese (2.2%) were projected for PFBC systems. Emission levels, however, were not projected for aluminum, molybdenum, nickel, or titanium. The retention of chromium may result from the formation of stable spinel complexes, typically cobalt ($CoCrO_4$) or magnesium chromate ($MgCrO_4$), or that enrichment and consequently lower emission concentrations, may have resulted from adsorption/condensation mechanisms of chromium with the entrained ash - both of which have not been accounted for in the first level noninteractive FBC equilibrium model.

The current work[53] on the pressurized FBC at the Exxon miniplant provides additional information that illustrates the fate of the trace and minor elements during combustion and the projected flue gas emission concentration. Analytical techniques determining the trace and minor element concentration in the feedstock materials and resulting ash include ICP (Inductively Coupled Plasma Emission Spectroscopy), NAA

---

*Westinghouse equilibrium projections at 927°C are indicated in parentheses.

(Neutron Activation Analysis), and SSMS (Spark Source Mass Spectroscopy). Variations in the resulting percent ratios of the mass of elements in the flue gas to the total mass of each element in all input streams were noted: Aluminum, 0.006-0.04 percent; cobalt, 0.20-43.42 percent; chromium 7.57-9.84 percent; iron, 0.07-1.65 percent; molybdenum, 15.02-18.26 percent; manganese 0.23-33.88 percent; nickel, 3.22-7.26 percent; and titanium 0.003-0.01 percent.* The thermodynamic equilibrium projection for the trace and minor elements considered in this study, with the exception of chromium and molybdenum, are within the concentration ranges Exxon reported. When the potential stream locations where partitioning of the elements occurs through gas/ash interactions are reviewed, it is evident that depletion of the elements from the flue gas results particularly at the secondary cyclone. It is at this location that gaseous chromium and molybdenum may be removed from the effluent stream, thus lowering the projected thermodynamic equilibrium volatilization percentage.

The current studies have only begun to determine the possible reactions of trace elements throughout FBC processes. Although a complete understanding of the process would require knowledge of the compounds in which these elements are combined in the feedstock material and of the resulting chemical phases and the kinetics of each reaction that occurs during combustion, the thermodynamic projects at equilibrium provide a first-level approximation of the possible distri-bution of the elements or phases characteristic of the effluent and solid materials. Further comparison of the initial projections with future reported data from FBC units and conventional power stations, and an inclusion of additional elements and their interactions with emphasis given to systems modeling and partitioning mechanisms, will provide a more complete understanding of the trace and minor element chemistry in the FBC process.

---

*Exxon test conditions: 890°C bed temperature, 832°C secondary cyclone temperature, 1.5 m^3/min superficial gas velocity, 3.3 m bed height, 40% excess air, 86.3 kg/hr coal feed rate, 13.2 kg/hr sorbent feed rate, 900 kPa; feedstock materials: 2 percent sulfur Champion coal and 0.6 percent sulfur Kentucky coal, and Pfizer No. 1337 dolomite.

7. REFERENCES

1. Newby, R. A., N. H. Ulerich, E. P. O'Neill, D. F. Ciliberti, and D. L. Keairns, Effect of SO_2 Emission Requirements on Fluidized Bed Combustion Systems; Preliminary Technical/Economic Assessment. Report to EPA, Westinghouse Research and Development Center, Pittsburgh, PA, August 1978, EPA-600/7-78-163, NTIS PB 286 971/7ST.

2. Alvin, M. A., E. P. O'Neill, L. N. Yannapoulos, and D. L. Keairns, Evaluation of Trace Element Release from Fluidized Bed Combustion Systems. Report to EPA, Westinghouse Research and Development Center, Pittsburgh, PA, March 1978, EPA-600/7-78-050, NTIS PB 281 321.

3. Exxon Research and Engineering, Linden, NJ, Monthly Progress Report No. 113 to EPA, July 1979, EPA Contract 68-02-1312.

4. Ciliberti, D. F., D. L. Keairns, and D. H. Archer, Particulate Control for Fluidized Bed Combustion Processes. Proceedings of the Fifth International Fluidization Conference, Washington, DC, December 12-14, 1977, McLean, VA: The Mitre Corporation, 1978.

5. Keairns, D. L., et al. Fluidized Bed Combustion Process Evaluation - Phase II - Pressurized Fluidized Bed Coal Combustion Development, Report to EPA, Westinghouse Research Laboratories Pittsburgh, PA, September 1975, EPA-650/2-75-027c, NTIS PB 246 116.

6. Levenspiel, O., D. Kunii, and T. Fitzgerald, The Processing of Solids of Changing Size in Bubbling Fluidized Beds, Powder Technology, 2 (1968/69) 87-96.

7. PFBC Component Test and Integration Unit, Title 1 report to DOE, Stearns-Roger Engineering Co., March 1978, Contract EY-76-C-02-4085.

8. Yagi, S., D. Kunii, Studies on Combustion of Carbon Particles In Flames and Fluidized Beds, 5th International Symposium on Combustion, 231-244 (1955).

9. Yagi, S., and T. Aochi, Paper presented at the Society of Chemical Engineers (Japan) Spring Meeting (1955).

10. Merrick, D., and J. Highley, Particle Size Reduction and Elutriation In a Fluidized Bed Process, AIChE Symposium Series No. 137, Vol. 70, 1974, 366.

11. Menguturk, M., and E. F. Sverdrup, Tolerance of a Large Electric Utility Turbine to Erosion Damage by Coal-Ash Gas Particles, ASTM Symposium on Erosion, Vail, CO, October 24-26, 1977.

12. Lancaster, B. W., and D. F. Ciliberti, Advanced Coal Gasification System for Electric Power Generation, Report to ERDA, Westinghouse Research Laboratories, Pittsburgh, PA, January 1974, Contract E(49-18)-1514.

13. Zeldovich, J., The Oxidation of Nitrogen in Combustion and Explosions, Acta Physicochemica, URSS, 21(4): 577; 1946.

14. Furusawa, T, et al., Abatement of Nitric Oxide Emission in Fluidized Bed Combustion of Coal, J. Chem. Eng'g, Japan, 11(5): 377; 1978.

15. Pereira, F. J., et al., NO_x Emission from Fluidized Bed Coal Combustion, 15th Symp. (International) on Combustion, Tokyo, August 25-31, 1974, Pittsburgh: The Combustion Institute; 1975: 1149-1156.

16. Jonke, A. A., et al., Reduction of Atmospheric Pollution by the Application of Fluidized Bed Combustion, Argonne National Laboratory, Argonne, IL, 1969, ANL/ES-CEN-1001.

17. Kirner, W., The Occurrence of N in Coal, Chemistry of Coal Utilization, Vol. 1, H. H. Lowry, ed. New York: John Wiley & Sons, Inc.; 1945.

18. Beér, J. M., and G. B. Martin, Application of Advanced Technology for NO_x Control: Alternate Fuels and Fluidized Bed Coal Combustion, AIChE Symposium Series, 74(175): 93; 1974.

19. Pereira, F. J., J. M. Beér, and B. M. Gibbs, Nitric Oxide Emissions from Fluidized Coal Combustion, The Combustion Institute, Central States Section Spring Meeting, April 5-6, 1976.

20. Chronowski, R. A., and B. Molayem, NO_x Emissions from Atmospheric Fluidized-Bed Boilers, presented at ASME-IEEE Joint Power Generation Conference, Portland, OR, Sept. 28 - Oct. 1, 1975.

21. Pereira, F. J., Nitric Oxide Emission from Fluidized Coal Combustion, PhD thesis, The University of Sheffield, England, 1975.

22. Vogel, G. J., et al., Reduction of Atmospheric Pollution by the Application of Fluidized-Bed Combustion and Regeneration of Sulfur-Containing Additives, Argonne National Laboratory, Argonne, IL, 1974, ANL/ES-CEN-1007.

23. Hammons, G., and A. Skopp, NO_x Formation and Control in Fluidized-Bed Coal Combustion Processes, ASME Winter Annual Meeting, Washington, DC, 1971.

24. Gibbs, B, and J. M. Beér, Concentration and Temperature Distributions in a Fluidized Bed Coal Combustor, Proceedings of Combustion Institute: European Symposium, F. Weinberg, ed., New York: Academic Press; 1973.

25. Ruch, R. R., H. J. Gluskoter, and N. F. Shimp, Occurrence and Distribution of Potentially Volatile Trace Elements in Coal. Report to EPA, Illinois State Geological Survey, July 1974, EPA-640/2-74-054, NTIS PB 238 091.

26. Lyon, W. S., Trace Element Measurements at the Coal-Fired Steam Plant. Cleveland: CRC Press; 1977.

27. Magee, E. M., H. J. Hall, and G. M. Varga, Jr., Potential Pollutants in Fossil Fuels. Report to EPA, Esso Research & Engineering Co., Linden, NJ, June 1973, NTIS PB 225 039.

28. Klein, D. H., A. W. Andren, and N. Bolton, Mass Balance for Thirty-three Elements at a Coal Fired Power Plant, Oak Ridge National Laboratories, Oak Ridge, TN, 1974.

29. Wewerka, E. M., J. M. Williams, P. L. Wanek, and J. D. Olsen, Environmental Contamination from Trace Elements in Coal Preparation Wastes. A Literature Review, Los Alamos Scientific Laboratory, Los Alamos, NM, NTIS PB 267 339.

30. Weir, A., The Environmental Effects of Trace Elements in the Pond Disposal of Ash and Flue Gas Desulfurizaton Sludge. Report to EPRI, Research Project 202, Southern California Edison Co., Rosemead, CA, September 1975.

31. Murthy, K. S., D. W. Hissong, R. A. Schilling, K. C. Sekkar, and H. Nack, First Topical Report on Engineering Review of Fluidized-Bed Combustion Emissions. Report to EPA, Contract 68-02-2138, Battelle Memorial Laboratories, Columbus, OH.

32. Kaakinen, J. W., Trace Element Study in a Pulverized-Coal-Fired Power Plant, Dissertation, Boulder, CO: University of Colorado; 1974.

33. Bertine, K. K., and E. P. Goldberg, Fossil Fuel Combustion and the Major Sedimentary Cycles, Science, 173: July 1971; 233-35.

34. Merryman, E. L., A. Levy, G. W. Felton, K. T. Liu, Method for Analyzing Emissions from Atmospheric Fluidized Bed Combustors. Report to EPA, Battelle Memorial Laboratories, Columbus, OH, April 1977, EPA-600/7-77-034, NTIS PB 271 514.

35. Cowheard, C. M., M. Marcus, C. M. Guenther, J. L. Spigarelli, Hazardous Emisson Characteristics of Utility Boilers. Report to EPA, Midwest Research Institute, Kansas City, MO, July 1975, EPA-650/2-75-066, NTIS PB 245 017.

36. Cato, G. A., Field Testing, Trace Element and Organic Emissions from Industrial Boilers. Report to EPA, KVB Engineering Inc., Tustin, CA, October 1976, EPA-600/2-76-086b.

37. Watt, J. D., and D. J. Thorne, Composition and Pozzolanic Properties of Pulverized Fuel Ashes, I. Composition of Fly Ashes from Some British Power Stations and Properties of Their Component Particles, Journal of Applied Chemistry, 15: 585; December 1965.

38. Miller, W. G., Relationships between Minerals and Selected Trace Elements in Some Pennsylvanian Age Coals of Northwestern Illinois, M. S. thesis, Urbana, IL: University of Illinois; 1974.

39. Natusch, D. F. S., J. R. Wallace, and C. A. Evans, Jr., Toxic Trace Elements: Preferential Concentration in Respirable Particles, Science, 183: 202; 1974.

40. Duffin, R. J., E. L. Peterson, and C. Zener, Geometric Programming, New York: John Wiley and Sons; 1967.

41. Chase, M. W., J. L. Curnutt, H. Prophet, R. A. McDonald, and A. N. Syverud, JANAF Thermochemical Tables, Journal of Physical and Chemical Reference Data, National Bureau of Standards, 2nd Edition, and 1974-1975 supplements.

42. Hertzberg, G., Molecular Spectra and Molecular Structure I-III, New York: D. Van Nostrand Co., Inc.; 1966.

43. Glassner, A., The Thermochemical Properties of the Oxides, Fluorides and Chlorides to 2500 K, Argonne National Laboratory, Argonne, IL, ANL-5750, 1975.

44. Barin, J., and O. Knacke, Thermochemical Properties of Inorganic Substances, Berlin: Springer-Verlag; 1978.

45. Oppermann, Von H., Fur Anorzanische and Allgemeine Chemie, Band 359 (52); 1968.

46. Krasnov, K. S., Handbook: Molecular Constants of Inorganic Compound, Khimiya; 1968.

47. National Bureau of Standards, NBS TN 270-3, Selected Values of Chemical Thermodynamic Properties, 1968.

48. Feber, R. C., Heats of Dissociation of Gaseous Halide, Los Alamos Scientific Laboratory, Los Alamos, NM, LA-3164, TSC-4, Chemistry TID-3500 (40th ed.), 1965.

49. Schick, H. L., Thermodynamics of Certain Refractory Compounds, New York: Academic Press; 1966.

50. Cleland, J. G., G. L. Kingsbury, Minimum Acute Toxicity Effluent (MATE) Values for Organic and Inorganic Compounds from Fossil Energy Processes, A Subset of Multimedia Goals for Environmental - Assessment Use in Rapid Screening of Effluents, Research Triangle Institute, Research Triangle Park, NC., EPA-68-02-2612, draft May 10, 1977.

51. Fulkerson, W., Allen Steam Plant Study, Energy Division, Annual Progress Report for Period Ending December 31, 1974, ORNL-5030, April 1975.

52. Swift, W. M., G. J. Vogel, A. F. Panek, and A. A. Jonke, Trace Element Mass Balances around a Bench Scale Combustor. Proceedings of the 4th International Conference on Fluidized Bed Combustion, December 1975. McLean, VA: The Mitre Corporation; 1976.

53. A Regenerative Limestone Process for Fluidized Bed Coal Combustion and Desulfurization. Monthly Report No. 95, January 1, 1978 - January 31, 1978 to EPA, Exxon Research and Engineering Company, Linden, NJ, Contract 68-02-1312.

APPENDIX A

NITROGEN OXIDE EMISSIONS IN FLUID-BED COMBUSTION EXPERIMENTS

This appendix presents the data collection used for the NO_x regression analyses. Reference numbers are the first entry, and these correlate with the reference list provided at the end of the data. In the case of fluidized-bed combustor operating conditions, some investigators have reported the expanded bed depth, whereas others have reported the settled bed depth, and again some have differentiated between the initial and final settled bed depths. Thus, to identify the format in which bed depth has been reported, we have assigned a bed depth code (see Nomenclature at end of this appendix) as shown in the following data collection. Some of these NO_x emission data have been plotted in figures as a function of temperature, with excess air level as parameter. These plots indicate that the NO_x emissions increase with increasing excess air and/or temperature.

FILE	SOURCE	RUN #	P(kPa)	%EX AIR	Ca/S	TEMP C	SUP VEL	B DEP	CD	NOXppm	%DESUL	COAL	WT% N
1	EXX(9/76)	2.1	395	27.50	0.0	861.0	2.46	0.76	2		0.00	ARKWRIGHT	1.50
2	EXX(9/76)	3.1A	395	11.80	0.0	395.0	2.50	0.92	2		0.00	ARKWRIGHT	1.50
3	EXX(9/76)	3.1B	395	-8.90	0.0	939.0	2.50	0.92	2		0.00	ARKWRIGHT	1.50
4	EXX(9/76)	4.1	1033	78.90	0.0	885.0	1.69	0.92	2		0.00	ARKWRIGHT	1.50
5	EXX(9/76)	4.3	922	115.00	0.0	919.0	1.89	0.00	0		0.00	ARKWRIGHT	1.50
6	EXX(9/76)	5.1	912	98.90	0.0	849.0	1.88	0.00	0		0.00	ARKWRIGHT	1.50
7	EXX(9/76)	5.2	896	96.10	0.0	889.0	1.98	0.00	0		0.00	ARKWRIGHT	1.50
8	EXX(9/76)	6.1	902	87.80	0.0	949.0	1.96	0.92	2		0.00	ARKWRIGHT	1.50
9	EXX(9/76)	6.2	912	100.00	0.0	938.0	1.91	0.00	0		0.00	ARKWRIGHT	1.50
10	EXX(9/76)	7.1	912	23.20	0.0	876.0	1.84	1.53	2		0.00	ARKWRIGHT	1.50
11	EXX(9/76)	7.2	912	36.70	0.0	884.0	1.89	0.00	0		0.00	ARKWRIGHT	1.50
12	EXX(9/76)	7.3	698	0.00	0.0	880.0	2.10	0.00	0		0.00	ARKWRIGHT	1.50
13	EXX(9/76)	7.4	912	34.30	4.0	877.0	1.73	1.98	3		0.00	ARKWRIGHT	1.50
14	EXX(9/76)	8.4	907	67.00	1.6	908.0	1.83	0.58	2		0.00	ARKWRIGHT	1.50
15	EXX(9/76)	8.4A	906	15.00	0.0	906.0	1.77	1.30	3		0.00	ARKWRIGHT	1.50
16	EXX(9/76)	9.1	932	80.50	1.0	881.0	1.76	0.61	2		0.00	ARKWRIGHT	1.50
17	EXX(9/76)	10.1	901	114.00	1.2	916.0	1.96	0.61	2		0.00	ARKWRIGHT	1.50
18	EXX(9/76)	10.2	901	87.60	1.2	891.0	1.84	0.58	2		0.00	ARKWRIGHT	1.50
19	EXX(9/76)	10.3	912	93.90	1.2	912.0	2.04	1.12	2	90	0.00	ARKWRIGHT	1.50
20	EXX(9/76)	11.1	915	139.00	0.0	909.0	2.05	0.61	2	45	0.00	ARKWRIGHT	1.50
21	EXX(9/76)	11.2	912	95.80	0.0	915.0	1.89	0.84	2	162	0.00	ARKWRIGHT	1.50
22	EXX(9/76)	12.1	922	66.50	1.2	903.0	1.78	0.76	2	170	0.00	ARKWRIGHT	1.50
23	EXX(9/76)	12.1A	922	50.00	1.2	903.0	1.78	0.76	2	165	0.00	ARKWRIGHT	1.50
24	EXX(9/76)	12.1B	922	51.00	1.2	903.0	1.78	0.76	2	160	0.00	ARKWRIGHT	1.50
25	EXX(9/76)	12.1C	922	58.00	1.2	903.0	1.78	0.76	2	170	0.00	ARKWRIGHT	1.50
26	EXX(9/76)	12.1D	922	49.00	1.2	903.0	1.78	0.76	2	160	0.00	ARKWRIGHT	1.50
27	EXX(9/76)	12.1E	922	40.00	1.2	903.0	1.78	0.76	2	155	0.00	ARKWRIGHT	1.50
28	EXX(9/76)	12.1F	922	46.00	1.2	903.0	1.78	0.76	2	165	0.00	ARKWRIGHT	1.50
29	EXX(9/76)	12.1G	922	39.00	1.2	903.0	1.78	0.76	2	170	0.00	ARKWRIGHT	1.50
30	EXX(9/76)	12.1H	922	44.00	1.2	903.0	1.78	0.76	2	160	0.00	ARKWRIGHT	1.50
31	EXX(9/76)	12.1I	922	38.00	1.2	903.0	1.78	0.76	2	160	0.00	ARKWRIGHT	1.50
32	EXX(9/76)	12.1J	922	37.00	1.2	903.0	1.78	0.76	2	165	0.00	ARKWRIGHT	1.50
33	EXX(9/76)	12.1K	922	55.00	1.2	903.0	1.78	0.76	2	175	0.00	ARKWRIGHT	1.50
34	EXX(9/76)	12.1L	922	28.00	1.2	903.0	1.78	0.76	2	160	0.00	ARKWRIGHT	1.50
35	EXX(9/76)	12.1M	922	28.00	1.2	903.0	1.78	0.76	2	155	0.00	ARKWRIGHT	1.50
36	EXX(9/76)	12.1N	922	28.00	1.2	903.0	1.78	0.76	2	170	0.00	ARKWRIGHT	1.50
37	EXX(9/76)	12.1O	922	18.00	1.2	903.0	1.78	0.76	2	150	0.00	ARKWRIGHT	1.50
38	EXX(9/76)	12.1P	922	22.00	1.2	903.0	1.78	0.76	2	150	0.00	ARKWRIGHT	1.50
39	EXX(9/76)	12.1Q	922	21.00	1.2	903.0	1.78	0.76	2	160	0.00	ARKWRIGHT	1.50
40	EXX(9/76)	12.2	912	27.30	1.2	896.0	1.83	1.27	2	130	0.00	ARKWRIGHT	1.50
41	EXX(9/76)	13.2	912	48.70	1.2	910.0	1.86	0.89	2	130	0.00	ARKWRIGHT	1.10
42	EXX(9/76)	13.2A	912	34.00	1.2	910.0	1.86	0.89	2	140	0.00	ARKWRIGHT	1.10
43	EXX(9/76)	13.2B	912	32.00	1.2	910.0	1.86	0.89	2	135	0.00	ARKWRIGHT	1.10
44	EXX(9/76)	13.2C	912	28.00	1.2	910.0	1.86	0.89	2	135	0.00	ARKWRIGHT	1.10
45	EXX(9/76)	13.2D	912	22.00	1.2	910.0	1.86	0.89	2	125	0.00	ARKWRIGHT	1.10
46	EXX(9/76)	13.2E	912	17.00	1.2	910.0	1.86	0.89	2	115	0.00	ARKWRIGHT	1.10
47	EXX(9/76)	13.2F	912	7.00	1.2	910.0	1.86	0.89	2	75	0.00	ARKWRIGHT	1.10
48	EXX(9/76)	14.1A	902	86.80	1.2	909.0	1.84	0.84	2		0.00	ARKWRIGHT	1.10
49	EXX(9/76)	14.1B	912	61.00	1.2	916.0	1.83	1.33	3		0.00	ARKWRIGHT	1.10
50	EXX(9/76)	14.2	912	22.50	1.2	934.0	1.91	1.33	2		0.00	ARKWRIGHT	1.10
51	EXX(9/76)	15.1A	907	44.20	1.2	910.0	1.92	1.04	2		0.00	ARKWRIGHT	1.10
52	EXX(9/76)	15.1B	902	24.00	1.2	902.0	2.09	1.93	3		0.00	ARKWRIGHT	1.10
53	EXX(9/76)	15.2	912	62.20	1.2	916.0	1.83	1.92	2		0.00	ARKWRIGHT	1.10
54	EXX(9/76)	15.3A	921	27.10	1.2	889.0	1.87	1.80	2		0.00	ARKWRIGHT	1.10
55	EXX(9/76)	15.3B	902	23.60	1.2	901.0	2.09	2.29	3		0.00	ARKWRIGHT	1.10
56	EXX(9/76)	15.4	912	25.00	1.2	905.0	2.03	2.29	2		0.00	ARKWRIGHT	1.10
57	EXX(9/76)	16.1	821	8.90	1.4	882.0	1.83	0.78	2		0.00	CHAMPION	1.60
58	EXX(9/76)	16.1A	821	18.00	1.4	882.0	1.83	0.78	2	225	0.00	CHAMPION	1.60
59	EXX(9/76)	16.1B	821	10.00	1.4	882.0	1.83	0.78	2	225	0.00	CHAMPION	1.60
60	EXX(9/76)	16.1C	821	10.00	1.4	882.0	1.83	0.78	2	205	0.00	CHAMPION	1.60
61	EXX(9/76)	16.1D	821	6.00	1.4	882.0	1.83	0.78	2	140	0.00	CHAMPION	1.60
62	EXX(9/76)	16.1E	821	3.00	1.4	882.0	1.83	0.78	2	130	0.00	CHAMPION	1.60
63	EXX(9/76)	16.1F	821	2.00	1.4	882.0	1.83	0.78	2	125	0.00	CHAMPION	1.60
64	EXX(9/76)	16.1G	826	-3.10	1.4	875.0	1.84	1.75	3		0.00	CHAMPION	1.60
65	EXX(9/76)	6.3	932	31.00	1.4	893.0	2.05	0.84	2		0.00	CHAMPION	1.60
66	EXX(9/76)	17.1A	906	16.70	1.4	898.0	2.13	0.74	2		0.00	CHAMPION	1.60
67	EXX(9/76)	17.1B	913	35.30	0.0	863.0	2.03	1.95	3		0.00	CHAMPION	1.60
68	EXX(9/76)	18.1	935	57.30	1.4	899.0	1.71	0.66	2		0.00	CHAMPION	1.60
69	EXX(9/76)	18.3	958	61.50	1.4	910.0	1.86	0.76	2	140	0.00	CHAMPION	1.60
70	EXX(9/76)	19.2	922	30.40	1.4	874.0	1.81	0.71	2		0.00	CHAMPION	1.60
71	EXX(9/76)	19.2A	922	65.00	1.4	874.0	1.81	0.71	2	210	0.00	CHAMPION	1.60
72	EXX(9/76)	19.2B	922	44.00	1.4	874.0	1.81	0.71	2	175	0.00	CHAMPION	1.60
73	EXX(9/76)	19.2C	922	33.00	1.4	874.0	1.81	0.71	2	170	0.00	CHAMPION	1.60
74	EXX(9/76)	19.2D	922	32.00	1.4	874.0	1.81	0.71	2	160	0.00	CHAMPION	1.60
75	EXX(9/76)	19.2E	922	21.00	1.4	874.0	1.81	0.71	2	140	0.00	CHAMPION	1.60
76	EXX(9/76)	19.2F	922	15.00	1.4	874.0	1.81	0.71	2	120	0.00	CHAMPION	1.60
77	EXX(9/76)	19.2G	922	15.00	1.4	874.0	1.81	0.71	2	115	0.00	CHAMPION	1.60
78	EXX(9/76)	19.2H	922	9.00	1.4	874.0	1.81	0.71	2	90	0.00	CHAMPION	1.60
79	EXX(9/76)	19.3	922	5.70	1.4	879.0	1.89	1.45	2		0.00	CHAMPION	1.60
80	EXX(9/76)	19.3A	922	9.00	1.4	879.0	1.89	1.45	2	65	0.00	CHAMPION	1.60
81	EXX(9/76)	19.3B	922	5.00	1.4	879.0	1.89	1.45	2	80	0.00	CHAMPION	1.60
82	EXX(9/76)	19.3C	922	11.00	1.4	879.0	1.89	1.45	2	45	0.00	CHAMPION	1.60
83	EXX(9/76)	19.3D	922	7.00	1.4	879.0	1.89	1.45	2	80	0.00	CHAMPION	1.60
84	EXX(9/77)	19.2	930	6.60	1.4	872.0	1.90	0.71	2	147	0.00	CHAMPION	1.61
85	EXX(9/77)	19.3	930	6.00	1.4	871.0	1.90	1.45	2	78	56.40	CHAMPION	1.61
86	EXX(9/77)	19.4	925	15.00	2.5	880.0	1.99	1.58	2	125	69.00	CHAMPION	1.61
87	EXX(9/77)	19.5	935	15.00	2.5	892.0	2.00	1.98	2	91	67.00	CHAMPION	1.61
88	EXX(9/77)	19.6A	930	15.00	2.5	884.0	2.02	1.58	2	104	68.00	CHAMPION	1.61
89	EXX(9/77)	19.6B	930	22.00	2.5	825.0	1.94	1.60	3	127	58.00	CHAMPION	1.61
90	EXX(9/77)	19.7A	930	9.10	2.5	879.0	1.98	1.96	2	102	73.00	CHAMPION	1.61

FILE	SOURCE	RUN #	P(kPa)	%EX AIR	Ca/S	TEMP C	SUP VEL	B DEP	CD	NOXppm	%DESUL	COAL	WT% N
91	EXX(9/77)	19.7B	970	9.60	2.5	937.0	2.18	1.27	3	141	83.50	CHAMPION	1.61
92	EXX(9/77)	19.9A	930	10.00	2.5	870.0	1.79	1.09	2	135	66.00	CHAMPION	1.61
93	EXX(9/77)	19.9B	930	20.00	2.5	926.0	2.40	1.88	3	105	81.90	CHAMPION	1.61
94	EXX(9/77)	20.1A	930	11.00	3.3	870.0	2.06	1.85	2	117	54.00	CHAMPION	1.57
95	EXX(9/77)	20.1B	930	12.00	3.3	827.0	1.83	0.00	0	95	53.00	CHAMPION	1.57
96	EXX(9/77)	20.1C	930	18.50	3.3	927.0	2.32	1.32	3	157	0.00	CHAMPION	1.57
97	EXX(9/77)	20.2A	930	18.00	1.5	927.0	2.30	1.22	2	200	71.20	CHAMPION	1.57
98	EXX(9/77)	20.2B	930	13.70	3.3	927.0	2.30	1.65	3	195	86.30	CHAMPION	1.57
99	EXX(9/77)	21	930	14.00	3.3	870.0	2.00	1.60	2	195	60.00	CHAMPION	1.57
100	EXX(9/77)	21B	930	18.00	3.3	930.0	2.20	2.11	3	210	0.00	CHAMPION	1.57
101	EXX(9/77)	22	930	28.00	0.0	870.0	1.90	2.11	2		0.00	CHAMPION	1.57
102	EXX(9/77)	23	930	12.00	1.3	885.0	1.82	1.19	2	110	0.00	CHAMPION	1.57
103	EXX(9/77)	25	930	8.00	1.3	970.0	1.75	1.37	2	125	0.00	CHAMPION	1.57
104	EXX(9/77)	26A	930	9.50	3.7	927.0	2.10	1.12	2	185	90.80	CHAMPION	1.57
105	EXX(9/77)	26B	930	11.50	3.7	885.0	1.90	2.28	3	180	81.20	CHAMPION	1.57
106	EXX(9/77)	27.1	930	18.90	0.5	880.0	2.01	4.00	0	207	55.00	CHAMPION	1.57
107	EXX(9/77)	27.2	930	15.40	0.5	927.0	2.15	4.00	0	199	57.10	CHAMPION	1.57
108	EXX(9/77)	27.3	930	15.30	0.5	902.0	1.98	3.00	0	176	55.60	CHAMPION	1.57
109	EXX(9/77)	27.4	930	20.50	0.5	829.0	1.07	0.00	0	200	62.00	CHAMPION	1.57
110	EXX(9/77)	27.5	930	12.10	2.5	829.0	1.72	6.00	0	189	97.80	CHAMPION	1.62
111	EXX(9/77)	27.6	930	14.50	0.8	829.0	1.72	5.00	0	143	80.00	CHAMPION	1.62
112	EXX(9/77)	27.7	930	12.40	1.5	835.0	1.72	6.00	0	135	97.20	CHAMPION	1.62
113	EXX(9/77)	27.8	930	12.60	1.5	878.0	1.83	7.00	0	128	98.00	CHAMPION	1.62
114	EXX(9/77)	27.9	930	13.10	1.5	922.0	2.09	5.00	0	164	98.50	CHAMPION	1.62
115	EXX(9/77)	27.10	930	7.80	0.7	883.0	1.87	5.00	0	93	72.00	CHAMPION	1.62
116	EXX(9/77)	27.11	930	11.00	0.7	931.0	2.23	7.00	0	109	70.00	CHAMPION	1.62
117	EXX(9/77)	27.12	930	23.00	0.7	834.0	1.94	7.00	0	130	71.00	CHAMPION	1.62
118	EXX(9/77)	27.13	930	13.50	0.3	888.0	2.02	6.00	0	110	46.00	CHAMPION	1.60
119	EXX(9/77)	27.14	930	14.60	0.7	892.0	2.04	6.00	0	100	64.00	CHAMPION	1.60
120	EXX(9/77)	27.15	930	8.20	1.0	889.0	1.88	5.00	0	103	71.00	CHAMPION	1.60
121	EXX(9/77)	27.16	930	10.40	0.7	841.0	1.74	5.00	0	94	87.00	CHAMPION	1.60
122	EXX(9/77)	27.17	930	13.80	0.7	891.0	1.97	6.00	0	95	72.00	CHAMPION	1.60
123	EXX(9/77)	27.18	930	8.20	1.0	909.0	2.09	7.00	0	97	84.50	CHAMPION	1.60
124	EXX(9/77)	27.19	930	12.30	1.5	907.0	2.08	7.00	0	101	90.00	CHAMPION	1.60
125	EXX(9/77)	27.20	930	12.10	0.0	895.0	2.03	7.00	0	91	11.00	CHAMPION	1.60
126	EXX(9/77)	27.21	930	10.90	0.0	846.0	1.67	5.00	0	65	14.00	CHAMPION	1.60
127	EXX(9/77)	28.1	930	40.00	0.0	840.0	2.13	1.02	2	134	10.00	CHAMPION	1.60
128	EXX(9/77)	28.2	930	35.00	0.0	870.0	2.16	0.00	0	145	13.50	CHAMPION	1.60
129	EXX(9/77)	28.3	930	18.00	0.0	920.0	2.13	0.00	0	125	9.00	CHAMPION	1.60
130	EXX(9/77)	28.4	930	4.50	0.0	920.0	1.40	0.00	0	41	1.60	CHAMPION	1.60
131	EXX(9/77)	28.5	930	21.00	0.0	930.0	2.65	9.70	3	146	3.60	CHAMPION	1.60
132	EXX(9/77)	29	930	19.00	3.7	875.0	2.16	0.80	2	137	55.70	CHAMPION	1.60
133	EXX(9/77)	30.1	920	13.70	3.7	885.0	2.15	1.60	2	50	49.70	CHAMPION	1.60
134	EXX(9/77)	30.2	920	17.20	3.7	929.0	2.50	0.00	0		89.10	CHAMPION	1.60
135	EXX(9/77)	30.3	920	13.90	3.7	885.0	2.10	0.00	0		64.50	CHAMPION	1.60
136	EXX(9/77)	30.4	920	16.10	3.7	835.0	1.90	2.26	3	70	32.10	CHAMPION	1.60
137	EXX(9/77)	31	520	23.00	2.5	838.0	1.96	1.60	2	55	66.00	CHAMPION	1.60
138	EXX(9/77)	32.1	600	13.00	2.5	950.0	2.20	1.40	2	80	76.40	CHAMPION	1.60
139	EXX(9/77)	32.2	600	16.00	1.5	947.0	2.10	0.00	0	106	60.00	CHAMPION	1.60
140	EXX(9/77)	32.3	600	20.00	0.7	836.0	1.50	0.90	3	89	66.00	CHAMPION	1.60
141	EXX(9/77)	33	920	23.40	2.5	918.0	1.56	0.76	2	147	0.00	CHAMPION	1.60
142	EXX(9/77)	34	932	20.90	0.7	900.0	1.50	2.29	2	52	0.00	CHAMPION	1.60
143	EXX(9/77)	35	930	45.80	0.7	905.0	1.54	2.26	2	72	61.60	CHAMPION	1.60
144	EXX(9/77)	36.1	930	42.00	0.7	900.0	1.40	1.40	2	94	65.60	CHAMPION	1.40
145	EXX(9/77)	36.2	930	96.00	0.7	913.0	3.00	1.70	3	159	75.60	CHAMPION	1.40
146	EXX(9/77)	37	930	92.00	0.7	902.0	2.96	1.68	2	121	46.00	CHAMPION	1.40
147	EXX(9/77)	38.1	930	47.00	0.7	891.0	2.08	1.14	2	135	40.00	CHAMPION	1.40
148	EXX(9/77)	38.2	930	44.00	0.7	894.0	2.09	0.00	0	127	45.00	CHAMPION	1.40
149	EXX(9/77)	38.3	930	94.00	0.7	762.0	1.85	0.00	0	125	48.00	CHAMPION	1.40
150	EXX(9/77)	38.4	930	94.00	1.5	762.0	1.84	0.00	0	149	71.00	CHAMPION	1.40
151	EXX(9/77)	38.5	930	112.00	1.5	690.0	1.9	0.00	0	114	76.00	CHAMPION	1.40
152	EXX(9/77)	38.6	930	78.00	1.5	684.0	1.30	2.26	3	102	82.00	CHAMPION	1.40
153	EXX(9/77)	39.1	902	68.00	2.5	750.0	1.52	1.22	2	120	0.00	CHAMPION	1.40
154	EXX(9/77)	39.2	902	60.00	2.5	674.0	1.40	0.00	0	174	0.60	CHAMPION	1.40
157	EXX(5/78)	41.1	912	44.00	0.8	889.0	1.60	2.30	2	111	68.00	CHAMPION	1.36
158	EXX(5/78)	41.2	912	37.00	0.8	875.0	1.50	2.00	3	127	100.00	ARKWRIGHT	1.07
159	EXX(5/78)	43.1	840	24.00	1.2	940.0	1.70	1.40	2	80	98.00	ILLINOIS#6	1.17
160	EXX(5/78)	43.2	880	42.00	0.7	845.0	1.80	2.10	3	120	60.00	ILLINOIS#6	1.17
161	EXX(5/78)	43.3	885	25.00	0.7	940.0	1.80	1.60	2	90	63.00	ILLINOIS#6	1.17
162	EXX(5/78)	43.4	940	25.00	1.2	940.0	1.70	1.60	2	79	96.00	ILLINOIS#6	1.17
163	EXX(5/78)	43.5	940	25.00	0.5	945.0	1.70	2.20	3	75	44.00	ILLINOIS#6	1.17
164	EXX(5/78)	45.1	780	37.00	0.7	880.0	1.40	2.30	2		65.00	CHAMPION	1.36
165	EXX(5/78)	45.2	780	40.00	0.7	885.0	1.40	0.00	0		92.00	CHAMPION	1.36
166	EXX(5/78)	45.3	780	33.00	1.3	890.0	1.40	0.00	0		84.00	CHAMPION	1.36
167	EXX(5/78)	45.4	780	30.00	1.0	870.0	1.40	0.00	0		82.00	CHAMPION	1.36
168	EXX(5/78)	45.5	780	28.00	0.0	875.0	1.40	0.00	0		56.00	CHAMPION	1.36
169	EXX(5/78)	45.6	780	27.00	0.0	875.0	1.40	2.20	3		62.00	CHAMPION	1.36
170	EXX(5/78)	46.1	940	37.00	2.5	920.0	1.30	1.80	2	80	90.00	CHAMPION	1.36
171	EXX(5/78)	46.2	940	47.00	2.5	865.0	1.20	2.30	3	120	86.00	CHAMPION	1.36
172	EXX(5/78)	46.3	940	40.00	2.5	760.0	1.00	2.30	2	120	55.00	CHAMPION	1.36
173	EXX(5/78)	46.4	940	35.00	1.5	865.0	1.40	2.00	3	150	64.00	CHAMPION	1.36
174	EXX(5/78)	47	1075	18.00	1.5	885.0	2.20	2.10	2	100	2.70	CHAMPION	1.36
175	EXX(5/78)	48	930	39.00	1.4	875.0	1.50	1.50	2	92	58.00	CHAMPION	1.36
176	EXX(5/78)	50.1A	910	41.00	1.2	890.0	1.20	1.60	2	97	69.00	CHAMP/KY	1.50
177	EXX(5/78)	50.1B	915	45.00	1.2	890.0	1.20	0.00	0	102	70.00	CHAMP/KY	1.50
178	EXX(5/78)	50.2	900	63.00	1.2	805.0	1.20	0.00	0	136	86.00	CHAMP/KY	1.50
179	EXX(5/78)	50.3	900	40.00	1.2	890.0	1.30	3.20	0	128	95.00	CHAMP/KY	1.50
180	EXX(5/78)	50.4	900	40.00	1.2	890.0	1.30	3.30	0	124	96.00	CHAMP/KY	1.50
181	EXX(5/78)	50.5	900	36.00	1.2	895.0	1.40	2.20	0	119	29.00	CHAMP/KY	1.40
182	EXX(5/78)	51	932	46.00	1.4	871.0	1.50	1.90	2	143	71.00	CHAMP/KY	1.40
183	EXX(5/78)	52	930	38.00	1.2	890.0	1.50	1.70	2	107	0.00	CHAMP/KY	1.40

FILE	SOURCE	RUN #	P(kPa)	%EX AIR	Ca/S	TEMP C	SUP VEL	B DEP	CD	NOXppm	%DESUL	COAL	WT% N
184	EXX(5/78)	54	595	29.00	0.0	910.0	1.90	2.70	0		31.00	CHAMP/KY	1.54
185	EXX(5/78)	55	570	13.00	0.0	930.0	2.10	2.50	0	110	30.00	CHAMP/KY	1.54
186	EXX(5/78)	56	800	34.00	0.6	815.0	1.40	1.80	2	104	93.00	CHAMP/KY	1.54
187	EXX(5/78)	57	810	14.00	0.7	935.0	1.40	1.60	3	35	87.00	CHAMP/KY	1.54
188	EXX(5/78)	59.1	890	33.00	0.7	956.0	1.60	3.70	0	78	88.00	CHAMP/KY	1.54
189	EXX(5/78)	59.2	873	26.00	0.0	949.0	1.70	1.30	3	55	66.00	CHAMP/KY	1.54
190	ANL(6/74)	VAR 1	810	15.00	2.9	785.0	0.63	0.90	0	190	0.00	ARKWRIGHT	1.66
191	ANL(6/74)	VAR 2	810	15.00	2.9	852.0	1.44	0.90	0	210	0.00	ARKWRIGHT	1.66
192	ANL(6/74)	VAR 3	810	15.00	1.1	857.0	0.63	0.90	0	140	0.00	ARKWRIGHT	1.66
193	ANL(6/74)	VAR 4	810	15.00	1.9	899.0	0.69	0.90	0	180	0.00	ARKWRIGHT	1.66
194	ANL(6/74)	VAR 5	810	15.00	1.0	795.0	3.40	0.90	0	150	0.00	ARKWRIGHT	1.66
195	ANL(6/74)	VAR 6	810	15.00	2.0	852.0	1.08	0.90	0	190	0.00	ARKWRIGHT	1.66
196	ANL(6/74)	VAR 6	810	15.00	2.1	949.0	1.08	0.90	0	180	0.00	ARKWRIGHT	1.66
197	ANL(6/74)	VAR 6	810	15.00	2.0	[illegible]	1.05	0.90	0	160	0.00	ARKWRIGHT	1.66
198	ANL(6/74)	VAR 7	810	15.00	2.2	793.0	1.26	0.90	0	150	0.00	ARKWRIGHT	1.66
199	ANL(6/74)	VAR 8	810	15.00	2.2	888.0	1.08	0.90	0	270	0.00	ARKWRIGHT	1.66
200	ANL(6/74)	VAR 9	810	15.00	1.0	907.0	1.47	0.90	0	120	0.00	ARKWRIGHT	1.66
201	NCB(9/71)		354	25.00	0.7	798.8	0.60	1.12	1		39.00	WELBECK	1.50
202	NCB(9/71)		354	28.04	0.7	798.8	0.60	1.12	1	80	57.00	WELBECK	1.50
203	NCB(9/71)		354	32.07	0.9	798.8	0.60	1.12	1	120	39.00	WELBECK	1.50
204	NCB(9/71)		354	29.62	0.9	798.8	0.60	1.12	1	130	85.00	WELBECK	1.50
205	NCB(9/71)		354	16.66	1.4	798.8	0.60	1.12	1	80	94.00	PITTSBURGH	1.40
206	NCB(9/71)		354	27.27	1.8	798.8	0.60	1.12	1	130	96.00	PITTSBURGH	1.40
207	NCB(9/71)		354	30.43	1.9	798.8	0.60	1.12	1	90	96.00	PITTSBURGH	1.40
208	NCB(9/71)		506	42.85	1.8	798.8	0.60	1.12	1	100	95.00	PITTSBURGH	1.40
209	NCB(9/71)		506	33.75	1.6	798.8	0.60	1.12	1	160	95.00	PITTSBURGH	1.40
210	NCB(9/71)		506	32.07	1.9	798.8	0.60	1.12	1		95.00	PITTSBURGH	1.40
211	NCB(9/71)		506	38.15	1.5	798.8	0.60	1.12	1	140	94.00	PITTSBURGH	1.40
212	NCB(9/71)		506	33.75	2.0	798.8	0.60	1.12	1	190	98.00	PITTSBURGH	1.40
213	NCB(9/71)		506	20.68	1.8	798.8	0.60	1.12	1	90	66.00	PITTSBURGH	1.40
214	NCB(9/71)		506	22.09	2.3	798.8	0.60	1.12	1	90	77.00	PITTSBURGH	1.40
215	NCB(9/71)		506	33.75	1.0	798.8	0.60	1.12	1	140	95.00	PITTSBURGH	1.40
216	EXX11/73		607	97.00	0.0	737.7	1.80	0.12	1	310	8.00	ARKWRIGHT	1.49
217	EXX11/73		658	77.00	0.0	926.6	1.98	0.30	1	300	34.00	ARKWRIGHT	1.49
218	EXX10/75		930	9.10	2.5	879.4	1.95	1.57	2	102	73.00	ARKWRIGHT	1.49
219	EXX12/73		658	88.00	0.0	998.8	1.95	0.60	1	365	72.00	ARKWRIGHT	1.49
231	EXX3/75		805	21.00	0.0	870.0	1.50	0.75	2	190	68.50	ARKWRIGHT	1.49
232	EXX3/75		805	37.00	0.0	865.0	1.41	0.75	4	199	62.00	ARKWRIGHT	1.49
233	EXX3/75		805	62.00	0.0	893.8	1.05	0.75	4	191	69.00	ARKWRIGHT	1.49
234	EXX3/75		395	61.00	0.0	875.0	1.41	0.45	2	220	69.50	ARKWRIGHT	1.49
239	EXX9/75		805	12.00	0.0	913.8	1.14	0.75	2	175	82.60	ARKWRIGHT	1.49
240	EXX9/75		805	16.00	0.0	925.0	1.14	0.75	4	151	70.50	ARKWRIGHT	1.49
241	EXX9/75		805	17.00	0.0	887.2	1.17	0.75	2	231	85.60	ARKWRIGHT	1.49
242	EXX9/75		310	33.00	0.0	902.7	1.83	0.36	2	208	61.60	ARKWRIGHT	1.49
243	EXX(9/76)		700	44.00	0.0	875.0	1.53	0.49	1	160	98.00	ARKWRIGHT	1.49
244	EXX(9/76)		800	15.00	0.0	850.0	1.23	0.42	4	205	86.00	ARKWRIGHT	1.49
245	EXX2/74		658	56.00	0.0	871.1	1.50	0.60	1	335	91.00	ARKWRIGHT	1.49
246	EXX2/74		638	61.00	0.0	943.3	1.86	0.60	1	370	89.00	ARKWRIGHT	1.49
247	EXX2/74		628	27.00	0.0	910.0	1.86	0.60	1	240	69.00	ARKWRIGHT	1.49
248	EXX3/74		628	58.00	0.0	946.1	1.86	0.60	1	250	91.00	WYOMING	0.90
249	EXX3/74		628	43.00	0.0	737.7	1.56	0.60	1	230	35.00	ILLINOIS	1.20
250	EXX4/74		840	43.00	0.0	848.8	1.74	0.60	1	220	87.40	ARKWRIGHT	1.49
251	EXX11/74		861	0.00	0.0	860.0	1.35	0.50	1	170	76.40	ARKWRIGHT	1.49
252	EXX1/74		658	45.00	0.0	1093.3	2.43	0.60	1	470	54.00	ARKWRIGHT	1.49
253	EXX1/74		658	26.00	0.0	954.4	2.07	0.36	4	610	6.00	ARKWRIGHT	1.49
254	EXX1/74		658	110.00	0.0	793.3	1.86	0.60	1	300	89.00	ARKWRIGHT	1.49
255	EXX(9/76)		810	46.00	0.0	870.0	1.08	0.45	4		84.00	ARKWRIGHT	1.49
256	EXX(9/76)		800	5.00	0.0	895.0	1.55	0.86	1		97.00	ARKWRIGHT	1.49
257	EXX6/73		820	209.00	0.0	821.1	1.68	0.60	4	380	54.00	ARKWRIGHT	1.49
258	EXX6/73		820	203.00	0.0	893.3	1.83	0.60	4	340	54.00	ARKWRIGHT	1.49
259	EXX7/73		871	130.00	0.0	843.3	1.14	0.60	1	410	85.50	ARKWRIGHT	1.49
260	EXX11/73		658	8.00	0.0	137.7	1.89	0.37	1		50.00	ARKWRIGHT	1.49
261	EXX1/75		800	30.00	0.0	920.0	1.23	0.50	2	330	97.30	ARKWRIGHT	1.49
262	EXX1/75		800	42.00	0.0	910.0	1.26	0.50	2		99.70	ARKWRIGHT	1.49
263	EXX1/75		800	58.00	0.0	972.2	1.20	0.26	4	160	84.00	ARKWRIGHT	1.49
264	EXX3/75		800	0.00	0.0	885.0	1.57	0.80	2		96.70	ARKWRIGHT	1.49
265	EXX5/75		800	32.00	0.0	911.1	1.12	0.45	2	201	66.00	ARKWRIGHT	1.49
266	EXX6/75		800	31.00	0.0	887.2	1.38	0.75	2	176	62.80	ARKWRIGHT	1.49
267	EXX6/75		811	14.00	0.0	850.0	1.41	0.75	2	153	60.30	ARKWRIGHT	1.49
268	EXX6/75		800	24.00	0.0	857.2	1.44	0.75	4	166	43.70	ARKWRIGHT	1.49
269	EXX6/75		800	25.00	0.0	751.1	1.08	0.75	2	217	67.90	ARKWRIGHT	1.49
270	EXX6/75		800	17.00	0.0	867.2	1.92	0.75	2	160	60.80	ARKWRIGHT	1.49
271	EXX7/75		800	22.00	0.0	877.2	1.08	0.54	2	198	85.40	ARKWRIGHT	1.49
273	ARG(10/74)		810	16.66	2.9	790.5	0.63	0.90	0	190	94.78	ARKWRIGHT	5.08
274	ARG(10/74)		810	16.66	2.9	851.6	1.44	0.90	0	210	94.35	ARKWRIGHT	5.08

FILE	SOURCE	RUN #	P(kPa)	%EX AIR	Ca/S	TEMP C	SUP VEL	B DEP	CD	NOXppm	%DESUL	COAL	WT% N
275	ARG(10/74)		810	16.66	1.1	857.2	0.63	0.90	0	140	84.78	ARKWRIGHT	5.08
276	ARG(10/74)		810	16.66	1.9	898.8	0.69	0.90	0	180	94.78	ARKWRIGHT	5.08
277	ARG(10/74)		810	16.66	1.0	793.3	1.02	0.90	0	150	70.43	ARKWRIGHT	5.08
278	ARG(10/74)		810	16.66	2.0	851.6	1.08	0.90	0	190	92.61	ARKWRIGHT	5.08
279	ARG(10/74)		810	16.66	2.1	848.8	1.08	0.90	0	180	80.87	ARKWRIGHT	5.08
280	ARG(10/74)		810	16.66	2.0	843.3	1.05	0.90	0	160	91.74	ARKWRIGHT	5.08
281	ARG(10/74)		810	16.66	2.2	793.3	1.26	0.90	0	150	88.70	ARKWRIGHT	5.08
282	ARG(10/74)		810	16.66	3.2	887.7	1.08	0.90	0	270	94.35	ARKWRIGHT	5.08
283	ARG(10/74)		810	16.66	1.0	907.2	1.47	0.90	0	120	63.04	ARKWRIGHT	5.08
284	ARG(10/74)		810	16.66	1.1	851.6	1.08	0.90	0	150	72.00	SAN JUAN	1.14
285	ARG(10/74)		810	16.66	1.1	848.8	1.05	0.90	0	130	85.00	GLENHAROLD	0.72
286	ARG(10/74)		810	16.66	1.2	904.4	1.02	0.90	0	150	80.87	ARKWRIGHT	5.08
287	ARG(10/74)		1013	23.52	2.9	843.3	0.90	0.90	0	200	93.91	ARKWRIGHT	5.08
288	ARG2/75		810	17.31	4.0	954.4	1.05	0.90	0	150	85.00	ARKWRIGHT	5.08
289	ARG2/75		810	17.00	1.4	898.8	1.35	0.90	0	160	83.00	ARKWRIGHT	5.08
290	ARG2/75		810	44.00	1.1	898.8	1.35	0.90	0		76.00	ARKWRIGHT	5.08
291	ARG2/75		810	44.00	1.4	898.8	1.35	0.90	0	211	71.00	ARKWRIGHT	5.08
292	ARG2/75		810	44.00	1.9	898.8	1.35	0.90	0	182	86.00	ARKWRIGHT	5.08
293	ARG2/75		810	44.00	2.9	898.8	1.35	0.90	0	215	93.00	ARKWRIGHT	5.08
294	ARG2/75		810	75.00	1.3	898.8	1.35	0.90	0	245	57.00	ARKWRIGHT	5.08
295	ARG2/75		810	75.00	1.5	898.8	1.35	0.90	0	180	86.00	ARKWRIGHT	5.08
296	ARG2/75		810	75.00	2.1	898.8	1.35	0.90	0	266	93.00	ARKWRIGHT	5.08
297	ARG2/75		810	75.00	2.9	898.8	1.35	0.90	0	190	92.00	ARKWRIGHT	5.08
298	ARG10/74		810	16.66	1.5	954.4	1.05	0.90	0	135	96.00	ARKWRIGHT	5.08
299	ARG10/74		810	15.38	1.1	954.4	1.05	0.90	0	130	87.00	ARKWRIGHT	5.08
300	ARG10/74		810	16.02	1.7	954.4	1.05	0.90	0	84	68.00	ARKWRIGHT	5.08
301	ARG10/74		810	15.38	1.4	954.4	1.05	0.90	0	110	57.00	ARKWRIGHT	5.08
302	ARG11/74		810	16.66	1.5	898.8	1.35	0.90	0	180	81.00	ARKWRIGHT	5.08
303	ARG11/74		810	40.93	1.4	898.8	1.35	0.90	0	225	71.00	ARKWRIGHT	5.08
304	ARG1/75		810	17.97	2.7	954.4	1.05	0.90	0	130	77.00	ARKWRIGHT	5.08
305	ARG12/74		810	16.02	1.8	954.4	1.05	0.90	0	84	72.00	ARKWRIGHT	5.08
306	ARG12/74		810	15.38	1.4	954.4	1.05	0.90	0	110	63.00	ARKWRIGHT	5.08
307	ARG12/74		810	16.02	1.5	898.8	1.05	0.90	0	95	62.00	ARKWRIGHT	5.08
308	ARG12/74		810	17.97	1.4	898.8	1.05	0.90	0	93	56.00	ARKWRIGHT	5.08
309	ARG9/74		810	16.66	1.2	898.8	0.99	0.90	0	130	82.00	ARKWRIGHT	5.08
310	ARG11/75		810	17.00	1.3	843.3	0.92	0.90	0	160	90.00	ARKWRIGHT	5.08
311	ARG11/75		810	17.00	1.4	843.3	0.83	0.90	0	170	92.00	ARKWRIGHT	5.08
312	ARG11/75		810	17.00	1.3	843.3	0.72	0.90	0	180	93.00	ARKWRIGHT	5.08
313	ARG11/75		810	17.00	1.4	843.3	0.80	0.90	0	210	89.00	ARKWRIGHT	5.08
314	ARG11/75		810	17.00	2.0	843.3	1.08	0.90	0	190	92.60	ARKWRIGHT	5.08
315	ARG11/75		810	17.00	2.0	843.3	1.08	0.90	0	180	90.90	ARKWRIGHT	5.08
316	ARG11/75		810	17.00	2.0	843.3	1.05	0.90	0	160	91.70	ARKWRIGHT	5.08
317	ARG11/75		810	17.00	2.1	843.3	0.95	0.90	0	135	92.60	ARKWRIGHT	5.08
318	ARG12/75		820	17.00	1.5	840.0	0.98	0.90	0	150	89.10	ARKWRIGHT	5.08
319	ARG(4/76)		810	17.00	1.6	900.0	0.92	1.08	0	300	86.00	ARKWRIGHT	5.08
320	ARG(4/76)		810	17.00	1.6	900.0	0.95	1.08	0	120	86.00	ARKWRIGHT	5.08
330	EXX11/75		825	22.00	0.0	870.0	1.09	0.23	2		93.30	ARKWRIGHT	1.49
331	EXX11/75		633	27.00	0.0	900.0	1.44	0.50	1	240	49.00	ARKWRIGHT	1.49
332	EXX11/75		851	43.00	0.0	880.0	1.40	0.51	1	220	60.00	ARKWRIGHT	1.49
333	EXX11/75		810	8.00	0.0	690.0	1.12	1.01	1	220	99.00	ARKWRIGHT	1.49
334	EXX11/75		820	5.00	0.0	850.0	1.25	0.50	1	180	93.00	ARKWRIGHT	1.49
335	EXX11/75		810	0.00	0.0	350.0	0.57	1.00	1	170	99.00	ARKWRIGHT	1.49
336	EXX11/75		820	19.00	0.0	920.0	1.46	0.50	1	150	99.00	ARKWRIGHT	1.49
337	EXX11/75		861	1.00	0.0	860.0	1.33	0.50	1	170	64.00	ARKWRIGHT	1.49
338	EXX11/75		810	24.00	0.0	827.2	1.20	0.50	1	180	98.00	ARKWRIGHT	1.49
339	EXX11/75		810	13.00	0.0	855.0	1.25	0.50	1	170	99.99	ARKWRIGHT	1.49
340	EXX11/75		810	29.00	0.0	840.0	1.05	0.54	1		85.00	ARKWRIGHT	1.49
341	EXX11/75		810	0.00	0.0	885.0	1.55	0.80	1		93.00	ARKWRIGHT	1.49
342	EXX11/75		810	32.00	0.0	911.1	1.12	0.45	1	201	51.00	ARKWRIGHT	1.49
343	EXX11/75		810	31.00	0.0	887.2	1.37	0.75	1	176	49.00	ARKWRIGHT	1.49
344	EXX11/75		810	14.00	0.0	850.0	1.40	0.75	1	153	42.00	ARKWRIGHT	1.49
345	EXX11/75		810	25.00	0.0	751.1	1.07	0.75	1	217	34.00	ARKWRIGHT	1.49
346	EXX11/75		810	17.00	0.0	867.2	1.62	0.75	1	160	41.00	ARKWRIGHT	1.49
347	EXX11/75		810	22.00	0.0	877.2	1.08	0.54	1	198	54.00	ARKWRIGHT	1.49
348	EXX11/75		815	21.00	0.0	870.0	1.50	0.75	1	190	68.50	ARKWRIGHT	1.49
349	EXX11/75		400	61.00	0.0	875.0	0.42	0.45	1	220	69.50	ARKWRIGHT	1.49
350	EXX11/75		815	12.00	0.0	913.8	1.15	0.75	1	175	82.60	ARKWRIGHT	1.49
351	EXX11/75		815	17.00	0.0	887.2	1.17	0.75	1	231	85.60	ARKWRIGHT	1.49
352	EXX11/75		314	33.00	0.0	902.7	1.82	0.47	1	208	61.60	ARKWRIGHT	1.49
372	ARG(7/76)		810	17.00	2.0	840.0	1.08	0.90	0	190	92.60		
373	ARG(7/76)		810	17.00	2.0	840.0	1.08	0.90	0	180	90.90		
374	ARG(7/76)		810	17.00	2.0	840.0	1.05	0.90	0	160	91.70		
375	ARG(7/76)		810	17.00	2.1	840.0	0.95	0.90	0	135	92.60		
376	ARG(7/76)		810	17.00	1.3	840.0	0.92	0.90	0	160	90.00		
377	ARG(7/76)		810	17.00	1.4	840.0	0.83	0.90	0	170	92.00		
378	ARG(7/76)		810	17.00	1.3	840.0	0.72	0.90	0	180	93.00		
379	ARG(7/76)		810	17.00	1.4	840.0	0.80	0.90	0	210	90.00		
380	EXX(1/74)		810	43.00	0.0	804.4	1.17	0.60	1	310	84.40	ARKWRIGHT	1.49
381	EXX(1/74)		810	23.00	0.0	904.4	1.29	0.60	1	290	86.00	ARKWRIGHT	1.49
382	EXX(1/74)		537	104.00	0.0	804.4	1.62	0.60	1	340	86.80	ARKWRIGHT	1.49
383	EXX(1/74)		537	153.00	0.0	848.8	1.74	0.60	1	450	72.20	ARKWRIGHT	1.49
384	EXX(1/74)		810	209.00	0.0	821.1	1.68	0.60	1	380	54.30	ARKWRIGHT	1.49
385	EXX(1/74)		810	203.00	0.0	893.3	1.83	0.60	1	340	54.30	ARKWRIGHT	1.49
386	EXX1/76		820	1.00	0.0	875.0	1.02	0.60	1	140	83.10	ARKWRIGHT	1.49
387	EXX1/76		820	0.00	0.0	880.0	1.02	0.60	4	112	77.50	ARKWRIGHT	1.49
388	EXX1/76		820	6.00	0.0	850.0	0.98	0.60	4	122	51.50	ARKWRIGHT	1.49
389	EXX5/76		810	57.00	0.0	850.0	1.14	0.75	1	201	52.30	ILLINOIS#6	1.24
390	EXX5/76		820	55.00	0.0	830.0	1.11	0.75	4	210	39.20	ILLINOIS#6	1.24
391	EXX5/76		820	60.00	0.0	850.0	1.16	0.75	4	230	26.00	ILLINOIS#6	1.24
392	EXX5/76		820	61.00	0.0	902.2	1.16	0.60	1	239	86.60	ILLINOIS#6	1.24
393	EXX5/76		820	70.00	0.0	882.2	1.15	0.60	4	240	58.60	ILLINOIS#6	1.24
394	EXX5/76		820	104.00	0.0	882.7	1.14	0.60	4	251	45.60	ILLINOIS#6	1.24
395	EXX5/76		820	119.00	0.0	837.7	1.13	0.60	0	241	99.99	WESTERN	0.96
396	EXX5/76		820	120.00	0.0	825.0	1.10	0.60	4	299	99.99	WESTERN	0.96

[illegible]	[illegible]	[illegible]	P(kPa)	%EX AIR	Ca/S	TEMP C	SUP VEL	B DEP	CD	NOXppm	%DESUL	COAL	WT% N
402	EXXn/76		820	114.00	0.0	850.0	1.13	0.60	4	261	88.40	WESTERN	0.96
403	EXXn/76		820	157.00	0.0	850.0	1.12	0.60	4	291	93.30	WESTERN	0.96
404	EXXn/76		820	153.00	0.0	842.7	1.13	0.60	4	272	93.60	WESTERN	0.96
415	CC(3/70)		156	24.26	7.3	926.6	0.45	0.90	0	240	99.99	DISCO CHAR	1.42
416	CC(3/70)		156	21.38	7.9	982.2	0.45	0.90	0	270	97.90	DISCO CHAR	1.42
417	CC(3/70)		156	31.25	8.3	982.2	0.90	0.90	0	130	98.20	DISCO CHAR	1.42
418	CC(3/70)		156	24.26	8.0	1037.7	0.90	0.90	0	270	99.00	DISCO CHAR	1.42
419	CC(3/70)		156	32.91	4.2	982.2	0.90	0.90	0	60	94.50	CRESAPCHAR	1.55
420	CC(3/70)		156	28.83	2.0	982.2	0.90	0.90	0	103	90.70	CRESAPCHAR	1.55
421	CC(3/70)		156	25.74	4.0	982.2	0.90	0.90	0	116	93.60	IRELAND	1.37
422	CC(3/70)		156	23.52	1.8	982.2	0.90	0.90	0	44	88.50	IRELAND	1.37
423	CC(3/70)		156	28.83	1.4	982.2	0.90	0.90	0	152	87.00	IRELAND	1.37
424	CC(3/70)		156	28.04	0.9	982.2	0.90	0.90	0	90	74.10	IRELAND	1.37
425	CC(3/70)		156	25.74	3.6	982.2	0.90	0.90	0	340	66.50	IRELAND	1.37
426	CP(10/75)		405	286.00	1.5	793.3	2.07	0.60	1	118	43.50	ILLINOIS	1.36
427	CP(10/75)		405	282.00	3.4	782.2	2.07	0.60	1	166	56.10	ILLINOIS	1.36
428	CP(10/75)		405	317.00	1.4	763.8	1.92	0.60	1	45	38.10	ILLINOIS	1.36
429	CP(10/75)		405	310.00	3.3	798.8	1.95	0.60	1	65	69.40	ILLINOIS	1.36
430	CP(10/75)		405	329.00	1.4	796.1	1.92	0.60	1	36	66.20	ILLINOIS	1.36
431	CP(10/75)		405	299.00	3.3	797.2	1.98	0.60	1	63	69.50	ILLINOIS	1.36
432	CP(10/75)		405	318.00	1.6	801.1	2.01	0.60	1	70	57.90	ILLINOIS	1.36
433	CP(10/75)		405	297.00	1.5	798.8	1.98	0.60	1	78	57.50	ILLINOIS	1.36
434	CP(9/75)		405	366.00	1.4	785.0	2.01	0.60	1	73	43.80	ILLINOIS	1.36
436	CP(9/75)		101	172.72	1.2	915.5	1.84	0.60	1	185	91.10	ILLINOIS	1.36
439	CP(9/75)		101	150.00	1.3	871.1	1.80	0.60	1	326	98.70	ILLINOIS	1.36
441	CP(9/75)		101	139.76	0.6	912.7	1.83	0.60	1	258	50.00	ILLINOIS	1.36
443	CP(9/75)		101	183.78	0.9	912.7	1.83	0.60	1	221	75.30	ILLINOIS	1.36
444	PER(10/70)		101	20.68	1.7	871.1	3.90	0.50	1	300	54.50	OHIO #8	2.50
445	PER(10/70)		101	22.09	1.4	837.7	3.90	0.50	1	360	43.00	OHIO #8	2.50
446	PER(10/70)		101	18.64	1.1	948.8	3.90	0.37	1	340	2.60	OHIO #8	2.50
447	PER(10/70)		101	20.00	1.6	937.7	3.90	0.37	1	340	13.20	OHIO #8	2.50
448	PER(10/70)		101	17.97	2.2	937.7	3.90	0.37	1	300	29.00	OHIO #8	2.50
449	PER(10/70)		101	17.31	1.1	854.4	3.90	0.50	1	280	21.00	OHIO #8	2.50
450	PER(10/70)		101	20.00	1.6	854.4	3.90	0.50	1	280	37.00	OHIO #8	2.50
451	PER(10/70)		101	16.66	2.4	854.4	3.90	0.50	1	280	48.00	OHIO #8	2.50
452	PER(10/70)		101	17.97	1.1	804.4	3.90	0.50	1	260	28.20	OHIO #8	2.50
453	PER(10/70)		101	15.38	1.7	804.4	3.90	0.50	1	220	45.00	OHIO #8	2.50
454	PER(10/70)		101	16.66	1.1	804.4	3.90	0.50	1	160	39.00	OHIO #8	2.50
455	PER(10/70)		101	16.66	0.7	860.0	3.90	0.50	1	240	28.20	OHIO #8	2.50
456	PER(10/70)		101	16.66	0.9	860.0	3.90	0.50	1	200	41.00	OHIO #8	2.50
457	PER(10/70)		101	17.97	0.9	810.0	3.90	0.50	1	200	54.00	OHIO #8	2.50
458	PER(10/70)		101	15.38	1.1	987.7	3.90	0.32	1	260	25.00	OHIO #8 WA	0.99
459	PER(10/70)		101	16.02	1.4	965.5	3.90	0.32	1	230	40.00	OHIO #8 WA	0.99
460	PER(10/70)		101	16.66	1.4	932.2	3.90	0.32	1	230	59.00	OHIO #8 WA	0.99
461	PER(10/70)		101	16.66	1.3	915.5	3.90	0.47	1	280	56.00	OHIO #8 WA	0.99
462	PER(10/70)		101	16.66	1.3	871.1	3.90	0.47	1		62.00	OHIO #8 WA	0.99
463	PER(10/70)		101	14.13	1.4	898.8	3.90	0.50	1	280	68.00	OHIO #8 WA	0.99
464	PER(10/70)		101	15.38	2.4	843.3	3.90	0.47	1	300	65.30	OHIO #8 WA	0.99
465	PER(10/70)		101	16.66	2.4	871.1	3.90	0.54	1	260	81.80	OHIO #8 WA	0.99
466	PER(10/70)		101	16.66	2.2	871.1	3.90	0.54	1	260	77.40	OHIO #8 WA	0.99
467	PER(10/70)		101	16.02	2.2	871.1	3.90	0.54	1	260	83.50	OHIO #8 WA	0.99
468	PER(10/70)		101	16.66	1.7	843.3	3.90	0.60	1	240	71.50	OHIO #8	2.50
469	PER(10/70)		101	17.97	1.7	826.6	3.90	0.60	1	240	74.20	OHIO #8	2.50
470	PER(10/70)		101	16.66	1.7	904.4	3.90	0.50	1	220	64.20	OHIO #8	2.50
471	PER(10/70)		101	17.97	1.9	860.0	3.90	0.50	1	220	70.90	OHIO #8	2.50
472	PER(10/70)		101	16.02	2.0	854.4	3.90	0.50	1	320	74.00	OHIO #8	2.50
473	PER(10/70)		101	0.00	2.4	871.1	3.90	0.50	1	260	71.60	OHIO #8 WA	0.99
474	PER(10/70)		101	0.00	2.2	871.1	3.90	0.50	1	260	64.90	OHIO #8 WA	0.99
475	PER(10/70)		101	0.00	1.7	871.1	3.90	0.50	1	240	60.00	OHIO #8	2.50
476	PER(10/70)		101	0.00	2.0	882.2	3.90	0.50	1	240	73.50	OHIO #8	2.50
477	PER(10/70)		101	0.00	2.0	882.2	3.90	0.50	1	240	73.50	OHIO #8	2.50
478	PER(10/70)		101	0.00	1.4	882.2	3.90	0.50	1	250	50.00	OHIO #8 WA	0.99
479	PER(10/70)		101	0.00	1.8	882.2	3.90	0.50	1	250	60.40	OHIO #8 WA	0.99
480	PER(10/70)		101	0.00	1.3	882.2	3.90	0.50	1	270	53.80	OHIO #8 WA	0.99
481	PER(10/70)		101	0.00	1.6	882.2	3.90	0.50	1	270	61.50	OHIO #8 WA	0.99
482	PER(10/70)		101	0.00	1.6	876.6	3.90	0.50	1	290	61.90	OHIO #8 WA	0.99
483	PER(10/70)		101	0.00	1.8	876.6	3.90	0.50	1	290	64.90	OHIO #8 WA	0.99
484	PER(10/70)		101	0.00	1.8	876.6	3.90	0.50	1	290	70.50	OHIO #8 WA	0.99
485	NCB(9/71)		101	23.52	2.9	776.6	2.40	0.60	1	410	73.00	PITTSBURGH	1.40
486	NCB(9/71)		101	27.27	1.8	771.1	2.40	0.60	1		74.00	PITTSBURGH	1.40
487	NCB(9/71)		101	25.74	1.8	837.7	2.40	0.60	1	480	78.00	PITTSBURGH	1.40
488	NCB(9/71)		101	22.09	0.6	848.8	2.40	0.60	1		44.00	PITTSBURGH	1.40
489	NCB(9/71)		101	24.26	0.6	915.5	2.40	0.60	1		16.00	PITTSBURGH	1.40
490	NCB(9/71)		101	22.09	1.7	915.5	2.40	0.60	1		48.00	PITTSBURGH	1.40
491	NCB(9/71)		101	26.50	0.6	776.6	2.40	0.60	1		69.00	PITTSBURGH	1.40
492	NCB(9/71)		101	21.38	4.7	898.8	2.40	0.60	1	480	64.00	PITTSBURGH	1.40
493	NCB(9/71)		101	36.36	5.5	843.3	2.40	0.60	1	480	82.00	PITTSBURGH	1.40
494	NCB(9/71)		101	11.11	2.4	848.8	0.90	0.60	1		90.50	PITTSBURGH	1.40
495	NCB(9/71)		101	12.90	1.9	843.8	0.90	0.60	1		97.50	PITTSBURGH	1.40
496	NCB(9/71)		101	14.13	1.1	798.8	0.90	0.60	1		55.00	ILLINOIS	1.30
497	NCB(9/71)		101	11.70	2.2	798.8	0.90	0.60	1		67.00	ILLINOIS	1.30
498	NCB(9/71)		101	12.29	3.2	798.8	0.90	0.60	1		94.00	ILLINOIS	1.30
499	NCB(9/71)		101	17.31	0.8	798.8	0.60	0.60	1		55.00	WELBECK	1.50
500	NCB(9/71)		101	17.31	0.8	798.8	0.60	0.60	1		52.00	WELBECK	1.50
501	NCB(9/71)		101	17.31	0.8	798.8	0.90	0.60	1		45.00	WELBECK	1.50
502	NCB(9/71)		101	12.29	1.8	798.8	0.90	0.60	1		81.00	WELBECK	1.50
503	NCB(9/71)		101	11.70	2.9	798.8	0.90	0.60	1		97.00	WELBECK	1.50
504	NCB(9/71)		101	1.44	0.8	798.8	0.90	0.60	1		48.00	WELBECK	1.50
505	NCB(9/71)		101	14.13	1.8	798.8	0.60	0.60	1		85.00	WELBECK	1.50

FILE	SOURCE	RUN #	P(kPa)	%EX AIR	Ca/S	TEMP C	SUP VEL	B DEP	CD	NOXppm	%DESUL	COAL	WT% N
506	NCB(9/71)		101	13.51	1.3	798.8	0.90	0.60	1		25.00	PARK HILL	1.30
507	NCB(9/71)		101	10.52	2.7	798.8	0.90	0.60	1		78.00	PARK HILL	1.30
508	NCB(9/71)		101	21.38	1.5	815.5	2.40	0.60	1	430	55.00	PITTSBURGH	1.40
509	NCB(9/71)		101	20.00	0.4	821.1	2.40	0.60	1		14.00	PITTSBURGH	1.40
510	NCB(9/71)		101	15.38	3.0	832.2	2.40	0.60	1		86.00	PITTSBURGH	1.40
511	NCB(9/71)		101	22.80	1.8	848.8	2.40	0.60	1		32.00	PITTSBURGH	1.40
512	NCB(9/71)		101	20.00	0.8	854.4	2.40	0.60	1	380	26.00	PITTSBURGH	1.40
513	NCB(9/71)		101	22.09	2.4	843.3	2.40	0.60	1	490	59.00	PITTSBURGH	1.40
514	NCB(9/71)		101	22.80	0.7	843.3	2.40	0.60	1	500	21.00	PITTSBURGH	1.40
515	NCB(9/71)		101	22.09	2.4	854.4	2.40	0.60	1	390	61.00	PITTSBURGH	1.40
516	NCB(9/71)		101	25.00	1.6	851.1	2.40	0.60	1		46.00	PITTSBURGH	1.40
517	NCB(9/71)		101	56.71	1.4	846.6	2.40	0.60	1		54.00	PITTSBURGH	1.40
518	NCB(9/71)		101	19.31	1.0	848.8	2.40	0.60	1		40.00	PITTSBURGH	1.40
519	NCB(9/71)		101	20.68	2.3	843.3	2.40	0.60	1		76.00	PITTSBURGH	1.40
520	NCB(9/71)		101	20.68	3.8	848.8	2.40	0.60	1		85.00	PITTSBURGH	1.40
521	NCB(9/71)		101	20.68	0.6	843.3	2.40	0.60	1		24.00	PITTSBURGH	1.40
522	NCB(9/71)		101	22.09	2.4	848.8	2.40	0.60	1		74.00	PITTSBURGH	1.40
523	NCB(9/71)		101	23.52	1.9	815.5	2.40	0.60	1		67.00	PITTSBURGH	1.40
524	NCB(9/71)		101	21.38	2.6	832.2	1.80	0.60	1		85.00	PITTSBURGH	1.40
525	NCB(9/71)		101	32.91	2.6	854.4	3.30	0.60	1	330	77.00	PITTSBURGH	1.40
526	NCB(9/71)		101	32.07	2.8	843.3	2.10	0.60	1	510	82.00	PITTSBURGH	1.40
527	NCB(9/71)		101	40.93	2.6	843.3	3.30	0.60	1	410	77.00	PITTSBURGH	1.40
528	NCB(9/71)		101	26.50	2.6	904.4	2.40	0.60	1	500	58.00	PITTSBURGH	1.40
529	NCB(9/71)		101	20.68	2.6	848.8	1.80	0.60	1	470	83.00	PITTSBURGH	1.40
530	NCB(9/71)		101	26.50	1.7	843.3	2.40	0.60	1	530	69.00	PITTSBURGH	1.40
531	NCB(9/71)		101	25.74	2.2	798.8	1.20	0.66	1		81.00	PITTSBURGH	1.40
532	NCB(9/71)		101	22.09	2.2	748.8	1.20	0.66	1		50.00	PITTSBURGH	1.40
533	NCB(9/71)		101	19.31	2.2	848.8	1.20	0.66	1		83.00	PITTSBURGH	1.40
534	NCB(9/71)		101	25.00	1.3	848.8	1.20	0.66	1		58.00	PITTSBURGH	1.40
535	NCB(9/71)		101	17.31	2.2	848.8	1.20	0.63	1		76.00	PITTSBURGH	1.40
536	NCB(9/71)		101	18.64	3.3	848.8	1.20	0.66	1		91.00	PITTSBURGH	1.40
537	NCB(9/71)		101	14.13	1.2	848.8	1.20	0.63	1		60.00	PITTSBURGH	1.40
538	NCB(9/71)		101	16.66	2.2	798.8	0.90	0.69	1		84.00	PITTSBURGH	1.40
539	NCB(9/71)		101	16.02	3.3	798.8	0.93	0.63	1		98.00	PITTSBURGH	1.40
540	NCB(9/71)		101	16.02	1.1	848.8	2.43	0.63	1	470	34.00	PITTSBURGH	1.40
541	NCB(9/71)		101	16.02	2.3	848.8	2.43	0.63	1	515	56.00	PITTSBURGH	1.40
542	NCB(9/71)		101	13.51	2.9	848.8	2.40	0.63	1		68.00	PITTSBURGH	1.40
543	NCB(9/71)		101	17.97	1.0	843.8	1.20	0.63	1		49.00	PITTSBURGH	1.40
544	NCB(9/71)		101	14.13	1.0	848.8	0.90	0.60	1		49.00	PITTSBURGH	1.40
545	NCB(9/71)		101	17.97	1.7	848.8	1.20	0.63	1		65.00	PITTSBURGH	1.40
546	NCB(9/71)		101	17.97	1.6	848.8	2.40	0.66	1	445	51.00	PITTSBURGH	1.40
547	NCB(9/71)		101	12.90	1.9	848.8	2.34	1.05	1		57.00	PITTSBURGH	1.40
548	NCB(9/71)		101	15.38	5.7	848.8	2.40	1.08	1	560	97.00	PITTSBURGH	1.40
549	NCB(9/71)		101	16.66	6.0	848.8	2.40	1.08	1	400	99.99	PITTSBURGH	1.40
550	NCB(9/71)		101	11.11	1.1	798.8	0.90	0.60	1		42.00	PARK HILL	1.30
551	NCB(9/71)		101	13.51	2.6	798.8	0.90	0.60	1		84.00	PARK HILL	1.30
552	NCB(9/71)		101	10.52	0.8	798.8	0.90	0.60	1		50.00	PARK HILL	1.30
553	NCB(9/71)		101	12.90	1.0	798.8	0.90	0.60	1		31.00	PITTSBURGH	1.40
554	NCB(9/71)		101	11.70	2.1	798.8	0.90	0.60	1		52.00	PITTSBURGH	1.40
555	NCB(9/71)		101	12.90	3.1	798.8	0.90	0.60	1		88.00	PITTSBURGH	1.40
556	NCB(9/71)		101	15.38	1.5	798.8	0.90	0.60	1		47.00	ILLINOIS	1.30
557	NCB(9/71)		101	14.13	2.2	798.8	0.90	0.60	1		63.00	ILLINOIS	1.30
558	NCB(9/71)		101	16.02	3.3	798.8	0.90	0.60	1		78.00	ILLINOIS	1.30
559	NCB(9/71)		101	14.75	1.1	698.8	0.90	0.60	1		15.00	ILLINOIS	1.30
560	NCB(9/71)		101	12.90	2.2	698.8	0.90	0.60	1		18.00	ILLINOIS	1.30
561	NCB(9/71)		101	14.75	1.1	798.8	0.90	0.90	1		51.00	ILLINOIS	1.30
562	NCB(9/71)		101	14.13	2.1	798.8	0.90	0.90	1		72.00	ILLINOIS	1.30
563	NCB(9/71)		101	12.90	1.1	798.8	0.90	0.60	1		61.00	ILLINOIS	1.30
564	NCB(9/71)		101	13.51	3.6	798.8	0.90	0.60	1		93.00	ILLINOIS	1.30
565	NCB(9/71)		101	13.51	0.9	798.8	0.90	0.60	1		43.00	PITTSBURGH	1.40
566	NCB(9/71)		101	11.70	1.7	798.8	0.90	0.60	1		71.00	PITTSBURGH	1.40
567	NCB(9/71)		101	12.29	2.6	798.8	0.90	0.60	1		91.00	PITTSBURGH	1.40
568	NCB(9/71)		101	11.11	0.9	798.8	0.90	0.60	1		38.00	PITTSBURGH	1.40
569	NCB(9/71)		101	13.51	0.9	798.8	0.90	0.60	1		43.00	PITTSBURGH	1.40
570	NCB(9/71)		101	14.13	1.9	798.8	0.90	0.60	1		80.00	WELBECK	1.50
571	NCB(9/71)		101	16.66	3.1	798.8	1.20	0.63	1	234	83.00	PITTSBURGH	1.40
572	NCB(9/71)		101	21.38	2.6	748.8	1.23	0.63	1		72.00	PITTSBURGH	1.40
573	NCB(9/71)		101	16.02	2.7	848.8	1.14	0.63	1	244	73.00	PITTSBURGH	1.40
574	NCB(9/71)		101	22.09	2.7	798.8	1.20	0.63	1		74.00	PITTSBURGH	1.40
575	NCB(9/71)		101	15.38	2.2	798.8	0.63	1.11	1	360	83.00	PITTSBURGH	1.40
576	NCB(9/71)		101	17.31	1.6	798.8	0.66	1.14	1	392	99.00	PITTSBURGH	1.40
577	NCB(9/71)		101	16.66	2.5	848.8	2.40	0.81	1		62.00	PITTSBURGH	1.40
578	NCB(9/71)		101	18.64	5.4	848.8	2.40	0.81	1	390	87.00	PITTSBURGH	1.40
579	NCB(9/71)		101	19.31	5.3	848.8	2.43	1.20	1	360	88.00	PITTSBURGH	1.40
580	NCB(9/71)		101	14.75	5.2	848.8	2.40	2.10	1	400	93.00	PITTSBURGH	1.40
581	NCB(9/71)		101	16.66	5.0	848.8	2.40	1.65	1	425	87.00	PITTSBURGH	1.40
582	NCB(9/71)		101	16.66	1.8	848.8	2.40	0.63	1		38.00	PITTSBURGH	1.40
583	NCB(9/71)		101	19.31	2.1	848.8	2.40	0.63	1		50.00	PITTSBURGH	1.40
584	NCB(9/71)		101	19.31	2.8	848.8	2.37	0.66	1		64.00	PITTSBURGH	1.40
585	NCB(9/71)		101	18.64	2.8	848.8	2.40	1.14	1		64.00	PITTSBURGH	1.40
586	NCB(9/71)		101	17.31	3.0	848.8	1.23	0.69	1		72.00	PITTSBURGH	1.40
587	ARG(7/69)		101	200.00	3.5	871.1	0.93	0.37	0		67.00	ILLINOIS	1.31
588	ARG(7/69)		101	200.00	5.1	871.1	0.93	0.37	4		74.00	ILLINOIS	1.31
589	ARG(7/69)		101	60.00	1.4	871.1	0.96	0.37	0		42.00	ILLINOIS	1.31
590	ARG(7/69)		101	60.00	2.8	871.1	0.96	0.37	0		75.00	ILLINOIS	1.31
591	ARG(7/69)		101	130.00	2.0	871.1	1.38	0.37	0		61.00	ILLINOIS	1.31
592	ARG(7/69)		101	130.00	2.9	871.1	1.38	0.37	4		74.00	ILLINOIS	1.31
593	ARG(7/69)		101	130.00	4.0	871.1	1.38	0.37	4		87.00	ILLINOIS	1.31
594	ARG(7/69)		101	56.00	1.5	871.1	1.38	0.37	0		29.00	ILLINOIS	1.31
595	ARG(7/69)		101	56.00	2.1	871.1	1.38	0.37	4		51.00	ILLINOIS	1.31
596	ARG(7/69)		101	56.00	2.6	871.1	1.38	0.37	4		60.00	ILLINOIS	1.31
597	ARG(7/69)		101	20.00	2.5	871.1	0.90	0.37	0		72.00	ILLINOIS	1.31
598	ARG(7/69)		101	22.50	4.2	871.1	0.90	0.37	0		86.00	ILLINOIS	1.31
599	ARG(7/69)		101	11.00	1.9	871.1	0.90	0.60	0	440	68.00	ILLINOIS	1.31

FILE	SOURCE	RUN #	P(kPa)	%EX AIR	Ca/S	TEMP C	SUP VEL	B DEP	CD	NOXppm	%DESUL	COAL	WT% N
600	ARG(7/69)		101	23.50	2.4	871.1	0.90	0.60	0	400	53.00	ILLINOIS	1.11
601	ARG(7/69)		101	15.00	2.6	871.1	0.90	0.60	0	400	52.00	ILLINOIS	1.11
602	ARG(7/69)		101	20.50	2.2	871.1	0.90	0.60	0	360	87.00	ILLINOIS	1.11
603	ARG(6/70)		101	17.97	2.2	871.1	0.90	0.60	0	420	79.00	ILLINOIS#6	1.18
604	ARG(6/70)		101	20.00	1.7	871.1	0.90	0.60	0	500	64.00	ILLINOIS#6	1.18
605	ARG(6/70)		101	7.69	1.2	871.1	0.90	0.60	4	400	41.00	ILLINOIS#6	1.18
606	ARG(6/70)		101	13.51	1.7	871.1	0.90	0.60	4	460	65.00	ILLINOIS#6	1.18
607	ARG(6/70)		101	16.66	3.0	871.1	0.90	0.60	4	500	79.00	ILLINOIS#6	1.18
608	ARG(6/70)		101	20.00	1.3	871.1	2.70	0.60	0	420	51.00	ILLINOIS#6	1.18
609	ARG(6/70)		101	18.64	1.7	871.1	2.70	0.60	4	400	59.00	ILLINOIS#6	1.18
610	ARG(6/70)		101	12.29	1.6	871.1	2.70	0.60	0	550	18.00	ILLINOIS#6	1.18
611	ARG(6/70)		101	20.00	1.0	871.1	2.70	0.60	0	520	39.00	ILLINOIS#6	1.18
612	ARG(6/70)		101	5.00	1.0	871.1	2.70	0.60	0	510	33.00	ILLINOIS#6	1.18
613	ARG(6/70)		101	13.51	2.4	871.1	2.70	0.60	4	510	71.00	ILLINOIS#6	1.18
614	ARG(6/70)		101	13.51	2.4	871.1	2.70	0.60	4	470	69.00	ILLINOIS#6	1.18
615	ARG(6/70)		101	7.69	2.4	871.1	2.70	0.60	4	420	64.00	ILLINOIS#6	1.18
616	ARG(6/70)		101	20.00	1.5	843.3	0.90	0.60	0	600	58.00	ILLINOIS#6	1.18
617	ARG(6/70)		101	20.68	2.0	843.3	0.90	0.60	4	600	67.00	ILLINOIS#6	1.18
618	ARG(6/70)		101	14.13	2.0	843.3	0.90	0.60	4	600	83.00	ILLINOIS#6	1.18
619	ARG(6/70)		101	22.09	4.2	843.3	0.90	0.60	4	650	89.00	ILLINOIS#6	1.18
620	ARG(6/70)		101	8.80	3.4	843.3	0.90	0.60	4	600	82.00	ILLINOIS#6	1.18
621	ARG(6/70)		101	16.66	1.5	898.8	0.90	0.60	0	580	54.00	ILLINOIS#6	1.18
622	ARG(6/70)		101	20.00	2.6	898.8	0.90	0.60	4	600	74.00	ILLINOIS#6	1.18
623	ARG(6/70)		101	20.00	3.0	898.8	0.90	0.60	4	600	81.00	ILLINOIS#6	1.18
624	ARG(6/70)		101	21.38	3.0	898.8	0.90	0.60	4	640	86.00	ILLINOIS#6	1.18
625	ARG(6/70)		101	23.52	2.4	898.8	0.90	0.60	0		60.00	ILLINOIS#6	1.18
626	ARG(6/70)		101	23.52	0.8	898.8	0.90	0.60	4		55.00	ILLINOIS#6	1.18
627	ARG(6/70)		101	18.64	0.6	898.8	0.90	0.60	4		43.00	ILLINOIS#6	1.18
628	ARG(6/70)		101	16.02	0.8	898.8	0.90	0.60	4		42.00	ILLINOIS#6	1.18
629	ARG(6/70)		101	14.13	4.0	843.3	0.90	0.60	0	530	95.00	ILLINOIS#6	1.18
630	ARG(6/70)		101	14.13	1.7	843.3	0.90	0.60	4	550	59.00	ILLINOIS#6	1.18
631	ARG(6/70)		101	14.13	0.6	843.3	0.90	0.60	4	690	32.00	ILLINOIS#6	1.18
632	ARG(6/70)		101	14.13	2.4	843.3	0.90	0.60	4	530	73.00	ILLINOIS#6	1.18
633	ARG(6/70)		101	0.00	1.2	871.1	0.90	0.60	0		53.00	ILLINOIS#6	1.18
634	ARG(6/70)		101	0.00	2.0	871.1	0.90	0.60	4		65.00	ILLINOIS#6	1.18
635	ARG(6/70)		101	15.38	1.6	871.1	0.85	0.60	0	500	87.00	ILLINOIS#6	1.18
636	ARG(6/70)		101	16.66	1.5	871.1	0.85	0.60	0	550	78.00	ILLINOIS#6	1.18
637	ARG(6/70)		101	16.66	0.6	871.1	0.85	0.60	0	350	45.00	ILLINOIS#6	1.18
638	ARG(6/70)		101	17.97	1.2	871.1	0.85	0.60	4	395	69.00	ILLINOIS#6	1.18
639	ARG(6/70)		101	11.70	1.5	871.1	0.85	0.60	0	365	66.00	ILLINOIS#6	1.18
640	ARG(6/70)		101	13.51	2.1	871.1	0.85	0.60	4	400	83.00	ILLINOIS#6	1.18
641	ARG(6/70)		101	16.66	2.6	871.1	0.84	0.60	0	380	79.00	ILLINOIS#6	1.18
642	ARG(6/70)		101	12.00	2.3	871.1	0.84	0.60	4	220	83.00	ILLINOIS#6	1.18
643	ARG(6/70)		101	20.00	2.5	871.1	0.84	0.60	4	320	79.00	ILLINOIS#6	1.18
644	ARG(6/70)		101	20.00	2.3	871.1	0.84	0.60	4	400	74.00	ILLINOIS#6	1.18
645	ARG(6/70)		101	23.52	2.2	871.1	0.84	0.60	4	440	[illegible]	[illegible]	[illegible]
646	ARG(6/70)		101	23.52	2.2	904.4	0.84	0.60	4	380	91.00	ILLINOIS#6	1.18
647	ARG(6/70)		101	19.31	2.5	760.0	0.84	0.60	4	250	44.00	ILLINOIS#6	1.18
648	ARG(6/70)		101	16.66	2.5	787.7	0.84	0.60	4	230	65.00	ILLINOIS#6	1.18
649	ARG(6/70)		101	20.00	2.5	815.5	0.84	0.60	4	360	91.00	ILLINOIS#6	1.18
650	ARG(6/70)		101	19.31	2.5	843.3	0.84	0.60	4	430	91.00	ILLINOIS#6	1.18
651	ARG(6/70)		101	18.64	2.5	871.1	0.84	0.60	4	430	86.00	ILLINOIS#6	1.18
652	ARG(6/70)		101	17.97	2.5	760.0	0.84	0.60	4	270	53.00	ILLINOIS#6	1.18
653	ARG(6/70)		101	20.00	1.5	871.1	0.73	0.60	4	75	99.00		0.00
654	ARG(6/70)		101	11.11	2.1	871.1	0.73	0.60	4	60	92.00		0.00
655	ARG(6/70)		101	19.31	1.8	871.1	0.81	0.60	4	75	95.00		0.00
656	ARG(6/70)		101	18.64	1.8	871.1	0.81	0.60	4	75	95.00		0.00
657	ARG(6/70)		101	17.97	1.6	871.1	0.81	0.60	4	100	90.00		0.00
658	ARG(6/70)		101	17.97	1.4	871.1	0.81	0.60	4	100	84.00		0.00
659	ARG(6/74)		101	16.66	1.6	898.8	1.65	0.60	0	135	16.00		0.00
660	ARG(6/74)		101	16.66	4.1	843.3	0.96	0.60	4	110	60.00		0.00
661	ARG(6/74)		101	16.66	11.9	843.3	0.96	0.60	4	140	90.00		0.00
662	ARG(6/74)		101	16.66	5.4	843.3	0.90	0.60	4	150	88.00		0.00
663	ARG(6/74)		101	16.66	6.0	787.7	0.93	0.60	4	140	78.00		0.00
664	ARG(6/74)		101	16.66	6.0	898.8	0.93	0.60	4	130	66.00		0.00
665	ARG(6/74)		101	5.00	4.0	787.7	0.99	0.60	4	190	68.00		0.00
666	EXX(2/71)		101	54.41	13.8	887.7	0.90	0.30	1		80.00	PITTSBURGH	1.30
667	EXX(2/71)		101	23.52	10.4	871.1	0.90	0.30	1		80.00	PITTSBURGH	1.30
668	EXX(2/71)		101	22.80	6.6	871.1	0.90	0.15	1		80.00	PITTSBURGH	1.30
669	EXX(2/71)		101	20.68	6.4	871.1	0.90	0.09	1		80.00	PITTSBURGH	1.30
670	EXX(2/71)		101	25.00	17.4	871.1	0.90	0.39	1		80.00	PITTSBURGH	1.30
671	EXX(2/71)		101	20.68	8.8	926.6	0.93	0.15	1		80.00	PITTSBURGH	1.30
672	EXX(2/71)		101	22.80	11.9	815.5	0.90	0.15	1		80.00	PITTSBURGH	1.30
673	EXX(2/71)		101	11.70	3.7	982.2	0.90	0.15	1		80.00	PITTSBURGH	1.30
674	EXX(2/71)		101	29.62	6.2	871.1	1.20	0.15	1	600	80.00	PITTSBURGH	1.30
675	EXX(2/71)		101	12.90	6.2	871.1	0.60	0.15	1	600	80.00	PITTSBURGH	1.30
676	EXX(2/71)		101	27.27	7.3	871.1	0.90	0.15	1	700	80.00	PITTSBURGH	1.30
677	EXX(2/71)		101	25.00	10.6	871.1	0.90	0.30	1	700	80.00	PITTSBURGH	1.30
678	EXX(2/71)		101	40.00	10.0	871.1	0.90	0.15	1	700	80.00	PITTSBURGH	1.30
679	EXX(2/71)		101	9.37	11.9	926.6	0.81	0.15	1	750	80.00	PITTSBURGH	1.30
680	EXX(2/71)		101	18.64	6.3	871.1	0.90	0.15	1	650	80.00	PITTSBURGH	1.30
681	EXX(2/71)		101	22.80	5.4	871.1	0.90	0.15	1	650	80.00	PITTSBURGH	1.30
682	EXX(2/71)		101	15.38	3.8	871.1	0.90	0.15	1	750	80.00	PITTSBURGH	1.30
683	EXX(2/71)		101	17.97	6.5	871.1	0.90	0.15	1	800	80.00	PITTSBURGH	1.30
684	EXX(2/71)		101	19.31	5.6	926.6	0.81	0.15	1	750	80.00	PITTSBURGH	1.30
685	B&W(3/77)		101	14.75	2.7	848.3	2.49	0.46	0	285	65.70		0.86
686	B&W(3/77)		101	13.51	0.5	850.0	2.50	0.49	0	212	39.60		0.86
687	B&W(3/77)		101	16.66	1.5	894.4	2.46	0.42	0	334	48.40		0.86
688	B&W(3/77)		101	16.66	1.4	838.8	2.48	0.50	0	215	50.60		0.86
689	B&W(3/77)		101	17.31	1.5	774.4	2.37	0.57	0	300	24.40		0.86
690	B&W(3/77)		101	16.02	1.8	838.3	3.57	0.61	0	213	42.20		0.86
691	B&W(3/77)		101	16.66	1.7	770.0	1.31	0.86	0	56	36.80		0.86
692	B&W(3/77)		101	16.02	2.1	829.4	2.40	0.41	0	213	59.60		0.76
693	B&W(3/77)		101	19.31	2.2	842.2	2.43	0.41	0	285	60.50		0.76
694	B&W(3/77)		101	16.66	3.5	857.7	2.49	0.41	0	322	73.50		0.76
695	B&W(3/77)		101	18.64	1.1	845.0	2.45	0.42	0	233	44.00		0.76
696	B&W(3/77)		101	17.97	1.1	850.0	2.45	0.42	0	303	28.40		0.76
697	B&W(3/77)		101	16.66	2.4	818.8	2.39	0.39	0	238	54.80		0.76
698	B&W(3/77)		101	14.75	3.4	825.5	2.39	0.41	0		70.00		0.76
699	B&W(3/77)		101	20.00	0.8	845.0	2.41	0.40	0	269	28.70		0.76
700	B&W(3/77)		101	14.75	2.0	845.0	2.49	0.40	0	246	52.70		0.76
701	B&W(3/77)		101	17.31	2.1	819.4	1.43	0.28	0	296	65.50		0.76
702	B&W(3/77)		101	16.02	2.3	850.5	2.48	0.33	0	190	64.50		0.76
703	B&W(3/77)		101	16.66	2.1	865.0	2.54	0.42	0	199	94.10		0.76
704	B&W(3/77)		101	17.31	1.8	829.4	1.38	0.30	0	313	78.20		0.76
705	B&W(3/77)		101	16.66	1.6	845.0	2.46	0.36	0	265	79.10		0.76

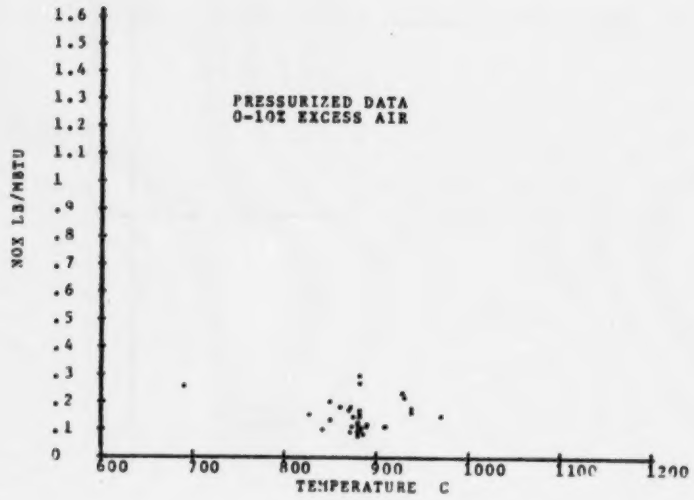
PRESSURIZED DATA
0-10% EXCESS AIR
NOX LB/MBTU
1.6
1.5
1.4
1.3
1.2
1.1
1
.9
.8
.7
.6
.5
.4
.3
.2
.1
0
600
700
800
900
1000
1100
1200
TEMPERATURE C

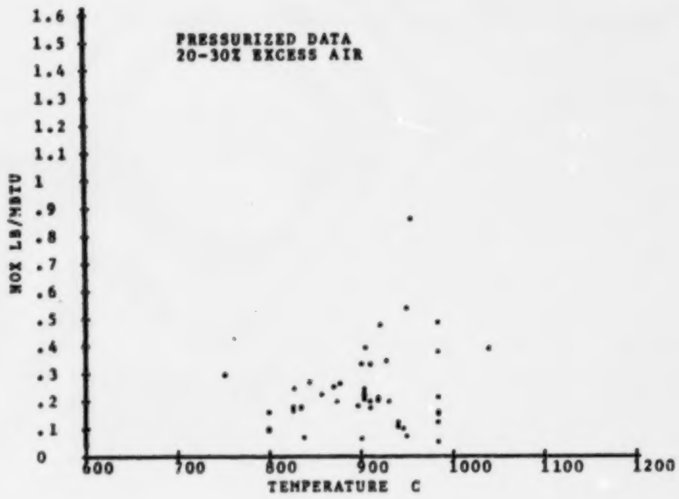
PRESSURIZED DATA
20-30% EXCESS AIR
NOX LB/MBTU
1.6
1.5
1.4
1.3
1.2
1.1
1
.9
.8
.7
.6
.5
.4
.3
.2
.1
0
600
700
800
900
1000
1100
1200
TEMPERATURE C

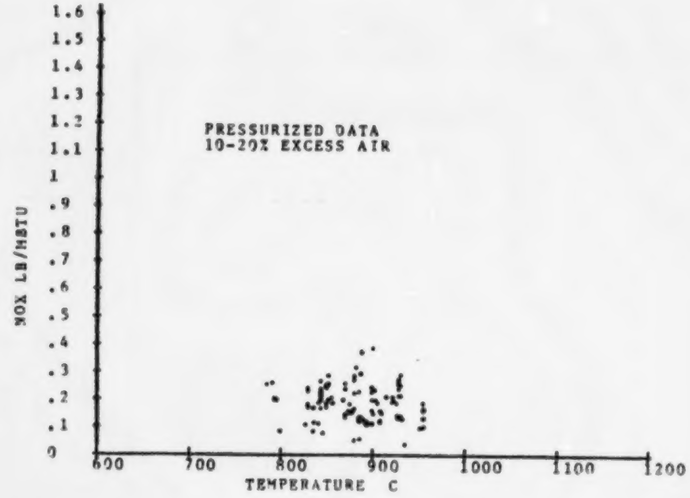
PRESSURIZED DATA
10-20% EXCESS AIR
NOX LB/MBTU
1.6
1.5
1.4
1.3
1.2
1.1
1
.9
.8
.7
.6
.5
.4
.3
.2
.1
0
600
700
800
900
1000
1100
1200
TEMPERATURE C

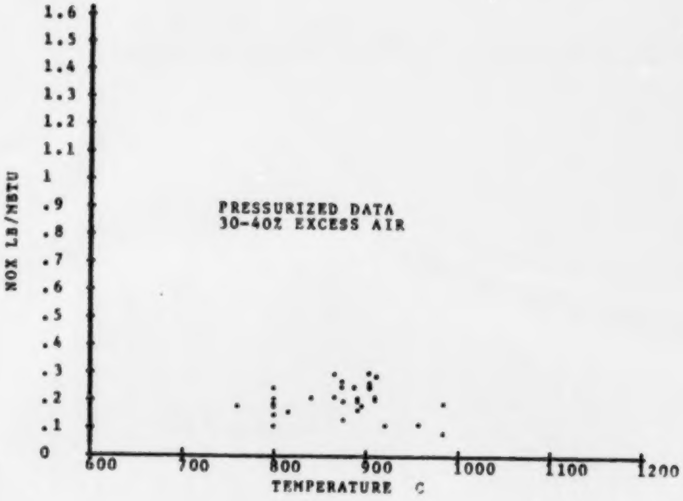
PRESSURIZED DATA
30-40% EXCESS AIR
NOX LB/MBTU
1.6
1.5
1.4
1.3
1.2
1.1
1
.9
.8
.7
.6
.5
.4
.3
.2
.1
0
600
700
800
900
1000
1100
1200
TEMPERATURE C

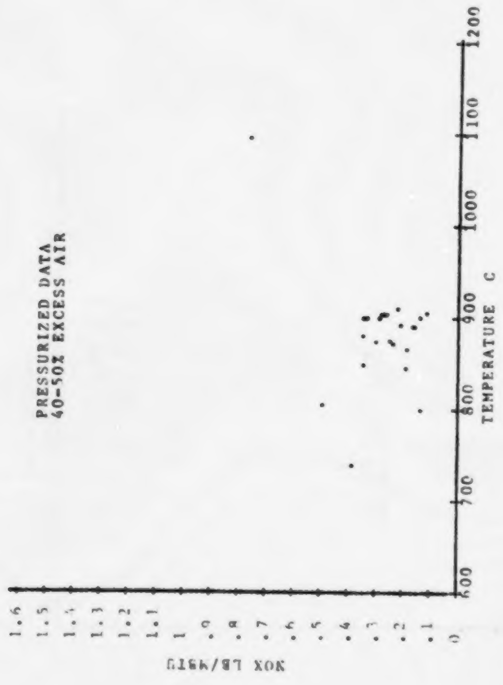
PRESSURIZED DATA
40-50% EXCESS AIR
NOX LB/MBTU
0
.1
.2
.3
.4
.5
.6
.7
.8
.9
1
1.1
1.2
1.3
1.4
1.5
1.6
TEMPERATURE C
600
700
800
900
1000
1100
1200

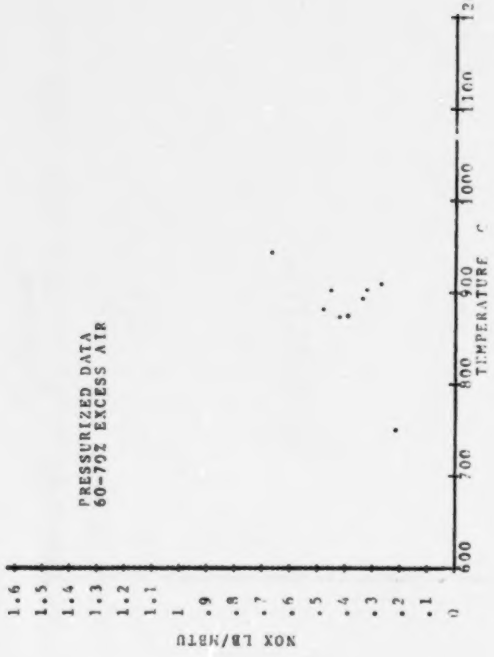
PRESSURIZED DATA
60-70% EXCESS AIR
NOX LB/MBTU
0
.1
.2
.3
.4
.5
.6
.7
.8
.9
1
1.1
1.2
1.3
1.4
1.5
1.6
TEMPERATURE C
600
700
800
900
1000
1100
1200

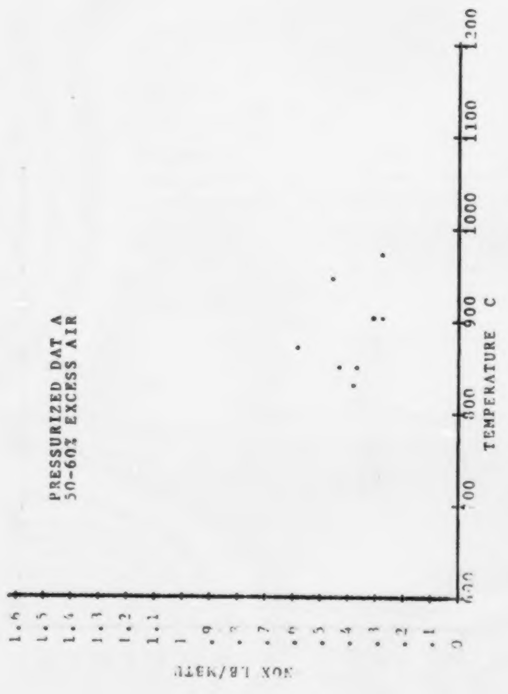
PRESSURIZED DAT A
50-60% EXCESS AIR
NOX LB/MBTU
0
.1
.2
.3
.4
.5
.6
.7
.8
.9
1
1.1
1.2
1.3
1.4
1.5
1.6
TEMPERATURE C
600
700
800
900
1000
1100
1200

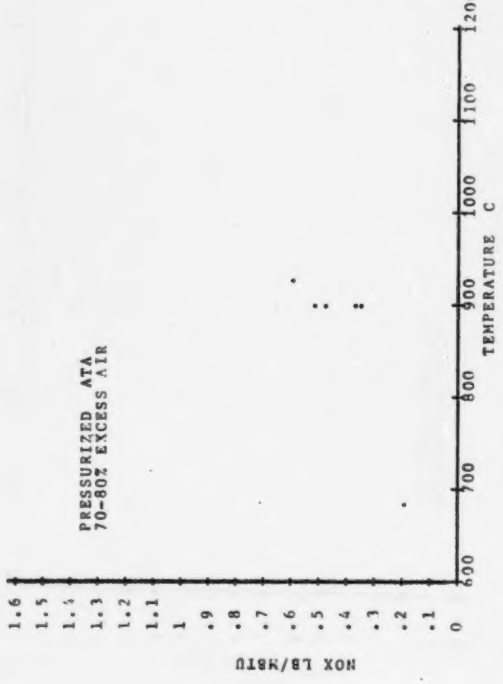
PRESSURIZED ATA
70-80% EXCESS AIR
NOX LB/MBTU
0
.1
.2
.3
.4
.5
.6
.7
.8
.9
1
1.1
1.2
1.3
1.4
1.5
1.6
TEMPERATURE C
600
700
800
900
1000
1100
1200

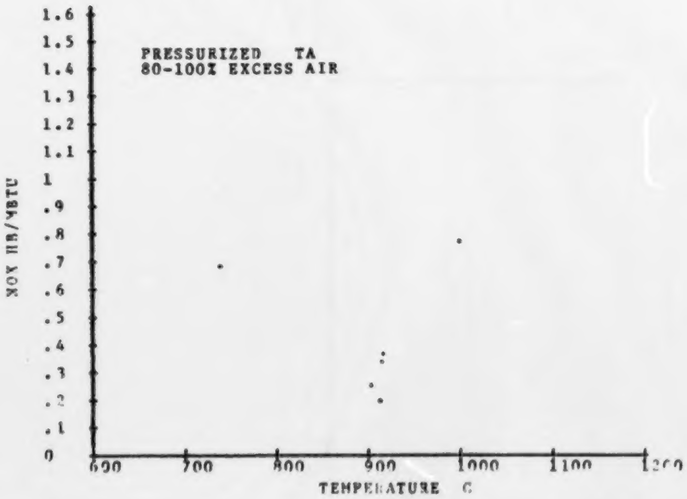
PRESSURIZED TA
80-100% EXCESS AIR
NOX LB/MBTU
1.6
1.5
1.4
1.3
1.2
1.1
1
.9
.8
.7
.6
.5
.4
.3
.2
.1
0
600
700
800
900
1000
1100
1200
TEMPERATURE C

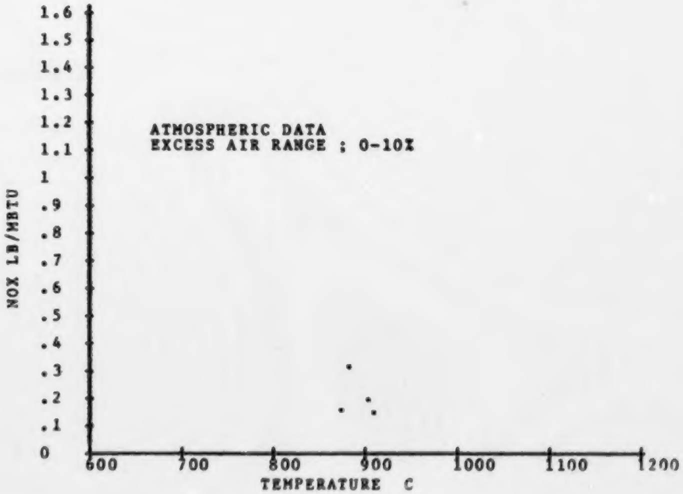
ATMOSPHERIC DATA
EXCESS AIR RANGE ; 0-10%
NOX LB/MBTU
1.6
1.5
1.4
1.3
1.2
1.1
1
.9
.8
.7
.6
.5
.4
.3
.2
.1
0
600
700
800
900
1000
1100
1200
TEMPERATURE C

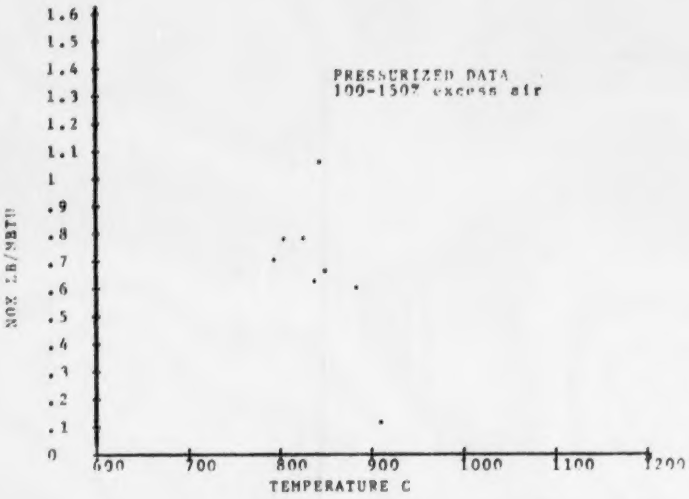
PRESSURIZED DATA
100-150% excess air
NOX LB/MBTU
1.6
1.5
1.4
1.3
1.2
1.1
1
.9
.8
.7
.6
.5
.4
.3
.2
.1
0
600
700
800
900
1000
1100
1200
TEMPERATURE C

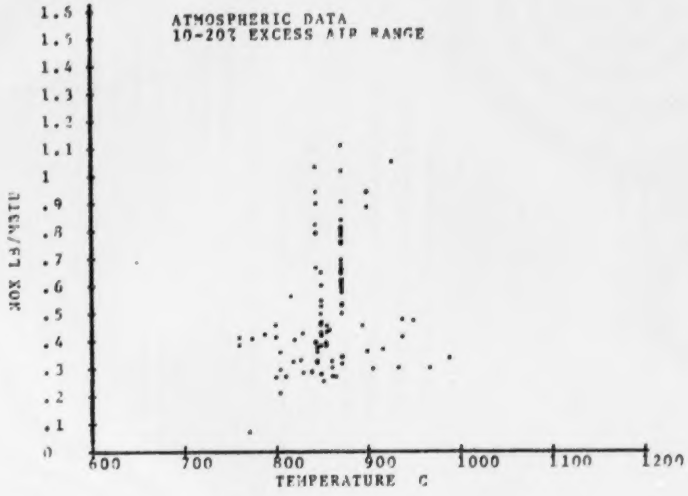
ATMOSPHERIC DATA
10-20% EXCESS AIR RANGE
NOX LB/MBTU
1.6
1.5
1.4
1.3
1.2
1.1
1
.9
.8
.7
.6
.5
.4
.3
.2
.1
0
600
700
800
900
1000
1100
1200
TEMPERATURE C

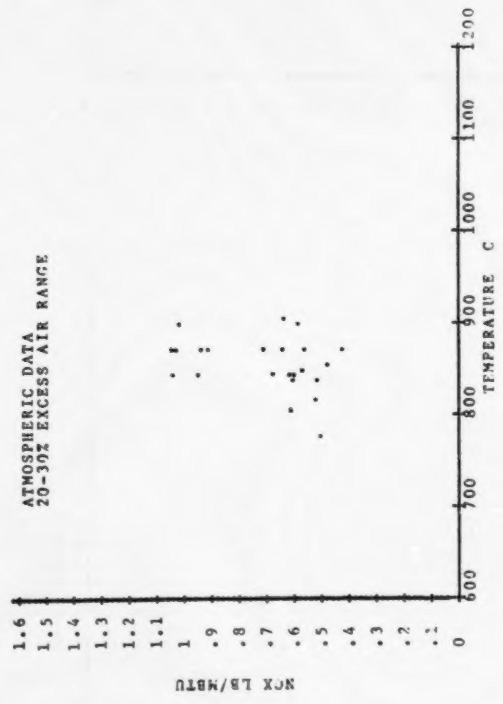
ATMOSPHERIC DATA
20-30% EXCESS AIR RANGE
NOX LB/MBTU
1.6
1.5
1.4
1.3
1.2
1.1
1
.9
.8
.7
.6
.5
.4
.3
.2
.1
0
TEMPERATURE C
600
700
800
900
1000
1100
1200

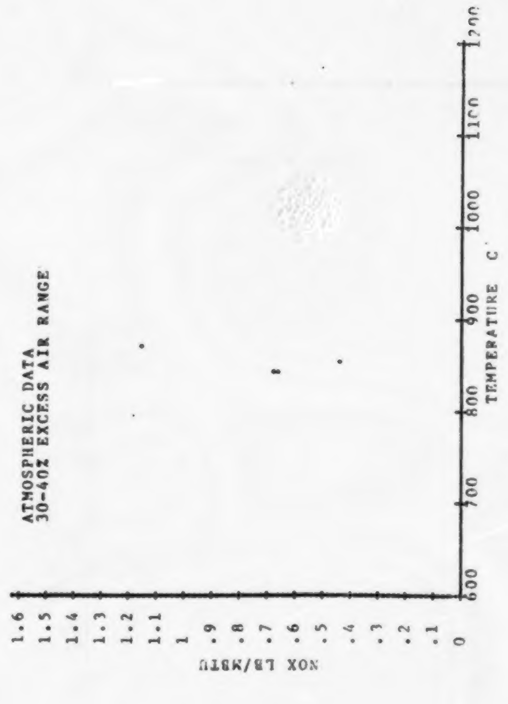
ATMOSPHERIC DATA
30-40% EXCESS AIR RANGE
NOX LB/MBTU
1.6
1.5
1.4
1.3
1.2
1.1
1
.9
.8
.7
.6
.5
.4
.3
.2
.1
0
TEMPERATURE C
600
700
800
900
1000
1100
1200

REFERENCE LIST

File Numbers	Reference, equipment
1-83	Hoke, R. C. et al., Studies of the Pressurized Fluidized-bed Coal Combustion Process. Report to U.S. EPA, Exxon Research and Engineering Company, Linden, NJ, September 1976, EPA-600/7-76-011. Exxon fluidized-bed combustion miniplant; 12.5 in internal diameter combustor.
84-156	Hoke, R. C. et al., Studies of the Pressurized Fluidized-bed Coal Combustion Process. Report to U.S. EPA, Exxon Research and Engineering Company, Linden, NJ, September 1977, EPA-600/7-77-107. Exxon fluidized-bed combustion miniplant; 12.5 in internal diameter combustor.
157-189	Hoke, R. C. et al., Miniplant Studies of Pressurized Fluidized-bed Coal Combustion. Third Annual Report to U.S. EPA, Exxon Research and Engineering Company, Linden, NJ, April 1978, EPA-600/7-78-069. Exxon fluidized-bed combustion miniplant; 12.5 in internal diameter combustor.
190-200	Vogel, G. J. et al., Reduction of Atmospheric Pollution by the Application of Fluidized-bed Combustion and Regeneration of Sulfur Containing Additives, Annual Report July 1973 - June 1974. ANL/ES-CEN-1007 and EPA-650/2-74-104.

File Numbers	Reference, equipment
201-215	Reduction of Atmospheric Pollution. Report to EPA, National Coal Board, London, UK, September 1971, Reference No. DHB 060971. 24 in. x 48 in. continuous fluid-bed combustor
216-219 231-234 239-271 330-352 386-396 402-404	Hoke, R. C., et al., A Regenerative Process for Fluidized Bed Coal Combustion and Desulfurization, Monthly Reports prepared under contracts 68-02-0617, 68-02-1451, and 68-02-1312 to EPA, Esso Research and Engineering Company, Linden, NJ. 216-218, 12/73; 4.5 in. diameter batch fluid-bed combustor 219, 12/73; 4.5 in. diameter batch fluid-bed combustor 231-234, 8/75; 4.5 in. diameter batch fluid-bed combustor 239-242, 9/75; 4.5 in. diameter batch fluid-bed combustor 243, 244, 4/73; 4.5 in. diameter batch fluid-bed combustor 245-247, 2/74; 4.5 in. diameter batch fluid-bed combustor 248, 249, 3/74; 4.5 in. diameter batch fluid-bed combustor 250, 4/74; 4.5 in. diameter batch fluid-bed combustor 251, 11/74; 4.5 in. diameter batch fluid-bed combustor 252-254, 1/74; 4.5 in. diameter batch fluid-bed combustor 255-258, 6/73; 4.5 in. diameter batch fluid-bed combustor

File Numbers	Reference, equipment
	259, 7/73; 4.5 in. diameter batch fluid-bed combustor
	260, 11/73; 4.5 in. diameter batch fluid-bed combustor
	261-263, 1/75; 4.5 in. diameter batch fluid-bed combustor
	264, 3/75; 4.5 in. diameter batch fluid-bed combustor
	265, 5/75; 4.5 in. diameter batch fluid-bed combustor
	266-270, 6/75; 4.5 in. diameter batch fluid-bed combustor
	271, 7/75; 4.5 in. diameter batch fluid-bed combustor
	330-352, 11/75; 4.5 in. diameter batch fluid-bed combustor
	386-388, 1/76; 4.5 in. diameter batch fluid-bed combustor
	389-396, 5/76; 4.5 in. diameter batch fluid-bed combustor
	402-404, 6/76; 4.5 in. diameter batch fluid-bed combustor
273-287	A Development Program on Pressurized Fluidized-Bed Combustion. Interim Report No. 1 to Office of Coal Research and EPA, Argonne National Laboratory, Argonne, IL, October 1974, Contract No. 14-32-0001-1543. 6 in. diameter continuous fluid-bed combustor
288-318	Jonke, A. A., A Development Program on Pressurized Fluidized-Bed Combustion, Monthly Progress Reports by Argonne National Laboratory, Argonne, IL, Work

File Numbers	Reference, equipment
	performed under an agreement between the U.S. Atomic Energy Commission and the Office of Coal Research, U.S. Department of Interior, Contract No. 14-32-0001-1543. 6 in. diameter continuous fluid-bed combustor 288-297, 2/75 298-301, 10/74 302, 303, 11/74 304, 1/75 305-308, 12/74 309, 9/74 310-317, 11/75 318, 12/75
319-320	Jonke, A. A., A Development Program on Pressurized Fluidized-Bed Combustion. Quarterly Report to ERDA and EPA, Argonne National Laboratory, Argonne, IL, April 1976, EPA Contract IAG-D5-E681. 6 in. diameter continuous fluid-bed combustor
372-379	Jonke, A. A., A Development Program on Pressurized Fluidized-Bed Combustion. Annual Report to ERDA and EPA, Argonne National Laboratory, Argonne, IL, July 1976, EPA Contract IAG-D5-E681 6 in. diameter continuous fluid-bed combustor
380-385	Hoke, R. C., et al., A Regenerative Limestone Process for Fluidized-Bed Coal Combustion and Desulfurization, Esso Research and Engineering Company, Linden, NJ, January 1974, NTIS PB 231 374. 4 in. diameter batch fluid-bed combustor

File Numbers	Reference, equipment
415-425	Zielke, C. W., H. E. Lebowitz, R. T. Struck, and E. Gorin, Sulfur Removal During Combustion of Solid Fuels in a Fluidized-Bed of Dolomite, J. of Air Pollution Control Association, 20 (3): 164-69; March 19790. 4 in. diameter continuous fluid-bed combustor
426-433	Energy Conversion from Coal Utilizing CPU-400 Technology. Annual Report to ERDA, Combustion Power Company, Inc., Menlo Park, CA, October 1975, No. 1 TR-75-10-123. 9-1/2 ft. diameter continuous fluid-bed combustor
434-443	Energy Conversion from Coal Utilizing CPU-400 Technology. Quarterly Report to ERDA, Combustion Power Company, Inc., Menlo Park, CA, July-September 1975, No. 4 TR-75-126. 9-1/2 ft. diameter continuous fluid-bed combustor

REFERENCE LIST - ATMOSPHERIC COMBUSTION

File Numbers	Reference, equipment
444-484	Robinson, E. B., et al., Characterization and Control of Gaseous Emissions from Coal-Fired Fluidized-bed Boilers. Interim Report to NAPCA, Pope, Evans and Robbins, Alexandria, VA, October 1970. 18 in. x 72 in. continuous fluid-bed combustor
485-586	Reduction of Atmospheric Pollution. Report to EPA, National Coal Board, London, UK, Reference No. DHB 060971, September 1971. 485-490, 508, 530; 27 in. diameter continuous fluid-bed combustor 494, 495; 12 in. x 12 in. continuous fluid-bed combustor 496-507; 6 in. diameter continuous fluid-bed combustor 531-549; 36 in. x 18 in. continuous fluid-bed combustor
587-602	Carls, E. L., et al., Reduction of Atmospheric Pollution by the Application of Fluidized-Bed Combustion. Report to NAPCA and U.S. Atomic Energy Commission, Argonne National Laboratory, Argonne, IL, July 1968 - July 1969, ANL/ES-CEN-1001. 6 in. diameter continuous fluid-bed combustor

File Numbers	Reference, equipment
603-658	Jonke, A. A., et al., Reduction of Atmospheric Pollution by the Application of Fluidized-Bed Combustion. Report to NAPCA, Argonne National Laboratory, Argonne, IL, July 1969 - July 1970, ANL/ES/CEN-1002. 6 in. diameter continuous fluid-bed combustor
659-665	Vogel, G. J., et al., Reduction of Atmospheric Pollution by the Application of Fluidized-Bed Combustion and Regeneration of Sulfur-Containing Additives. Annual Report to EPA, Argonne National Laboratory, Argonne, IL, July 1971 - June 1972, ANL/ES-CEN-1005 and EPA-R2-73-253. 6 in. diameter continuous fluid-bed combustor
666-684	Hammons, G. A. and A. Skopp, A Regenerative Limestone Process for Fluidized Bed Coal Combustion and Desulfurization. Report to Air Pollution Control Office, Esso Research and Engineering Company, Linden, NJ, February 28, 1971, Contract CPA 70-19. 3 in. diameter continuous fluid-bed combustor
685-705	Lange, H. B., et al., SO_2 Absorption in Fluidized-Bed Combustion of Coal-Effect of Limestone Particle Size, Final Report to EPRI, The Babcock and Wilcox Company, Alliance, OH, January 1978, EPRI FP-667. 3 ft. x 3 ft. fluid-bed combustor

NOMENCLATURE

Sup vel = Superficial velocity, m/s

B Dep = Bed depth, m

CD = Bed depth code

- 0 - Expanded bed depth
- 1 - Settled bed depth
- 2 - Initial settled bed depth
- 3 - Final settled bed depth
- 4 - Bed from previous run

APPENDIX B

LITERATURE SUMMARY OF NITROGEN OXIDE EMISSIONS IN FLUIDIZED-BED COMBUSTION

Dwg. 2620C80

Source	Materials Used	Type of Experimentation	Direct Results	Mechanistic Studies	Method of Determination	Conclusions
1. Exxon (2/71)	Grove limestone Coal - Pittsburgh bituminous	Fluid-bed, batch combustor, 3 in. dia, 870 - 980°C 2.5 - 6% O_2 atmospheric pressure	- NO_x emission is constant in an inert bed - NO_x emissions from a fluid bed of lime at zero conversion are higher than those from an inert bed - NO_x decreases as SO_2 increases in limestone beds - NO_x reduced upon addition of SO_2 to a fluid bed of partly sulfated stone - NO_x emission not affected by injection of SO_2 to an inert bed ($CaSO_4$) when N_2 is transport gas but in air NO_x was reduced - NO_x increased from 1100 to 1500 ppm as temperature was raised from 670 - 980°C (Note: These were not at same SO_2 levels) - NO_x not affected by varying excess air	Simulated Gas Studies - $CaSO_4$ is not a NO_x decomposition catalyst - NO and SO_2 react in the presence of an activated site - SO_2 and NO do not react at 888°C in 1 second, only in partly sulfated beds	- Gas temperature lowered to 149°C, passed through cyclone and fritted SS filter, then air-cooled condenser - Whittaker polarographic analyzer continuously monitors NO_x (full response to NO, 80% to NO_2)	- NO_x reduction mechanism proposed 1) $CaO + SO_2 \rightarrow CaSO_3$ $CaSO_3 + 2NO \rightarrow CaSO_3{\cdot}(NO)_2$ $CaSO_3{\cdot}(NO)_2 \rightarrow CaSO_4 + N_2O$ $N_2O \rightarrow N_2 + 1/2\ O_2$ 2) Unidentified mechanism for inert beds with large excess O_2 present - Excess air has no effect on NO_x emission since oxidation of fuel N_2 occurs at bed entrance where O_2 level is fairly independent of excess air
2. Exxon (12/71)	Grove limestone Coal - Pittsburgh bituminous	Fluid-bed batch combustor, 3 in. diameter Electrically heated fixed beds 670 - 980°C, 2.5 - 6% O_2, atmospheric pressure	- NO_2 emission negligible - Increasing temperature from 816 to 927°C Doubles reduction of NO in presence of steam Little effect with no steam	Studies in fixed bed ● NO - SO_2 $CaO + SO_2 \rightarrow CaSO_3$ $2CaSO_3 + 2NO \rightarrow 2CaSO_4 + N_2$ ● NO - CO $2CO + 2NO \rightarrow 2CO_2 + N_2$	Gas temperature lowered to 149°C, passed through cyclone, filter, air-cooled and water-cooled condensers - Whittaker polarographic NO_x analyzer - Beckman Model NO 1R315B NO analyzer - Du Pont Model 461 NO_x analyzer ● NO_2 - absorption of visible light ● NO-oxidation to NO_2 under 414 kPa O_2 presence	- The NO - CO Reaction 1) Catalyzed by CaO more than $CaSO_4$, more than Alundum 2) Second order in NO and CO 3) Ea = 25 - 33 kJ/mole (704 - 927 °C) 4) Decreasing temperature or excess air increases CO there by decreasing NO emissions 5) Addition of steam minimizes the need for an active solid surface - The NO - SO_2 Reaction 1) CaO necessary 2) Order = 0.5 in NO with no O_2 3) Negative temperature dependence (rate increases by a factor of 5 in reducing temperature from 871 - 760°C, decrease in rate coincides with increase in $CaSO_3$ thermodynamic stability) - 2-Stage Combustor Proposed 1) Phase one operating at Stoichiometric conditions, NO - CO reaction promoted 2) Add secondary air at a higher point to complete combustion and provide SO_2 for reaction with remaining NO

Dwg. 2620C77

Source	Materials Used	Type of Experimentation	Direct Results	Mechanistic Studies	Method of Determination	Conclusions
3. Exxon (1/74)	Grove limestone and Tymochtee dolomite Coal-Arkwright, 2.5% S	Batch fluidized-bed combustor, 10.2 cm diameter 760 - 870°C, 506 - 810 kPa, 20 - 200% excess air, 0.6 m settled bed height	300 - 400 ppm NO_x possibly due to high excess air	Reaction of CO and NO studied in a 2.54 cm diameter SS fixed bed $2NO + 2CO \rightarrow 2CO_2 + N_2$	Off gas passed through cyclones, cooler, and filter Beckman Model NO 1 R 315 analyzer for NO	- The reaction $NO + CO \rightarrow CO_2 + N_2$ is inhibited by CO_2 to a large extent and by O_2 and N_2 to a slight extent - Temperature in range of 870 - 927°C in presence of CO_2 has no effect conversion of NO
4. Exxon (9/76)	Limestone 1359, and Tymochtee dolomite Coal-Pittsburgh Seam (Champion), 2%; Pittsburgh Seam (Arkwright), 2.6% S; Illinois No. 6, 4% S; western subbituminous, 0.7% S	Batch fluidized-bed combustor 11.4 cm dia; 540-850 kPa; 620-979°C; 0-153% excess air; 0.17-1.03 m settled bed height; miniplant combuster, 31.8 cm dia; 395-1033 kPa; 871-949°C, 0-139% excess air	NO_x emissions increased with increase in excess air excess air levels of 15 to 20%, emissions ranged from 86 to 129 ng NO_2/J. NO_x emissions with inert alundum beds very similar to those measured from runs with limestone or dolomite beds. NO_x emissions measured in the miniplant and batch combustors in close agreement		For batch combustors, Thermo-Electron 10B NO/NO_x (chemiluminescence) For miniplant - Beckman 315B (infrared)	Excess air is the primary variable; at 800 kPa bed material, inert or sulfur-capturing sorbent seems to have no effect on NO_x emissions
5. Exxon (9/77)	Limestone 1359 and Dolomite 1337 Coal - Pittsburgh Seam (Champion), 2% S; Illinois No. 6, 4% S; western subbituminous, 0.7% S	Batch fluidized-bed combustor, 11.4 cm dia.; 800 kPa; 800-979°C; 0-157% excess air; 0.32-0.77 m settled bed height; Miniplant combustor, 31.8 cm dia.; 520-930 kPa; 674-954°C; 5-112% excess air; 2-7 m expanded bed height	NO_x emissions increased with increase in excess air; in the range of 15 to 20% excess air, average emissions 90-130 ng/J; at low excess air levels, NO_x emissions in the batch unit slightly higher than in the miniplant; high excess air levels NO_x emissions in batch unit significantly higher than in the miniplant			- Excess air and temperature are the only significant variables - Temperature seems to have a secondary effect
6. Exxon (4/78)	Limestone 1359 and Dolomite 1337 Coal - Pittsburgh Seam (Champion) 2% S; Illinois No. 6, 4.2% S	Miniplant combustor, 31.8 cm dia; 570-1075 kPa; 760-956°C; 13-63% excess air; 2.5-7.2 m expanded bed height	NO_x emissions followed the trend developed in earlier studies. An upset period of one run resulted in poor combustion and formation of about 1800 ppm CO and 10-20 ppm NO_x indicating two-stage combustion could limit NO_x emissions			- Excess air is the primary variable and temperature has secondary effect on NO_x emissions Two-stage combustion may be a possibility for limiting NO_x emissions in pressurized operations to very low levels

Dwg. 2625C10

7. Argonne (7/69)	Limestones 1359, 1360, and dolomite 1337 No limestone used in Argon substitution experiments Coal - Illinois, 4.5% S	Bench-scale fluid-bed combustor, 15 cm dia. Atmospheres of N_2/O_2 and Ar/O_2 atmospheric pressure	Increasing O_2 in flue gas from 2.6 to 11.8% (14 to 128% excess air) increased NO emission from 400 - 500 ppm. Reduction in NO with SO_2 upon addition of limestone $NO_2 + SO_2 \rightleftarrows NO + SO_3$	- NO values were higher than possibly obtained by equilibrium $N_2 + O_2 \rightleftarrows 2\,NO$ in fluid-bed combustion of coal - Argon substitution for N_2 showed same NO in flue gas	NO_2 - by gas chromatography, unsuccessful NO. SO_2 Beckman infrared analyzer	NO in flue gas comes from reaction of solid nitrogeneous material in coal
8. Argonne (6/70)	Tymochtee dolomite Coal - Illinois Seam No. 6, 4.5% S	Bench-scale fluid-bed combustor, 15 cm dia. SS pipe 870°C, 0.9 m/s 0.6 - 2.7 m bed height atmospheric pressure	- Experiments with natural gas had NO < 100 ppm as expected in nitrogen fixation equilibrium - Initial NO of 600 ppm reduced to 200 ppm in a fluid bed of limestone - NO_x removal is inversely proportional to Ca/S molar ratio - NO_x removal is inversely proportional to velocity of gas - NO removal is proportional to gas residence time	The reaction $NO_2 + SO_2 \rightleftarrows SO_3 + NO$ is not the mechanism for NO removal with SO_2 since NO_2 levels remain constant	NO_2 - 1) phenoldisulfonic acid procedure 2) mass spec NO/NO_2 3) fast NO_2 analyzer NO infrared analyzer Sampling in 1.3 cm diameter SS tube. Passed through sintered nickel filter to remove fines and a condenser and refrigerator	Injection of Al_2O_3 and ZrO_2 had no effect on emissions Co_3O_4 increased NO emissions, had no effect on SO_2 emissions NO_x emission from a partly sulfated lime bed was 20 - 40% lower than emission over an inert bed
9. Argonne (6/73)	Limestone 1359 Coal - Peabody, 4% S	Bench scale fluid-bed combustor, 15 cm dia., atmospheric pressure	- NO emissions increased with excess air (50 - 250%) - NO emissions tended to be lower at higher temperatures, possibly because NO - CO reaction increases with temperature	Less than stoichiometric air was added to a fluid bed When air was added above the bed NO emission increased. Possible reasons 1) NO & CO reduction stopped 2) the excess air oxidized NH_3 etc. to NO	Infrared analyzer	No dependence of NO emission on temperature or gas velocity
10. Argonne (10/74)	Tymochtee dolomite coals - Arkwright, 2.82% S subbituminous, 0.78% S lignite, 0.9% S	Continuous, fluid-bed combustor 15 cm diameter - 788 - 899°C - Ca/S of 1, 2, and 3 - velocity of 0.6 - 1.5 m/s - pressure, 8 - 10 atm - 0.9 m bed height - 15% excess air	- NO emissions were low 270 ppm at Ca/S of 3.2, 888°C, 1.1 m 120 ppm at Ca/S of 1, 907°C, 1.5 m - Reduced Ca/S produced higher SO_2 levels and lower NO levels	Effect of Pressure - Greatly increased NO with decreased pressure in Alundum bed (to 1600 ppm at 101.3 kPa) - Smaller increase in NO with decreasing pressure in coal and dolomite bed (500 ppm at 101.3 kPa)	IR analyzer Gas passed through sintered SS filter	- NO levels at pressure are significantly lower than at 101.3 kPa - Temperature in range of 788 - 899°C has no effect on NO emission - Reduced Ca/S gives lower NO emissions

Dwg. 2620C76

	Source	Materials Used	Type of Experimentation	Direct Results	Mechanistic Studies	Method of Determination	Conclusions
11.	Argonne (6/79)	Limestone 1359 and Tymochtee dolomite Coal - Pittsburgh bituminous, 2.82% S	Bench-scale, fluid-bed combustor, 15 cm diameter, 810 kPa pressure 954°C	NO increased with O_2 in flue gas 3% O_2 - 160 ppm NO 6% O_2 - 200 ppm NO 9% O_2 - 230 ppm NO	Effect of precalcination of sorbent on NO emission	Infrared analyzer	- Additive type does not effect NO emission - Precalcination of sorbent does not effect NO emission
12.	Argonne (12/79)	Grove limestone and Tymochtee dolomite Coals - -Arkwright, 2.82% S - San Juan, 0.78% S - Glenharold, 0.53% S	Continuously operated, fluid-bed combustor 788 - 899°C Ca/S of 1 to 3, gas velocity of 0.6 - 1.5 m/s 810 kPa pressure, 0.9 m fluidized-bed height, 3% O_2	- NO levels were very low (120 - 270 ppm) - Increasing Ca/S, increased NO_x - Coal & sorbent particle size has no significant effect on NO_x - Additive type has effect on NO_x - NO_x increases with O_2 concentration - Temperature variation (788 - 899°C) has little or no effect on flue gas composition - Increase in NO emission occurs when pressure is decreased	CO levels in flue gas - In presence of dolomite, increase with decreasing pressure - Without sorbent-CO level is minimum at 405 kPa pressure	NO_x infrared analyzers	Increasing NO emissions with increasing Ca/S ratio - the only independent variable with a significant effect based on regression analysis considering temperature (788 - 899°C), gas velocity (0.6 - 1.5 m/s) and Ca/S (1 - 3)
13.	Argonne (7/76)	Tymochtee dolomite (370 and 740 um) Coal - Arkwright, 2.8% S (150 and 640 um)	Continuously operated, fluid-bed combustor 840°C, 810 kPa, 17% excess air, 1.07 m/s, 0.9 m bed height	- NO was low (120 - 150 ppm) in all four runs - NO_2 levels of 40 - 60 ppm were higher than the expected 5 - 10 ppm		Chemiluminescence analyzer	Particle size of coal and sorbent have no effect on NO emissions
14.	Pope, Evans and Robbins (10/70)	Limestone 1359 and dolomite 1337 Coals - No. 8 Pittsburgh, 4.5% S Pike County, low S and N	Continuously operated, fluid-bed combustor 810 - 971°C 1.27 - 30 cm bed depth 1.8 - 4 m/s atmospheric pressure	- NO varied from 320 ppm (1% O_2) to 440 ppm (5% O_2) - NO_2 emission was very low - Use of sorbent had an unclear effect on NO emission. In two cases a reduction in NO was observed with additive addition	A change from low to high nitrogen coal caused a small increase in NO emission	- Infrared absorption - Total NO_x by phenoldisulfonic acid determination	- No consistent correlation between temperature and NO emission at constant O_2 concentration - NO emission is independent of bed height

Dwg. 2620C78

Source	Materials Used	Type of Experimentation	Direct Results	Mechanistic Studies	Method of Determination	Conclusions
15. **National Coal Board (9/71)**	**U.K. limestone, limestone 1359, limestone 18, U.K. dolomite, and dolomite 1337** **Coal** **- Illinois, 4.4% S** **- Pittsburgh, 2.8% S** **- Park Hill, 2.5% S** **- Welbeck, 1.5% S**	Continuous fluid-bed combustor: 69 cm diameter 91 cm × 46 cm 122 cm × 61 cm pressurized 749 - 927 °C 0.46 - 2.1 m bed height 0.61 - 3.35 m/s 101.3 - 506.5 kPa	- NO emissions were generally in the range of 320 - 600 ppm - in 91 cm combustor NO_x increased as SO_2 decreased - NO_x reduced to 100 ppm when coal size was reduced from 3175 µm to 1680 µm		Flue gas withdrawn through silica probe (steel probe used for pressurized combustor) and bubbled through water to remove soluble gases - About 5% NO_x was soluble and analyzed by Saltzman's method - Remaining NO_x analyzed two ways 1) Saltzman's method - spectrophotometric 2) BCURA NO_x box, NO oxidized to NO_2 and electrical current measured	- No correlation was found between NO_x emissions and gas velocity, temperature, Ca/S molar ratio or SO_2 concentration - In pressurized operation NO_x was lower, NO emission increasing with decreasing SO_2
16. **NRDC/ BCURA (7/74)**	**U.K. limestone and Dolomite 1337; Coal - Pittsburgh, 3% S; Illinois, 3.5% S**	Continuous fluidized-bed combustor, 0.91 m × 0.61 m; 584 kPa; 900-954 °C; 14-20% excess air; 1.1-1.4 m fluidized bed height	NO_x emissions generally 86 ng NO_2/J (150 ppm) or lower; however in one test higher values of 255 ng NO_2/J observed	With higher concentrations of SO_2 in the exhaust gas, relatively lower NO_x emission observed	NO_x measured using chemiluminescence monitor	- Excess air is the primary variable. Significant increase in NO_x emissions were observed for excess air levels in the range of 0-6%. - SO_2 may possibly inhibit the formation or promote the dissociation of NO_x in FBC
17. **NRDC/ NCURL (9/77)**	**Dolomite 1337; Coal-Illinois 6, 3% S**	Continuous fluidized-bed combustor, 0.91 m × 0.61 m;	NO_x emissions between 129-215 ng NO_2/J (90-180 ppm); higher emissions observed on increasing the temperature from 865 to 902 °C and superficial velocity from 0.8 to 2.1 m/s		Thermo Electron Corporation 'chemiluminescence' monitor	NO_x emissions increased on decreasing the gas residence time (increasing superficial velocity), and/or increasing the temperature
18. **Pereira, Beer, Gibbs (4/76)**	**No limestone Bed material - inert silica-based clinker** **Coal - 1.7% S and 1.4% N**	30 × 30 cm sectioned continuous combustor 650 - 850 °C −25 - +40% excess air 0.61 m bed depth 0.9 m/s velocity atmospheric pressure 7.5 cm diameter batch combustor 600 - 950 °C 10 - 40 cm/s velocity atmospheric pressure	NO emissions increase linearly with temperature (650 - 800 °C) at 2.26 ppm/°C At temperatures above 800 °C, the emissions level off Batch combustor NO_x emissions reach a maximum at 750 °C NO emissions (mole/g of coal) increase with excess air levels Regression analysis gives ppm NO = −1093 + 2.26 T - 203 N (N = ratio of actual to stoichiometric air T = °C)	Reduction of NO by char 1) increased reaction as temperature raised above 800 °C 2) increased reduction as particle size of char is reduced (Experiments in batch combustor with no oxygen) 90% reduction NO emission at 930 °C with 100 µm particles Temperature maximum for NO emissions - Emissions increasing up to 750 °C due to decrease in reduction by unburnt CO, H_2 and hydrocarbons - Emissions decrease at higher temperature due to reduction by char	Continuous monitoring of NO with chemiluminescent analyzer	- NO formation occurs preferentially in regions of high O_2 concentration, close to the distributor and coal feed points - NO reduction occurs in the bed and freeboard. In the freeboard, the reduction is due to chemical reaction rather than mixing - NO is reduced by hot char in the absence of oxygen. The amount reduced increases with temperature and decreasing char particle size

REFERENCE FOR LITERATURE SUMMARY

1. Hammons, G. A., and A. Skopp, A Regenerative Limestone Process for Fluidized Bed Coal Combustion and Desulfurization. Final report to Air Pollution Control Office, Esso Research and Engineering Company, Linden, NJ, February 28, 1971, Contract CPA 70-19.
2. Skopp, H., et al., Studies of the Fluidized Lime-Bed Coal Combustion Desulfurization System, Part 2: Factors Affecting NO_x Formation and Control in Fluidized Bed Combustion, Esso Research and Engineering Company, Linden, NJ, December 31, 1971, NTIS PB 210 246.
3. Hoke, R. C., et al., A Regenerative Limestone Process for Fluidized-Bed Coal Combustion and Desulfurization, Esso Research and Engineering Company, Linden, NJ, January 1974, NTIS PB 231 374.
4. Hoke, R. C., et al., Studies of the Pressurized Fluidized-Bed Coal Combustion Process, Report to EPA, Exxon Research and Engineering Co., Linden, NJ, September 1967, EPA-600/7-76-011.
5. Hoke, R. C., et al., Studies of the Pressurized Fluidized-Bed Coal Combustion Process, Report to EPA, Exxon Research and Engineering Co., Linden, NJ, September 1977, EPA-600/7-77-107.
6. Hoke, R. C., et al., Miniplant Studies of Pressurized Fluidized-Bed Coal Combustion, Report to EPA, Exxon Research and Engineering Co., Linden, NJ, April 1978, EPA-600/7-78-069.
7. Carls, E. L., et al., Reduction of Atmospheric Pollution by the Application of Fluidized Bed Combustion, Annual report to NAPCA and U.S. Atomic Energy Commission, Argonne National Laboratory, Argonne, IL, July 1968-July 1969, ANL/ES-CEN-1001.
8. Jonke, A. A., et al., Reduction of Atmospheric Pollution by the Application of Fluidized-Bed Combustion, Annual report to NAPCA, Argonne National Laboratory, Argonne, IL, July 1969-July 1970, ANL/ES-CEN-1002.
9. Vogel, G. J., et al., Reduction of Atmospheric Pollution by the Application of Fluidized-Bed Combustion and Regeneration of Sulfur-Containing Additives, Report to EPA, Argonne National Laboratory, Argonne, IL, June 1973, EPA-R2-73-253.

10. A Development Program on Pressurized Fluidized-Bed Combustion. Interim Report No. 1 to Office of Coal Research and EPA, Argonne National Laboratory, Argonne, IL, October 1974, Contract No. 14-32-0001-1543.

11. Vogel, G. J., et al., A Development Program on Pressurized Fluidized-Bed Combustion, Annual Report to ERDA, Argonne National Laboratory, Argonne, IL, July 1975. ANL/ES-CEN-1011.

12. Vogel, G. J.., et al., Recent ANL Bench-Scale, Pressurized-Fluidized-Bed Studies, Argonne National Laboratory, Argonne, IL, Proceedings of the Fourth International Conference on Fluidized-Bed Combustion, Washington, DC, December 9-11, 1975.

13. Jonke, A. A., A Development Program on Pressurized Fluidized-Bed Combustion, Report to ERDA and EPA, Argonne National Laboratory, Argonne, IL, July 1976.

14. Robinson, E. B., et al., Characterization and Control of Gaseous Emmissions from Coal-Fired Fluidized-Bed Boilers, Interim Report To NAPCA, Pope, Evans and Robbins, October 1970.

15. Reduction of Atmospheric Pollution, Report to EPA, National Coal Board, London, UK, September 1971, Reference No. DHB 060971.

16. Pressurized Fluidized Bed Combustion, Report to Office of Coal Research, National Research Development Corporation, London, UK, July 1974, Contract No. 14-32-0001-1511, NTIS PB-234 591.

17. Roberts, A. G., et al., Pressurized Fluidized Bed Combustion, Report to U. S. ERDA, Report No. 43, National Research Development Corporation, London, UK, September 1977, FE-1511-43.

18. Pereira, F. J., J. M. Beer, and B. M. Gibbs, Nitric Oxide Emissions from Fluidized Coal Combustion, the Combustion Institute, Central States Section, Spring Meeting, April 5-6, 1976.

APPENDIX C

EFFECTS OF PRESSURE, EXCESS AIR, AND GASEOUS SULFUR CONTENT ON VOLATILE TRACE AND MINOR SPECIES AT EQUILIBRIUM IN FBC PROCESSES*

---

*In this section PP stands for partial pressure.

EFFECT OF PRESSURE, EXCESS AIR AND SULFUR CONTENT ON VOLATILE ALUMINUM SPECIES AT EQUILIBRIUM

GAS PHASE	PRESSURE, 1520.4→101.3KPA (15→1ATM)	EXCESS AIR, 10 → 300%	SULFUR REMOVAL, 0 → 90%
ALCL3	INCREASED PPALCL3 AT LOW TEMPERATURES	DECREASED PPALCL3	INCREASED PPALCL3 AT LOW TEMPERATURES
	DECREASED PPALCL3 AT HIGH TEMNPERATURES		
ALOCL	INCREASED PPALOCL	INCREASED PPALOCL AT LOW TEMPERATURES	INCREASED PPALOCL AT LOW TEMPERATURES
		DECREASED PPALOCL AT HIGH TEMPERATURES	
ALCL2	INCREASED PPALCL2	DECREASED PPALCL2	INCREASED PPALCL2
ALO2	INCREASED PPALO2	DECREASED PPALO2	INCREASED PPALO2
ALOH	INCREASED PPALOH	DECREASED PPALOH	DECREASED PPALOH
ALCL	INCREASED PPALCL	DECREASED PPALCL	DECREASED PPALCL
ALO	INCREASED PPALO	DECREASED PPALO	SLIGHTLY DECREASED PPALO AT 10% EXCESS AIR
AL2CL6	DECREASED AL2CL6	DECREASED PPAL2CL6	NO EFFECT

EFFECT OF PRESSURE, EXCESS AIR AND SULFUR CONTENT ON VOLATILE CHROMIUM SPECIES AT EQUILIBRIUM

GAS PHASE	PRESSURE, 1520.4→101.3KPA (15→1ATM)	EXCESS AIR, 10 → 300%	SULFUR REMOVAL, 0 → 90%
CRO2CL2	DECREASED PPCRO2CL2	DECREASED PPCRO2CL2	INCREASED PPCRO2CL2 FOR 10% EXCESS AIR
CRO4H2	DECREASED PPCRO4H2	INCREASED PPCRO4H2 FOR 10% TO 100% EXCESS AIR	INCREASED PPCRO4H2 ESPECIALLY FOR 10% AND 100% EXCESS AIR
		DECREASED PPCRO4H2 FOR 100% TO 300% EXCESS AIR	
CRO2OH	NO EFFECT	INCREASED PPCRO2OH	INCREASED PPCRO2OH ESPECIALLY FOR 10% TO 100% EXCESS AIR
CRO3	INCREASED PPCRO3	INCREASED PPCRO3	INCREASED PPCRO3 AT 10% TO 100% EXCESS AIR AT 1 AND 5 ATM
CRO2	INCREASED PPCRO2	INCREASED PPCRO2	INCREASED PPCRO2 AT 10% TO 100% EXCESS AIR
CRCL3	INCREASED PPCRCL3 AT LOW TEMPERATURES	DECREASED PPCRCL3	DECREASED PPCRCL3 AT 100% EXCESS AIR AT LOW TEMPERATURES
	DECREASED PPCRCL3 AT HIGH TEMPERATURES		NO EFFECT AT HIGH TEMPERATURES; AT 100% OR 300% EXCESS AIR
CRCL2	INCREASED PPCRCL2	DECREASED PPCRCL2	NO EFFECT

EFFECT OF PRESSURE, EXCESS AIR AND SULFUR CONTENT ON VOLATILE CHROMIUM SPECIES AT EQUILIBRIUM (Cont)

CRCL4	DECREASED PPCRCL4	DECREASED PPCRCL4	DECREASED PPCRCL4 AT LOW TEMPERATUES FOR 10% AND 100% EXCESS AIR INCREASED PPCRCL4 AT HIGH TEMPERATURES FOR 10% AND 100% EXCESS AIR NO EFFECT FOR 300% EXCESS AIR
CRO	INCREASED PPCRO	DECREASED PPCRO	SLIGHTLY DECREASED PPCRO FOR HIGH TEMPERATURES IN 10% EXCESS AIR
CRCL	DECREASED PPCRCL	DECREASED PPCRCL	SLIGHTLY DECREASED PPCRCL AT 10% EXCESS AIR AT HIGH TEMPERATURES
CR	INCREASED PPCR	DECREASED PPCR	DECREASED PPCR AT 100% EXCESS AIR NO EFFECT FOR 100% AND 300% EXCESS AIR

EFFECT OF PRESSURE, EXCESS AIR AND SULFUR CONTENT ON VOLATILE COBALT SPECIES AT EQUILIBRIUM

GAS PHASE	PRESSURE, 1520.4→101.3KPA (15→1ATM)	EXCESS AIR, 10 → 300%	SULFUR REMOVAL, 0 → 90%
COCL2	INCREASED PPCOCL2	DECREASED PPCOCL2	INCREASED PPCOCL2
COCL3	DECREASED PPCOCL3	DECREASED PPCOCL3	INCREASED PPCOCL3 AT LOW TEMPERATURES NO EFFECT AT HIGH TEMPERATURES
CO2CL4	INCREASED PPCO2CL4 AT LOW TEMPERATURES DECREASED PPCO2CL4 AT HIGH TEMPERATURES	DECREASED PPCO2CL4	INCREASED PPCO2CL4 AT LOW TEMPERATURES NO EFFECT AT HIGH TEMPERATURES
COCL	INCREASED PPCOCL AT LOW TEMPERATURES INCREASED PPCOCL AT HIGH TEMPERATURES FOR 10% AND 100% EXCESS AIR, AND 0% AND 90% SULFUR REMOVAL DECREASED PPCOCL AT HIGH TEMPERATURES FOR 300% EXCESS AIR AND 0% AND 90% SULFUR REMOVAL	DECREASED PPCOCL	INCREASED PPCOCL AT LOW TEMPERATURES NO EFFECT AT HIGH TEMPERATURES

EFFECT OF PRESSURE, EXCESS AIR AND SULFUR CONTENT ON VOLATILE IRON SPECIES AT EQUILIBRIUM

GAS PHASE	PRESSURE, 1520.4→101.3KPA (15→1ATM)	EXCESS AIR, 10 → 300%	SULFUR REMOVAL, 0 → 90%
FE(OH)2	INCREASED PPFE(OH)2	DECREASED PPFE(OH)2	INCREASED PPFE(OH)2 AT LOW TEMPERATURES
FECL2	INCREASED PPFECL2	DECREASED PPFECL2	INCREASED PPFECL2 AT LOW TEMPERATURES
FECL3	INREASED PPFECL3 AT LOW TEMPERATURES DECREASED PPFECL3 AT HIGH TEMPERATURES	DECREASED PPFECL3	INCREASED PPFECL3 AT LOW TEMPERATURES
FEO	INCREASED PPFEO	DECREASED PPFEO FOR 10%, 100%, 300% EXCESS AIR FOR 90% SULFUR REMOVAL INCREASED PPFEO FOR 800K IN 0% SULFUR REMOVAL, DECREASED PPFEO AT HIGHER TEMPERATURES	INCREASED PPFEO AT LOW TEMPERATURES FOR 10% EXCESS AIR DECREASED PPFEO AT HIGH TEMPERATURES
FE2CL4	FOR 0% SULFUR REMOVAL: INCREASED PPFECL4 AT LOW TEMPERATURES, DECREASED PPFECL4 AT HIGH TEMPERATURES FOR 90% SULFUR REMOVAL: DECREASED PPFECL4	DECREASED PPFE2CL4	INCREASED PPFE2CL4 AT LOW TEMPERATURES DECREASED PPFE2CL4 AT HIGH TEMPERATURES FOR 10% EXCESS AIR

EFFECT OF PRESSURE, EXCESS AIR AND SULFUR CONTENT ON VOLATILE
IRON SPECIES AT EQUILIBRIUM (Cont)

FECL	INCREASED	DECREASED PPFECL	INCREASED PPFECL AT LOW TEMPERATURES FOR 15, 10, 5 ATMOSPHERES. SLIGHT DECREASED PPFECL AT HIGH TEMPERATURES FOR 10% EXCESS AIR
(FECL3)2	FOR 0% SULFUR REMOVAL: INCREASED PP(FECL3)2 AT LOW TEMPERATURES DECREASED PP(FECL3)2 AT HIGH TEMPERATURES FOR 90% SULFUR REMOVAL: DECREASED PP(FECL3)2	DECREASED PP(FECL3)2	INCREASED PP(FECL3)2 AT LOW TEMPERATURES
FE	INCREASED PPFE	DECREASED PPFE	DECREASED PPFE FOR 10% EXCESS AIR

EFFECT OF PRESSURE, EXCESS AIR AND SULFUR CONTENT ON VOLATILE MANGANESE SPECIES AT EQUILIBRIUM

GAS PHASE	PRESSURE, 1520.4→101.3KPA (15→1ATM)	EXCESS AIR, 10 → 300%	SULFUR REMOVAL, 0 → 90%
MNCL2	INCREASED PPMNCL2	DECREASED PPMNCL2	INCREASED PPMNCL2 AT LOW TEMPERATURES NO EFFECT AT HIGH TEMPERATURES
MNCL	INCREASED PPMNCL	DECREASED PPMNCL	INCREASED PPMNCL AT LOW TEMPERATURES NO EFFECT AT HIGH TEMPERATURES
MNO	INCREASED PPMNO	INCREASED PPMNO AT LOW TEMPERATURES DECREASED PPMNO AT HIGH TEMPERATURES	INCREASED PPMNO AT LOW TEMPERATURES NO EFFECT AT HIGH TEMPERATURES
MN	INCREASED PPMN	DECREASED PPMN AT HIGH TEMPERATURES	INCREASED PPMN AT LOW TEMPERATURES SLIGHT DECREASE IN PPMN AT HIGH TEMPERATURES FOR 10% EXCESS AIR

EFFECT OF PRESSURE, EXCESS AIR AND SULFUR CONTENT ON VOLATILE MOLYBDENUM SPECIES AT EQUILIBRIUM

GAS PHASE	PRESSURE, 1520.4→101.3KPA (15→1ATM)	EXCESS AIR, 10 → 300%	SULFUR REMOVAL, 0 → 90%
MOO2(OH)2	NO EFFECT	DECREASED PPMOO2(OH)2	SLIGHT INCREASE IN PPMOO2(OH)2 AT LOW TEMPERATURES NO EFFECT AT HIGH TEMPERATURES
MOO2CL2	INCREASED PPMOO2CL2 NO EFFECT AT HIGH TEMPERATURES	DECREASED PPMOO2CL2	SLIGHT DECREASE IN PPMOO2CL2 AT LOW TEMPERATURES FOR 10% EXCESS AIR NO EFFECT AT HIGH TEMPERATURES
MOO3	NO EFFECT	NO EFFECT	NO EFFECT
MOO2	INCREASED PPMOO2	DECREASED PPMOO2	SLIGHT DECREASE IN PPMOO2 FOR 10% EXCESS AIR
MOCL4	SLIGHT INCREASE IN PPMOCL4 AT LOW TEMPERATURES FOR 10% EXCESS AIR INCREASE AT LOW TEMPERATURES FOR 100% AND 300% EXCESS AIR DECREASE IN PPMOCL4 AT 1200K FOR 10% 100% AND 300% EXCESS AIR	DECREASED PPMOCL4	DECREASE IN PPMOCL4 PARTICULARLY FOR 10% EXCESS AIR
MOO	NO EFFECT	DECREASED PPMOO	DECREASE IN PPMOO AT 1 ATM FOR 10% EXCESS AIR; OTHERWISE, NO EFFECT
MOCL5	DECREASED PPMOCL5	DECREASED PPMOCL5	DECREASED PPMOCL5 FOR 10% AND 100% EXCESS AIR
MOCL6	DECREASED PPMOCL6	DECREASED PPMOCL6	NO EFFECT

EFFECT OF PRESSURE, EXCESS AIR AND SULFUR CONTENT ON VOLATILE NICKEL SPECIES AT EQUILIBRIUM

GAS PHASE	PRESSURE, 1520.4→101.3KPA (15→1ATM)	EXCESS AIR, 10 → 300%	SULFUR REMOVAL, 0 → 90%
NICL2	INCREASED PPNICL2 AT LOW TEMPERATURES	DECREASED PPNICL2	SLIGHTLY DECREASED PPNICL2 AT LOW TEMPERATURES
	NO CHANGE IN PPNICL2 AT T>1000K		NO EFFECT AT T>1000K
NI(OH)2	SLIGHTLY INCREASED PPNI(OH)2 AT LOW TEMPERATURES	DECREASED PPNI(OH)2	INCREASED PPNI(OH)2 AT LOW TEMPERATURES
	NO CHANGE AT T>1000K		NO EFFECT AT ELEVATED TEMPERATURES
NICL	INCREASED PPNICL AT ALL TEMPERATURES	DECREASED PPNICL	DECREASED PPNICL AT 600K FOR 10% EXCESS AIR
			SLIGHT INCREASE IN PPNICL AT LOW TEMPERATURES FOR 100% AND 300% EXCESS AIR
			NO EFFECT AT ELEVATED TEMPERATURES
NIO	INCREASED PPNIO AT LOW TEMPERATURES	INCREASED PPNIO AT T<1000K	INCREASED PPNIO AT 700K
	NO EFFECT AT T>1000K	AT T>1000K NO CHANGE IS DETECTED	NO EFFECT AT T>1000K
NI	INCREASED PPNI AT ALL TEMPERATURES		INCREASED PPNI AT 800K
			SLIGHT DECREASE IN PPNI AT T>1000K
NIH	INCREASED PPNIH AT ALL TEMPERATURES	DECREASED PPNIH	INCREASED PPNIH AT 900K
			SLIGHT DECREASE IN PPNIH AT ELEVATED TEMPERATURES

APPENDIX D

EQUILIBRIUM CALCULATIONS FOR FBC OPERATION AT 100 PERCENT EXCESS AIR, 90 PERCENT SULFUR REMOVAL AND 1013 kPa (10 atm) TOTAL PRESSURE

```
ALUMINUM - FLUID BED COMBUSTION GAS
      100% EXCESS AIR
       90% SULFUR REMOVAL
        10 ATMOSPHERES TOTAL  PRESSURE

TEMP.\COMPOUND
 (K)  \  AL2O3 (C)  AL2(SO4)3 (C)  ALCL3 (G)    ALOCL (G)    ALCL2 (G)
  300    .0000       .4160-02      .0000        .0000        .0000
  400    .1975-01    .4160-02      .5612-32     .0000        .0000
  500    .1975-01    .4160-02      .1128-25     .0000        .0000
  600    .1975-01    .4158-02      .5471-22     .8027-36     .0000
  700    .1986-01    .4041-02      .9764-20     .4755-30     .3593-35
  800    .2390-01    .0000         .3605-18     .9121-26     .1326-30
  900    .2390-01    .0000         .5485-17     .1878-22     .4405-27
 1000    .2390-01    .0000         .4802-16     .8296-20     .2843-24
 1100    .2390-01    .0000         .2712-15     .1183-17     .5440-22
 1200    .2390-01    .0000         .1148-14     .7319-16     .4300-20

TEMP.\COMPOUND
 (K)  \   ALO2 (G)      ALOH (G)      ALCL (G)      ALO (G)       AL2CL6 (G)
  300     .0000         .0000         .0000         .0000         .0000
  400     .0000         .0000         .0000         .0000         .0000
  500     .0000         .0000         .0000         .0000         .0000
  600     .0000         .0000         .0000         .0000         .0000
  700     .0000         .0000         .0000         .0000         .0000
  800     .1213-33      .0000         .0000         .0000         .4657-36
  900     .6367-29      .4298-35      .1687-35      .0000         .1507-34
 1000     .3747-25      .1246-30      .3772-31      .2268-35      .2447-33
 1100     .4495-22      .5490-27      .1324-27      .4842-31      .2232-32
 1200     .1636-19      .5882-24      .1178-24      .1933-27      .1430-31
```

```
IRON - FLUID BED COMBUSTION GAS
      100% FXCESS AIR
       90% SULFUR REMOVAL
        10 ATMOSPHERES TOTAL  PRESSURE

TEMP.\COMPOUND
 (K)  \   FE2O3 (S) FE2(SO4)3 (S) FE(OH)2 (G) FECL2 (G)    FECL3 (G)
  300     .1303-01     .4160-02     .0000        .0000        .5063-26
  400     .1303-01     .4160-02     .0000        .1019-28     .3794-19
  500     .1303-01     .4160-02     .9430-29     .7185-22     .2561-15
  600     .1303-01     .4159-02     .3884-23     .1122-17     .2669-13
  700     .1308-01     .4107-02     .3858-19     .5860-15     .2947-12
  800     .1576-01     .1426-02     .3736-16     .5084-13     .1308-11
  900     .1719-01     .0000        .7691-14     .1489-11     .3715-11
 1000     .1719-01     .0000        .5349-12     .2151-10     .8337-11
 1100     .1719-01     .0000        .1704-10     .1820-09     .1523-10
 1200     .1719-01     .0000        .3018-09     .1064-08     .2492-10

TEMP.\COMPOUND
 (K)  \   FEO (G)       FE2CL4 (G)      FECL (G) (FECL3)2 (G) FE (G)
  300     .0000         .0000         .0000        .1998-34     .0000
  400     .0000         .0000         .0000        .4361-27     .0000
  500     .0000         .2409-35      .0000        .3153-23     .0000
  600     .0000         .1633-29      .0000        .1076-21     .0000
  700     .1627-36      .6833-26      .0000        .2248-21     .0000
  800     .1999-30      .2287-23      .1602-32     .2173-21     .0000
  900     .1031-25      .1769-21      .5202-28     .1732-21     .5076-33
 1000     .5811-22      .5444-20      .2036-24     .1399-21     .2727-28
 1100     .6581-19      .8209-19      .1696-21     .1064-21     .1960-24
 1200     .2248-16      .7713-18      .4511-19     .8435-22     .3134-21
```

(C) moles

(G) atmospheres

```
TITANIUM - FLUID BED COMBUSTION GAS
       100% EXCESS AIR
        90% SULFUR REMOVAL
         10 ATMOSPHERES TOTAL  PRESSURE

    \
TEMP.\COMPOUND
 (K)   \     TIO2 (C)       TICL4 (G)      TICL3 (G)      TICL2 (G)      TICL (G)
 300         .1460-02       .2294-34       .0000          .0000          .0000
 400         .1460-02       .1517-26       .0000          .0000          .0000
 500         .1460-02       .3207-22       .0000          .0000          .0000
 600         .1460-02       .5078-20       .8916-34       .0000          .0000
 700         .1460-02       .5797-19       .1178-29       .0000          .0000
 800         .1460-02       .2577-18       .1119-26       .0000          .0000
 900         .1460-02       .7312-18       .2105-24       .1832-35       .0000
1000         .1460-02       .1679-17       .1378-22       .9714-32       .0000
1100         .1460-02       .3147-17       .4032-21       .1041-28       .0000
1200         .1460-02       .5341-17       .6723-20       .3466-26       .7676-36

    \
TEMP.\COMPOUND
 (K)   \     TIOCL2 (G)     TIOCL (G)      TIO2 (G)       TIO (G)
 300         .0000          .0000          .0000          .0000
 400         .0000          .0000          .0000          .0000
 500         .0000          .0000          .0000          .0000
 600         .1361-30       .0000          .0000          .0000
 700         .2945-26       .0000          .1081-36       .0000
 800         .4367-23       .0000          .8480-31       .0000
 900         .1188-20       .1143-22       .3160-26       .0000
1000         .1039-18       .8068-29       .1399-22       .0000
1100         .3890-17       .1105-25       .1318-19       .1031-32
1200         .7915-16       .4497-23       .3896-17       .8097-29

COBALT - FLUID BED COMBUSTION GAS
       100% EXCESS AIR
        90% SULFUR REMOVAL
         10 ATMOSPHERES TOTAL  PRESSURE

    \
TEMP.\COMPOUND
 (K)   \     COSO4 (S)      CO3O4 (S)      COO (S)        COCL2 (G)      COCL3 (G)
 300         .1617-04       .0000          .0000          .0000          .0000
 400         .1618-04       .0000          .0000          .6780-31       .2499-27
 500         .1618-04       .0000          .0000          .1952-23       .8667-22
 600         .1619-04       .0000          .0000          .1086-18       .1743-18
 700         .1619-04       .0000          .0000          .6502-15       .7353-16
 800         .1619-04       .0000          .0000          .7355-12       .1058-13
 900         .1619-04       .0000          .0000          .1835-09       .5198-12
1000         .1610-04       .0000          .0000          .1783-07       .1383-10
1100         .0000          .5201-05       .0000          .9051-07       .2421-10
1200         .0000          .4668-05       .0000          .3246-06       .3573-10

    \
TEMP.\COMPOUND
 (K)   \     CO2CL4 (G)     COCL (G)
 300         .0000          .0000
 400         .0000          .0000
 500         .0000          .0000
 600         .5150-31       .0000
 700         .1873-25       .4245-31
 800         .7798-21       .3827-25
 900         .3424-17       .1749-20
1000         .3911-14       .1086-16
1100         .1803-13       .1650-14
1200         .5560-13       .1001-12

*MASS CONSTRAINTS WERE NOT SATISFIED: ERROR OF 0.1-0.4% RESULTED IN THE
CALCULATIONS
```

```
CHROMIUM - FLUID BED COMBUSTION GAS
      100% EXCESS AIR
        90% SULFUR REMOVAL
         10 ATMOSPHERES TOTAL  PRESSURE

TEMP.\COMPOUND
 (K)   \    CR203   (S)  CRO2CL2 (G)    CRO4H2 (G)    CRO2OH (G)     CRO3 (G)
  300       .1306-04      .4154-07       .6155-16      .3902-33     .0000
  400       .1306-04      .6644-06       .2029-12      .5198-24     .7476-32
  500       .5686-05      .2169-05       .2608-10      .1395-18     .9271-25
  600       .5791-05      .2138-05       .6795-09      .5544-15     .4704-20
  700       .9060-05      .1176-05       .7157-08      .2016-12     .1044-16
  800       .1306-04      .6264-06       .4270-07      .1652-10     .3302-14
  900       .1306-04      .3618-06       .1746-06      .5036-09     .2854-12
 1000       .1306-04      .2338-06       .5435-06      .7670-08     .9972-11
 1100*      .8579-05      .1605-06       .1395-05      .7081-07     .1805-09
 1200*      .2790-05      .1158-06       .3085-05      .4485-06     .1995-08

TEMP.\COMPOUND
 (K)   \    CRO2  (G)    CRCL3 (G)      CRCL2 (G)     CRCL4 (G)      CRO (G)
  300       .0000         .0000          .0000         .5471-27     .0000
  400       .0000         .2930-33       .0000         .2698-21     .0000
  500       .0000         .1338-26       .0000         .2949-18     .0000
  600       .1678-33      .1114-22       .1660-31      .6530-17     .0000
  700       .1841-27      .2910-20       .9871-27      .1882-16     .0000
  800       .6030-23      .1433-18       .3088-23      .2927-16     .2324-36
  900       .1908-19      .2706-17       .1505-20      .3700-16     .6004-31
 1000       .1178-16      .2839-16       .2112-18      .4514-16     .1253-26
 1100*      .2221-14      .1881-15       .1174-16      .5141-16     .4201-23
 1200*      .1721-12      .8902-15       .3277-15      .5618-16     .3581-20

TEMP.\COMPOUND
 (K)   \    CRCL  (G)    CR (G)
  300       .0000        .0000
  400       .0000        .0000
  500       .0000        .0000
  600       .0000        .0000
  700       .0000        .0000
  800       .1976-36     .0000
  900       .1819-31     .0000
 1000       .1669-27     .1548-35
 1100*      .2835-24     .5195-31
 1200*      .1366-21     .3024-27

*MASS CONSTRAINTS WERE NOT SATISFIED:
       ERROR OF 2% RESULTED IN THE CALCULATIONS
```

```
MANGANESE - FLUID BFD COMBUSTION GAS
      100% EXCESS AIR
       90% SULFUR REMOVAL
        10 ATMOSPHERES TOTAL  PRESSURE
    \
TEMP.\COMPOUND
 (K)   \    MNSO4 (S)     MN2O3 (S)     MN3/4 (S)     MNCL2 (G)     MNCL (G)
 300        .8991-04      .0000         .0000         .0000         .0000
 400        .8993-04      .0000         .0000         .2744-31      .0000
 500        .8993-04      .0000         .0000         .1273-23      .0000
 600        .8988-04      .0000         .0000         .9795-19      .0000
 700        .8989-04      .0000         .0000         .7455-15      .1591-32
 800        .8989-04      .0000         .0000         .1018-11      .2661-26
 900        .8989-04      .0000         .0000         .2956-09      .1981-21
1000        .0000         .4491-04      .0000         .1563-07      .8772-16
1100        .0000         .4470-04      .0000         .7825-07      .1644-15
1200        .0000         .4397-04      .0000         .2928-06      .1255-13

    \
TEMP.\COMPOUND
 (K)   \    MNO (G)       MN (G)
 300        .0000         .0000
 400        .0000         .0000
 500        .0000         .0000
 600        .0000         .0000
 700        .0000         .0000
 800        .1478-32      .0000
 900        .1448-26      .1023-30
1000        .5032-22      .1619-25
1100        .5125-19      .5707-22
1200        .1609-16      .5051-19


MOLYBDENUM - FLUID BED COMBUSTION GAS
      100% EXCESS AIR
       90% SULFUR REMOVAL
        10 ATMOSPHERES TOTAL  PRESSURE
    \
TEMP.\COMPOUND
 (K)   \    MOO3 (S)      H2MOO4 (G)    MOO2CL2 (G)   MOO3 (G)      MOO2 (G)
 300        .7882-05      .3396-19      .3875-15      .0000         .0000
 400        .7868-05      .2771-13      .2554-10      .0000         .0000
 500        .7784-05      .9663-10      .1231-07      .2001-29      .0000
 600        .5462-05      .2224-07      .3314-06      .8422-23      .0000
 700*       .0000         .1159-05      .2008-05      .4602-18      .0000
 800        .0000         .8902-06      .2532-06      .6263-16      .1782-33
 900        .0000         .1073-05      .7003-07      .4091-14      .3688-29
1000        .0000         .1122-05      .2183-07      .1015-12      .9090-26
1100        .0000         .1143-05      .8095-08      .1352-11      .5174-23
1200        .0000         .1158-05      .3466-08      .1144-10      .9955-21

    \
TEMP.\COMPOUND
 (K)   \    MOCL4 (G)     MOO (G)       MOCL5 (G)     MOCL6 (G)
 300        .0000         .0000         .0000         .0000
 400        .0000         .0000         .0000         .0000
 500        .4201-36      .0000         .1074-35      .0000
 600        .8282-31      .0000         .1043-31      .0000
 700        .1628-27      .0000         .1818-29      .0000
 800        .1330-26      .0000         .2248-29      .0000
 900        .9093-26      .0000         .3504-29      .6880-37
1000        .3638-25      .0000         .4302-29      .6775-37
1100        .1082-24      .0000         .4867-29      .6452-37
1200        .2616-24      .6864-35      .5311-29      .6073-37

*MASS CONSTRAINTS WERE NOT SATISFIED: ERROR OF 17% RESULTED IN THE
CALCULATIONS
```

```
NICKEL - FLUID BED COMBUSTION
      100% EXCESS AIR
       90% SULFUR REMOVAL
        10 ATMOSPHERES TOTAL  PRESSURE

     \
TEMP.\COMPOUND
 (K)   \    NISO4 (S)     NIO (S)         NICL2 (G)      NI(OH)2 (G) NICL (G)
  300       .3580-04      .0000           .0000          .0000       .0000
  400       .3582-04      .0000           .4242-31       .0000       .0000
  500       .3582-04      .0000           .2116-23       .2242-30    .0000
  600       .3575-04      .0000           .1765-18       .5026-24    .4779-35
  700       .3576-04      .0000           .1456-14       .7790-19    .9219-28
  800       .3577-04      .0000           .2148-11       .1212-14    .4858-22
  900       .3576-04      .0000           .6712-09       .2511-11    .1485-17
 1000       .0000         .3562-04        .2874-07       .4869-09    .2454-14
 1100       .0000         .3521-04        .8949-07       .5283-08    .1513-12
 1200       .0000         .3399-04        .2278-06       .3859-07    .4614-11

     \
TEMP.\COMPOUND
 (K)   \    NIO (G)       NI (G)          NIH (G)
  300       .0000         .0000           .0000
  400       .0000         .0000           .0000
  500       .0000         .0000           .0000
  600       .0000         .0000           .0000
  700       .1728-35      .0000           .0000
  800       .2995-28      .1463-33        .0000
  900       .1430-22      .4908-27        .5905-33
 1000       .2135-18      .3494-22        .1287-27
 1100       .8044-16      .4735-19        .4356-24
 1200       .1113-13      .1907-16        .3757-21
```

```
FLUORINE - FLUID BED COMBUSTION
       100% EXCESS AIR
        90% SULFUR REMOVAL
         10 ATMOSPHERES TOTAL PRESSURE
    \
TEMP.\COMPOUND
 (K)   \     HF (G)        KF (G)        NAF (G)       SO2F2 (G)
  300        .1112-06      .0000         .0000         .3271-04
  400        .2083-05      .2339-36      .0000         .3172-04
  500        .1150-04      .4851-28      .5256-29      .2701-04
  600        .3363-04      .1663-22      .2430-23      .1595-04
  700        .6178-04      .2443-18      .4192-19      .1875-06
  800        .6538-04      .3119-15      .6043-16      .7292-07
  900        .6553-04      .7676-13      .1729-13      .4512-08
 1000        .6553-04      .6548-11      .1694-11      .3922-09
 1100        .6553-04      .2744-09      .7913-10      .4108-10
 1200        .6553-04      .6417-08      .1906-08      .5472-11

BERYLLIUM - FLUID BED COMBUSTION
       100% EXCESS AIR
        90% SULFUR REMOVAL
         10 ATMOSPHERES TOTAL PRESSURE
    \
TEMP.\COMPOUND
 (K)   \     BESO4 (S)     BE(OH)2 (G)
  300        .3918-04      .4830-20
  400        .3918-04      .1032-12
  500        .3918-04      .2545-08
  600        .0000         .2763-05
  700        .0000         .5750-05
  800        .0000         .5750-05
  900        .0000         .5766-05
 1000        .0000         .5765-05
 1100        .0000         .5765-05
 1200        .0000         .5768-05
MERCURY - FLUID BED COMBUSTION
       100% EXCESS AIR
        90% SULFUR REMOVAL
         10 ATMOSPHERES TOTAL PRESSURE
    \
TEMP.\COMPOUND
 (K)   \     HGCL2 (G)     HG (G)        HGO (G)       HG2 (S)       HGCL (G)
  300        .2353-07      .6042-35      .1513-33      .0000         .0000
  400        .2382-07      .7201-26      .2538-25      .0000         .4237-31
  500        .2474-07      .3054-20      .3287-20      .0000         .3942-25
  600        .2760-07      .3997-16      .1944-16      .1445-34      .5888-21
  700        .2770-07      .5759-13      .1584-13      .1949-28      .6925-18
  800        .2780-07      .1579-10      .2829-11      .1053-23      .1497-15
  900        .2781-07      .1262-08      .1617-09      .5170-20      .9797-14
 1000        .1086-07      .1671-07      .1636-08      .7309-18      .1091-12
 1100        .9380-09      .2622-07      .2057-08      .1504-17      .1468-12
 1200        .7934-10      .2939-07      .1915-08      .1621-17      .1328-12
LEAD - FLUID BED COMBUSTION
       100% EXCESS AIR
        90% SULFUR REMOVAL
         10 ATMOSPHERES TOTAL PRESSURE
    \
TEMP.\COMPOUND
 (K)   \     PBCL4 (G)     PBCL2 (G)     PBO (G)       PBCL (G)
  300        .5931-05      .0000         .0000         .0000
  400        .5931-05      .0000         .0000         .0000
  500        .5931-05      .7634-33      .0000         .0000
  600        .5930-05      .7740-26      .0000         .0000
  700        .5928-05      .1360-20      .1894-30      .1098-29
  800        .5928-05      .1343-16      .7129-24      .1119-23
  900        .5932-05      .1726-13      .9530-19      .5344-19
 1000        .5932-05      .5341-11      .1240-14      .3011-15
 1100        .5931-05      .5869-09      .2960-11      .3584-12
 1200        .5894-05      .3439-07      .2675-08      .1863-09
```